ADULT STEM CELL-DERIVED KIDNEY ORGANOIDS TO MODEL TISSUE PHYSIOLOGY AND DISEASE

Frans Schutgens

ISBN: 978-94-6182-843-9
Author: Frans Schutgens
Cover illustration: Frans Schutgens
Layout and printing: Off Page, Amsterdam

ADULT STEM CELL-DERIVED KIDNEY ORGANOIDS TO MODEL TISSUE PHYSIOLOGY AND DISEASE

NIERORGANOÏDEN UIT VOLWASSEN STAMCELLEN OM FYSIOLOGIE EN ZIEKTE TE MODELLEREN
(met een samenvatting in het Nederlands)

Proefschrift

ter verkrijging van de graad van doctor aan de Universiteit Utrecht
op gezag van de rector magnificus, prof.dr. G.J. van der Zwaan,
ingevolge het besluit van het college voor promoties
in het openbaar te verdedigen op dinsdag 21 november 2017
des ochtends te 10.30 uur

door

Frans Willem Godfried Schutgens
geboren op 10 juni 1987 te Beek

Promotoren:
Prof. dr. H.C. Clevers
Prof. dr. M.C. Verhaar

Copromotoren:
Dr. M.B. Rookmaaker
Dr. R.G.J. Vries

CONTENTS

OUTLINE AND SCOPE OF THE THESIS

"Organoid" is defined[1] as a 3D structure grown from stem cells and consisting of organ-specific cell types that self-organizes through cell sorting and spatially restricted lineage commitment. Organoids can be derived from either adult stem cells (ASCs) or pluripotent stem cells (PSCs).

In **Chapter 1**, the development of ASC-derived organoid cultures for other organs than the kidney is described and it is explained why organoids are a valuable tool for biology and medicine. In addition, we address the state-of-the-art of kidney ASC cultures and how the field of nephrology may benefit from ASC-derived organoid cultures. An adequate ASC-derived kidney organoid culture system does not exist, although in theory such system would have useful applications.

The other cell source for establishing organoid cultures are PSCs, either embryonic or induced. For the kidney, organoid cultures derived from PSCs have been well-established. In order to gain insight into growth conditions that allow expansion and differentiation of kidney cells, published protocols to differentiate PSCs into kidney organoids are reviewed in **Chapter 2**.

In **Chapter 3**, the development of ASC-derived kidney organoid culture is described. Cultures can be established from mouse and human kidney tissue, as well as from human urine. Organoids can be expanded for 6 months while remaining genetically stable and can be used to model infectious and malignant disease. Kidney organoids derived from the urine of cystic fibrosis patients can be used to predict treatment efficacy *ex vivo*.

In **Chapter 4**, a living organoid biobank of pediatric kidney tumors is established. This biobank contains the most common types of pediatric kidney tumors, such as Wilms tumor, malignant rhabdoid tumor of the kidney and renal cell carcinoma. Organoid lines from tumor and matching normal tissue can be efficiently established and reflect the primary tissue on histology.

In **Chapter 5**, organoid-derived cells are integrated with an 'organ-on-a-chip' platform, to allow high-throughput transporter and toxicity studies, and with a hollow fiber platform, to create 'living membranes.' Organoids may function as an autologous cell source for these technologies, thereby broadening the scope of applications of the culture system.

In **Chapter 6**, a population of murine kidney cells with a relatively high organoid-forming capacity is described. *In vivo* tracing of these cells yields mono-clonal expansions during kidney development, adult homeostasis and repair.

In **Chapter 7**, the findings of this thesis are summarized and the implications for future research are discussed.

REFERENCE

1. Clevers, H. Modeling Development and Disease with Organoids. *Cell* **165**, 1586-1597, doi:10.1016/j.cell.2016.05.082 (2016).

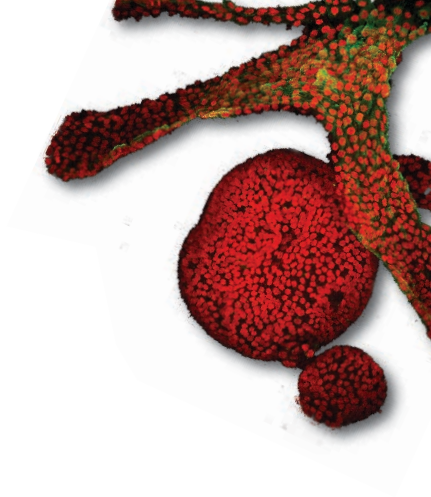

CHAPTER 1

DEVELOPMENT AND APPLICATION OF HUMAN ADULT STEM OR PROGENITOR CELL ORGANOIDS

ABSTRACT

Adult stem or progenitor cell organoids are 3D adult-organ-derived epithelial structures that contain self-renewing and organ-specific stem or progenitor cells as well as differentiated cells. This organoid culture system was first established in murine intestine and subsequently developed for several other organs and translated to humans. Organoid cultures have proved valuable for basic research and for the study of healthy tissue homeostasis and the biology of disease. In addition, data from proof-of-principle experiments support promising clinical applications of adult stem or progenitor cell organoids. Although renal organoids have many potential applications, an adult stem or progenitor cell organoid culture system has not yet been developed for the kidney. The development of such a system is likely to be challenging because of the intricate renal architecture. Differentiated 3D cultures and stem or progenitor cell 3D sphere cultures are, however, available for the kidney. These cultures indicate the feasibility of renal organoid culture and provide a solid basis for its development. In this Review, we discuss the state-of-the-art of human adult stem or progenitor cell organoid culture and the potential of renal organoids as tools in basic and clinical research.

Maarten B. Rookmaaker*[1], Frans Schutgens*[1,2], Marianne C. Verhaar[1], Hans Clevers[2]

[1] Department of Nephrology and Hypertension, University Medical Centre Utrecht, the Netherlands
[2] Hubrecht Institute–Royal Netherlands Academy of Arts and Sciences, Utrecht, the Netherlands
* Contributed equally to the work

Nature Reviews Nephrology 11, 546–554 (2015)

INTRODUCTION

Although chronic kidney disease is a major, worldwide public health problem with an increasing incidence,[1] current treatment remains limited to reducing inflammation, optimization of cardiovascular risk factors and supportive care. New therapeutic approaches are urgently required and better understanding of physiological and pathophysiological mechanisms of renal damage and repair will facilitate their development.

The kidney contains many cell types and has a complex architecture, which complicates *in vivo* studies. Although 2D cell culture models are valuable for the study of renal pathophysiology, 3D culture models are thought to be superior in mimicking the *in vivo* situation. Two main types of adult 3D kidney models are currently in use; 3D models of differentiated cells are mainly used for transport and toxicity studies, whereas 3D sphere cultures propagate putative stem or progenitor cell populations, enabling study of the dynamics of these cells.

Integration of these existing adult 3D kidney models into a uniform culture system would combine culture of differentiated epithelial cells with physiological cell turnover by proliferation and differentiation of stem or progenitor cells. An integrated culture system would more accurately resemble the *in vivo* situation than the current models and would also provide an unlimited source of differentiated and undifferentiated organ-specific cells. An integrated adult-cell-derived 3D culture system was first developed for the intestine and subsequently for several other organs. These organoid culture systems comprise adult-organ-derived *ex vivo* cultured epithelial structures that can be expanded indefinitely and stem or progenitor cells that are able to self-renew and to differentiate into the cells of the organ-specific epithelium.[2] Of note, these models reflect the epithelial components of an organ but lack vascular and stromal cells.

As an adult stem or progenitor cell organoid culture system has not yet been described for the kidney, we review the development of intestinal adult stem cell organoid culture, the organoid culture systems available for other organs and their applications. We then discuss the challenges and feasibility of the development of kidney organoid culture and the potential kidney-specific applications of organoids.

ORGANOID CULTURE

The term organoid culture has been used for a wide array of culture systems, but all organoid cultures share multiple features (Figure 1).[3] Organoid culture involves the culture of multicellular structures known as organoids that contain multiple cell types and are intended to represent organ structure and function, and to model maintenance and repair *ex vivo*. Organoids have the capacity of self-organization, which is the spontaneous ordering of a cell population and an essential process in organogenesis.[3] This process involves cells sorting on the basis of differential expression of cell adhesion molecules and lineage specification.[4] Self-organization is distinct from recellularization of decellularized or printed matrices in which external architectural cues are provided.[5,6] Organoids are 3D structures—differentiated cells better maintain their *in vivo* characteristics when cultured in 3D than when cultured in 2D.[7] Moreover, the finding that culture of floating spheres enables expansion of embryonic neuronal stem cells that retain their multi-lineage potential[8] led to recognition of

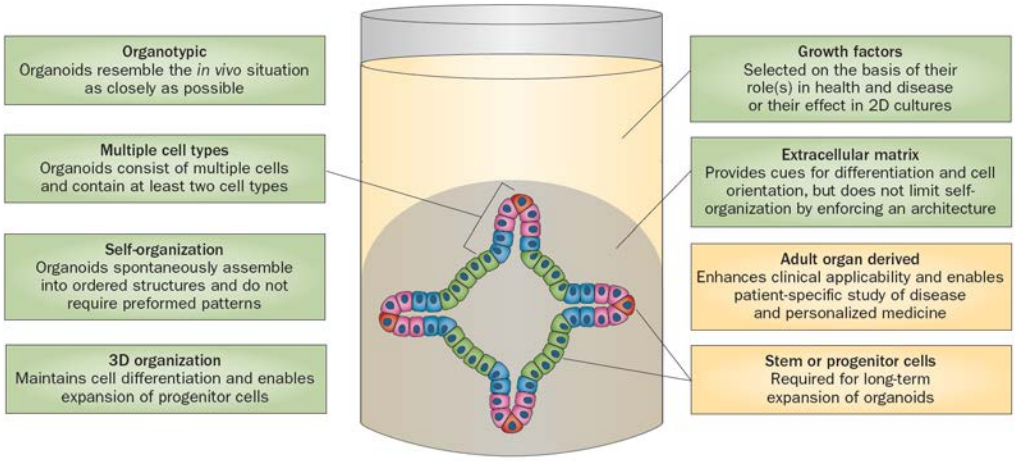

Figure 1. Human adult progenitor or stem cell organoid culture. Although most organoid culture systems share several characteristics (green boxes), some aspects depend on the specific type of organoid culture (orange boxes). For example, all organoid cultures are 3D, but organoids can be derived either from embryonic or adult cells.

the importance of 3D organization for stem and progenitor cell culture. Similar cultures for other tissues, including retina, pancreas and skin, have been developed.[9-11]

Organoids are suspended in an extracellular matrix (ECM). As matrix components seem to be vital for cell differentiation and orientation, organoid cultures have been set up in laminin-rich Matrigel, which enables the expansion and differentiation of primary human breast epithelial cells[12, 13] and stem-cell-enriched populations of murine prostate cells.[12, 13] Furthermore, organoid culture requires specific culture media, growth factors and other media components, which are often selected based on their effect on cell proliferation and differentiation during embryonic development, normal adult cell turnover and regeneration. In addition, factors that are related to pathophysiological states, such as hyperplasia and tumour formation, have proved of use to enhance organoid expansion.[14]

ADULT STEM OR PROGENITOR CELL ORGANOIDS

In this Review, we discuss an adult epithelial-tissue-derived stem or progenitor cell based organoid culture system that was developed in our laboratory for the intestine and several other organs. Thus, in this article we define organoids as adult organ-derived *ex vivo* cultured 3D epithelial structures that can be expanded indefinitely and contain stem or progenitor cells that are able to self-renew and to differentiate into the cells of the organ-specific epithelium (Figure 1). This organoid culture system has proved valuable for fundamental research as many aspects of adult tissue pathophysiology are represented *ex vivo*. In addition, the use of adult patient-derived organoids enables several diagnostic and therapeutic applications. The presence of stem or progenitor cells enables long-term expansion, ensuring sufficient material for *ex vivo* models and clinical applications. Notably this system—like most organoid culture systems—lacks nerve innervation,

blood supply and mesenchymal support. Several other organoid culture models using different cell sources, such as embryonic stem cells or induced pluripotent stem cells have been described in the literature with their own fields of application.[15, 16]

Development of the culture system

The identification of tissue-specific stem or progenitor cell markers in epithelial organs led to the development of the adult organoid culture system. Following the identification of leucine-rich repeat-containing G-protein coupled receptor 5 (Lgr5) as an intestinal stem cell marker, a 3D culture system was set up that enables long-term expansion and multi-lineage differentiation of intestinal stem cells.[17] When cultured in a 3D extracellular matrix with culture media resembling the *in vivo* situation in terms of growth factor composition, single Lgr5$^+$ cells develop into structures with distinct intestinal crypt and villus-domains, containing all differentiated cell types found in the instestine in near-physiological ratios.[14] The matrix consists of a collagen and laminin-rich Matrigel, as laminins constitute an important part of the crypt basal lamina *in vivo*. Factors that induce stem cell expansion, as seen in crypt hyperplasia (Wnt and Noggin) and in intestinal epithelial cell proliferation (epidermal growth factor [EGF]) are included in the culture media. These conditions enable prolonged expansion of the size and number of crypt-villus structures and maintenance of the multi-lineage differentiation potential of the Lgr5$^+$ stem cell population.

The intestinal organoid culture system has been adapted to culture stem or progenitor cells from other organs with high or low cell turnover. For example, organoid cultures have been set up for Lgr5$^+$ stem or progenitor cells of colon crypts and the pyloric glands of the stomach.[18, 19] Importantly, Lgr5 expression is not a requirement for organoid culture development; subsets of basal tracheal cells that express low-affinity nerve growth factor receptor[20] and a subset of lung epithelial cells that express epithelial cell adhesion molecule[20, 21] can give rise to organoids. Organoid culture systems have also been developed for several organs with low self-renewal, such as the prostate.[22, 23] Interestingly, in adult murine liver, Lgr5$^+$ stem or progenitor cells are absent in healthy tissue but are induced upon damage. These induced Lgr5$^+$ cells have clonal expansion capacity and multi-lineage differentiation potential, with the capacity to differentiate into bile duct cells and hepatocytes.[24] Analogously, in adult murine pancreas, damage induced Lgr5$^+$ cells clonally expand in organoid culture and can be directed towards either an endocrine or pancreatic duct fate.[25]

As murine organoid culture conditions do not enable long-term culture of human organoids, several strategies have been used to identify the factors that are required for such cultures. Factors, such as nicotinamide and a TGF-β-inhibitor, that are involved in human tissue homeostasis, tumour development and epithelial cell culture were evaluated, and proved to enable the long-term culture of human adult tissue derived organoids.[19, 26, 27] Translation of liver organoid culture involved a different approach. Gene expression profiles of human organoids, cultured in murine organoid culture media, were analysed to identify upregulated pathways involved in growth arrest and downregulated proliferative pathways.[28] Subsequently, factors that inhibit and stimulate these pathways, respectively, were added to the culture media. Using these strategies, human organoid culture systems have now been developed for the stomach, small intestine, colon, lung, pancreas, liver and prostate.[19, 20, 23, 26, 27, 29]

APPLICATIONS OF ORGANOID CULTURE

Study of healthy tissue homeostasis

Organoid cultures are useful tools for basic research and hold great promise for diagnostic and therapeutic applications (Figure 2). Moreover, they can be used to study homeostasis of healthy tissue, enabling the real time study of differentiation, dedifferentiation, gene function and cell–cell interactions, as well as the identification of factors affecting differentiation states.[30, 31] In intestinal organoids, Notch inhibition enables steering of progenitor cells into differentiated daughter cells of the secretory lineage, reflecting the *in vivo* situation.[32, 33] Conversely, secretory cells can dedifferentiate and regain stemness upon damage *in vivo* and after Wnt3A exposure *in vitro*.[33-35] Whole library screening has been performed in this organoid culture system to identify epigenetically active compounds involved in intestinal stem cell differentiation.[36]

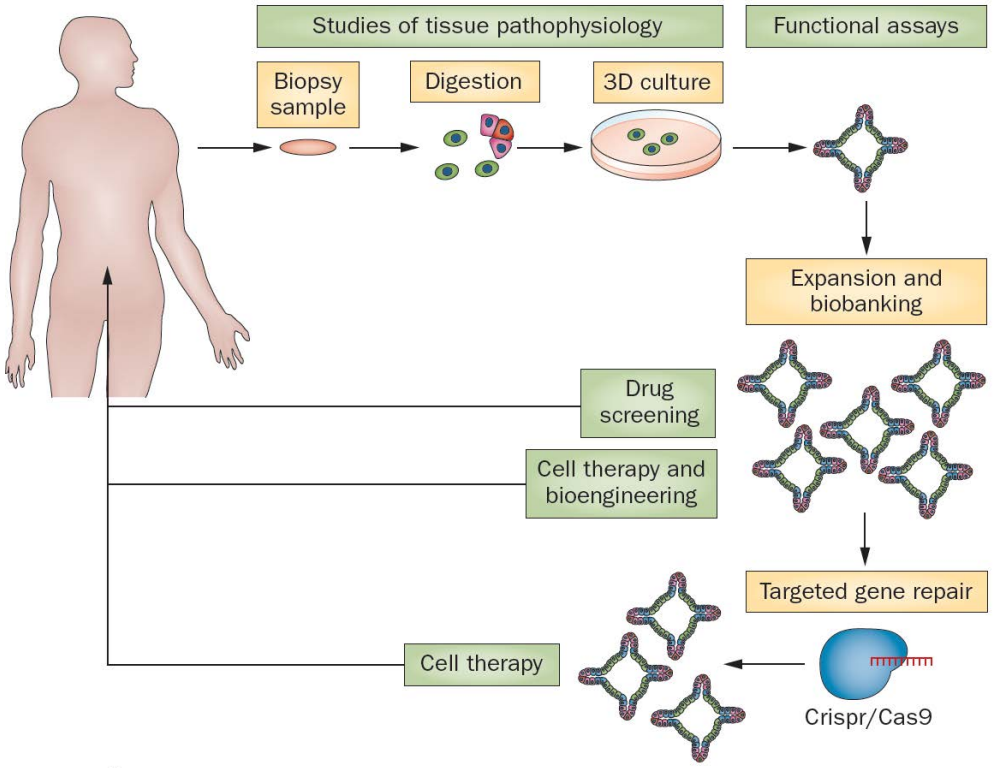

Figure 2. Applications of organoid culture. The various steps in the establishment of an organoid culture (yellow boxes) enable specific fundamental and clinical applications (green boxes). After digestion of biopsy material the cells are seeded in a 3D matrix. A subset of these cells will develop into organoids. The development of organoids from tissue biopsy samples mimics aspects of tissue organization and turnover in health and disease which enables studies of tissue homeostasis. Functional assays can be performed using developed organoids. In addition, organoids can be expanded and used as a screening tool to test drug efficacy and toxicity in pre-clinical trials or for personalized medicine. Expanded organoids from a single patient might also be used for bioengineering and cell therapy, possibly in combination with targeted gene repair.

Gene function in tissue homeostasis and signalling has been studied in the crypt-villus structure of intestinal organoids using recombinant viruses, conditional knock-out models and small-interfering RNA.[37-39] Importantly, organoid culture enables the functional evaluation of genes that are difficult to study in knock-out mice because of embryonic lethality.

Organoid culture also enables the determination of cell–cell interactions, for example in the intestinal crypt. When single intestinal Lgr5$^+$ cells are seeded in Matrigel, the percentage of cells that develop into organoids is low.[40] The observation that co-culturing single intestinal Lgr5$^+$ cells with Paneth cells profoundly increases the efficiency of organoid culture indicates that Paneth cells constitute a niche for Lgr5$^+$ stem cells.[40] Indeed, Paneth cells are essential *in vivo* for stem cell proliferation and differentiation by paracrine secretion of growth factors such as Wnt3 and EGF.[40, 41]

Functional assays

As sphere formation efficacy is a parameter for stemness, the organoid-forming efficiency of single cells of a putative stem or progenitor cell population is a functional assay in its own right. Other stem cell characteristics, such as self-renewal and multi-lineage differentiation can also be studied in organoid culture, as demonstrated in cells derived from normal tissue and from adenomas.[42-45]

Transporter function can be assessed in organoids with wild type transporters as well as in those with mutant transporters.[46, 47] For example, the function of the cAMP-dependent chloride channel, cystic fibrosis transmembrane conductance regulator (CFTR), which is mutated in patients with cystic fibrosis, can be assessed intestinal organoids using a swelling assay. In wild-type organoids, forskolin treatment increases intracellular cAMP levels, resulting in increased CFTR-dependent chloride transport into the lumen and swelling of the organoid. Such swelling does not occur in organoids with mutant CFTR channels, but can be restored using CFTR-rescuing compounds.[47]

Study of diseased tissue

Patient-derived organoids enable study of the biology of disease. For example, organoids have been derived from patients with colorectal cancers and from patients with hereditary diseases.[19] The organoid culture system is particularly interesting for the latter owing to the genetic stability of organoids.[26] Intestinal organoids from patients with hereditary diseases, such as microvillus inclusion disease (MVID) and multiple intestinal atresia (MIA), reflect the *in vivo* histology of these diseases. Organoids from patients with MVID are characterized by loss of microvilli and subapical accumulation of vesicles, whereas those from patients with MIA display disrupted polarity, growth and differentiation.[48, 49]

Molecular pathogenesis can also readily be studied in organoids. This application is illustrated by the organoid swelling assay for CFTR function: in biopsy-derived rectal organoids from patients with cystic fibrosis, forskolin-induced swelling is reduced or absent; the extent of swelling correlates with disease severity.[47] Gastric gland organoids have been shown to respond to *H. pylori* exposure by mounting a substantial inflammatory response, indicating that organoids enable modelling of bacterial epithelial infection with live follow-up.[50] The effect of rotavirus infection on the intestine has also been experimentally modelled in organoids.[51]

Expansion of patient-derived organoids enables genetic screening and the *ex vivo* study of cell signalling pathways in the diseased state. Cancer-derived organoids (termed tumouroids) from the prostate consistently display abnormalities in the p53 and retinoblastoma tumour suppressor

pathways, suggesting a crucial role of these pathways in disease development.[23] Colon organoids derived from patients with inflammatory bowel disease were expanded *ex vivo* to obtain sufficient DNA to screen for non-coding DNA regulatory regions associated with this disease.[52] In addition, organoids can be used to investigate the effect of a potentially pathogenic mutation on organoid function and/or morphology. A study using organoid cultures showed that mutations in *RHOA* that are frequently found in patients with gastric cancer, contribute to tumourigenesis by decreasing anoikis.[53] Similarly, mutations in syntaxin-3, found in patients with MVID who lack typical myosin Vb mutations, induce a MVID phenotype in healthy organoids, indicating the pathogenicity of this mutation in variant MVID.[49]

Drug screening

By establishing living biobanks, organoid cultures can be used to assess the therapeutic and/or toxic effects of compounds on healthy and diseased tissue. Proof-of-principle for this application was provided by the establishment of a living biobank from 20 patients with colorectal cancer in which the major subtypes of this cancer are represented.[54] Biobanks of healthy or patient-derived human organoids enable high-throughput analysis of the effects of compounds in a heterogeneous target population. For example, exposure of lung organoids to high concentrations of tobacco smoke components decreased cell viability, whereas sub-toxic doses increased secreted protein levels and cytokine release and induced goblet cell hyperplasia and hypertrophy.[55] This organoid response to tobacco smoke components is comparable to the *in vivo* response. Moreover, high-throughput analysis of organoid cultures from patients with MIA showed that Rho kinase inhibitors restored the defects in cell polarity.[48]

Organoids might also enable the reaction of an individual to a drug or (after expansion) a panel of drugs to be predicted. For example, human colorectal tumouroids have been used to evaluate resistance to irinetocan.[56] In this study, the relevance of a culture system containing both tumour-initiating cells and differentiated cells was underlined, as differentiated cells confer drug resistance to the tumour-initiating cells. The CFTR-forskolin assay shows patient-specific drug responses in organoids from patients with the same mutation.[47] Use of organoid culture systems to predict individual drug responses might lay a foundation for organoid use in personalized medicine.

Therapy

Organoid culture has been successfully applied as a cell therapy in proof-of-principle animal experiments using models of intestinal and hepatic damage. Single-cell-derived murine colon organoids were shown to home to damaged colon epithelium upon transplantation and engraftment for >6 months was observed.[57] In fumarylacetoacetate hydrolase mutant mice, a model of liver failure that is lethal without rescue, liver organoids derived from single $Lg5^{+}$ liver cells integrated into the recipient's liver upon transplantation and significantly increased survival.[24]

Interestingly, patient-derived organoids are amenable to gene therapy. CRISPR/Cas9 mediated correction of a CFTR mutation in intestinal organoids derived from patients with cystic fibrosis restores the functional transport defect, assessed by forskolin–CFTR assay.[58] This finding provides proof-of-principle for gene repair of adult stem or progenitor cells derived from organoids cultured from patients with a monogenetic defect.

DEVELOPMENT OF RENAL ORGANOID CULTURES

Challenges

Adult stem or progenitor cell organoid culture systems have been successfully developed for progressively more complex organs, but are not yet available for the kidney. Two aspects that require particular attention when the development of renal organoid culture is considered are the existence of adult renal stem or progenitor cells and the complex renal architecture.

The exact nature of the stem or progenitor cells that are involved in tubular maintenance and repair in the adult kidney is heavily debated.[59, 60] Whether a committed stem or progenitor cell population is constitutively present in the adult kidney or whether differentiated tubular cells dedifferentiate, proliferate and replace damaged epithelium remains unclear. One might argue that the absence of constitutively present stem or progenitor cells would preclude the development of adult stem or progenitor cell derived renal organoids. In the liver, however, the existence of stem or progenitor cells is also heavily debated and constitutively present stem or progenitor cells do not seem to contribute to normal homeostasis.[61, 62] There is evidence that upon toxic injury, stem or progenitor cells residing in the bile ducts are induced, most likely through dedifferentiation.[63] However, this notion is also controversial, as data suggest that regardless of the mechanism of damage, the majority of hepatocyte regeneration is due to the proliferation of pre-existing hepatocytes—a mechanism that is comparable to what has been found in the kidney.[64, 65] Despite these controversies, our group demonstrated that long-term culture of genomically stable human adult liver derived organoids is possible.[26] Moreover, in the pancreas, stem or progenitor cells are absent during homeostasis and can be induced from the exocrine ducts upon damage, but long-term expansion of adult-derived pancreas organoids is possible.[29] Thus, independent of the presence of stem or progenitor cells in healthy adult tissue, organoid culture is possible for the liver and pancreas. Whether this finding also applies to the kidney remains to be elucidated.

The intricate architecture of the kidney, which is generated during embryonic development in a process that involves reciprocal interaction of the ureteric bud and metanephric mesenchyme, might complicate development of organoid culture. However, organoids can be cultured from adult lung, an organ that is also dependent on interactions between epithelial and mesenchymal structures for its development.[21, 66] In addition, nephrons consist of distinct segments with specific functions that might each have a separate committed stem or progenitor cell population.[67] Consequently, kidney organoid cultures might be segment-specific and require segment-specific culture conditions. However, for the intestine segment commitment has not posed a problem: stomach, small intestine and colon organoids can be cultured using different culture conditions.[19, 26]

Feasibility and progress

3D culture models of the developing kidney have been in use for a long time. Classic developmental biology experiments have been carried out using embryonic whole kidney explants, and subsequently with distinct embryonic kidney compartments or specific cell populations.[5, 68-70] Protocols for *ex vivo* differentiation of induced pluripotent or embryonic stem cells into 3D structures with renal phenotypes have also been developed.[71, 72, 73, 74] These models are of great value for the investigation of renal development and nephrogenesis, as in contrast to adult models, they contain discrete stem cell compartments.

The feasibility of the development of an adult stem or progenitor cell organoid culture system for the kidney is supported by the existence of 3D differentiated renal cell cultures. Compared with 2D cultures, 3D cultures are superior in maintaining renal cell differentiation and morphology. For example, isolated tubular cells cultured in a monolayer dedifferentiate quickly, exemplified by rapid loss of cytochrome P450 activity, whereas in 3D culture persistent expression of cytochrome P450 is observed.[7] Considering the crucial role of cytochromes in drug metabolism, it is not surprising that drug toxicity studies carried out in 3D cultures (even after prolonged culture of primary cells) are superior to 2D toxicity studies.[75] In addition, 3D culture models display the aberrant histology of renal disease; immortalized murine tubular epithelial cells from a model of autosomal dominant polycystic kidney disease (ADPKD) cultured in a silk scaffold matrix with collagen or Matrigel show the reversed polarity of epithelial cells that is typical for ADPKD *in vivo*.[76] Furthermore, a 3D spheroid model of differentiated tubular cells maintains apicobasal polarity and a luminal compartment.[77] This technology, therefore, seems particularly useful for the study of the morphological abnormalities that are characteristic of ciliopathies.

In addition to differentiated 3D structures, multi-cellular 3D epithelial cell cultures are of value for the identification and study of renal stem or progenitor cell populations, as sphere-forming capacity is a stem or progenitor cell characteristic. Subpopulations of $CD133^+$ cells have been proposed as adult renal stem or progenitor cells[58] and sphere-forming capacity of a subpopulation of $CD133^+$ adult human kidney-derived cells that expresses CD24 and high levels of aldehyde dehydrogenase has been demonstrated.[78, 79] Long-term culture, multi-lineage potential and expansion of these spheres was not reported. In accordance with these findings, adult human primary kidney cells cultured in suspension aggregate to form spheres that contain cells that co-express CD133 and marker genes for embryonic renal stem cells.[80] Although a large part of this spheroid formation can be attributed to clonal expansion, as assessed by genetic labelling, cell aggregation also contributes. This finding might reflect the need for a stem cell niche, such as that formed by the Paneth cell for $Lgr5^+$ intestinal stem cells.[40] Upon passage new spheres form, but clonal expansion has not been shown. Transplantation of sphere-derived cells to a chick chorioallantoic membrane resulted in tubulogenesis and the expression of segment-specific tubular proteins, indicating multi-potency of the sphere-derived stem or progenitor cells.[80] As cultured human kidney epithelial cells uniformly express CD133 and CD24, a follow up study was designed to obtain more specific markers for sphere-forming cells. A subset of $CD133^+CD24^+$ cells that re-express the embryonic mesenchymal marker neural cell adhesion molecule 1, which is important during kidney development, was found to have sphere-forming capacity.[81, 82] Consistent with this finding, a PKH26 or PKH2 label-retaining $CD133^+CD24^-$ population was identified within spheres cultured from single human adult kidney cells.[83] This population is capable of self-renewal and differentiation into multiple renal cell types when cultured in differentiation conditions.

In the studies discussed above, specific subpopulations of $CD133^+$ cells were cultured to assess stem or progenitor cell potential. In order to prove that segment-specific progenitor cells exist, a different approach was taken, wherein bulk adult murine cells were cultured: single cells were grown into 3D structures and subsequent co-staining with segment-specific markers showed that each structure had a segment-specific phenotype.[67] This fate restriction was also observed in *in vivo* fate mapping experiments, suggesting that 3D kidney culture faithfully recapitulates the *in vivo*

situation. These data are in line with our finding that segment-specific progenitors exist during embryonic development.[84] By contrast, another study found that a cluster of cultured adult rat cells from the proximal S3 segment gives rise to 3D structures that, based on morphology and marker expression, contain glomeruli as well as cells from all tubular segments.[85] Long-term culture and functional studies of these structures will be very interesting. The availability of 3D differentiated cultures and the progress made with sphere cultures of renal stem or progenitor cells indicate the feasibility of the development of a human kidney adult stem or progenitor cell organoid culture.

POTENTIAL APPLICATIONS OF RENAL ORGANOIDS

Renal organoid cultures established from kidney biopsy samples would be valuable for the study of the pathophysiology of renal epithelia and would provide an unlimited source of renal epithelial stem or progenitor cells. Various applications of organoid cultures are of particular interest for kidney research.

Study of healthy tissue homeostasis

High-throughput screening of genes and factors that are involved in renal stem or progenitor cell proliferation and differentiation would contribute to our understanding of renal homeostasis. As regeneration often mirrors mechanisms that act during development and homeostasis, the unravelling of these factors would facilitate the development of regeneration-enhancing therapeutic strategies. Renal organoid culture might also help to clarify the role of pathways that are known to be involved in development in kidney homeostasis and disease. For example, Wnt signalling is essential for kidney development, but its role in tissue homeostasis is poorly understood. Some evidence suggests that Wnt signalling promotes fibrosis,[86] whereas other data suggest that knockdown of Wnt signalling leads to cystic disease.[86, 87]

Functional assays

Evaluation of putative renal stem or progenitor cell populations using organoid cultures might help to clarify whether kidney regeneration is reserved to a limited number of stem or progenitor cells that are always present in the kidney, or whether it involves proliferation of dedifferentiated epithelial cells. If the latter is the case, renal organoid cultures could be employed to identify the factors that are necessary for the induction of this cellular plasticity and to investigate whether a specific niche for renal stem cells exists (that is, a kidney equivalent of the intestinal Paneth cell).

Renal organoids could also be applied to assess the function of transporters in differentiated epithelial cells *ex vivo*. Dysfunction of tubular epithelial cell transporters as a result of genetic abnormalities or exposure to drugs or toxins might result in renal disease. Assays to evaluate tubular transporters *ex vivo* that make use of fluorescent substrates are available and organoid swelling might be an additional read-out.[88-90]

Study of disease

Renal organoids could facilitate research regarding the pathophysiological mechanisms of kidney cancer, genetic diseases and infections. Kidney tumouroids would enable the study of genes,

pathways and growth factors that are involved in the development and progression of cancer and could, therefore, be a valuable tool for the development of targeted kidney cancer treatments. Organoids derived from patients with genetic diseases, such as ADPKD could be used to study the role of proteins in disease development and progression, for example ADPKD organoids might display typical cell polarity defects,[91] enabling the study of the development of this disease phenotype. The CFTR–forskolin swelling assay is also of particular interest in ADPKD, as CFTR has a role in progression of this disease.[92] Furthermore, renal organoids might be used to model kidney-specific infections. For example, polyoma BK virus, which specifically affects the collecting duct and results in graft failure in up to 10% of kidney transplant recipients, could be studied in a tubule-segment-specific organoid culture.[93, 94]

Drug screening

Drug-induced nephrotoxicity is the cause of up to 25% of cases of acute kidney injury in the intensive care unit,[95] highlighting the need for better pre-clinical drug toxicity screening. Currently such screening is predominantly performed using 2D cell cultures, which have serious disadvantages in comparison to 3D cultures, and in animal models, which are hampered by interspecies differences and the use of inbred strains that do not reflect the heterogeneous human population.[96] A biobank of renal organoids derived from the general population might function as a heterogeneous source of human renal 3D cultures for nephrotoxicity studies.

Biobanks of organoids, with or without disease phenotypes, could also be used for early-phase efficacy studies. For example, the efficacy of compounds that target transporters (such as diuretics and sodium/glucose cotransporter 2 inhibitors) can be studied in organoids with straightforward read-outs such as swelling.[97] The effect of drugs on cyst growth in ADPKD could be assessed in a similar fashion. At an individual patient level, tumour organoids enable robotized, high-throughput, chemotherapeutic sensitivity screens for personalized medicine. Use of this technology might reduce the costs of drug development and boost research towards therapies for rare genetic diseases.

Therapy

Renal stem or progenitor cells derived from kidney organoids might be used as cellular therapies. Injection of mesenchymal stem cells as a treatment for renal disease has yielded promising results, but the integration of these cells at the sites of regeneration is low and the benefits are mainly attributed to paracrine effects of the infused cells.[98, 99] Although the complex architecture of the kidney might not enable organoids to integrate at sites of regeneration upon transplantation, paracrine effects of kidney-specific stem or progenitor cells derived from organoid culture could be beneficial.

In addition, *ex vivo* expanded organoids might be used as a source of renal cells for the development of bioartificial kidneys, such as the renal assist device (RAD). This device combines conventional haemodialysis with a live tubule cell cartridge,[100] which partly restores the endocrine and immune functions of the kidney. The results of phase I and phase II trials of the device are promising.[100] A major hurdle, however, in upscaling the RAD to commercial use is the lack of access to a reliable source of renal cells.[101] Organoid culture might provide a limitless, possibly autologous,

cell source. Moreover, kidney organoids might function as a source of cells for decellularized renal scaffolds. ECM scaffolds obtained from rat, mouse and human kidneys have been successfully re-cellularized using epithelial and endothelial cell lines, leading to urine production and kidney function.[102] This highly relevant proof-of-principle could benefit from organoid culture: re-cellularized renal scaffolds with genetically repaired, autologous tubular stem or progenitor cells could be developed as a method to generate functional, implantable kidneys.[6]

CONCLUSIONS

Human adult stem or progenitor cell organoid cultures have been developed for a number of organs over the past decade and the scope of their applications in basic and clinical research is expanding rapidly. The development of such an organoid culture system for the kidney is feasible and would be of particular interest because of its complex 3D organization, which is directly related to its function. Moreover, research into diseases that affect this delicate architecture, such as ciliopathies, would benefit from the development of a 3D culture model that recapitulates disease development and morphology. As 3D organization is required to maintain the differentiation of kidney epithelial cells, organoids would facilitate functional assessment of renal epithelia *ex vivo*. Furthermore, the combination of limitless expansion potential and organ-specific epithelial differentiation would enable the development of living biobanks derived from renal biopsies. Such biobanks would enable high-throughput screening of pharmaceutical compounds for therapeutic and toxic effects in a heterogeneous patient population. Conversely, organoids from individual patients could enable *ex vivo* evaluation of therapeutic and/or toxic effects of multiple compounds on these individuals, enabling personalized medicine. A renal organoid culture system might, therefore, bridge the gap between traditional model systems and clinical trials. Finally, the limitless expansion of autologous renal stem or progenitor cells and differentiated epithelial cells might boost the development of bioartificial kidneys and the generation of functional, implantable kidneys for transplantation.

REFERENCES

1. Coresh, J. et al. Prevalence of chronic kidney disease in the United States. *JAMA* **298**, 2038-47 (2007).
2. Forster, R. et al. Human intestinal tissue with adult stem cell properties derived from pluripotent stem cells. *Stem Cell Reports* **2**, 838-52 (2014).
3. Shamir, E.R. & Ewald, A.J. Three-dimensional organotypic culture: experimental models of mammalian biology and disease. *Nat Rev Mol Cell Biol* **15**, 647-64 (2014).
4. Lancaster, M.A. & Knoblich, J.A. Organogenesis in a dish: modeling development and disease using organoid technologies. *Science* **345**, 1247125 (2014).
5. Unbekandt, M. & Davies, J.A. Dissociation of embryonic kidneys followed by reaggregation allows the formation of renal tissues. *Kidney Int* **77**, 407-16 (2010).
6. Bonandrini, B. et al. Recellularization of well-preserved acellular kidney scaffold using embryonic stem cells. *Tissue Eng Part A* **20**, 1486-98 (2014).
7. Xu, J., Patton, D., Jackson, S.K. & Purcell, W.M. In-vitro maintenance and functionality of primary renal tubules and their application in the study of relative renal toxicity of nephrotoxic drugs. *J Pharmacol Toxicol Methods* **68**, 269-74 (2013).
8. Reynolds, B.A. & Weiss, S. Clonal and population analyses demonstrate that an EGF-responsive mammalian embryonic CNS precursor is a stem cell. *Dev Biol* **175**, 1-13 (1996).
9. Seaberg, R.M. et al. Clonal identification of multipotent precursors from adult mouse pancreas that generate neural and pancreatic lineages. *Nat Biotechnol* **22**, 1115-24 (2004).
10. Toma, J.G. et al. Isolation of multipotent adult stem cells from the dermis of mammalian skin. *Nat Cell Biol* **3**, 778-84 (2001).
11. Tropepe, V. et al. Retinal stem cells in the adult mammalian eye. *Science* **287**, 2032-6 (2000).
12. Petersen, O.W., Ronnov-Jessen, L., Howlett, A.R. & Bissell, M.J. Interaction with basement membrane serves to rapidly distinguish growth and differentiation pattern of normal and malignant human breast epithelial cells. *Proc Natl Acad Sci U S A* **89**, 9064-8 (1992).
13. Lawson, D.A., Xin, L., Lukacs, R.U., Cheng, D. & Witte, O.N. Isolation and functional characterization of murine prostate stem cells. *Proc Natl Acad Sci U S A* **104**, 181-6 (2007).
14. Sato, T. et al. Single Lgr5 stem cells build crypt-villus structures in vitro without a mesenchymal niche. *Nature* **459**, 262-5 (2009).
15. McCracken, K.W. et al. Modelling human development and disease in pluripotent stem-cell-derived gastric organoids. *Nature* **516**, 400-404 (2014).
16. Watson, C.L. et al. An in vivo model of human small intestine using pluripotent stem cells. *Nat Med* **20**, 1310-1314 (2014).
17. Barker, N. et al. Identification of stem cells in small intestine and colon by marker gene Lgr5. *Nature* **449**, 1003-7 (2007).
18. Barker, N. et al. Lgr5(+ve) stem cells drive self-renewal in the stomach and build long-lived gastric units in vitro. *Cell Stem Cell* **6**, 25-36 (2010).
19. Sato, T. et al. Long-term expansion of epithelial organoids from human colon, adenoma, adenocarcinoma, and Barrett's epithelium. *Gastroenterology* **141**, 1762-72 (2011).
20. Rock, J.R. et al. Basal cells as stem cells of the mouse trachea and human airway epithelium. *Proc Natl Acad Sci U S A* **106**, 12771-5 (2009).
21. McQualter, J.L., Yuen, K., Williams, B. & Bertoncello, I. Evidence of an epithelial stem/progenitor cell hierarchy in the adult mouse lung. *Proc Natl Acad Sci U S A* **107**, 1414-9 (2010).
22. Karthaus, W.R. et al. Identification of Multipotent Luminal Progenitor Cells in Human Prostate Organoid Cultures. *Cell* (2014).
23. Gao, D. et al. Organoid cultures derived from patients with advanced prostate cancer. *Cell* **159**, 176-87 (2014).
24. Huch, M. et al. In vitro expansion of single Lgr5+ liver stem cells induced by Wnt-driven regeneration. *Nature* **494**, 247-50 (2013).
25. Huch, M. et al. Unlimited in vitro expansion of adult bi-potent pancreas progenitors through the Lgr5/R-spondin axis. *EMBO J* **32**, 2708-21 (2013).
26. Bartfeld, S. et al. In Vitro expansion of human gastric epithelial stem cells and their responses to bacterial infection. *Gastroenterology* **148**, 126-136 e6 (2015).

27. Karthaus, W.R. et al. Identification of multipotent luminal progenitor cells in human prostate organoid cultures. *Cell* **159**, 163-75 (2014).

28. Huch, M. et al. Long-term culture of genome-stable bipotent stem cells from adult human liver. *Cell* **160**, 299-312 (2015).

29. Boj, S.F. et al. Organoid models of human and mouse ductal pancreatic cancer. *Cell* **160**, 324-38 (2015).

30. Schwank, G., Andersson-Rolf, A., Koo, B.K., Sasaki, N. & Clevers, H. Generation of BAC transgenic epithelial organoids. *PLoS One* **8**, e76871 (2013).

31. Middendorp, S. et al. Adult stem cells in the small intestine are intrinsically programmed with their location-specific function. *Stem Cells* **32**, 1083-91 (2014).

32. VanDussen, K.L. et al. Notch signaling modulates proliferation and differentiation of intestinal crypt base columnar stem cells. *Development* **139**, 488-97 (2012).

33. van Es, J.H. et al. Dll1+ secretory progenitor cells revert to stem cells upon crypt damage. *Nat Cell Biol* **14**, 1099-104 (2012).

34. Buczacki, S.J. et al. Intestinal label-retaining cells are secretory precursors expressing Lgr5. *Nature* **495**, 65-9 (2013).

35. Roth, S. et al. Paneth cells in intestinal homeostasis and tissue injury. *PLoS One* **7**, e38965 (2012).

36. Cao, L. et al. Development of intestinal organoids as tissue surrogates: Cell composition and the Epigenetic control of differentiation. *Mol Carcinog* (2013).

37. Koo, B.K. et al. Controlled gene expression in primary Lgr5 organoid cultures. *Nat Methods* **9**, 81-3 (2012).

38. de Lau, W. et al. Lgr5 homologues associate with Wnt receptors and mediate R-spondin signalling. *Nature* **476**, 293-7 (2011).

39. Fafilek, B. et al. Troy, a tumor necrosis factor receptor family member, interacts with lgr5 to inhibit wnt signaling in intestinal stem cells. *Gastroenterology* **144**, 381-91 (2013).

40. Sato, T. et al. Paneth cells constitute the niche for Lgr5 stem cells in intestinal crypts. *Nature* **469**, 415-8 (2011).

41. van Es, J.H. et al. Notch/gamma-secretase inhibition turns proliferative cells in intestinal crypts and adenomas into goblet cells. *Nature* **435**, 959-63 (2005).

42. Schepers, A.G. et al. Lineage tracing reveals Lgr5+ stem cell activity in mouse intestinal adenomas. *Science* **337**, 730-5 (2012).

43. Basak, O. et al. Mapping early fate determination in Lgr5+ crypt stem cells using a novel Ki67-RFP allele. *EMBO J* (2014).

44. Takeda, N. et al. Interconversion between intestinal stem cell populations in distinct niches. *Science* **334**, 1420-4 (2011).

45. Gracz, A.D., Ramalingam, S. & Magness, S.T. Sox9 expression marks a subset of CD24-expressing small intestine epithelial stem cells that form organoids in vitro. *Am J Physiol Gastrointest Liver Physiol* **298**, G590-600 (2010).

46. Mizutani, T. et al. Real-time analysis of P-glycoprotein-mediated drug transport across primary intestinal epithelium three-dimensionally cultured in vitro. *Biochem Biophys Res Commun* **419**, 238-43 (2012).

47. Dekkers, J.F. et al. A functional CFTR assay using primary cystic fibrosis intestinal organoids. *Nat Med* **19**, 939-45 (2013).

48. Bigorgne, A.E. et al. TTC7A mutations disrupt intestinal epithelial apicobasal polarity. *J Clin Invest* **124**, 328-37 (2014).

49. Wiegerinck, C.L. et al. Loss of syntaxin 3 causes variant microvillus inclusion disease. *Gastroenterology* **147**, 65-68 e10 (2014).

50. Bartfeld, S. et al. In Vitro Expansion of Human Gastric Epithelial Stem Cells and Their Responses to Bacterial Infection. *Gastroenterology* (2014).

51. Finkbeiner, S.R. et al. Stem cell-derived human intestinal organoids as an infection model for rotaviruses. *MBio* **3**, e00159-12 (2012).

52. Mokry, M. et al. Many inflammatory bowel disease risk loci include regions that regulate gene expression in immune cells and the intestinal epithelium. *Gastroenterology* **146**, 1040-7 (2014).

53. Wang, K. et al. Whole-genome sequencing and comprehensive molecular profiling identify new driver mutations in gastric cancer. *Nat Genet* **46**, 573-82 (2014).

54. van de Wetering, M. et al. Prospective Derivation of a Living Organoid Biobank of Colorectal Cancer Patients. *Cell* **161**, 933-945.

55. Balharry, D., Sexton, K. & BeruBe, K.A. An in vitro approach to assess the toxicity of inhaled tobacco smoke components: nicotine, cadmium, formaldehyde and urethane. *Toxicology* **244**, 66-76 (2008).

56. Emmink, B.L. et al. Differentiated human colorectal cancer cells protect tumor-initiating cells from irinotecan. *Gastroenterology* **141**, 269-78 (2011).

57. Yui, S. et al. Functional engraftment of colon epithelium expanded in vitro from a single adult Lgr5(+) stem cell. *Nat Med* **18**, 618-23 (2012).

58. Schwank, G. et al. Functional repair of CFTR by CRISPR/Cas9 in intestinal stem cell organoids of cystic fibrosis patients. *Cell Stem Cell* **13**, 653-8 (2013).

59. O'Brien, L.L. & McMahon, A.P. Induction and patterning of the metanephric nephron. *Seminars in Cell & Developmental Biology* **36**, 31-38 (2014).

60. Kusaba, T. & Humphreys, B.D. Controversies on the origin of proliferating epithelial cells after kidney injury. *Pediatr Nephrol* **29**, 673-9 (2014).

61. Tornovsky-Babeay, S. et al. Type 2 diabetes and congenital hyperinsulinism cause DNA double-strand breaks and p53 activity in beta cells. *Cell Metab* **19**, 109-21 (2014).

62. Yanger, K. & Stanger, B.Z. Facultative stem cells in liver and pancreas: fact and fancy. *Dev Dyn* **240**, 521-9 (2011).

63. Huch, M., Boj, S.F. & Clevers, H. Lgr5(+) liver stem cells, hepatic organoids and regenerative medicine. *Regen Med* **8**, 385-7 (2013).

64. Yanger, K. et al. Adult Hepatocytes Are Generated by Self-Duplication Rather than Stem Cell Differentiation. *Cell Stem Cell* **15**, 340-349.

65. Kusaba, T., Lalli, M., Kramann, R., Kobayashi, A. & Humphreys, B.D. Differentiated kidney epithelial cells repair injured proximal tubule. *Proc Natl Acad Sci U S A* **111**, 1527-32 (2014).

66. Rock, J.R. & Hogan, B.L. Epithelial progenitor cells in lung development, maintenance, repair, and disease. *Annu Rev Cell Dev Biol* **27**, 493-512 (2011).

67. Rinkevich, Y. et al. In vivo clonal analysis reveals lineage-restricted progenitor characteristics in mammalian kidney development, maintenance, and regeneration. *Cell Rep* **7**, 1270-83 (2014).

68. Grobstein, C. Inductive Epithelio-mesenchymal Interaction in Cultured Organ Rudiments of the Mouse. *Science* **118**, 52-55 (1953).

69. Giuliani, S. et al. Ex vivo whole embryonic kidney culture: a novel method for research in development, regeneration and transplantation. *J Urol* **179**, 365-70 (2008).

70. Karavanova, I.D., Dove, L.F., Resau, J.H. & Perantoni, A.O. Conditioned medium from a rat ureteric bud cell line in combination with bFGF induces complete differentiation of isolated metanephric mesenchyme. *Development* **122**, 4159-4167 (1996).

71. Xia, Y. et al. Directed differentiation of human pluripotent cells to ureteric bud kidney progenitor-like cells. *Nat Cell Biol* **15**, 1507-15 (2013).

72. Xia, Y. et al. The generation of kidney organoids by differentiation of human pluripotent cells to ureteric bud progenitor-like cells. *Nat Protoc* **9**, 2693-704 (2014).

73. Takasato, M. et al. Directing human embryonic stem cell differentiation towards a renal lineage generates a self-organizing kidney. *Nat Cell Biol* **16**, 118-26 (2014).

74. Lam, A.Q. et al. Rapid and efficient differentiation of human pluripotent stem cells into intermediate mesoderm that forms tubules expressing kidney proximal tubular markers. *J Am Soc Nephrol* **25**, 1211-25 (2014).

75. Astashkina, A.I., Mann, B.K., Prestwich, G.D. & Grainger, D.W. Comparing predictive drug nephrotoxicity biomarkers in kidney 3-D primary organoid culture and immortalized cell lines. *Biomaterials* **33**, 4712-21 (2012).

76. Subramanian, B. et al. Tissue-engineered three-dimensional in vitro models for normal and diseased kidney. *Tissue Eng Part A* **16**, 2821-31 (2010).

77. Giles, R.H., Ajzenberg, H. & Jackson, P.K. 3D spheroid model of mIMCD3 cells for studying ciliopathies and renal epithelial disorders. *Nat Protoc* **9**, 2725-31 (2014).

78. Angelotti, M.L. et al. Characterization of renal progenitors committed toward tubular lineage and their regenerative potential in renal tubular injury. *Stem Cells* **30**, 1714-25 (2012).

79. Lindgren, D. et al. Isolation and characterization of progenitor-like cells from human renal proximal tubules. *Am J Pathol* **178**, 828-37 (2011).

80. Buzhor, E. et al. Kidney spheroids recapitulate tubular organoids leading to enhanced tubulogenic potency of human kidney-derived cells. *Tissue Eng Part A* **17**, 2305-19 (2011).

81. Buzhor, E. et al. Reactivation of NCAM1 defines a subpopulation of human adult kidney epithelial cells with clonogenic and stem/progenitor properties. *Am J Pathol* **183**, 1621-33 (2013).

82. Harari-Steinberg, O. et al. Identification of human nephron progenitors capable of generation of kidney structures and functional repair of chronic renal disease. *EMBO Mol Med* **5**, 1556-68 (2013).

83. Bombelli, S. et al. PKH(high) cells within clonal human nephrospheres provide a purified adult renal stem cell population. *Stem Cell Res* **11**, 1163-77 (2013).

84. Barker, N. et al. Lgr5(+ve) stem/progenitor cells contribute to nephron formation during kidney development. *Cell Rep* **2**, 540-52 (2012).

85. Kitamura, S., Sakurai, H. & Makino, H. Single Adult Kidney Stem/Progenitor Cells Reconstitute 3-Dimensional Nephron Structures in Vitro. *STEM CELLS*, n/a-n/a (2014).

86. Lancaster, M.A. et al. Impaired Wnt-[beta]-catenin signaling disrupts adult renal homeostasis and leads to cystic kidney ciliopathy. *Nat Med* **15**, 1046-1054 (2009).

87. He, W. et al. Wnt/ -Catenin Signaling Promotes Renal Interstitial Fibrosis. *Journal of the American Society of Nephrology* **20**, 765-776 (2009).

88. Schophuizen, C.S. et al. Cationic uremic toxins affect human renal proximal tubule cell functioning through interaction with the organic cation transporter. *Pflügers Archiv - European Journal of Physiology* **465**, 1701-1714 (2013).

89. Schophuizen, C.M. et al. Cationic uremic toxins affect human renal proximal tubule cell functioning through interaction with the organic cation transporter. *Pflugers Arch* **465**, 1701-14 (2013).

90. Sullivan, L.P., Grantham, J.A., Rome, L., Wallace, D. & Grantham, J.J. Fluorescein transport in isolated proximal tubules in vitro: epifluorometric analysis. *Am J Physiol* **258**, F46-51 (1990).

91. Wilson, P.D. Apico-basal polarity in polycystic kidney disease epithelia. *Biochimica et Biophysica Acta (BBA) - Molecular Basis of Disease* **1812**, 1239-1248 (2011).

92. Hanaoka, K. & Guggino, W.B. cAMP regulates cell proliferation and cyst formation in autosomal polycystic kidney disease cells. *J Am Soc Nephrol* **11**, 1179-87 (2000).

93. Hirsch, H.H. et al. Polyomavirus-associated nephropathy in renal transplantation: interdisciplinary analyses and recommendations. *Transplantation* **79**, 1277-86 (2005).

94. Yamanaka, K. et al. Immunohistochemical features of BK virus nephropathy in renal transplant recipients. *Clin Transplant* **26 Suppl 24**, 20-4 (2012).

95. Pannu, N. & Nadim, M.K. An overview of drug-induced acute kidney injury. *Crit Care Med* **36**, S216-23 (2008).

96. Seok, J. et al. Genomic responses in mouse models poorly mimic human inflammatory diseases. *Proc Natl Acad Sci U S A* **110**, 3507-12 (2013).

97. Nair, S. & Wilding, J.P. Sodium glucose cotransporter 2 inhibitors as a new treatment for diabetes mellitus. *J Clin Endocrinol Metab* **95**, 34-42 (2010).

98. Hopkins, C., Li, J., Rae, F. & Little, M.H. Stem cell options for kidney disease. *J Pathol* **217**, 265-81 (2009).

99. Pleniceanu, O., Harari-Steinberg, O. & Dekel, B. Concise review: Kidney stem/progenitor cells: differentiate, sort out, or reprogram? *Stem Cells* **28**, 1649-60 (2010).

100. Humes, H.D., Buffington, D., Westover, A.J., Roy, S. & Fissell, W.H. The bioartificial kidney: current status and future promise. *Pediatr Nephrol* **29**, 343-51 (2014).

101. Westover, A.J. et al. A bio-artificial renal epithelial cell system conveys survival advantage in a porcine model of septic shock. *Journal of Tissue Engineering and Regenerative Medicine*, n/a-n/a (2014).

102. Song, J.J. et al. Regeneration and Experimental Orthotopic Transplantation of a Bioengineered Kidney. *Nature medicine* **19**, 646-651 (2013).

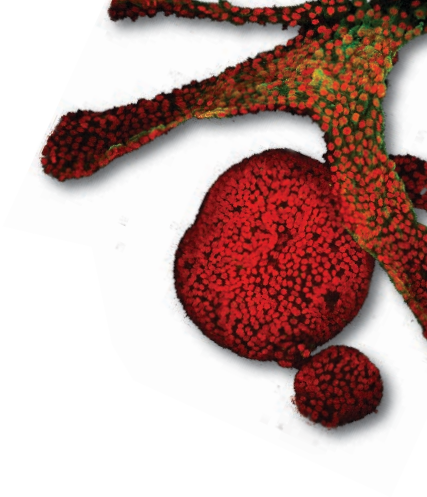

CHAPTER 2

PLURIPOTENT STEM CELL-DERIVED KIDNEY ORGANOIDS: AN *IN VIVO*-LIKE *IN VITRO* TECHNOLOGY

ABSTRACT

Organoids are self-organizing multicellular structures that contain multiple cell types, represent organ structure and function, and can be used to model organ development, maintenance and repair *ex vivo*. Organoid cultures, derived from embryonic stem cells, induced pluripotent stem cells or adult stem cells, and cultured in extracellular matrix (ECM), have been developed for multiple organs. For the kidney, pluripotent stem cell-derived organoid technology has rapidly developed in the last three years. Here, we review available PSC differentiation protocols, focusing on the pluripotent stem cells to initiate the organoid culture, as well as on growth factors and ECM used to regulate differentiation and expansion. In addition, we will discuss the read-out strategies to evaluate organoid phenotype and function. Finally, we will indicate how the choice of both culture parameters as well as read-out strategy should be tailored to specific applications of the organoid culture.

Frans Schutgens[1,2], Marianne C. Verhaar[2], Maarten B. Rookmaaker[2]

[1] Hubrecht Institute–Royal Netherlands Academy of Arts and Sciences, Utrecht, the Netherlands
[2] Department of Nephrology and Hypertension, University Medical Centre Utrecht, the Netherlands

European Journal of Pharmacology, Volume 790, 12-20 (2016)

INTRODUCTION

Organoids are self-organizing multicellular structures that represent tissue structure and function *in vitro*, and allow assessment and modeling of development, turnover and repair *ex vivo*. Organoids are organ-like 3D structures that are cultured in a three dimensional matrix and elegantly link *in vitro* and *in vivo* models. Organoid culture technology has been in the limelight for approximately a decade. The first adult-derived epithelial intestinal organoids were described for mouse intestine in 2009,[1] quickly followed by the development of human intestinal organoids [2] and organoids derived from other organs.[3-6] Around the same time, directing differentiation of pluripotent stem cells led to the establishment of pluripotent stem cell derived organoid cultures that contain stroma in addition to the epithelial compartment for many organs, including intestine, stomach, liver and brain.[7-10]

The resemblance to the *in vivo* situation makes organoid cultures highly relevant for both fundamental science as well as for clinical application. Organoid cultures have been applied to prove stemness,[11] for modeling of tumorigenesis[12] and for the investigation of infectious diseases.[6] Clinically, organoids may be applied for drug screening, both for personalized medicine, testing the efficacy of multiple drugs on one patient as well as for high throughput screening of one compound on organoids from multiple patients.[13] In proof of principle studies organoids have been used as an infinite source of cells for cell therapy in preclinical models of both liver[14] and colon disease.[15]

The kidney is a complex organ consisting of more than 20 different cell types arranged in a configuration that is crucial for proper organ function. The distinct cell types are characterized by differential gene expression per tubular segment, segment specific morphology (e.g. the presence of brush border in proximal tubule cells) and function (e.g. transport function and hormone sensitivity). The architecture of the nephron and its vasculature enables the reabsorption of 98% of the approximately 150 liters of plasma filtered in the glomerulus every day. Recently, renal organoids have been developed,[16-19] and although they cannot fully recapitulate the complex organization of the kidney, the organoids enable *ex vivo* modeling of nephrogenesis, renal cell homeostasis and function. Here, we will review distinct aspects of the available kidney organoid culture systems and highlight the importance of these aspects for potential applications. We will focus on kidney organoids derived from pluripotent stem cells and we will discuss different types of pluripotent stem cells, and how type, timing and sequence of growth factor administration and matrix influence cell expansion, differentiation and function. In addition, we will review the techniques used to evaluate organoid phenotype, morphology and function. We will discuss how specific application of the organoid culture (research, diagnostics, or therapy) directs choices of cell source, matrix and media (growth) factors as well as read-out strategies.

PLURIPOTENT STEM CELLS AS START CELLS

Pluripotent stem cells (PSCs) have by definition the capacity to form all cell types of the body. Directing differentiation towards kidney cells requires careful titration of expansion and differentiation of PSCs by modifying external cues, such as growth factors and matrix components (*see below*). PSCs derived from both embryonic tissue as well as PSCs derived from differentiated adult cells after forced dedifferentiation (induced PSCs (iPSCs)) have been used in renal organoid culture and will be described below.

Embryonic stem cells

Embryonic Stem Cells (ESCs) are PSCs derived from the inner cell mass of the blastocyst, the part that structurally gives rise to the embryo. Mouse ESCs were isolated for the first time in 1981[20] and nowadays, many mouse ESC lines are commercially available. The isolation and culture of human ESCs followed in 1998.[21] Subcutaneous transplantation of ESCs leads to the formation of teratomas that contain differentiated tissues from all germ layers (*endoderm, ectoderm and mesoderm*).[22] When ESCs are injected into blastocysts and transplanted into mice, they contribute to tissues from all germ layers.[23] *In vitro*, ESC lines can be differentiated into cell types of the three germ layers in 2D cell culture. 3D ESC-derived organoid cultures have been established by suspending embryonic cells – with or without pre-differentiation steps in 2D - in an ECM, often Matrigel, for organs from the three germ layers, for example intestine[10] and stomach[7] (*endoderm*); retina[24] and brain[8] (*ectoderm*); and heart[25] and kidney (*mesoderm*).

The differentiation of ESCs into kidney organoids has been a step by step process, where differentiation into progressively more differentiated structures was achieved. First, protocols for the differentiation into kidney precursor structures, such as the nephrogenic intermediate mesoderm[26] or ureteric bud,[19] were developed. The latter was created with mouse-human chimeric cultures. This was followed by protocols without chimerism that cultured specific kidney compartments that are present in adult kidney, such as the proximal tubule.[27] Subsequently, it became possible to culture organoids that included multiple kidney compartments, although vasculature, nerve innervation and a convergent urinary collecting duct system remain absent.[16-18,28,29]

An advantage of the use of ESCs compared to iPSCs is that no reprogramming process which poses risks of tumor formation (*see below*) is required. Drawbacks are the obvious ethical issues associated with the use of ESCs and that ESC-derived organoid cultures cannot be established from adult subjects.

Induced pluripotent stem cells

The discovery of the reprogramming factors by Yamanaka enabled dedifferentiation of differentiated, somatic adult cells into PSCs.[30] This invention revolutionized the field of stem cell biology: by (viral) introduction of Oct4, Sox2, cMyc and Klf4 it became possible for the first time to obtain a PSC population, derived from adult cells. This technique was first developed for mouse fibroblasts[30] and later also human fibroblasts,[31] and other somatic cell types have been used for reprogramming.[32,33]

Analogous to ESC differentiation, protocols have been developed for *in vivo* and *ex vivo* differentiation of iPSC. Similar to ESCs, subcutaneous transplantation of iPSCs into mice leads to teratoma formation that contain differentiated tissues from the three germ layers.[22] After micro-injection of mouse GFP-iPSCs into blastocysts, followed by *in vivo* development, GFP+ cells were found to contribute to tissues of all germ layers.[30] Differentiation protocols have been developed both for 2D and 3D cell culture, for other organs as well as for the kidney. The kidney iPSC differentiation protocols are roughly equal to the ESC protocols that are discussed above.[29] Some issues specific to iPSCs should be taken into account. Induction of pluripotency might not only require the introduction of the transcription factors mentioned above, but also epigenetic reprogramming.[34] Differentiated cell types used for the reprogramming into iPSC differentiate

more easily towards the organ of origin than towards other organ due to DNA methylation ("the epigenetic memory"), which ultimately affects differentiation.[35] This residual DNA methylation could be overcome by differentiation and serial reprogramming; addition of methylation-modifying drugs; or use of tissue that is embryonically similar to the target tissue. iPSC lines derived from adult human kidney cells are available, both directly isolated from kidney tissue,[36] as well as isolated from urine.[37]

The use of iPSCs for the generation of renal organoids has advantages when compared to ESCs. iPSCs can be easily obtained, even from cells shed with voiding, without the ethical concerns of ESCs. The accessibility of iPSC facilitates the generation of organoids from patients as well as healthy volunteers. However, the use of iPSC for the generation of renal organoid also has disadvantages. First, iPSCs are genetically instable as most reprogramming has been done by introducing the reprogramming factors by (lenti)viral infections that integrate semi-randomly into the genome, which poses a risk for later tumor formation. Of note, recent studies show that reprogramming with episomal plasmids that do not integrate into the genome is possible.[38,39] Second, epigenetic characteristics may not be completely reset after reprogramming, affecting cell behavior,[34] and reducing the similarity of iPSC-derived renal organoids to the *in vivo* kidney, if the iPSC line has been derived from cells from organs other than the kidney. Third, although iPSC technology in theory allows the development of autologous organoids and therefore transplantation, there are serious concerns that not adequately differentiated iPSC-derived renal organoids can give rise to teratomas upon transplantation.[40] Finally, iPSCs give rise to organoids with a lower efficiency than ESCs.[28]

GROWTH FACTORS

Mimicking *in vivo* kidney development by careful composition and timing of the growth factor mix will allow the *in vitro* differentiation of PSCs into renal lineages. Comparing protocols that are used to induce differentiation of PSCs into renal lineages (Figure 1), allows identification of factors that are indispensable, and factors that appear to be replaceable or redundant. We will first provide a context of kidney development focusing on the roles for growth factors and in this context we will discuss growth factors used for organoid development and differentiation from PSCs. Given the high similarity in growth factors used in the generation of renal organoid from ESCs and iPSCs, we discuss ESCs and iPSCs together.

Kidney development

Kidney development *in vivo* is a multi-step process requiring sequential growth factor signaling. The kidney is derived from the middle germ layer (*mesoderm*) that develops from ingression of specific populations of epithelial cells (*the primitive streak*) during the blastula phase. The primitive streak is a region of high Wnt signaling and it has been demonstrated in chick embryos that Wnt3a/Wnt5a gradients determine migratory behaviour in the primitive streak, with Wnt5a stimulating cell migration from the posterior streak and Wnt3a inhibiting migration from the anterior streak. [41]

Within the mesoderm a specific region, the intermediate mesoderm gives rise to the ureteric bud and metanephric mesenchyme that reciprocally interact to develop the kidney. Cells from

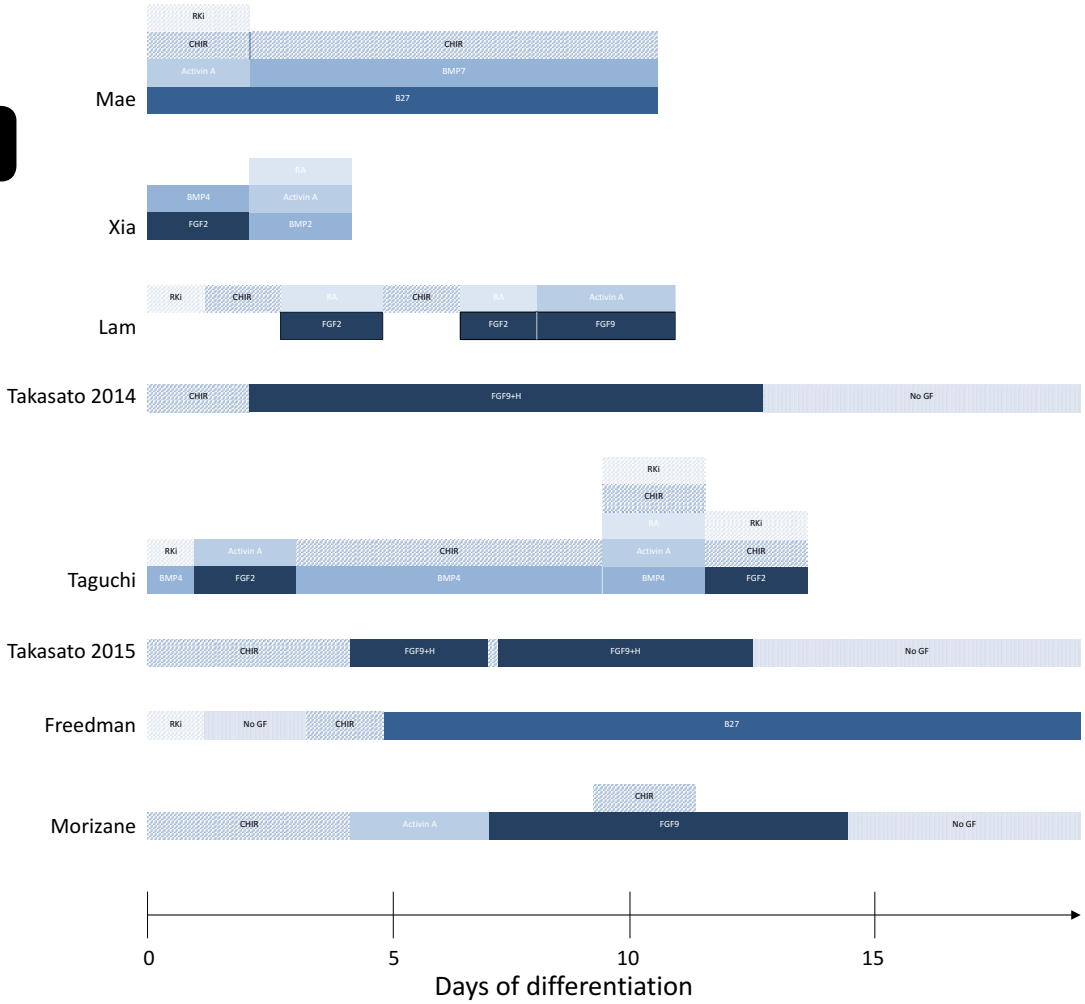

Figure 1. Overview of PSC differentiation protocols towards kidney lineages. The timeline below indicates days of differentiation. The same (classes of) added factors are depicted in the same color. In 3 papers,[18,26,27] multiple protocols are described of which only one is depicted: In [18]: two protocols are described and the one with the best differentiation is displayed. In [26]: only the single cell, serum free method is depicted. In [27]: instead of the last step, withdrawal of GFs leads to differentiation of structures towards proximal tubule like cells. Including the Activin A/FGF9 step leads to a nephron progenitor population as observed in the metanephric mesenchyme. Of note: [16,19,26] describe differentiation protocols only towards embryonic kidney structures. Rki: Rho-Kinase Inhibitor. CHIR: CHIR99201. BMP: Bone Morphogenetic Protein. FGF: Fibroblast Growth Factor. RA: Retinoic Acid. H: Heparin. GF: Growth Factor.

the primitive streak form the intermediate mesoderm, and further patterning of the mesoderm along the rostro-caudal axis depends on Fibroblast Growth Factor (FGF) / Retinoic Acid (RA) gradients, whereas the medio-lateral axis is dependent on Bone Morphogenetic Protein (BMP) gradients.[42-44] Indeed, FGF receptor signaling is crucial for *in vivo* kidney development: conditional FGFR1 and FGFR2 KO mice suffer from renal aplasia. Interestingly, knocking out specific FGFs, e.g.

FGF2 and FGF9, show no defects in intermediate mesoderm induction, which suggests *in vivo* redundancy in FGF signaling.[42,45,46] FGF signaling is inhibited by RA signaling: transcription of FGF8 is reduced by RA (produced on the rostral side of the embryo) and the other way around[47] and this creates a gradient forming distinct domains along the rostro-caudal axis.[42,48] High levels of BMP signaling are necessary and sufficient to induce lateral mesoderm gene expression and suppress intermediate and axial mesoderm, whereas low levels of BMP lead to intermediate mesoderm, and inhibition of BMP signaling by Noggin leads to paraxial mesoderm.[43,44]

The anterior side of the intermediate mesoderm develops into the ureteric bud / ureteric epithelium whereas the posterior develops into the metanephric mesenchyme.[17] This specification appears to result from differences in RA exposure, whereby high RA leads to a ureteric epithelium fate and inhibition of RA results in metanephric mesenchyme. Survival and reciprocal induction of the ureteric bud and the metanephric mesenchyme depend, amongst others, on Wnt-, tyrosine kinase-, BMP and Activin signaling. Canonical Wnt signaling, in particular mesenchyme-derived Wnt4[49] and ureteric bud derived Wnt9b,[50] are required to induce the metanephric mesenchyme to undergo a mesenchymal to epithelial transition and formation of renal vesicles: indeed, Wnt4 and Wnt9b knockout mice do not form nephrons. In embryos from FGFR1 or FGFR2 knock-outs, there is no metanephric mesenchyme present at E10.5, and the ureteric bud that is present, does neither elongate nor branch.[51] BMP4 is important for regulation of branching morphogenesis, by inhibiting ectopic branching at ureter stalk and stimulating growth of the branching ureteric bud into the metanephric mesenchyme.[52] Homozygous BMP7 KO mice[53] have renal dysplasia at birth and extensive apoptosis of the metanephric mesenchyme is observed: accordingly, BMP7 is absolutely required for nephron progenitor survival and proliferation and it does so in a mechanism that is dependent on Mitogen-Activated Protein Kinase (MAPK) signaling.[54] Activin A, derived from the ureteric bud, leads to reduced branching of the ureteric bud, whereas in metanephric mesenchyme cells it leads to growth and expression of epithelial differentiation markers in the metanephric mesenchyme, indicating that Activin A acts as differentiation compound in the metanephric mesenchyme.[55]

Once metanephric mesenchyme and ureteric bud have been formed and these structures can adequately and reciprocally interact, the system is robust and kidneys develop with minimal external cues as was demonstrated by *ex vivo* differentiation of these so called renal primordia.[56,57]

Wnt agonist CHIR99201

In all *in vitro* differentiation protocols, CHIR99201 is applied transiently as a Wnt agonist to induce primitive streak formation and/or at a later stage in the differentiation protocol to increase the number of nephron-like structures per organoid.[17] CHIR99201 is an aminopyrimidine that relatively specifically inhibits glycogen kinase 3β (GSK3β). By inhibiting GSK3β, β-catenin is not degraded and canonical Wnt signaling is activated.[58,59] Stimulating canonical Wnt signaling, with Wnt conditioned media or CHIR99201, has been shown to be essential for establishing and maintaining organoid cultures derived from many organs, both adult-derived and PSC-derived. [2,4,6,7]

CHIR99201 has also proved essential for differentiation towards kidney lineages: CHIR99201 addition to the media led to a more efficient differentiation of PSCs towards primitive streak, lateral plate mesoderm, followed by differentiation towards the intermediate mesoderm. Interestingly,

in kidney organoid cultures addition of CHIR was more efficient than Wnt3A protein alone.[27] This suggests that CHIR99201 exerts its effects not only through Wnt signaling and that off-target kinase inhibitory effects also play a role through mechanisms that remain to be elucidated.

CHIR99201 treatment also exemplifies that duration and timing of growth factor / inhibitor composition of the culture media is important for fate determination. Three days of CHIR99201 treatment at the primitive streak stage, leads later to anterior intermediate mesoderm formation (ureteric epithelium progenitors), whereas five days of CHIR99201 leads to posterior intermediate mesoderm formation (metanephric mesenchyme).[17]

Fibroblast Growth Factor signaling

Most protocols use transient FGF2 and/or FGF9 with or without heparin to induce intermediate mesoderm from primitive streak.[17,18,27] FGFs are encoded by 22 genes that bind to 4 FGF-tyrosine kinase receptors, of which different splice variants are known. FGFs have receptor specific affinities, with some having a broad signaling activity, whereas others are relatively specific: FGF1 is able to activate all FGFRs, whereas FGF7 activates only FGFR2b.[60,61] FGF2 (also known as basic FGF (bFGF) in [16,62]) and FGF9 have a relatively broad receptor affinity and both bind FGFR2 and -4 with comparable affinity.[61] In addition, FGFR activation requires heparin-sulfates, which are abundantly present at the cell surface, as a co-factor for receptor activation: heparin-like molecules bind both FGFs and FGFRs, facilitating interaction, allowing receptor dimerization[63] and thereby activation.[64,65] In addition, heparin-like molecules protect basal FGF from denaturation and enzymatic degradation.[66,67]

For the differentiation towards kidney organoids, stimulation of FGF signaling has proved useful for the induction of intermediate mesoderm from primitive streak. Indeed, most protocols include transient FGF2 or FGF9 stimulation in growth media at some point. Heparin-like compounds may be used to strengthen the FGF signal.[17,18]

Bone Morphogenetic Protein signaling

BMPs 2, 4 or 7 are transiently used in three protocols, predominantly to induce a (posterior) intermediate mesodermal cell fate.[19] The BMPs comprise twenty growth factors that are part of the TGFβ superfamily and are named after their first reported effects: stimulation of bone and cartilage formation. BMPs exert their effects by binding to one of two types of BMP receptors (BMPRs), each type having multiple members, and signaling through SMAD or MAPK pathways. Interestingly, BMP proteins can also signal through Activin receptors,[68] which may explain why in some protocols BMPs and Activin A are used simultaneously: potentially to prevent off-target effects.

BMP4 and -7 are important to induce a posterior intermediate mesodermal fate. The only protocol that uses BMP2 also uses BMP4 in an earlier step in the protocol, suggesting that BMP2 might be redundant. Interestingly, BMP inhibition is also required during the first four days of differentiation in one protocol.[29] Addition of a BMP4 antagonist (Noggin) is required for the differentiation of iPSCs, but not for ESCs in the same protocol. The authors suggest that intermediate mesoderm induction is highly sensitive to BMP4 signaling and that individual cell lines vary in endogenous BMP production. This suggests that the amount of BMP4 in cultures should be titrated in every individual cell line to optimize intermediate mesoderm induction.

Other factors

Factors used in some protocols, but not in others, appear dispensable, or can be replaced by other factors, but may increase expansion or differentiation efficiency. Here, factors that are used in at least two protocols will be briefly discussed.

Y27632 is an inhibitor of Rho-associated coiled-coil forming protein serine/threonine kinase (ROCK) family of protein kinases and is used transiently in some protocols[16,19,27,28] to prevent dissociated-induced apoptosis (anoikis) in single cell suspensions. Rho-kinase inhibition prevents anoikis[69] by a mechanism that is not well understood.[70] As single cells tend to undergo anoikis, it can be used to increase plating and culture efficiency.

Activin A, a molecule relevant for branching morphogenesis, is used in organoid culture to induce metanephric mesenchyme from intermediate mesoderm.[27] Activins are dimeric proteins, consisting of two β-subunits that occur as homodimers (β_A-β_A, named Activin A, or Activin B β_B-β_B) or heterodimers (β_A-β_A, or Activin AB). Activins are members of the TGFβ superfamily and act as cytokines by binding membrane-bound activing receptors that signal in a SMAD-dependent fashion. The Activin receptors share homology with receptors for other TGFβ-superfamily ligands, such as BMPs (*see above*).

Retinoic Acid (RA), a metabolite of vitamin A, is used to induce intermediate mesoderm,[16,27] or to stimulate outgrowth of ureteric epithelium.[17] RA acts by binding to one of 8 RA-receptors (RARs), which are transcription factors and induce of repress target gene expression by binding to retinoic acid response elements (RAREs) in the regulatory regions of target genes. The effect of RA in organoid differentiation, which is the stimulation of ureteric epithelium outgrowth, is confirmed in an experiment where addition of RA-receptor antagonist (AGN193109) to organoid culture induced a metanephric mesenchyme fate and inhibited formation of ureteric epithelium.[17]

B27 is used in two protocols reviewed[26,28] and in one[28] it is an indispensable reagent to obtain differentiated kidney organoids. B27 is a patented commercially available media supplement and although all its components (vitamins, proteins and other components), can be found on manufacturer's website, the exact quantity of each component is not listed. B27 was originally developed for the culture of neural stem cells. At present, it is used for the culture of adult-stem cell derived organoids from other organs[2] as well as in some protocols for PSC differentiation towards kidney organoids. No comments were made regarding its specific effects. Interestingly, RA is one of the components, which might be one of the reasons why B27 is of use. Indeed, in the protocols where B27 is used, RA is not added to the culture media.

MATRIX

Although classic 2D cell culture of homogenous cell populations has been of tremendous importance for the field of biology, 3D cultures better resemble the *in vivo* situation. For the kidney, 3D cultured proximal tubule in hydrogel cells better reflect the *in vivo* observed drug toxicity response (e.g. expression of Kidney Injury Molecule-1 (KIM1) and pro-inflammatory cytokines) than 2D cultured, immortalized proximal tubule cell lines.[71] In addition, the presence or absence of the third dimension affects cell fate: with the same differentiation protocol, initial 2D culture of undifferentiated PSCs leads to differentiation into cardiac lineages, whereas initial 3D culture steers

differentiation towards the kidney lineages.[28] Indeed when adult-derived intestinal organoids were successfully cultured for the first time, the ECM composition was collagen and laminin-rich, similar to the stem cell niche in vivo.[1] The choice of 3D matrix for the culture of renal organoids is crucial, as ECM composition affects differentiation[72] and the type will also affect the suitability for applications of the organoids. Use of an animal-derived immunogenic gel will make the organoids unsuitable for therapeutic application. Currently, several types of ECMs for 3D culture have been developed and these include animal derived ECM, either general or tissue-specific and synthetic matrices (reviewed in [73]).

Animal tissue-derived ECM matrix is to our knowledge the only matrix published to allow expansion, differentiation and passaging of renal organoids. Matrigel, the prototypical example, is a mixture derived from a mouse stromal tumor consisting of collagen and laminins. Matrigel is by far the most predominant source for ECM[1,3,6-10,74] for organoid cultures, including PSC-derived kidney organoids.

There are disadvantages associated with the use of Matrigel. As it is an animal product, batch-to-batch variability occurs and growth factors can be present, which makes it impossible to completely control the ECM. Of note, a growth factor-reduced version is available, which decreases the latter disadvantage. Matrigel is not kidney-specific, nor is Matrigel suitable for transplantation studies. Improved (synthetic) matrices might not only improve renal organoid culture but also allow better evaluation of specific matrix components on renal organoid expansion and differentiation, and even enable the generation of clinical grade renal organoids for cell therapy.

Tissue-specific matrices have been isolated, by decellularization and digestion of several (porcine) organs,[73,75] including the kidney.[72,76] As ECM composition *in vivo* is organ- and tissue-specific and provides an optimal micro-environment for cells of that particular organ, 3D cultures may benefit from a tissue-specific matrix. Accordingly, kidney-specific ECM increases the proliferation and metabolic activity of kidney stem cells, when compared to kidney cells cultured in bladder- or heart-derived ECM. Interestingly, even within an organ differences are observed: the proliferation of stem cells is lower in matrix derived from the renal papilla, where stem cells with a low cycling activity reside, when compared to cortex and medulla. Thus far, kidney organoid cultures have not yet been described in tissue-specific gels.

For synthetic matrices (reviewed in [73]), hydrogels are the prime candidates for application in organoid culture. Hydrogels consist of crosslinked polymers with a high water content, that allow transport of oxygen, nutrients and waste; modification of mechanical properties; and attachment of adhesion / signaling ligands to the polymer.[73,77] Hydrogels from natural materials include collagen-, fibrin- and polyglycan-based gels. When compared to non-natural hydrogels, the advantage is that these gels are bioactive and support the growth of many cell types, including chondrocytes[78] and valvular interstitial cells[73,79,80] thereby increasing the chances of successful organoid culture. For non-natural hydrogels, Poly(Ethylene Glycol) (PEG) hydrogels have shown encouraging results: ESC-derived cells, encapsulated in a PEG matrix can be cultured for 17 days and differentiate more efficiently to chondrocytes than the same cells cultured in 2D mono-layer culture.[81] Synthetic matrices, potentially containing organ-specific ECM cues attached to a polymer backbone to direct adhesion and differentiation of the embedded cells, would allow

clinical organoid transplantation. However, thus far it has proven difficult to use these gels for *in vitro* culture, and no synthetic matrices have been reported to allow the expansive or long term growth of (kidney) organoids.

EVALUATION OF ORGANOID CHARACTERISTICS

Evaluation of genetic, immunohistochemical, morphological and functional characteristics of renal organoids is not only crucial to identify level and direction of differentiation of the organoid tissue but also for their potential experimental, diagnostic and therapeutic application (Figure 2). The expression of genes and proteins linked to certain stages of renal development has been evaluated at different time points during expansion and differentiation of PSCs into renal organoids.

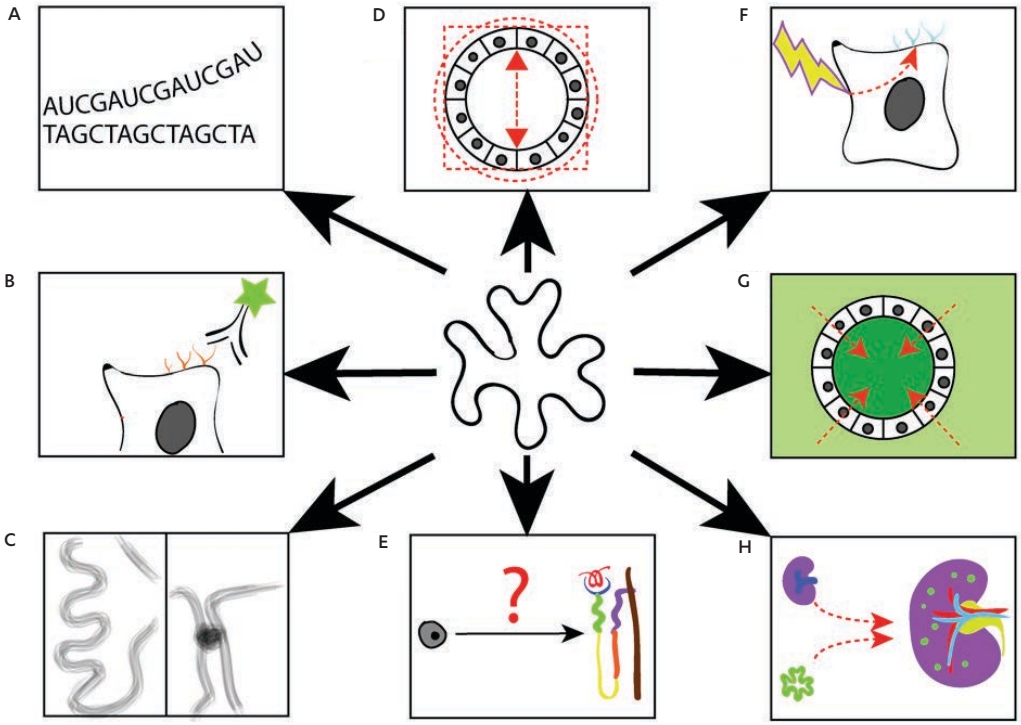

Figure 2. Evaluation of organoid characteristics. Organoids have been evaluated at RNA (A) and protein level (B, immunohistochemistry and Western blotting). Ultrastructural analysis has been done using electron microscopy (C). Morphology has been studied in healthy as well as mutated organoids (D). The use of PSC-derived organoids enabled evaluation of distinct factors on expansion and differentiation of stem cells (E). In differentiated renal organoids the effect of interventions on cell behavior, like the exposure to nephrotoxic drugs on the expression of injury molecules, has been evaluated (F). Transporter function of differentiated tubular epithelial cells has also been investigated and modulated in organoid culture (G). Renal stem cell capacity has been investigated by combining organoid-derived cells with embryonic and/or neonatal kidney cells to demonstrate active integration, participation and even nephron induction *in vivo* as well as *ex vivo* (H).

A wide variety of RNA and immunohistochemical markers has been used to determine cell types in kidney organoids, and markers that have been used in multiple protocols are depicted in Figure 3. [16,18,27,28,62,82-85] Beside the use of individual markers, gene profiling has been applied. Takasato et al performed RNA sequencing on renal organoids at different stages of differentiation and compared transcriptional profiles to transcriptomes of human fetal organs at different stages of development to determine tissue type and level of differentiation. [82]

Morphological characteristics of organoid tissue as well as individual cells have been evaluated using light and electron microscopy. Light microscopy showed that differentiated epithelial cells formed tubular structures when cultured in a 3D matrix.[27,85] Immunohistochemistry was used to demonstrate the presence and localization of proteins like SYNPO and ZO-1 in podocytes and the effect of PODXL on expression and, more specifically, the cellular localization of these proteins.[28] Immunohistochemistry was also used to evaluate lumen diameter of specific segments of differentiated renal organoids, and the effect of PKD genes on the diameter of the organoid lumen (i.e. cyst formation).[28] Electron microscopy has been used to assess the presence of tight junctions, brush borders and the mitochondrial density of differentiated proximal tubular cells.[28,82,84] Specific aspects of foot processes of podocytes have been assessed by electron microscopy. [82,84]

Functional characteristics of differentiated renal tissue have been assessed in organoid culture in physiological and pathophysiological conditions. Organoid culture allows evaluation of tissue-specific barrier and transport functions. Takasato and colleagues have demonstrated cubulin-mediated endocytosis of dextran (10kDa) by differentiated renal organoid cells with

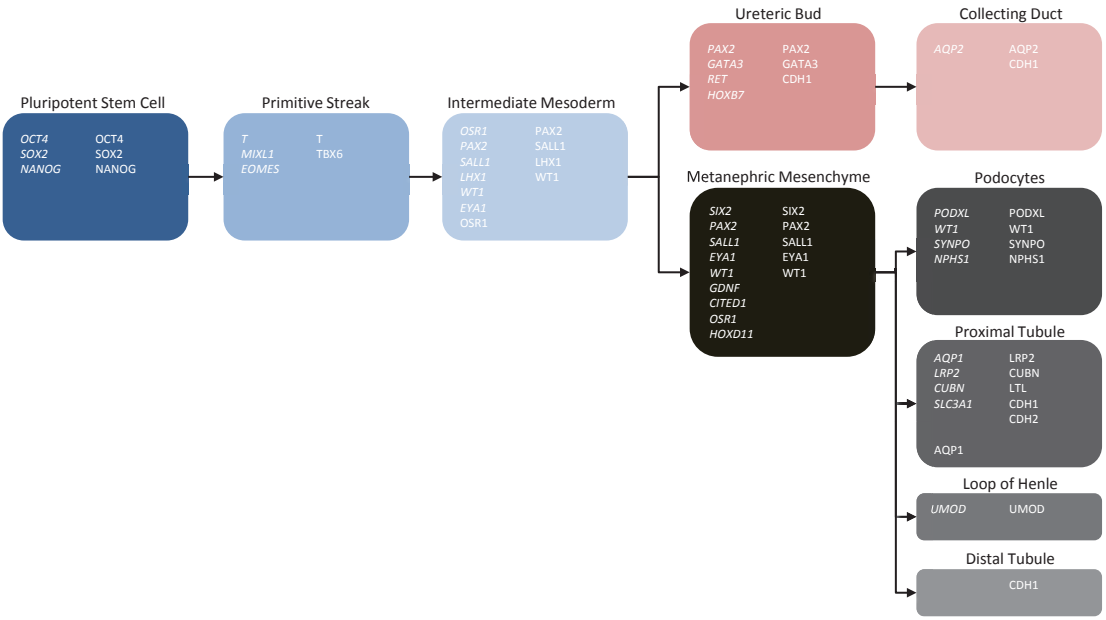

Figure 3. Differentiation markers used in PSC-derived renal organoids. Distinct markers have been used to identify differentiation direction and stage. Markers on RNA levels are in italics, markers on protein level are not.

a proximal tubular phenotype.[82] Freedman et al have demonstrated that dextran and methotrexate are actively transported into the lumen of renal organoids. They were able to inhibit the transport by inhibiting actin polymerization, suggesting that this transport is mediated by endocytosis, which is a process typical for proximal tubular cells.[28] Proximal tubule cells *in vivo* express KIM1 in response to nephrotoxins cisplatin and gentamicin. [28] In organoids, KIM1 expression was limited to cells with a proximal tubule phenotype, consistent with the *in vivo* situation. [84] Moreover, the induction of DNA damage marker yH2AX and subsequent apoptosis was also predominantly seen in cells with a proximal tubular phenotype in renal organoids in response to cisplatin, also consistent with the *in vivo* situation.[82,84]

Finally, differentiation of renal organoids from PSCs allows the evaluation of specific interventions on differentiation (capacity) and nephrogenic potential of renal stem and progenitor cells at specific levels of differentiation. The importance of Notch signaling for the differentiation of proximal tubular cells during renal organoids induction from PSCs has been demonstrated by the fact that Notch-inhibitor DAPT markedly suppressed the formation of tubular structures with a proximal phenotype during the generation of renal organoids from PSCs.[84] Several authors have demonstrated nephrogenic potential of renal organoid cells at different levels of differentiation by assessing their potential to integrate and participate in *ex vivo* cultured murine embryonic kidneys.[27,62,82,83] Participation of PSC-derived renal organoid cells in murine neonatal kidney development was used to assess nephrogenic potential *in vivo* of organoid-derived cells.[28]

OPTIMIZING CULTURE PARAMETERS FOR APPLICATION

Start cells, growth factors and matrix are important determinants for kidney organoid cultures. The specific application directs choices of each of these components used in organoid cultures. For modeling kidney development, ESCs are is currently the best option, as no reprogramming process with viral transfection is required for obtaining the cells and epigenetic memory is not an issue. For drug toxicity or efficacy screenings, iPSC or adult-derived organoids would be optimal, as these organoid lines can be derived from a broad population (healthy or with a specific disease) and would be ideal to capture genetic heterogeneity, picking up differences in drug response among the human population. For therapeutic purposes, the ideal cell source would be autologous, adult kidney stem cell-derived organoids. Although iPSCs can be used autologously, this would require reprogramming, which poses a risk for tumor formation upon transplantation (*see above*).

Growth factor composition can be used to differentiate into a particular segment of interest. When studying kidney development, decisions on growth factor composition can be made on the basis of both the embryonic kidney structure that is subject of study (e.g. metanephric mesenchyme or ureteric bud) as well as the stage of embryonic development (e.g. intermediate mesoderm or metanephric mesenchyme). For toxicity screening growth factor composition should direct differentiation in such way that the whole kidney is represented. Alternatively, organoids could be enriched for the proximal tubule, the major segment of drug-induced nephrotoxicity. When organoids are cultured for transplantation for therapeutic purposes, growth factors can be used to direct into the nephron segment where the defect is localized: i.e. proximal tubule in case of cystinosis. In addition, in experiments where adult-derived liver organoids [14] were transplanted,

organoids were cultured in expansion media, followed by culture in defined differentiation media to obtain functional, differentiated cells in the organoids, prior to transplantation.

The matrix that is most often used in organoid cultures is Matrigel and for some applications, such as drug screening, Matrigel may suffice as organoid matrix. For studying kidney development, use of a human kidney-specific ECM would be more relevant. For therapeutic purposes, a synthetic gel, preferably composed of non-natural components, would be necessary.

Many organoid read-out assays are available. The research question also determines which read-out assays are useful: for kidney development, the whole spectrum of differentiation characteristics from DNA to morphology and function might be used as read-out parameter. For drug-screening, read-out could be straightforward markers for apoptosis, such as caspase-3, or the clinically used proximal tubule damage marker KIM1. Indeed in proof-of-principle experiments, addition of known nephrotoxic compounds (gentamicin or cisplatin), led to dose-dependent death of the organoids, and an upregulation of KIM1.[28]

Taken together, the renal organoid model is a versatile *ex vivo* culture system at the crossroads of *in vitro* and *in vivo* experiments that can be adapted to its specific applications in basic science and the clinic.

ACKNOWLEDGMENTS

We thank Else Driehuis for help with the graphic design of figure 1.

REFERENCES

1. Sato, T. *et al*. Single Lgr5 stem cells build crypt-villus structures in vitro without a mesenchymal niche. *Nature* **459**, 262-265, doi:10.1038/nature07935 (2009).
2. Sato, T. *et al*. Long-term expansion of epithelial organoids from human colon, adenoma, adenocarcinoma, and Barrett's epithelium. *Gastroenterology* **141**, 1762-1772, doi:10.1053/j.gastro.2011.07.050 (2011).
3. Huch, M. *et al*. Long-Term Culture of Genome-Stable Bipotent Stem Cells from Adult Human Liver. *Cell*, doi:10.1016/j.cell.2014.11.050 (2014).
4. Boj, S. F. *et al*. Organoid models of human and mouse ductal pancreatic cancer. *Cell* **160**, 324-338, doi:10.1016/j.cell.2014.12.021 (2015).
5. Karthaus, W. R. *et al*. Identification of multipotent luminal progenitor cells in human prostate organoid cultures. *Cell* **159**, 163-175, doi:10.1016/j.cell.2014.08.017 (2014).
6. Bartfeld, S. *et al*. In vitro expansion of human gastric epithelial stem cells and their responses to bacterial infection. *Gastroenterology* **148**, 126-136 e126, doi:10.1053/j.gastro.2014.09.042 (2015).
7. McCracken, K. W. *et al*. Modelling human development and disease in pluripotent stem-cell-derived gastric organoids. *Nature* **516**, 400-404, doi:10.1038/nature13863 (2014).
8. Lancaster, M. A. *et al*. Cerebral organoids model human brain development and microcephaly. *Nature* **501**, 373-379, doi:10.1038/nature12517 http://www.nature.com/nature/journal/v501/n7467/abs/nature12517.html#supplementary-information (2013).
9. Takebe, T. *et al*. Generation of a vascularized and functional human liver from an iPSC-derived organ bud transplant. *Nat. Protocols* **9**, 396-409, doi:10.1038/nprot.2014.020 http://www.nature.com/nprot/journal/v9/n2/abs/nprot.2014.020.html#supplementary-information (2014).
10. Spence, J. R. *et al*. Directed differentiation of human pluripotent stem cells into intestinal tissue in vitro. *Nature* **470**, 105-109, doi:10.1038/nature09691 (2011).
11. Stange, D. E. *et al*. Differentiated Troy+ chief cells act as reserve stem cells to generate all lineages of the stomach epithelium. *Cell* **155**, 357-368, doi:10.1016/j.cell.2013.09.008 (2013).
12. Drost, J. *et al*. Sequential cancer mutations in cultured human intestinal stem cells. *Nature* **521**, 43-47, doi:10.1038/nature14415 http://www.nature.com/nature/journal/v521/n7550/abs/nature14415.html#supplementary-information (2015).
13. van de Wetering, M. *et al*. Prospective Derivation of a Living Organoid Biobank of Colorectal Cancer Patients. *Cell* **161**, 933-945, doi:10.1016/j.cell.2015.03.053 (2015).
14. Huch, M. *et al*. In vitro expansion of single Lgr5+ liver stem cells induced by Wnt-driven regeneration. *Nature* **494**, 247-250, doi:10.1038/nature11826 (2013).
15. Yui, S. *et al*. Functional engraftment of colon epithelium expanded in vitro from a single adult Lgr5(+) stem cell. *Nature medicine* **18**, 618-623, doi:10.1038/nm.2695 (2012).
16. Taguchi, A. *et al*. Redefining the in vivo origin of metanephric nephron progenitors enables generation of complex kidney structures from pluripotent stem cells. *Cell stem cell* **14**, 53-67, doi:10.1016/j.stem.2013.11.010 (2014).
17. Takasato, M. *et al*. Kidney organoids from human iPS cells contain multiple lineages and model human nephrogenesis. *Nature* **526**, 564-568, doi:10.1038/nature15695 http://www.nature.com/nature/journal/v526/n7574/abs/nature15695.html#supplementary-information (2015).
18. Takasato, M. *et al*. Directing human embryonic stem cell differentiation towards a renal lineage generates a self-organizing kidney. *Nature cell biology* **16**, 118-126, doi:10.1038/ncb2894 (2014).
19. Xia, Y. *et al*. Directed differentiation of human pluripotent cells to ureteric bud kidney progenitor-like cells. *Nature cell biology* **15**, 1507-1515, doi:10.1038/ncb2872 (2013).
20. Evans, M. J. & Kaufman, M. H. Establishment in culture of pluripotential cells from mouse embryos. *Nature* **292**, 154-156 (1981).
21. Thomson, J. A. *et al*. Embryonic Stem Cell Lines Derived from Human Blastocysts. *Science* **282**, 1145-1147 (1998).

22. Hentze, H. *et al*. Teratoma formation by human embryonic stem cells: evaluation of essential parameters for future safety studies. *Stem cell research* **2**, 198-210 (2009).

23. Bradley, A., Evans, M., Kaufman, M. H. & Robertson, E. Formation of germ-line chimaeras from embryo-derived teratocarcinoma cell lines. *Nature* **309**, 255-256 (1984).

24. Nakano, T. *et al*. Self-Formation of Optic Cups and Storable Stratified Neural Retina from Human ESCs. *Cell stem cell* **10**, 771-785, doi:10.1016/j.stem.2012.05.009.

25. Stevens, K. R., Pabon, L., Muskheli, V. & Murry, C. E. Scaffold-Free Human Cardiac Tissue Patch Created from Embryonic Stem Cells. *Tissue Engineering Part A* **15**, 1211-1222, doi:10.1089/ten.tea.2008.0151 (2008).

26. Mae, S.-I. *et al*. Monitoring and robust induction of nephrogenic intermediate mesoderm from human pluripotent stem cells. *Nature communications* **4**, 1367, doi:http://www.nature.com/ncomms/journal/v4/n1/suppinfo/ncomms2378_S1.html (2013).

27. Lam, A. Q. *et al*. Rapid and efficient differentiation of human pluripotent stem cells into intermediate mesoderm that forms tubules expressing kidney proximal tubular markers. *Journal of the American Society of Nephrology : JASN* **25**, 1211-1225, doi:10.1681/ASN.2013080831 (2014).

28. Freedman, B. S. *et al*. Modelling kidney disease with CRISPR-mutant kidney organoids derived from human pluripotent epiblast spheroids. *Nature communications* **6**, 8715, doi:10.1038/ncomms9715 (2015).

29. Morizane, R. *et al*. Nephron organoids derived from human pluripotent stem cells model kidney development and injury. *Nat Biotech* **33**, 1193-1200, doi:10.1038/nbt.3392

30. Takahashi, K. & Yamanaka, S. Induction of Pluripotent Stem Cells from Mouse Embryonic and Adult Fibroblast Cultures by Defined Factors. *Cell* **126**, 663-676, doi:10.1016/j.cell.2006.07.024.

31. Takahashi, K. *et al*. Induction of Pluripotent Stem Cells from Adult Human Fibroblasts by Defined Factors. *Cell* **131**, 861-872, doi:10.1016/j.cell.2007.11.019.

32. Aoi, T. *et al*. Generation of Pluripotent Stem Cells from Adult Mouse Liver and Stomach Cells. *Science* **321**, 699-702 (2008).

33. Stadtfeld, M., Brennand, K. & Hochedlinger, K. Reprogramming of Pancreatic β Cells into Induced Pluripotent Stem Cells. *Current Biology* **18**, 890-894, doi:10.1016/j.cub.2008.05.010.

34. Kim, K. *et al*. Epigenetic memory in induced pluripotent stem cells. *Nature* **467**, 285-290, doi:http://www.nature.com/nature/journal/v467/n7313/abs/nature09342.html#supplementary-information (2010).

35. Polo, J. M. *et al*. Cell type of origin influences the molecular and functional properties of mouse induced pluripotent stem cells. *Nat Biotech* **28**, 848-855, doi:http://www.nature.com/nbt/journal/v28/n8/abs/nbt.1667.html#supplementary-information (2010).

36. Song, B. *et al*. Generation of induced pluripotent stem cells from human kidney mesangial cells. *Journal of the American Society of Nephrology : JASN* **22**, 1213-1220, doi:10.1681/ASN.2010101022 (2011).

37. Zhou, T. *et al*. Generation of human induced pluripotent stem cells from urine samples. *Nat. Protocols* **7**, 2080-2089, doi:http://www.nature.com/nprot/journal/v7/n12/abs/nprot.2012.115.html#supplementary-information (2012).

38. Rao, M. S. & Malik, N. Assessing iPSC Reprogramming Methods for Their Suitability in Translational Medicine. *Journal of cellular biochemistry* **113**, 3061-3068, doi:10.1002/jcb.24183 (2012).

39. Briggs, J. A. *et al*. Integration-Free Induced Pluripotent Stem Cells Model Genetic and Neural Developmental Features of Down Syndrome Etiology. *Stem cells* **31**, 467-478, doi:10.1002/stem.1297 (2013).

40. Gutierrez-Aranda, I. *et al*. Human Induced Pluripotent Stem Cells Develop Teratoma More Efficiently and Faster Than Human Embryonic Stem Cells Regardless the Site of Injection. *Stem Cells (Dayton, Ohio)* **28**, 1568-1570, doi:10.1002/stem.471 (2010).

41. Sweetman, D., Wagstaff, L., Cooper, O., Weijer, C. & Münsterberg, A. The migration of paraxial and lateral plate mesoderm cells emerging from the late primitive streak is controlled by different Wnt signals. *BMC developmental biology* **8**, 1 (2008).

42. Takasato, M. & Little, M. H. The origin of the mammalian kidney: implications for recreating the kidney in vitro. *Development* **142**, 1937-1947 (2015).

43. Wijgerde, M., Karp, S., McMahon, J. & McMahon, A. P. Noggin antagonism of BMP4 signaling controls development of the axial skeleton in the mouse. *Developmental biology* **286**, 149-157 (2005).

44. James, R. G. & Schultheiss, T. M. Bmp signaling promotes intermediate mesoderm gene expression in a dose-dependent, cell-autonomous and translation-dependent manner. *Developmental biology* **288**, 113-125 (2005).

45. Dono, R., Texido, G., Dussel, R., Ehmke, H. & Zeller, R. Impaired cerebral cortex development and blood pressure regulation in FGF 2 deficient mice. *The EMBO journal* **17**, 4213-4225 (1998).

46. Ortega, S., Ittmann, M., Tsang, S. H., Ehrlich, M. & Basilico, C. Neuronal defects and delayed wound healing in mice lacking fibroblast growth factor 2. *Proceedings of the National Academy of Sciences* **95**, 5672-5677 (1998).

47. Kumar, S. & Duester, G. Retinoic acid controls body axis extension by directly repressing Fgf8 transcription. *Development* **141**, 2972-2977 (2014).

48. Duester, G. Retinoic acid synthesis and signaling during early organogenesis. *Cell* **134**, 921-931 (2008).

49. Stark, K., Vainio, S., Vassileva, G. & McMahon, A. P. Epithelial transformation of metanephric mesenchyme in the developing kidney regulated by Wnt-4. *Nature* **372**, 679-683 (1994).

50. Carroll, T. J., Park, J.-S., Hayashi, S., Majumdar, A. & McMahon, A. P. Wnt9b Plays a Central Role in the Regulation of Mesenchymal to Epithelial Transitions Underlying Organogenesis of the Mammalian Urogenital System. *Developmental cell* **9**, 283-292, doi:http://dx.doi.org/10.1016/j.devcel.2005.05.016 (2005).

51. Poladia, D. P. *et al.* Role of fibroblast growth factor receptors 1 and 2 in the metanephric mesenchyme. *Developmental biology* **291**, 325-339, doi:http://dx.doi.org/10.1016/j.ydbio.2005.12.034 (2006).

52. Miyazaki, Y., Oshima, K., Fogo, A., Hogan, B. L. M. & Ichikawa, I. Bone morphogenetic protein 4 regulates the budding site and elongation of the mouse ureter. *The Journal of clinical investigation* **105**, 863-873 (2000).

53. Dudley, A. T., Lyons, K. M. & Robertson, E. J. A requirement for bone morphogenetic protein-7 during development of the mammalian kidney and eye. *Genes & development* **9**, 2795-2807 (1995).

54. Blank, U., Brown, A., Adams, D. C., Karolak, M. J. & Oxburgh, L. BMP7 promotes proliferation of nephron progenitor cells via a JNK-dependent mechanism. *Development* **136**, 3557-3566 (2009).

55. Maeshima, A., Yamashita, S., Maeshima, K., Kojima, I. & Nojima, Y. Activin A Produced by Ureteric Bud Is a Differentiation Factor For Metanephric Mesenchyme. *Journal of the American Society of Nephrology* **14**, 1523-1534 (2003).

56. Hammerman, M. R. Transplantation of renal primordia: renal organogenesis. *Pediatric nephrology* **22**, 1991-1998 (2007).

57. Imberti, B. *et al.* Renal primordia activate kidney regenerative events in a rat model of progressive renal disease. *PloS one* **10**, e0120235 (2015).

58. Sato, N., Meijer, L., Skaltsounis, L., Greengard, P. & Brivanlou, A. H. Maintenance of pluripotency in human and mouse embryonic stem cells through activation of Wnt signaling by a pharmacological GSK-3-specific inhibitor. *Nature medicine* **10**, 55-63, doi:http://www.nature.com/nm/journal/v10/n1/suppinfo/nm979_S1.html (2004).

59. Niwa, H. Wnt: What's Needed To maintain pluripotency? *Nature cell biology* **13**, 1024-1026 (2011).

60. Zhang, X. *et al.* Receptor Specificity of the Fibroblast Growth Factor Family: THE COMPLETE MAMMALIAN FGF FAMILY. *The Journal of biological chemistry* **281**, 15694-15700, doi:10.1074/jbc.M601252200 (2006).

61. Ornitz, D. M. *et al.* Receptor Specificity of the Fibroblast Growth Factor Family. *Journal of Biological Chemistry* **271**, 15292-15297 (1996).

62. Xia, Y. *et al.* The generation of kidney organoids by differentiation of human pluripotent cells to ureteric bud progenitor-like cells. *Nature protocols* **9**, 2693-2704, doi:10.1038/nprot.2014.182 (2014).

63. Pantoliano, M. W. *et al.* Multivalent Ligand-Receptor Binding Interactions in the Fibroblast Growth Factor System Produce a Cooperative Growth Factor and Heparin Mechanism for Receptor Dimerization. *Biochemistry* **33**, 10229-10248, doi:10.1021/bi00200a003 (1994).

64. Yayon, A., Klagsbrun, M., Esko, J. D., Leder, P. & Ornitz, D. M. Cell surface, heparin-like molecules are required for binding of basic fibroblast growth factor to its high affinity receptor. *Cell* **64**, 841-848, doi:10.1016/0092-8674(91)90512-W (1991).

65. Goetz, R. & Mohammadi, M. Exploring mechanisms of FGF signalling through the lens of structural biology. *Nature reviews. Molecular cell biology* **14**, 166-180, doi:10.1038/nrm3528 (2013).

66. Saksela, O., Moscatelli, D., Sommer, A. & Rifkin, D. B. Endothelial cell-derived heparan sulfate binds basic fibroblast growth factor and protects it from proteolytic degradation. *The Journal of cell biology* **107**, 743-751 (1988).

67. Gospodarowicz, D. & Cheng, J. Heparin protects basic and acidic FGF from inactivation. *Journal of cellular physiology* **128**, 475-484, doi:10.1002/jcp.1041280317 (1986).

68. Yamashita, H. *et al*. Osteogenic protein-1 binds to activin type II receptors and induces certain activin-like effects. *The Journal of cell biology* **130**, 217-226 (1995).

69. Watanabe, K. *et al*. A ROCK inhibitor permits survival of dissociated human embryonic stem cells. *Nat Biotech* **25**, 681-686, doi:http://www.nature.com/nbt/journal/v25/n6/suppinfo/nbt1310_S1.html (2007).

70. Riento, K. & Ridley, A. J. ROCKs: multifunctional kinases in cell behaviour. *Nature reviews. Molecular cell biology* **4**, 446-456 (2003).

71. Astashkina, A. I., Mann, B. K., Prestwich, G. D. & Grainger, D. W. Comparing predictive drug nephrotoxicity biomarkers in kidney 3-D primary organoid culture and immortalized cell lines. *Biomaterials* **33**, 4712-4721, doi:10.1016/j.biomaterials.2012.03.001 (2012).

72. Gaetani, R. *et al*. Cardiac derived extracellular matrix enhances cardiogenic properties of human cardiac progenitor cells. *Cell transplantation* (2015).

73. Tibbitt, M. W. & Anseth, K. S. Hydrogels as extracellular matrix mimics for 3D cell culture. *Biotechnology and bioengineering* **103**, 655-663, doi:10.1002/bit.22361 (2009).

74. Karthaus, W. R. *et al*. Identification of Multipotent Luminal Progenitor Cells in Human Prostate Organoid Cultures. *Cell*, doi:10.1016/j.cell.2014.08.017 (2014).

75. Badylak, S. F. Regenerative medicine and developmental biology: the role of the extracellular matrix. *The Anatomical Record Part B: The New Anatomist* **287**, 36-41 (2005).

76. O'Neill, J. D., Freytes, D. O., Anandappa, A. J., Oliver, J. A. & Vunjak-Novakovic, G. V. The regulation of growth and metabolism of kidney stem cells with regional specificity using extracellular matrix derived from kidney. *Biomaterials* **34**, 9830-9841, doi:http://dx.doi.org/10.1016/j.biomaterials.2013.09.022 (2013).

77. Saha, K., Pollock, J. F., Schaffer, D. V. & Healy, K. E. Designing synthetic materials to control stem cell phenotype. *Current Opinion in Chemical Biology* **11**, 381-387, doi:http://dx.doi.org/10.1016/j.cbpa.2007.05.030 (2007).

78. Eyrich, D. *et al*. Long-term stable fibrin gels for cartilage engineering. *Biomaterials* **28**, 55-65 (2007).

79. Dawson, E., Mapili, G., Erickson, K., Taqvi, S. & Roy, K. Biomaterials for stem cell differentiation. *Advanced drug delivery reviews* **60**, 215-228 (2008).

80. Masters, K. S., Shah, D. N., Walker, G., Leinwand, L. A. & Anseth, K. S. Designing scaffolds for valvular interstitial cells: cell adhesion and function on naturally derived materials. *Journal of Biomedical Materials Research Part A* **71**, 172-180 (2004).

81. Hwang, N. S. *et al*. Effects of Three–Dimensional Culture and Growth Factors on the Chondrogenic Differentiation of Murine Embryonic Stem Cells. *Stem cells* **24**, 284-291 (2006).

82. Takasato, M. *et al*. Kidney organoids from human iPS cells contain multiple lineages and model human nephrogenesis. *Nature*, doi:10.1038/nature15695 (2015).

83. Mae, S. *et al*. Monitoring and robust induction of nephrogenic intermediate mesoderm from human pluripotent stem cells. *Nature communications* **4**, 1367, doi:10.1038/ncomms2378 (2013).

84. Morizane, R. *et al*. Nephron organoids derived from human pluripotent stem cells model kidney development and injury. *Nature biotechnology*, doi:10.1038/nbt.3392 (2015).

85. Kang, M. & Han, Y. M. Differentiation of human pluripotent stem cells into nephron progenitor cells in a serum and feeder free system. *PloS one* **9**, e94888, doi:10.1371/journal.pone.0094888 (2014).

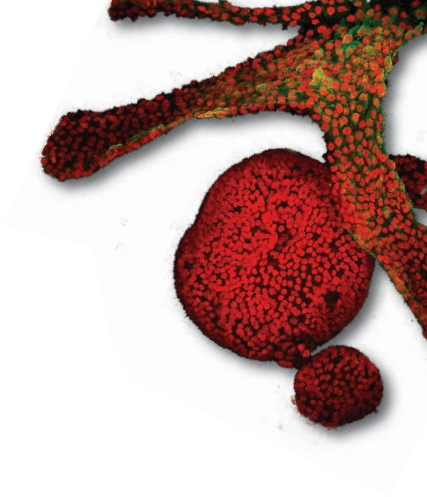

CHAPTER 3

MOUSE AND HUMAN ADULT KIDNEY-DERIVED ORGANOIDS AS PERSONALIZED DISEASE MODELS IN A DISH

ABSTRACT

Adult Stem Cell (ASC)-derived organoids are 3D epithelial structures that recapitulate essential aspects of their organ of origin. We have developed conditions for the long-term growth of primary kidney epithelial organoids. Cultures can be established from mouse and human kidney tissue, as well as from urine and can be expanded for at least 20 passages (> 6 months). Chromosome numbers remain normal. Human organoids represent proximal as well as distal nephron segments, as evidenced by gene expression, immunofluorescence and tubular functional analyses. BK virus infection of organoids recapitulates *in vivo* phenomena. Organoids can be established from Wilms nephroblastoma. Kidney organoids from Cystic Fibrosis (CF) patient's urine allow *ex vivo* assessment of treatment efficacy. Adult kidney-derived organoids allow studies of hereditary, infectious and malignant kidney disease in a personalized fashion.

Frans Schutgens[1,2], Maarten B. Rookmaaker[2], Carola Ammerlaan[1,2], Jitske Jansen[3], Marco Viveen[4], Francis Blokzijl[5], Annelotte Vonk[6], Karin M. de Winter - de Groot[7], Antoni P.A. Hendrickx[4], Ruben van Boxtel[5], Marry M. van den Heuvel – Eibrink[8], Ellen Heitzer[9], Edwin Cuppen[5], Jeffrey Beekman[6], Jean-Luc Murk[4,10], Rosalinde Masereeuw[3], Jarno Drost[8], Marianne C. Verhaar[2], Hans Clevers[1,8]

[1] Hubrecht Institute–Royal Netherlands Academy of Arts and Sciences, Utrecht, the Netherlands
[2] Department of Nephrology and Hypertension, University Medical Centre Utrecht, the Netherlands
[3] Division of Pharmacology, Utrecht Institute for Pharmaceutical Sciences, Utrecht University, the Netherlands
[4] Department of Medical Microbiology, University Medical Center Utrecht, the Netherlands
[5] Center for Molecular Medicine, Cancer Genomics Netherlands, Department of Genetics, University Medical Center Utrecht
[6] Regenerative Medicine Center Utrecht, the Netherlands
[7] Wilhelmina Children's Hospital, University Medical Center Utrecht, the Netherlands
[8] Princess Máxima Center for Pediatric Oncology, Utrecht, the Netherlands
[9] Institute of Human Genetics, Medical University of Graz, Austria
[10] Laboratory of Medical Microbiology and Immunology, St. Elisabeth TweeSteden Ziekenhuis, Tilburg, the Netherlands

Under review

INTRODUCTION

Organoid cultures can be established from embryonic stem cells or induced pluripotent stem cells, (collectively referred to as pluripotent stem cells (PSCs)) and from adult tissues.[1,2] PSC-derived "mini-kidney" organoids have been developed recently that contain cells from all kidney lineages.[3-8] ASC-derived organoids have been established for multiple organs and cancers derived thereof. [9-15] An ASC-derived human kidney organoid culture has not been developed yet.

RESULTS

Establishing and characterizing kidney organoids

To establish a culture protocol sustaining the growth of ASC-derived human kidney organoids, we adapted our protocol for the expansion of adult intestinal *Lgr5+* stem cells.[15,16] We resuspended tubular fragments, that were obtained after collagenase digestion of cortical human kidney, in Matrigel or BME (Figure 1A) and added culture media, containing *1)* Rspondin-conditioned medium to enhance canonical Wnt signaling, known to be essential for embryonic kidney development[17,18]; *2)* FGF10, to promote survival of kidney progenitor cells[19]; *3)* A8301, to inhibit the TGF-β receptors ALK4/5/7, preventing growth arrest and epithelial to mesenchymal transition[20]; *4)* the mitogen EGF; *5)* and Rho-kinase inhibitor to prevent anoikis of dissociated cells.[21]

Folded/branching organoids typically developed within 6 days after seeding (Figure 1B). The branching/folded structure of the organoids was confirmed with Hemotoxylin & Eosin (H&E) staining and Scanning Electron Microscopy (SEM) (Figure 1C, D). However, cystic structures consisting of a simple cuboid epithelium dominated in the culture after 4 or 5 passages (Figure 1E). Under optimized conditions, human organoids could be passaged 15 - 20 times with 1:3 weekly split ratios. Organoid lines could be established with 100% efficiency ($n > 30$) and retained a normal number of chromosomes over long-term culture (18 passages) (Figure 1O and Supplementary Figure 1).

To determine which kidney epithelial cell lineages are present in our cultures, we performed single cell RNA-sequencing. We sorted 192 organoid cells as well as 192 $Epcam^+$ epithelial cells from the primary cortical kidney tissue from which the organoids were derived. A median of 5937 genes per cell was detected and after removing cells with fewer than 4000 transcripts, 85 kidney cells and 142 organoid cells were subjected to unsupervised clustering using the validated rare cell type identification (RACEID and RACEID2) algorithms.[22,23] $Epcam^+$ kidney epithelial cells and organoid cells clustered separately. Organoid cells displayed higher expression of ribosomal genes, indicative of proliferation (Supplementary Figure 2),[22,24] which is not surprising as normal kidney tissue has a low turnover. We focused on the presence of differentiated epithelial cells from distinct nephron segments in the organoids. We first validated this approach for the kidney tissue-derived cells, and found predominantly non-overlapping expression of marker genes of the distinct nephron segments throughout the cell population: proximal tubule, loop of Henle, distal tubule and collecting duct (Supplementary Figure 3). The organoid cells were *PAX8+* and thus kidney-epithelial in nature (Supplementary Figure 4).[25] This was confirmed by protein staining (Supplementary Figure 4). Subsets of cells expressed collecting duct cell markers: the intercalated cell marker *SLC4A1* (Figure 1F) and the principal cell marker *AQP3* (Figure 1G), both confirmed at

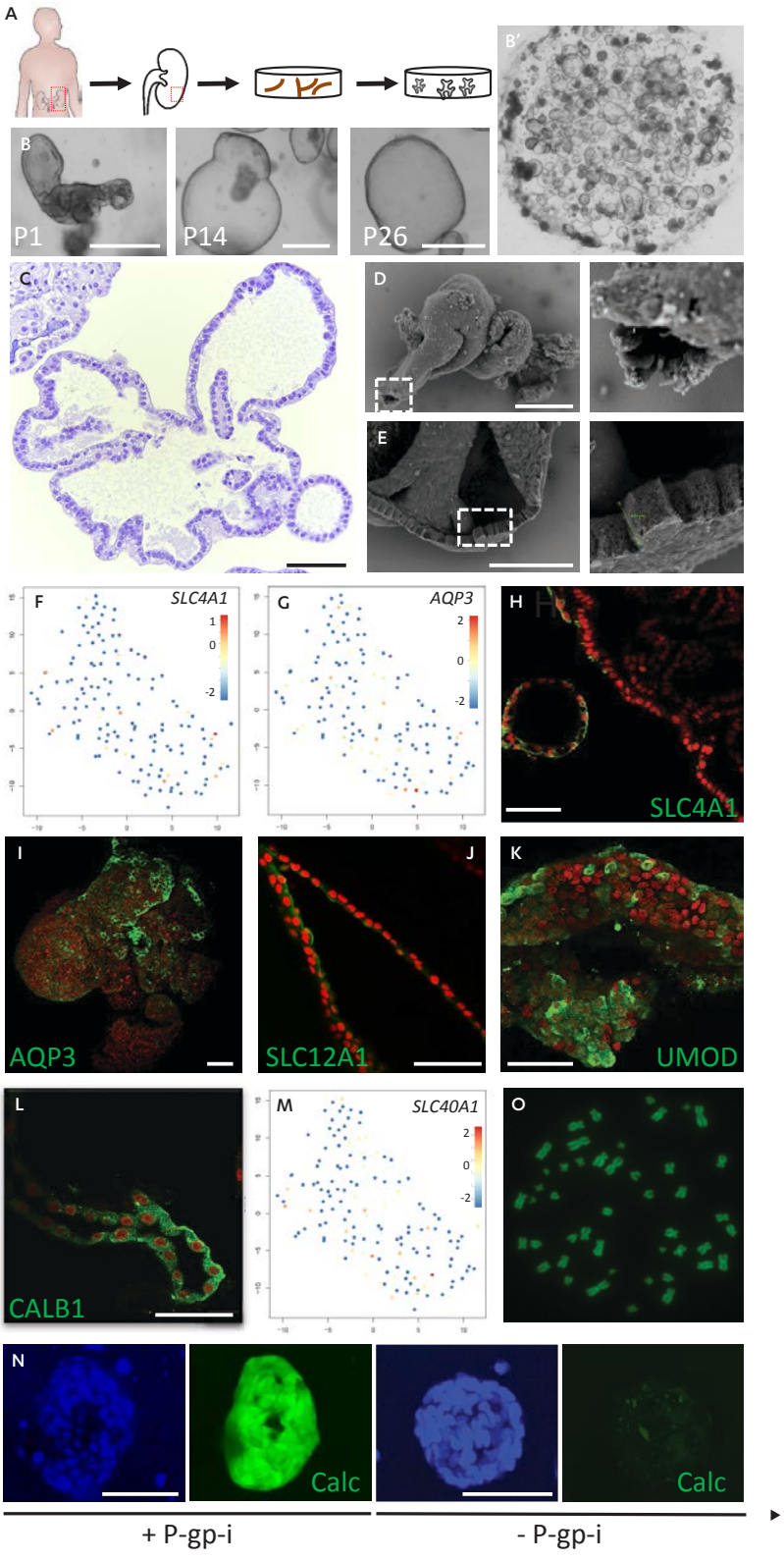
A
B
P1
P14
P26
B'
C
D
E
F
SLC4A1
G
AQP3
H
SLC4A1
I
AQP3
J
SLC12A1
K
UMOD
L
CALB1
M
SLC40A1
O
N
Calc
Calc
+ P-gp-i
- P-gp-i

Figure 1. Human kidney organoid culture. Scheme of the experimental protocol (A). In early passages, organoids have a folded structure and from passage 5 onwards, the cystic morphology predominates (B). H&E stain of P4 organoids, showing a cuboid epithelium (C) SEM image of P4 confirms the folded and tubular structure of organoids (D). Cystic organoids consist of a single layered epithelium with cells of approximately 10 µm in diameter, visualized with SEM (E). t-SNE maps for known marker genes with transcript counts color coded, with cells expressing alfa-intercalated cell marker SLC4A1 of the collecting duct (F) and principal cell of the collecting duct marker AQP3 (G). The expression of these markers was confirmed with immunofluorescence, SLC4A1 (H) AQP3 (I). A minority of the organoid cells express loop of Henle marker SLC12A1 (J) Expression of loop of Henle marker UMOD (K) and distal tubule marker CALB1 (L) were observed after withdrawal of growth factors. t-SNE map for proximal tubule marker gene *SLC40A1* with transcript counts color coded (M). Organoid display proximal tubule transporter function: by addition of a P-gp-specific inhibitor (+ P-gp-i), accumulation of calcein (Calc) is observed. This is not observed without inhibitor (- P-gp-i) (N). An example of a typical metaphase spread, from an organoid culture after 18 passages (O). Scale bars 75 µm, except B: 500 µm.

the protein level (Figure 1H, I). As the most abundant nephron-segment, cells expressed proximal tubule marker *SLC40A1* (Figure 1M). This predominant proximal tubule expression pattern could be validated with functional analyses (*see below*).

Under the described culture conditions (that were developed for initiation and expansion of organoids) no expression of loop of Henle-specific genes (*UMOD*, *SLC12A1*) and distal tubule marker *CALB1* were observed in the single cell RNA sequencing analysis. However, SLC12A1 was present in a minority of cells in a subset of organoids on the protein level (Figure 1J). Growth factor withdrawal, a method previously used to promote differentiation of organoids,[9] allowed detection of CALB1 and UMOD by immunofluorescence (Figure 1K,L and Supplementary Figure 5), suggesting the presence of progenitor cells for these segments. When cells in an organoid are positive for a segment-specific marker, generally the majority of the cells in that organoid are positive for that marker (Figure 1H-L), suggesting a nephron segment-specific phenotype of individual organoids.

We next evaluated whether the proximal tubule cells in the organoids were functional. We exposed organoids to a substrate (calcein-AM, which diffuses freely into cells) of the proximal tubule xenobiotics efflux pump P-glycoprotein (P-gp; *ABCB1*), in presence or absence of the P-gp-specific inhibitor PSC-833.[26] Thus, if P-gp is functional in organoids, accumulation of calcein-AM, which is intracellularly cleaved into the fluorescent calcein, is expected when P-gp-activity is blocked. An illustration of the experimental set-up is provided in Supplementary Figure 6. We observed accumulation of calcein in the presence of the inhibitor as assessed by confocal microscopy (Figure 1N). We quantified this by measuring fluorescence in a plate reader and found the difference to be significant (*P*-value = 0.004, Supplementary Figure 7).

Thus, under expansion conditions, proximal tubule cells are functional, collecting duct cells are present and a few loop of Henle cells are found. Growth factor withdrawal can be used as a strategy to increase the expression of loop of Henle and distal tubule markers.

Of note, by collagenase digestion of whole mouse kidneys, long-term mouse organoid cultures could be established with essentially 100% efficiency ($n > 10$) that remained folded / branching over passaging (Supplementary Figure 8A-D). Mouse organoid retained a normal number of chromosomes as well (Supplementary Figure 8H, I). To determine the presence of different kidney lineages to the mouse organoids, we compared gene expression of organoid lines with the contra-lateral adult kidney (n = 3) using RNA-sequencing (RNA-seq). Analysis of markers specific to the different adult kidney compartments revealed that (outer medullary) collecting duct genes

were upregulated, relative to complete adult kidney[27] (Supplementary Figure 8E). In accordance with the RNA-seq data, the collecting duct-specific aqp3 protein was predominantly present in the buds of the organoids (Supplementary Figure 8F). In a dehydrated state *in vivo*, increased ADH levels induce upregulation of the water channel AQP2 in the principal cells of the collecting duct. Indeed, *aqp2* mRNA increased 1.5 fold after 8 hours and 3.1 fold after 24 hours of desmopressin (the clinically used ADH-analogue) stimulation, comparable to the maximal *in vivo* ADH response[28] (Supplementary Figure 8G). Thus, under expansion conditions, mouse organoids enrich for distal nephron cells. The difference with the human organoids may be due to difference in starting material: for human cultures, we used cortical kidney tissue, whereas for mouse cultures, whole kidneys were digested.

Organoids to model infectious kidney disease

Subsequently, we set out to validate the renal organoid culture system as an *ex vivo* model to study acquired renal tubular pathophysiology. We infected human organoids with BK virus, a tubule-specific circular DNA virus for which currently no curative treatment exists. BK virus infections are responsible for the loss of 5-10% of donor organs in transplant recipients.[29] After infection of renal organoids with BK virus, H&E staining (Figure 2A) revealed that some nuclei of organoid cells increased in size in a patchy pattern. Immunohistochemistry for SV40 Large T antigen (used to diagnose BK nephropathy in kidney biopsies) demonstrated staining of the enlarged nuclei (Figure 2B). Both the patchy pattern of infection and the swelling of nuclei (termed "intranuclear basophilic viral inclusions") are observed in BK nephropathy kidney biopsies.[30] The scattered infection in organoids mimics the *in vivo* situation, in contrast to the more general infection observed in kidney cell lines.[31] The presence of viral particles in nuclei was confirmed by transmission electron microscopy (Figure 2C). In addition to productive infection with a laboratory BK virus strain, infection could be established using BK virus directly from BK virus patient's urine samples (Supplementary Figure 9). Moreover, we found that the number of virus copies increased exponentially during the first 10 days after infection (Figure 2D) using quantitative PCR. Viral DNA was sequenced at day 1 after infection of organoids and after 30 days of culture in organoids; no DNA changes were detected. Thus, BK virus expands stably in human kidney organoids.

Next, we tested whether virus particles that were produced in culture were infectious. We filtered culture supernatant 30 days after inoculation (having undergone 13 medium refreshments – thereby minimizing the contribution of virus particles used to establish infection). Incubation with the filtered supernatant was sufficient to establish infection and subsequent culturing increased the number of viral copies (Figure 2E), implying the active production of infectious viral particles.

Finally, we tested whether viral expansion could be reduced by anti-viral treatment of organoids. After incubation with BK-virus, organoids were cultured for 7 days in the presence of 10 - 320 µg/ml cidofovir (CDV, an inhibitor of DNA polymerase), a drug used clinically for the treatment of BK virus nephropathy.[32] The number of viral copies decreased significantly compared to control (P-value < 0.01, from 20 µg/ml onwards) in a dose-dependent manner (Figure 2F). The IC50 that we measured (approximately 10 µg/ml) is in the range of clinically obtained serum levels.[33]

Thus, BK virus infection in organoids mimics the clinical disease better than cell lines (where a high percentage of cells is infected[31]) and the model allows testing of treatment efficiency *ex vivo*.

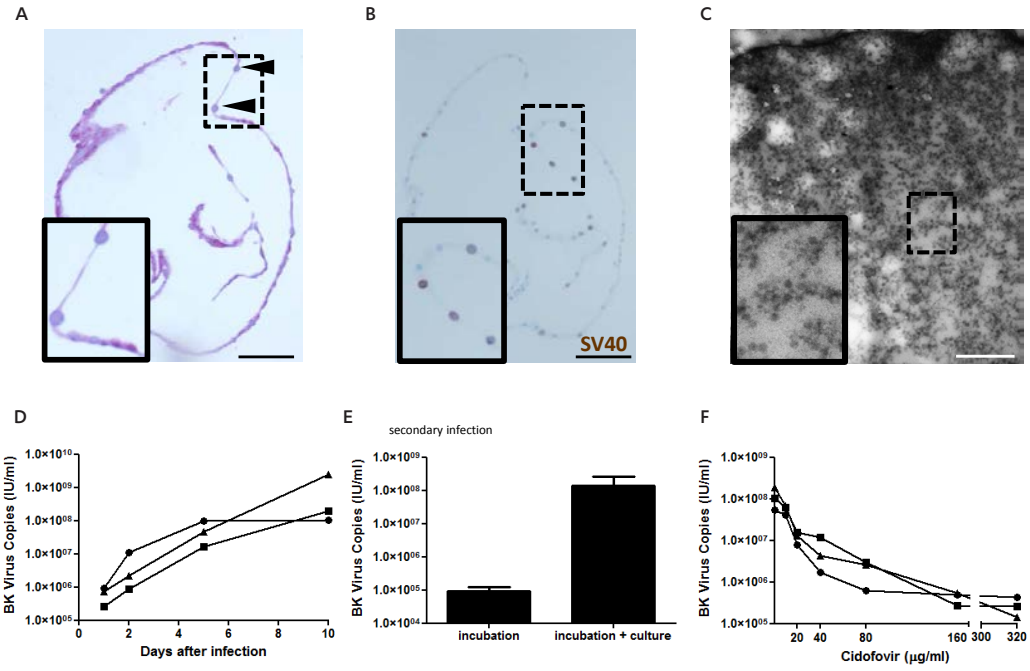

Figure 2. Modeling BK virus infection with human kidney organoids. H&E staining shows larger nuclei (intranuclear basophilic viral inclusions) in an infected organoid (A). The larger nuclei, present in a patchy pattern, stain for SV40 (B). Transmission electron microscopy shows the presence of viral particles in nuclei of an infected cell and are absent in negative control (C). BK virus particles increase exponentially in approximately the first ten days in culture (D, each line represents one independent experiment). Filtered supernatant of organoids infected with BK virus is infectious after incubation (*incubation*), and viral copies increase in number over time (*incubation + culture*) (E, average of $n = 3$ experiments is plotted; error bars represent standard deviation). The ratio of viral DNA / human DNA decreases significantly (P-value < 0.01) in the presence of cidofovir in a dose-dependent manner (F, each line represents one independent experiment). Scale bars 100 µm, except C: 500 nm.

Organoids from Wilms tumors

Wilms tumor, or nephroblastoma, is the most common pediatric solid tumor, accounting for 5% of all childhood malignancies.[34] Mutations in genes such as *WT1* or *CTNNB1* are believed to occur in kidney stem/progenitor cells during embryonic development. The resulting Wilms tumors have a typical tri-phasic histology with stroma, blastema and epithelium as components.[35] Copy number variations (CNVs) are observed in 75% of cases.[36,37] We established organoid lines from tumor and matching normal tissue of two nephroblastoma patients (Figure 3A, E). For the first nephroblastoma patient, tumor-derived organoids displayed a clearly different morphology compared to the healthy tissue-derived organoids, as assessed by phase-contrast microscopy (Figure 3A) and 6-day time-lapse imaging movies (*data not shown*). The most striking difference was the presence and expansion of a stromal (non-epithelial) compartment in culture, which was completely absent in healthy tissue-derived organoids. Time-lapse movies and SEM (Figure 3B) demonstrated that stromal cells were associated with the non-stromal structures in the organoid line. Histology showed that tumor organoids resembled the original tumor tissue, as the original tumor tissue

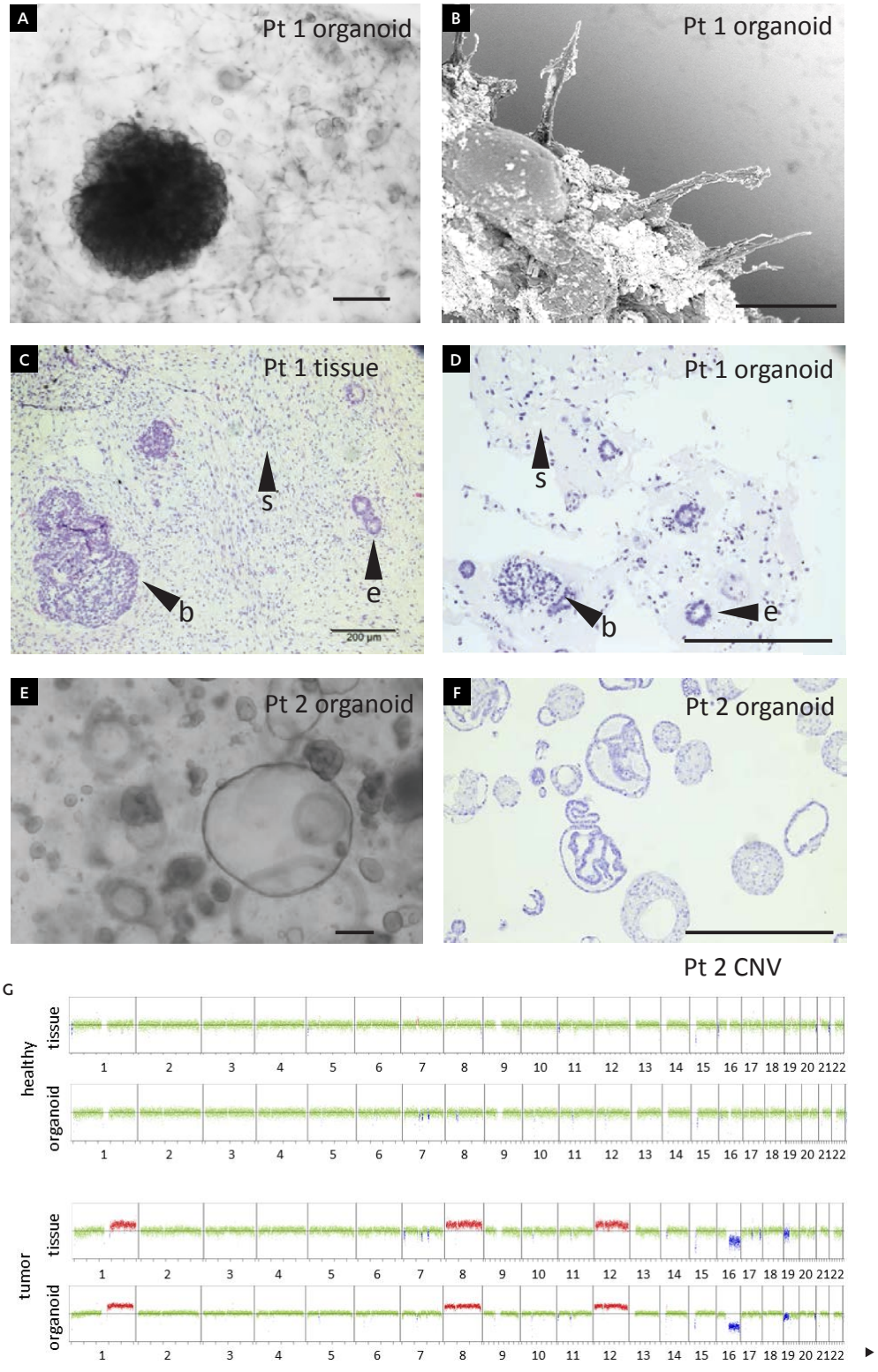
A
Pt 1 organoid
B
Pt 1 organoid
C
Pt 1 tissue
s
b
e
200 µm
D
Pt 1 organoid
s
b
e
E
Pt 2 organoid
F
Pt 2 organoid
Pt 2 CNV
G
healthy
tissue
organoid
tumor
tissue
organoid
1 2 3 4 5 6 7 8 9 10 11 12 13 14 15 16 17 18 19 20 21 22

▶ **Figure 3. Organoid lines can be established from Wilms tumor tissue.** Nephroblastoma-derived organoids have a different morphology than healthy tissue-derived organoids, as assessed with bright field microscopy (A), that shows expansion of the stromal compartment of the tumor, and SEM (B), that shows the association of stromal cells with non-stromal structures. H&E stains of the primary tumor tissue (C) and the organoid line (D) that both show the typical tri-phasic nephroblastoma histology, with blastema (arrow head, b), epithelium (arrow head, e) and stroma (arrow head, s) present. Organoids isolated from the second nephroblastoma patient do not have a different morphology as assessed with bright field (E) and H&E staining (F). Low-coverage whole genome sequencing shows that healthy tissue and the healthy organoid line do not display CNVs (G). However, in the tumor tissue and tumor organoid line, typical Wilms tumor CNVs, such as 1q gain, gain of chromosome 8 and 12, and 16q loss were identified (G). Scale bars 200 µm, except B: 100 µm.

(Figure 3C) also contained stroma, blastema and epithelium. All three components were present in the organoids (Figure 3D). By targeted sequencing, we found two frameshift mutations in the zinc finger DNA binding domains of *WT1*. In exon 10, we detected a heterozygous 4 base pair insertion in the tumor tissue and organoids that was absent in healthy tissue and organoids (Supplementary Figure 10). In exon 7, we found a heterozygous 8 base pair deletion in that was present in the tumor organoids and tissue, as well as in the healthy tissue and organoids, implying a germline mutation in *WT1* (Supplementary Figure 11).

For the second patient, we did not find striking histological differences between the healthy and the tumor line (Figure 3E,F). However, low coverage WGS revealed typical CNVs associated with nephroblastoma, including gain of 1q, chromosome 8, 12[38] and loss of 16q.[39] Importantly, identical CNVs were found in the primary tumor tissue (Figure 3G). These CNVs were absent in the healthy tissue and the organoids derived thereof, proving that the organoids were tumor-derived and that the organoid lines genetically reflected the primary tumor.

Nephroblastoma organoids from both patients could be expanded with a split ratio of 1:2-1:3 once every 10-14 days. In the first patient, the stromal compartment was still present in culture after >10 passages.

Organoids from urine

A limitation of the described culture system is that nephrectomy or biopsy is required to establish cultures. These invasive procedures are standard of care for only a limited number of kidney diseases. Thus, we set out to establish kidney organoid cultures from kidney epithelial cells shed in urine. By adaptation of previously described protocols [40], we were able to isolate and expand single cells from urine. In the same culture medium that we used for healthy human tissue, these single cells developed into organoids, typically two weeks after seeding. Urine-derived kidney organoid lines could be expanded over 10-15 passages with weekly passaging in a 1:3 ratio.

We established 3 independent organoid lines from healthy volunteers (pediatric and adult). Organoid cultures were almost exclusively derived from kidney epithelium, as demonstrated by PAX8+ staining of all organoids in two lines (Figure 4A). One line contained a mixed culture of PAX8+ and PAX8- structures. The PAX8-negative organoids were positive for the urothelial marker P63 and -in agreement- displayed a characteristic bladder urothelial structure (Figure 4B, B').

In addition, we established an organoid line from urine of a CF-patient (F508del/S1251N), from which an intestinal organoid line was already established. These organoids were PAX8+

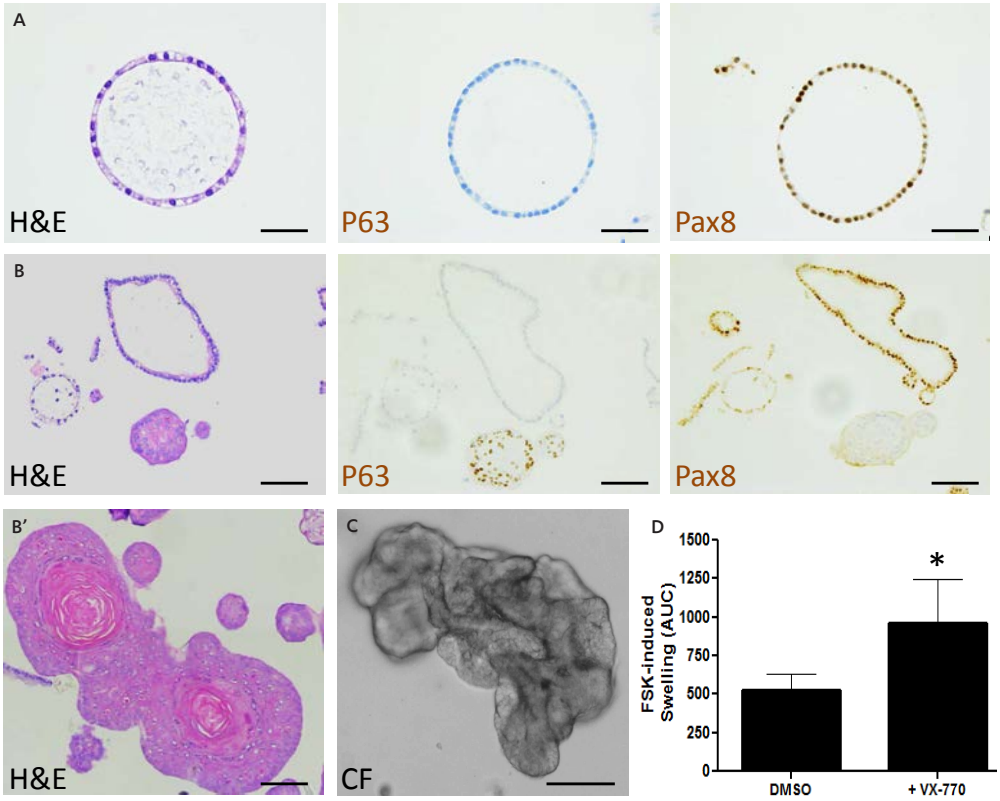

Figure 4. Organoid lines can be established from urine. Urine-derived organoids can originate from kidney epithelium, as demonstrated with Pax8-staining (A). However, also a combination of kidney (Pax8+) and urothelium (P63+) is observed (B). P63+ structures have a typical bladder urothelial organization (B') Typical phenotype of urine-derived CF kidney organoids after 10 passages (C). CF-urine organoids do not swell in response to FSK without VX-770 (DMSO), but swelling can be significantly increased by the addition of VX-770 (VX-770) (D, average of two independent experiments is plotted. Error bars represent standard deviation. * *P*-value = 0.02). Scale bars 100 µm.

(Supplementary Figure 12) and thus kidney-derived. Morphologically, the kidney organoids remained folded over long-term culture (~10 passages) (Figure 4C). This is analogous to the morphology of intestinal CF organoids that are also more folded while normal intestinal organoids are cystic.[41] As proof-of-principle for the evaluation of treatment efficacy, we performed the previously described forskolin swelling assay,[42] which is currently being used as *ex vivo* drug efficacy screen for CF on intestinal organoids (for which a rectal biopsy is required).[41,43] The addition of forskolin leads to swelling that is solely dependent on CFTR in intestinal organoids. Thus, in intestinal CF organoids, no swelling occurs, unless there is rest function of CFTR (as occurs with specific mutations, including F508del/S1251N[41]) or when an effective CFTR-restoring compound is present.

In the CF-line derived from urine, only minimal swelling occurred in response to opening the CFTR channel by forskolin. Swelling increased significantly (*P*-value = 0.02; Figure 4D) by pre-incubation with the CFTR-potentiator drug VX-770 (ivacaftor, Kaleydeco®), a registered drug for

treatment of F508del/S1251N mutations that also clinically had a beneficial effect on the patient. The intestinal organoids from the same patient showed similar results as the CF-urine organoids: forskolin induced limited swelling (demonstrating some residual CFTR function, as expected with F508del/S1251N mutations) and swelling increased by pre-incubation with the CF drug VX-770 (Supplementary Figure 13).

DISCUSSION

In this study, we report a robust organoid culture system for mouse, as well as human healthy and diseased kidney tissue. This enables expansion and differentiation of primary, functional renal epithelial cells with characteristics of distinct nephron segments, most notably the proximal tubule. We demonstrate the use of organoids for disease modeling, drug screening and transporter studies. We believe that our organoid culture system is complementary to the existing PSC-derived organoids.[3,5,6,44] It adds the unique feature of direct expansion of patient-derived renal tissue, from biopsy material and from urine, without the ethical issues related to embryonic stem cells or the disadvantages of reprogramming and resulting genetic instability of induced PSCs.[45]

There are, however, limitations of the culture system, some of which may be overcome in the future. Firstly, under the current culture conditions, we generate cells representing proximal, loop of Henle, distal tubules and collecting duct. Yet, glomerular cells are lacking. This may be overcome by adaptation of the culture medium or co-culture with endothelial cells.[46] Secondly, the culture system is purely epithelial in nature, lacking interstitial cells and vasculature. However, epithelial cells are often the primary substrate of disease and a reductionist system is powerful to investigate *ex vivo* epithelial cell dynamics.

Thus, we have established a culture system that allows disease modeling, drug screening and personalized medicine. Ultimately, our culture system may provide a nearly infinite source of autologous cells for the creation of bioartificial or bioengineered kidneys.[47,48]

MATERIAL AND METHODS

Mice and human tissue

All animal experiments were approved by the Animal Experimentation Committee of the Royal Dutch Academy of Science and UMC Utrecht. All experiments with human tissue were approved by the medical ethical committee of the University Medical Centre Utrecht and, if required, written informed consent from patients was obtained.

Organoid culture

Human tissue

From cortical kidney tissue, tubular fragments were isolated by collagenase digestion (C9407, Sigma) for 45 minutes at 1 mg/ml. Fragments were seeded in growth factor-reduced Matrigel (Corning) or Basement Membrane Extract (BME - R&D Systems) and cultured in medium (ADMEM / F12 supplemented with 1% penicillin / streptomycin, HEPES, Glutamax, N-acetylcysteine (1 mM, Sigma) and 1.5% B27 supplement (Gibco)), supplemented with 10% Rspo1-conditioned medium[49]

or 1% Rspo3-conditioned medium, the latter produced via the r-PEX protein expression platform (U-Protein Express), EGF (50 ng/ml, Peprotech), FGF-10 (100 ng/ml, Preprotech), Rho-kinase inhibitor Y-27632 (10 μM, Abmole) A8301 (5 μM, Tocris Bioscience), primocine (0.1 mg/ml, Invivogen).

Differentiation medium contained ADMEM / F12 supplemented with 1% penicillin / streptomycin, HEPES and Glutamax.

Human urine

Urine (30-50 ml was sufficient) was processed quickly after voiding and until processing, the sample was kept at 4° C. Rho-kinase inhibitor Y-27632 (10 μM, Abmole) and primocine (0.1 mg/ml, Invivogen) were added. After centrifugation, pellet was washed with medium (ADMEM / F12 supplemented with 1% penicillin / streptomycin, HEPES and Glutamax), supplemented with Rho-kinase inhibitor Y-27632 (10 μM, Abmole) and primocine (0.1 mg/ml, Invivogen). After a second centrifugation step, pellet was resuspended in growth factor-reduced Matrigel (Corning) or BME (R&D Systems) and cultured in the organoid culture medium described above.

Mouse

Kidneys were isolated and tubular fragments were isolated by collagenase digestion (C9407, Sigma) for 15 minutes at 0.5 mg/ml. Fragments were seeded growth factor-reduced Matrigel (Corning) and cultured in medium (ADMEM / F12 supplemented with 1% penicillin / streptomycin, HEPES, Glutamax), with 1.5% B27 supplement (Gibco), 40% Wnt3a conditioned medium (produced using stably transfected L cells) 10% Noggin conditioned medium, 10% Rspo1-conditioned medium,[49] EGF (50 ng/ml, Peprotech), FGF-10 (100 ng/ml, Preprotech); N-acetylcysteine (1.25 mM, Sigma) A8301 (5 μM), Tocris Bioscience), primocine (0.1 mg/ml, Invivogen).

Histology and immunohistochemistry

Tissues were fixed in 4% paraformaldehyde, dehydrated and embedded in paraffin. Sections were subjected to H&E and / or immunohistochemical staining. IHC was performed according to standard protocols on 3–4 μm sections. The primary antibodies were rabbit anti-Pax8 (1:500, 10336-1-AP, Proteintech), mouse anti-P63 (1:50, M7317, Dako) and mouse anti-SV-40 (1:100, bPAb416, Merck Millipore). Primary antibodies were dissolved in 0.05% Bovine Serum Albumin (BSA) in PBS. If required, a rabbit-anti-mouse-HRP (1:500, Dako) in PBS and 5% normal mouse serum was used. Goat-anti-Rabbit Powervision-Horse Radish Peroxidase (both Leica Biosystems) was used as tertiary antibody and counterstaining was done with with haematoxylin.

Immunofluorescence

For whole mount immunofluorescence staining, organoids were processed as previously described.[50] Rabbit anti-AQP-3 (1:100, 125219, Abcam), rabbit anti-AE1 / SLC4A1 (1:100, AE11-A, Alpha Diagnostics International), goat anti-calbindin D28K (1:200, N-18, Santa Cruz) were used as primary antibody. Sheep anti-UMOD (1:200) and rabbit anti-NKCC2 (1: 200) antibodies were kindly provided bij Prof. Hoenderop (Nijmegen, the Netherlands). Alexa Fluor 568 donkey anti-rabbit immunoglobulin G (IgG) or Alexa Fluor 568 donkey anti-goat IgG were used as secondary antibody (1:500; Invitrogen).

Nuclei were stained with Dapi (Thermo Scientific) or DRAQ5 (Biostatus). Immunofluorescence images were acquired using a confocal microscope (Leica, SP5 or SP8). Images were analyzed and processed using Leica LAS AF Lite or LAS X software (Leica SP5 or SP8 confocal).

Scanning electron microscopy

Organoids were fixed for 15 minutes with 1% (v/v) glutaraldehyde (Sigma) in phosphate buffered saline (PBS) at room temperature. Samples were subsequently serially dehydrated by consecutive 10 minute incubations in 2 ml of 10% (v/v), 25% (v/v) and 50% (v/v) ethanol-PBS, 75% (v/v) and 90% (v/v) ethanol-H_2O, and 100% ethanol (2x), followed by 50% ethanol-hexamethyldisilazane (HMDS) and 100% HMDS (Sigma). The samples were removed from the 100% HMDS and air-dried overnight at room temperature. After overnight evaporation of HMDS, samples were mounted onto 12 mm specimen stubs (Agar Scientific) and coated with gold to 1 nm using a Quorum Q150R sputter coater at 20 mA prior to examination with a Phenom PRO Table-top scanning electron microscope (PhenomWorld).

RNA sequencing of mouse organoids

For each organoid line (n=3) 4 wells of a 24 well plate (a total of 200 µl of Matrigel) were harvested with 1 ml TRIzol reagent. Two lines were 35 days in culture, one 70 days. Adult kidneys (n =3 mice) were snap frozen in liquid nitrogen, homogenized and subsequently treated with TRIzol reagent.

RNA was extracted using the TRIzol Plus RNA Purification Kit (Life Technologies) according to manufacturer's instructions and RNA samples were treated on column with PureLink DNase (Life Technologies). RNA quality was determined using a Bioanalyser 2100 (Agilent) with an RNA 6000 Nano Kit. Samples with a RNA Integrity Number greater than 9 were used for sequencing library preparation. Libraries were generated from 1 µg Total RNA using a TruSeq Stranded Total RNA kit with Ribo-zero human/mouse/rat (Illumina # RS-122-2201) per manufacturer's instructions. For final application, 11 cycles of PCR were used. Quality of the libraries was determined and libraries were quantified using a bioanalyser 2100 (Agilent) with a DNA 1000 Kit. Equimolar amounts of libraries were pooled and subjected to paired-end, 101 base-pair sequencing using an Illumina HiSeq 2000.

RNA sequencing analysis

RNA-seq reads were aligned to the mouse reference genome NCBIM37 using STAR [51]. The BAM files were sorted with Sambamba v0.5.1 [52] and transcript abundances were quantified with HTSeq-count [53]. Subsequently, DESeq 1.16.0 [54] was used to normalize gene counts and to test for differential expression between organoid and adult kidney. *P* values were adjusted for multiple testing using Benjamini-Hochberg FDR correction. Adjusted *P* values of < 0.05 were considered significantly up- or downregulated.

To determine which embryonic compartment organoids resemble the most in gene expression, we assessed the differential expression between adult mouse kidney and mouse organoids of available compartment- specific gene sets of embryonic mouse kidney and adult human kidney [27,55,56]. Mouse orthologs of human genes were found using biomaRt[57] and multiple mouse orthologs were

allowed. Gene symbols were converted to Ensembl Gene ID using org.Mm.eg.db[58] and genes that occurred in multiple segments or genes that we could not link to an Ensembl Gene ID were excluded from the analysis.

RNA-seq data can be found with GEO accession number: ERP019828, where "culture" refers to organoids and "kidney" to adult kidney.

Desmopressin stimulation

Organoids in 40 µl of Matrigel per condition were ADH-stimulated by removing the culture medium and addition of a 1:1 mix of organoid medium : 4 µg/ml Minrin (= desmopressinacetate, Ferring). In the control condition sterile PBS was added instead of Minrin. Samples were harvested 8, 24, or 48 hours after stimulation and RT-qPCR analysis on these samples was carried out as described below.

Real Time – Quantitative PCR (RT-qPCR)

Organoids were lysed and homogenised and total RNA was extracted with an RNEasy mini kit (Qiagen), according to the supplier's protocol. cDNA was synthesized from at least 500 ng RNA template, using the GoScript cDNA Synthesis Kit (Promega) as per manufacturer's instructions. Resulting cDNA was diluted (10x) and this was used to determine expression levels. The reference gene used was GAPDH (forward: ACCACTTTGGCATCGTGGAG; Reverse: GGGCCATCCACAGTCTTCTG; 60 degrees) and to detect AQP2 expression, the following primers were used: forward: ATGTGGGAACTCCGGTCCATA; reverse: ACGGCAATCTGGAGCACAG; 62 degrees.

The iQ SYBR Green Supermix (Bio-Rad) was used to multiply and measure the cDNA with a CFX96 Touch Real-Time PCR Detection System (Bio-Rad). Samples were run in triplicate in 20 µl reactions in the following PCR program: 95°C for 3 min, followed by 39 cycles of 10 s at 95°C, 30 s at the indicated annealing temperature and 30 s at 72°C, then 10 s at 95°C followed by a melt of the product from 65°C–95°C.

mRNA expression of AQP2 was normalised to GAPDH mRNA and expressed as fold change to controls with the ΔΔCT method.

Single cell sequencing

Sample and SORT-Seq library preparation

Samples were prepared according to the Sort-seq method as described previousy.[59] Briefly, Epcam+ primary kidney cells, FACSsorted (Facsjazz, BD) with Alexa-fluor 488 anti-human CD326 (Epcam, clone9C4; Biolegend), and the single cell suspension from passage 4 organoids (derived from the same tissue as the Epcam+ primary kidney cells) were single cell sorted into 384 well plates (Biorad) containing 5 µl vapor lock (Qiagen) 100-200 nl of RT primers, dNTPs and synthetic mRNA spike-ins.

Live single cells were selected on the basis of DAPI and forward/side scatter properties. After the sort, plates were spun down and frozen to -80 degrees until further processing.

RNA samples were processed into cDNA libraries as described previously[59,60] and on the basis of the CEl-seq2 technique. Illumina sequencing libraries were prepared with the TruSeq small RNA primers (Illumina) and sequenced paired-end at 75 bp read length the Illumina NextSeq. Primary cells and organoid cells were processed and sequenced in parallel.

Single Cell sequencing data Analysis

Paired-end reads from Illumina sequencing were aligned to the human transcriptome with BWA.[61] RaceID and RACEID2 analysis were performed as described.[22,23] Organoid cells with less than 4000 unique reads were discarded and samples with maximum expression less than 4 were discarded. Primary cell parameters with less than 4000 unique reads were discarded and samples with maximum expression less than 2 were discarded. In supplementary figures (Supplementary Figure 2 and 5) where organoid and primary cells were combined, cells with less than 2000 unique reads and samples with maximum expression less than 4 after down-sampling were discarded.

Karyotyping

Organoids were treated with 0.1 µg/ml colcemid (Gibco) for 16 h. Cultures were washed and dissociated into single cells using TrypLE (Gibco) and processed as previously described.[62] Slides were mounted with DAPI-containing Vectashield and analyzed on a DM6000 Leica microscope. At least 40 spreads were analyzed, in at least three independent experiments, from multiple organoid lines.

BK virus experiments

BK virus infection

Organoids were harvested, Matrigel was removed with cold ADMEM/F12, organoids were centrifuged, supernatant was taken off, and organoids were subsequently incubated in ADMEM/F12 with 1:100 BK virus (clinical isolate genotype BK1b-1, isolated from urine of an immunocompromised patient) for two hours at 37 degrees, with regular mixing. After incubation, organoids were centrifuged and after a wash step with ADMEM/F12, organoids were plated out in Matrigel. Samples were harvested either directly after incubation or after different periods in culture (1, 2, 5, 10 or 30 days after incubation) in 500 µl ADMEM/F12 and stored at -20°C until analysis.

Supernatant infection

400 µl of supernatant of a well (with 40 µl Matrigel) that was infected 10 days before was harvested and diluted 1:15 in ADMEM/F12. Subsequently, it was filtered with a Millex-GS 0.22 µm sterile filter unit (Merck Millipore Ltd) to remove cells, and this was used to infect organoids as described above. Samples were harvested either directly after incubation or after 10 days in culture in 500 µl ADMEM/F12 and stored at -20°C until analysis.

CDV inhibition experiment

Organoids were infected as described under BK virus infection. Organoids were cultured in organoid culture medium, supplemented with a range (0; 10; 20; 40; 80; 160; 320 µg/ml) of CDV (Selleckchem). A non-infected control was exposed to 80 µg/ml CDV. Organoids were harvested after 7 days of culture and during this period, culture media were refreshed twice. Samples were harvested in 500 µl ADMEM/F12 and stored at -20°C until analysis.

BK virus DNA extraction and real-time TaqMan PCR

Viral DNA was isolated using a MagNaPure 96 automated extraction system (Roche). Phocine Herpes Virus was added to the material prior to DNA extraction as an internal control. Samples were assayed in a 25 µl reaction mixture containing 10 µl isolate, Taqman universal PCR mastermix (applied Biosystems,

ABI), primers (300nM diagnostic primers; BK-forward: TGCTGATATTTGTGGSCTGTTTACTA; BK-reverse: CTCAGGCGRATCTTAAAATATCTTG) and fluorogenic probe (200nM diagnostic probe; probe A: CAGCTCTGGAACACAACAGTGGAGAGGC; Probe G: CAGCTC TGGGACACAACAGTGGAGAGGC) labelled with `5 reporter dye (FAM) and `3 quencher dye (TAMRA).

The amplification and detection were performed with an ABI 7500 system for 2 minutes at 50ºC, 10 minutes at 95ºC, and 45 cycles of 15 seconds at 95ºC and 1 minute at 60ºC. Samples were controlled for the presence of possible inhibitors of the amplification reaction by the indicated internal control, of which the signals had to be within the reference range.

In the CDV inhibition experiments, a PCR for human RNaseP was performed in parallel, to control for the quantity of human DNA.

Transmission EM

Organoids were infected as described under BK-virus infection and a negative control was included. Organoids (80 µl of Matrigel) were harvested after 10 days of culture. Matrigel was removed with recovery solution (Corning). Recovery solution was removed and 200 µl Karnovsky reagent was added. Samples were processed for transmission electron microscopy as described previously.[63]

Sequencing of BK virus DNA

The whole genome sequence of BK virus was obtained with the use of a modified sequence method described.[64] BK virus PCR fragments were obtained by fractional amplification of MagNAPure 96 total DNA isolates using the Superscript III one-step Reverse Transcriptase-PCR System with Platinum Taq High Fidelity kit (Invitrogen) and a 9800 Fast thermal cycler (ABI) according to the manufacturers protocol. PCR products were applied to a 1% agarose gel and purified from the gel with the use of GeneJet PCR purification kit (ThermoScientific). Isolated fragments were used for whole genome sequencing. Sequencing was performed by Macrogen Europe (Amsterdam, the Netherlands). The resulting sequence information was assembled into BK virus whole genome sequences through alignment with the reference BK virus genome GenBank accession no. V01108.

SV-40 stain

See histology and immunohistochemistry.

Genotyping

DNA from organoids and tissue was isolated with a gDNA ReliaPrep Kit (Promega) according to the manufacturer's instructions. Primers for PCR amplification of *WT1* with Phusion High-Fidelity Polymerase (Thermo Scientific), were, for exon 7[65]: fw (5'-ACCTACGTGAATGTTCACATGT-3'); rv (5'- GTTTGCCCAAGACTGGA-3' and for exon 10: fw (5'-GTGAAAAGCCCTTCAGCTGTC-3') and rv (5'-AAGGGTCAGGGGGACATGAT-3'). Products were clones into a CloneJET vector (Thermo Scientific) and sequenced using a T7 sequencing primer.

Low coverage whole genome sequencing for copy number profiling

Genome wide copy number alterations (CNA) were established using low-coverage whole genome sequencing. Shotgun libraries were prepared using the TruSeq Nano DNA Library Prep Kit (Illumina, San Diego, CA, USA) according to the manufacturer's recommendations.

Briefly, 50-180ng of input DNA (obtained with a Promega gDNA ReliaPrep Kit) from the primary tissues and the organoids were fragmented to 300bp in 130µl using the Covaris System (Covaris, Woburn, MA, USA). After concentrating the volume to 50µl end repair, A-tailing and adapter ligation were performed following the manufacturer's instructions. For selective amplification of the library fragments that have adapter molecules on both ends we used 12 PCR cycles. Libraries were quality checked on an Agilent Bioanalzyer using a DNA 7500 Chip (Agilent Technologies, Santa Clara, CA, USA) and quantified using qPCR with a commercially available PhiX library (Illumina, San Diego, CA, USA) as a standard. Libraries were pooled equimolarily and sequenced on an Illumina NextSeq in a 150bp single read run. Copy number analysis was performed as previously described.[66] Briefly, low-coverage whole-genome sequencing reads were mapped to the pseudo-autosomal-region (PAR)-masked genome and reads in different windows [~55kb] were counted and normalized by the total amount of reads. We further normalized read counts according to the GC-content using LOWESS-statistics. In order to avoid position effects we normalized the sequencing data with GC-normalized read counts of control samples. Subsequently we generated segments of similar copy-number values by applying circular binary segmentation (CBS) and Gain and Loss Analysis of DNA (GLAD).

P-gp transporter assay

Organoids were mechanically disrupted and seeded in BME on either glass bottom plates (for confocal imaging) or an opaque 96-well plate (for quantification in a fluorescence plate reader). Medium with or without P-gp-inhibitor PSC-833 (Tocris biosciences) at 5µM was added. The next day, calcein-AM (1µM; R&D Systems) was added with or without 5µM PSC-833. After 1 hour of incubation at 37° C, medium was removed and the cells were washed twice with 200 µl ice-cold Hank's Balanced Salt Solution (HBSS). Then, cells were either fixed in 2% (w/v) PFA (for confocal analysis) or cells were lysed by addition of 100 µl of 1% (v/v) Triton X-100 (fluorescent plate reader). Samples were used directly for analysis with a confocal microscope (SP5 or SP8, Leica) or a fluorescence plate reader (Ascent Fluoroskan FL microplate reader) with an excitation λ of 488 nm and an emission λ of 518 nm.

FSK swelling assay and intestinal organoid culture

The FSK-induced swelling assay and intestinal organoid culture was carried out as described before,[42] with the difference that swelling was measured for 3 hours after addition of FSK, in both intestinal as well as urine-derived organoids.

Statistical analysis

An unpaired *t*-test was performed to determine statistical differences when two groups were compared. In case of multiple groups, a one way ANOVA was performed, combined with Tukey post-hoc tests. A P -value < 0.05 was considered statistically significant.

Data availability

The data that support the findings of this study are available from the corresponding author on reasonable request.

ACKNOWLEDGMENTS

We thank the Hubrecht Imaging Center for assistance with (confocal) microscopy. We thank H. Begthel and J. Korving (both Hubrecht Institute) for preparation of histological and immunohistochemical specimens. We thank Dr. T. Nguyen and Dr. R. de Krijger for help with the analysis of histological specimens. We thank the Hubrecht FACS facility for help the sort of single (Epcam+) cells. Dr. G.P. Posthuma, (Department of Cell Biology and Institute of Biomembranes, UMC Utrecht, the Netherlands) for excellent support with transmission electron microscopy. We thank Prof. Dr. J. Hoenderop (Radboud UMC, the Netherlands) for kindly providing Umod and SLC12A1 antibodies. NC3R's for development of the kidney-on-a-chip assays (Nephrotube: CRACK-IT challenge).

This work was supported by a grant from the Dutch Kidney Foundation (DKF14OP04).

REFERENCES

1 Clevers, H. Modeling Development and Disease with Organoids. *Cell* **165**, 1586-1597, doi:10.1016/j.cell.2016.05.082 (2016).

2 Rookmaaker, M. B., Schutgens, F., Verhaar, M. C. & Clevers, H. Development and application of human adult stem or progenitor cell organoids. *Nat Rev Nephrol* **11**, 546-554, doi:10.1038/nrneph.2015.118 (2015).

3 Takasato, M. *et al*. Kidney organoids from human iPS cells contain multiple lineages and model human nephrogenesis. *Nature* **526**, 564-568, doi:10.1038/nature15695 http://www.nature.com/nature/journal/v526/n7574/abs/nature15695.html#supplementary-information (2015).

4 Morizane, R. *et al*. Nephron organoids derived from human pluripotent stem cells model kidney development and injury. *Nat Biotech* **33**, 1193-1200, doi:10.1038/nbt.3392 http://www.nature.com/nbt/journal/v33/n11/abs/nbt.3392.html#supplementary-information (2015).

5 Freedman, B. S. *et al*. Modelling kidney disease with CRISPR-mutant kidney organoids derived from human pluripotent epiblast spheroids. *Nature communications* **6**, 8715, doi:10.1038/ncomms9715 (2015).

6 Takasato, M. *et al*. Directing human embryonic stem cell differentiation towards a renal lineage generates a self-organizing kidney. *Nature cell biology* **16**, 118-126, doi:10.1038/ncb2894 (2014).

7 Taguchi, A. *et al*. Redefining the in vivo origin of metanephric nephron progenitors enables generation of complex kidney structures from pluripotent stem cells. *Cell stem cell* **14**, 53-67, doi:10.1016/j.stem.2013.11.010 (2014).

8 Mae, S.-I. *et al*. Monitoring and robust induction of nephrogenic intermediate mesoderm from human pluripotent stem cells. *Nature communications* **4**, 1367, doi:http://www.nature.com/ncomms/journal/v4/n1/suppinfo/ncomms2378_S1.html (2013).

9 Huch, M. *et al*. Long-Term Culture of Genome-Stable Bipotent Stem Cells from Adult Human Liver. *Cell* **160**, 299-312, doi:10.1016/j.cell.2014.11.050 (2015).

10 Boj, S. F. *et al*. Organoid models of human and mouse ductal pancreatic cancer. *Cell* **160**, 324-338, doi:10.1016/j.cell.2014.12.021 (2015).

11 Drost, J. *et al*. Sequential cancer mutations in cultured human intestinal stem cells. *Nature* **521**, 43-47, doi:10.1038/nature14415 http://www.nature.com/nature/journal/v521/n7550/abs/nature14415.html#supplementary-information (2015).

12 Gao, D. *et al*. Organoid cultures derived from patients with advanced prostate cancer. *Cell* **159**, 176-187, doi:10.1016/j.cell.2014.08.016 (2014).

13 Bartfeld, S. *et al*. In vitro expansion of human gastric epithelial stem cells and their responses to bacterial infection. *Gastroenterology* **148**, 126-136 e126, doi:10.1053/j.gastro.2014.09.042 (2015).

14 van de Wetering, M. *et al*. Prospective Derivation of a Living Organoid Biobank of Colorectal Cancer Patients. *Cell* **161**, 933-945, doi:10.1016/j.cell.2015.03.053 (2015).

15 Sato, T. *et al*. Single Lgr5 stem cells build crypt-villus structures in vitro without a mesenchymal niche. *Nature* **459**, 262-265, doi:10.1038/nature07935 (2009).

16 Sato, T. *et al*. Long-term expansion of epithelial organoids from human colon, adenoma, adenocarcinoma, and Barrett's epithelium. *Gastroenterology* **141**, 1762-1772, doi:10.1053/j.gastro.2011.07.050 (2011).

17 Stark, K., Vainio, S., Vassileva, G. & McMahon, A. P. Epithelial transformation of metanephric mesenchyme in the developing kidney regulated by Wnt-4. *Nature* **372**, 679-683 (1994).

18 Carroll, T. J., Park, J.-S., Hayashi, S., Majumdar, A. & McMahon, A. P. Wnt9b Plays a Central Role in the Regulation of Mesenchymal to Epithelial Transitions Underlying Organogenesis of the Mammalian Urogenital System. *Developmental cell* **9**, 283-292, doi:http://dx.doi.org/10.1016/j.devcel.2005.05.016 (2005).

19 Poladia, D. P. *et al*. Role of fibroblast growth factor receptors 1 and 2 in the metanephric mesenchyme. *Developmental biology* **291**, 325-339, doi:http://dx.doi.org/10.1016/j.ydbio.2005.12.034 (2006).

20 Xu, J., Lamouille, S. & Derynck, R. TGF-β-induced epithelial to mesenchymal transition. *Cell research* **19**, 156-172 (2009).

21 Watanabe, K. *et al*. A ROCK inhibitor permits survival of dissociated human embryonic stem cells. *Nat Biotech* **25**, 681-686, doi:http://www.nature.com/nbt/journal/v25/n6/suppinfo/nbt1310_S1.html (2007).

22 Grün, D. *et al*. Single-cell messenger RNA sequencing reveals rare intestinal cell types. *Nature* **525**, 251-255 (2015).

23 Grün, D. *et al.* De Novo Prediction of Stem Cell Identity using Single-Cell Transcriptome Data. *Cell stem cell* **19**, 266-277, doi:10.1016/j.stem.2016.05.010 (2016).

24 Zhou, X., Liao, W.-J., Liao, J.-M., Liao, P. & Lu, H. Ribosomal proteins: functions beyond the ribosome. *Journal of molecular cell biology*, mjv014 (2015).

25 Karafin, M. *et al.* Diffuse expression of PAX2 and PAX8 in the cystic epithelium of mixed epithelial stromal tumor, angiomyolipoma with epithelial cysts, and primary renal synovial sarcoma: evidence supporting renal tubular differentiation. *The American journal of surgical pathology* **35**, 1264-1273 (2011).

26 Jansen, J. *et al.* A morphological and functional comparison of proximal tubule cell lines established from human urine and kidney tissue. *Experimental cell research* **323**, 87-99, doi:http://dx.doi.org/10.1016/j.yexcr.2014.02.011 (2014).

27 Chabardes-Garonne, D. *et al.* A panoramic view of gene expression in the human kidney. *Proceedings of the National Academy of Sciences* **100**, 13710-13715 (2003).

28 Promeneur, D., Kwon, T.-H., Frøkiær, J., Knepper, M. A. & Nielsen, S. Vasopressin V2-receptor-dependent regulation of AQP2 expression in Brattleboro rats. *American Journal of Physiology-Renal Physiology* **279**, F370-F382 (2000).

29 Hirsch, H. H. *et al.* Polyomavirus-associated nephropathy in renal transplantation: interdisciplinary analyses and recommendations. *Transplantation* **79**, 1277-1286 (2005).

30 Bohl, D. L. & Brennan, D. C. BK Virus Nephropathy and Kidney Transplantation. *Clinical Journal of the American Society of Nephrology* **2**, S36-S46 (2007).

31 de Kort, H. *et al.* Primary human renal-derived tubular epithelial cells fail to recognize and suppress BK virus infection. *Transplantation* (2017).

32 Ganguly, N. *et al.* Low-dose cidofovir in the treatment of symptomatic BK virus infection in patients undergoing allogeneic hematopoietic stem cell transplantation: a retrospective analysis of an algorithmic approach. *Transplant Infectious Disease* **12**, 406-411, doi:10.1111/j.1399-3062.2010.00513.x (2010).

33 Cundy, K. C. *et al.* Clinical pharmacokinetics of cidofovir in human immunodeficiency virus-infected patients. *Antimicrobial agents and chemotherapy* **39**, 1247-1252 (1995).

34 Kalapurakal, J. A. *et al.* Management of Wilms' tumour: current practice and future goals. *The lancet oncology* **5**, 37-46 (2004).

35 Rivera, M. N. & Haber, D. A. Wilms' tumour: connecting tumorigenesis and organ development in the kidney. *Nature Reviews Cancer* **5**, 699-712 (2005).

36 Hohenstein, P., Pritchard-Jones, K. & Charlton, J. The yin and yang of kidney development and Wilms' tumors. *Genes & development* **29**, 467-482 (2015).

37 Hawthorn, L. & Cowell, J. K. Analysis of wilms tumors using SNP mapping array-based comparative genomic hybridization. *PloS one* **6**, e18941 (2011).

38 Hing, S. *et al.* Gain of 1q is associated with adverse outcome in favorable histology Wilms' tumors. *The American journal of pathology* **158**, 393-398 (2001).

39 Mengelbier, L. H. *et al.* Deletions of 16q in Wilms tumors localize to blastemal-anaplastic cells and are associated with reduced expression of the IRXB renal tubulogenesis gene cluster. *The American journal of pathology* **177**, 2609-2621 (2010).

40 Zhou, T. *et al.* Generation of human induced pluripotent stem cells from urine samples. *Nat. Protocols* **7**, 2080-2089, doi:http://www.nature.com/nprot/journal/v7/n12/abs/nprot.2012.115.html#supplementary-information (2012).

41 Dekkers, J. F. *et al.* Characterizing responses to CFTR-modulating drugs using rectal organoids derived from subjects with cystic fibrosis. *Science Translational Medicine* **8**, 344ra384-344ra384 (2016).

42 Dekkers, J. F. *et al.* A functional CFTR assay using primary cystic fibrosis intestinal organoids. *Nature medicine* **19**, 939-945, doi:10.1038/nm.3201 (2013).

43 Dekkers, J. F. *et al.* Potentiator synergy in rectal organoids carrying S1251N, G551D, or F508del CFTR mutations. *Journal of Cystic Fibrosis* **15**, 568-578 (2016).

44 Lam, A. Q. *et al.* Rapid and efficient differentiation of human pluripotent stem cells into intermediate mesoderm that forms tubules expressing kidney proximal tubular markers. *Journal of the American Society of Nephrology : JASN* **25**, 1211-1225, doi:10.1681/ASN.2013080831 (2014).

45 Gutierrez-Aranda, I. *et al.* Human Induced Pluripotent Stem Cells Develop Teratoma More Efficiently and Faster Than Human Embryonic Stem Cells Regardless the Site of Injection. *Stem Cells (Dayton, Ohio)* **28**, 1568-1570, doi:10.1002/stem.471 (2010).

46 VanDussen, K. L. *et al*. Notch signaling modulates proliferation and differentiation of intestinal crypt base columnar stem cells. *Development* **139**, 488-497, doi:10.1242/dev.070763 (2012).

47 Jansen, J. *et al*. Bioengineered kidney tubules efficiently excrete uremic toxins. *Scientific reports* **6**, 26715 (2016).

48 Jansen, J. *et al*. Biotechnological challenges of bioartificial kidney engineering. *Biotechnology advances* **32**, 1317-1327 (2014).

49 Kim, K.-A. *et al*. Mitogenic Influence of Human R-Spondin1 on the Intestinal Epithelium. *Science* **309**, 1256-1259 (2005).

50 Barker, N. *et al*. Lgr5(+ve) stem cells drive self-renewal in the stomach and build long-lived gastric units in vitro. *Cell stem cell* **6**, 25-36, doi:10.1016/j.stem.2009.11.013 (2010).

51 Dobin, A. *et al*. STAR: ultrafast universal RNA-seq aligner. *Bioinformatics* **29**, 15-21 (2013).

52 Tarasov, A., Vilella, A. J., Cuppen, E., Nijman, I. J. & Prins, P. Sambamba: fast processing of NGS alignment formats. *Bioinformatics* **31**, 2032-2034 (2015).

53 Anders, S., Pyl, P. T. & Huber, W. HTSeq—a Python framework to work with high-throughput sequencing data. *Bioinformatics* (2014).

54 Anders, S. & Huber, W. Differential expression analysis for sequence count data. *Genome Biology* **11**, 1-12, doi:10.1186/gb-2010-11-10-r106 (2010).

55 Schwab, K. *et al*. A catalogue of gene expression in the developing kidney. *Kidney international* **64**, 1588-1604 (2003).

56 Brunskill, E. W. *et al*. Atlas of Gene Expression in the Developing Kidney at Microanatomic Resolution. *Developmental cell* **15**, 781-791, doi:10.1016/j.devcel.2008.09.007 (2008).

57 Durinck, S., Spellman, P. T., Birney, E. & Huber, W. Mapping identifiers for the integration of genomic datasets with the R/Bioconductor package biomaRt. *Nature protocols* **4**, 1184-1191 (2009).

58 Carlson, M. org.Mm.eg.db: Genome wide annotation for Mouse. *R package* (2016).

59 Muraro, M. J. *et al*. A Single-Cell Transcriptome Atlas of the Human Pancreas. *Cell Systems* (2016).

60 Hashimshony, T. *et al*. CEL-Seq2: sensitive highly-multiplexed single-cell RNA-Seq. *Genome biology* **17**, 1 (2016).

61 Li, H. & Durbin, R. Fast and accurate short read alignment with Burrows–Wheeler transform. *Bioinformatics* **25**, 1754-1760 (2009).

62 Huch, M. *et al*. In vitro expansion of single Lgr5+ liver stem cells induced by Wnt-driven regeneration. *Nature* **494**, 247-250, doi:10.1038/nature11826 (2013).

63 Galmes, R. *et al*. Vps33B is required for delivery of endocytosed cargo to lysosomes. *Traffic* **16**, 1288-1305 (2015).

64 Tan, L. *et al*. Genetic variability among complete human respiratory syncytial virus subgroup A genomes: bridging molecular evolutionary dynamics and epidemiology. *PloS one* **7**, e51439 (2012).

65 Coppes, M. J., Liefers, G. J., Paul, P., Yeger, H. & Williams, B. R. Homozygous somatic Wt1 point mutations in sporadic unilateral Wilms tumor. *Proceedings of the National Academy of Sciences* **90**, 1416-1419 (1993).

66 Heitzer, E. *et al*. Tumor-associated copy number changes in the circulation of patients with prostate cancer identified through whole-genome sequencing. *Genome medicine* **5**, 1 (2013).

SUPPLEMENTARY INFORMATION

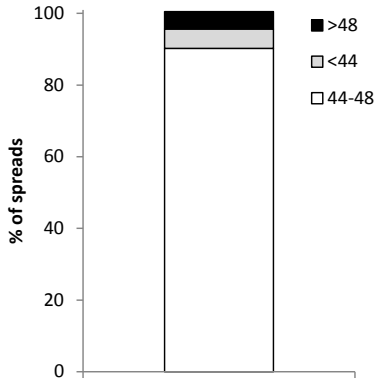

Supplementary Figure 1. Quantification of human metaphase spreads. > 40 spreads were quantified, from organoids in P11, P14 and P18 in 3 independent experiments.

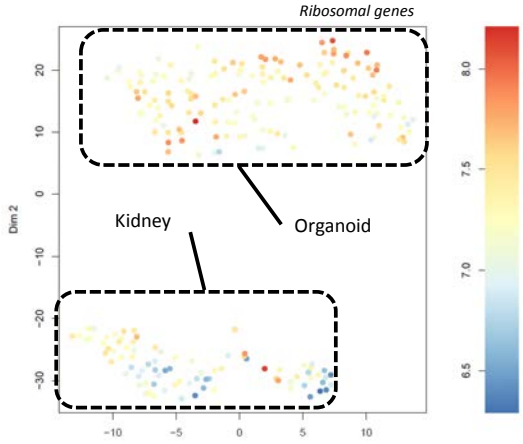

Supplementary Figure 2. Kidney organoids are more proliferative than primary kidney cells. The cells derived from organoids ("organoid") have a higher expression of ribosomal genes (indicating cell proliferation) and more cells express ribosomal genes, than the primary epithelial cells ("kidney") from which the organoids were derived, as shown on a transcript counts color coded t-SNE map.

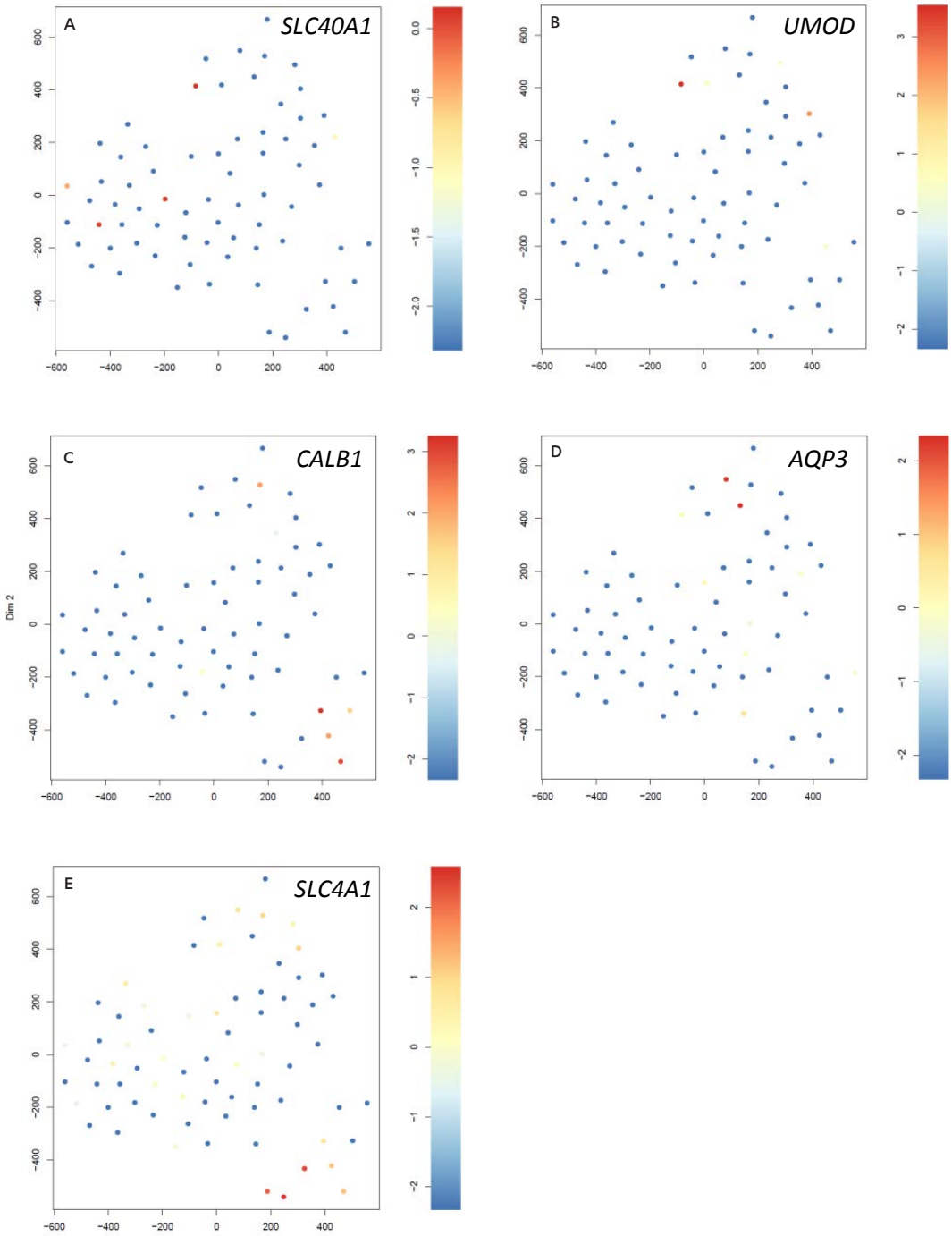

Supplementary Figure 3. Expression of marker genes in primary kidney epithelial cells. t-SNE maps for known marker genes with transcript counts color coded, with cells expressing proximal tubule marker *SLC40A1* (A), loop of Henle marker *UMOD* – note that there is one cell that overlaps with proximal tubule marker *SLC40A1* (B), distal tubule marker *CALB1* (C), collecting duct principal cell marker *AQP3* (D) and intercalated cell marker *SLC4A1* (E).

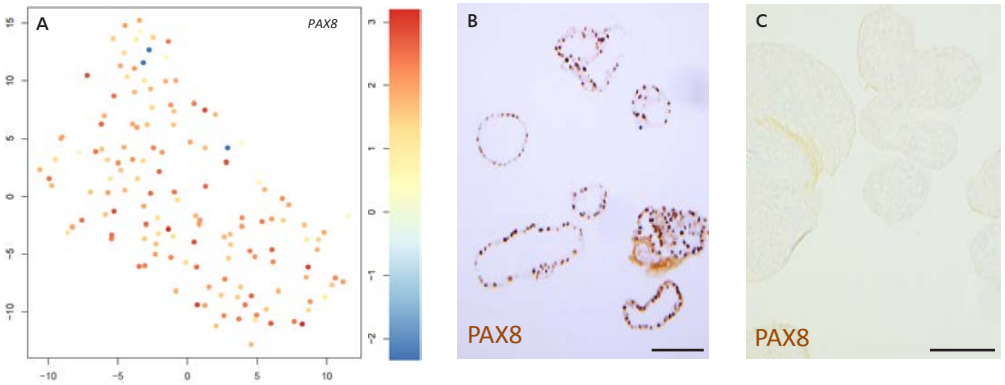

Supplementary Figure 4. Human kidney organoids are derived from kidney epithelium. t-SNE maps for marker genes with transcript counts color coded, show that virtually all organoid cells express the kidney epithelium marker *Pax8* (A). The expression of PAX8 is confirmed on the protein level (B) and a negative control does not show PAX8 staining (C).

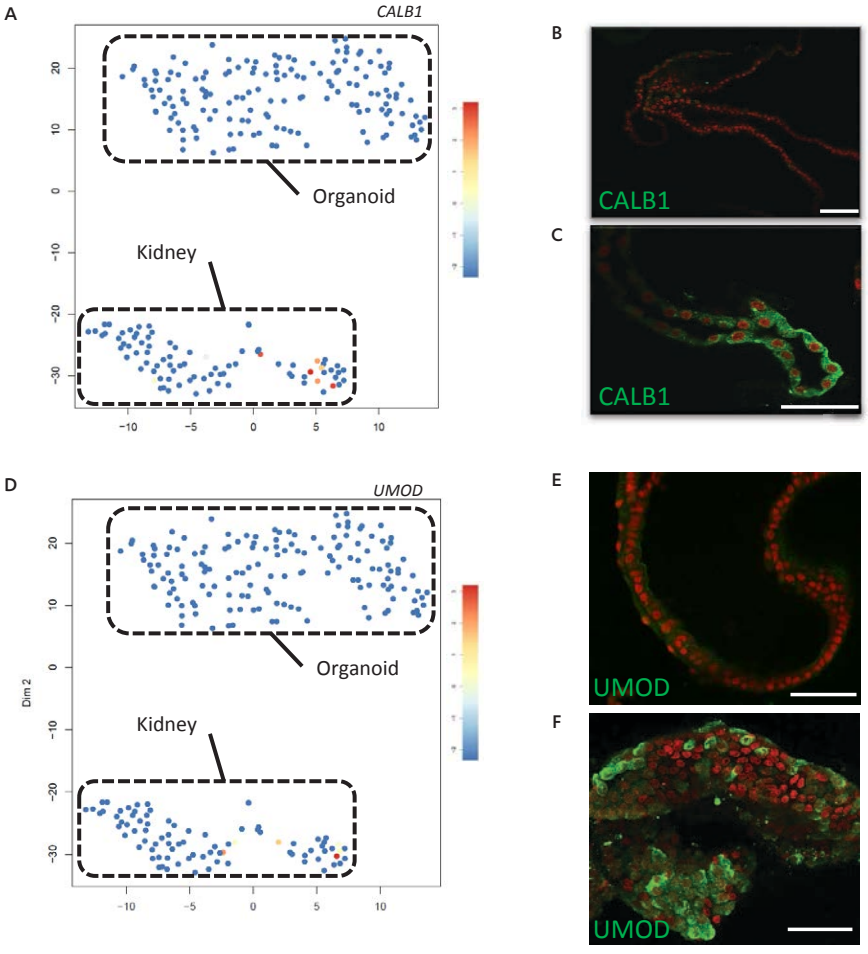

Supplementary Figure 5. Expression of distal tubule marker *CALB1* and loop of Henle marker *UMOD* can be induced by growth factor withdrawal. *CALB1* expression is absent in kidney organoids on the mRNA level, as ▶

Supplementary Figure 5. (continued)
shown with a transcript counts color coded t-SNE map (A) and protein level (B). By withdrawal of growth factors from the culture medium, CALB1 can be induced, as visualized with immunofluorescence (C). *UMOD* expression is absent in kidney organoids on the mRNA level, as shown with a transcript counts color coded t-SNE map (D) and protein level (E). By withdrawal of growth factors from the culture medium, UMOD can be induced, as visualized with immunofluorescence (F). Scale bar 75 µm.

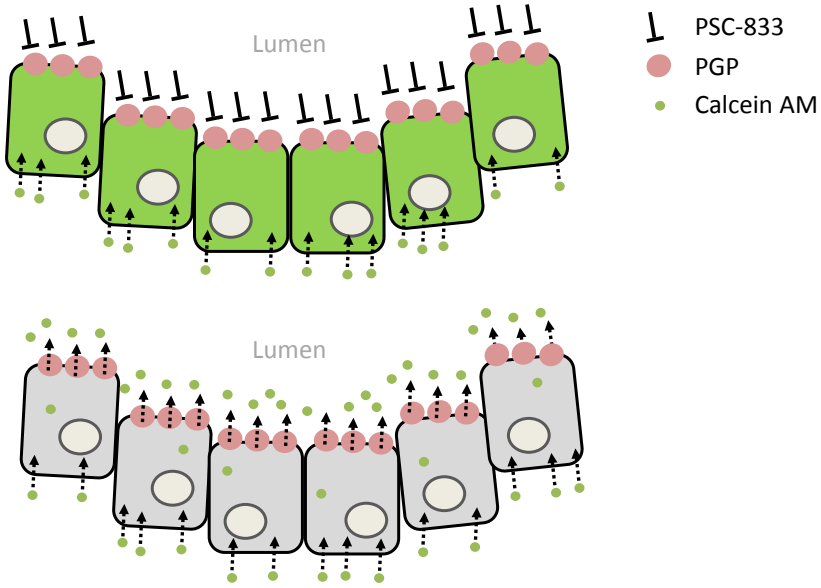

Supplementary Figure 6. Schematic representation of the proximal tubule functional assay. When organoids are exposed to calcein-AM, a substrate of P-gp (the xenobiotics efflux pump, located at the apical membrane) that diffuses freely into cells and that becomes fluorescent inside cells after cleaving the acetomethoxy group resulting in calcein, in the presence of an inhibitor (PSC-833) of P-gp, , calcein accumulates (A). In absence of the inhibitor, P-gp pumps calcein-AM from the cells, thereby preventing accumulation of fluorescent signal (B).

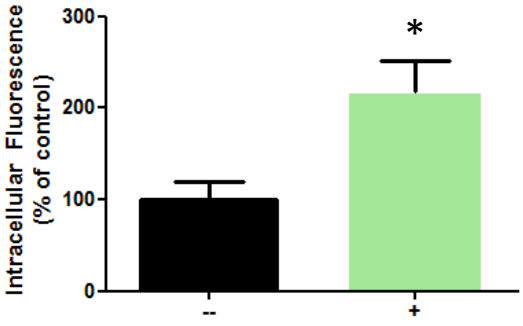

Supplementary Figure 7. P-gp is functional in human kidney organoids. In the presence of specific P-gp-inhibitor PSC-833, calcein accumulates in organoids, as measured by fluorescent plate reader. Quantification of n = 3 independent experiments. Error bars represent SEM. * = P < 0.004.

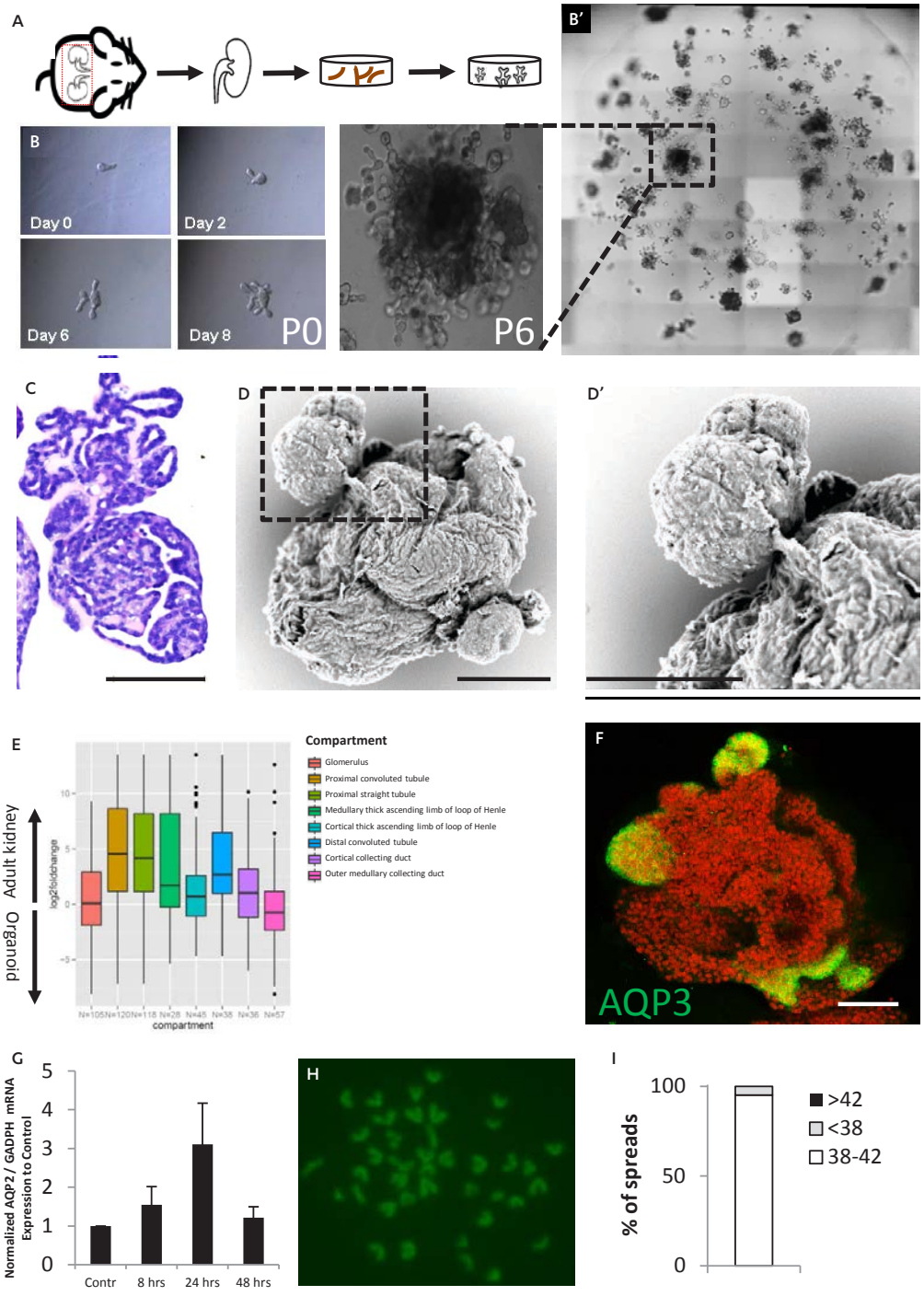
A
B
Day 0
Day 2
Day 6
Day 8
P0
P6
B'
C
D
D'
E
Adult kidney
Organoid
log2foldchange
compartment
N=105 N=120 N=118 N=28 N=45 N=38 N=36 N=57
Compartment
Glomerulus
Proximal convoluted tubule
Proximal straight tubule
Medullary thick ascending limb of loop of Henle
Cortical thick ascending limb of loop of Henle
Distal convoluted tubule
Cortical collecting duct
Outer medullary collecting duct
F
AQP3
G
Normalized AQP2 / GADPH mRNA Expression to Control
Contr
8 hrs
24 hrs
48 hrs
H
I
% of spreads
>42
<38
38-42

Supplementary Figure 8. Adult mouse kidney organoid culture. Mouse kidney organoid culture. Scheme of the experimental protocol (A). The development of mouse kidney epithelial cells into folded / branching structures after seeding (B). This branching / folded structure is maintained over time: an overview of a Matrigel droplet at passage 6 (B'). H&E stain at passage 7 (C). SEM image that displays the folded nature of the organoids (D), with D' as zoom of D. When assessing the expression levels of adult nephron compartments, organoids are upregulated for collecting duct genes, when compared to whole kidney. Gene lists were obtained from Garonne et al.[27] Number of genes per compartment is indicated below the graph (E). AQP3 expression is maintained over time (passage 7) in the budding parts of an organoid (F). Organoids respond to desmopressin stimulation by upregulating AQP2 expression (G, average of n = 3 independent experiments; error bars represent SEM). An example of a typical metaphase spread, from an organoid culture with passage number > 11 (H) Quantification of > 40 metaphase spreads in 3 independent experiments, from organoids from in P11, P15 and P16 (I). Scale bars 100 µm, except D & D': 50 µm.

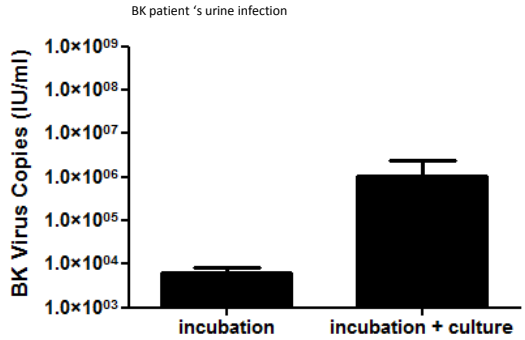

Supplementary Figure 9. Infection of organoids with urine from a patient suffering from BK virus-induced nephropathy. The number of virus particles after incubation with BK virus (*incubation*) or incubation and 10 days of culture (*incubation + culture*). The average of *n* = 3 experiments is plotted, error bars represent standard deviation.

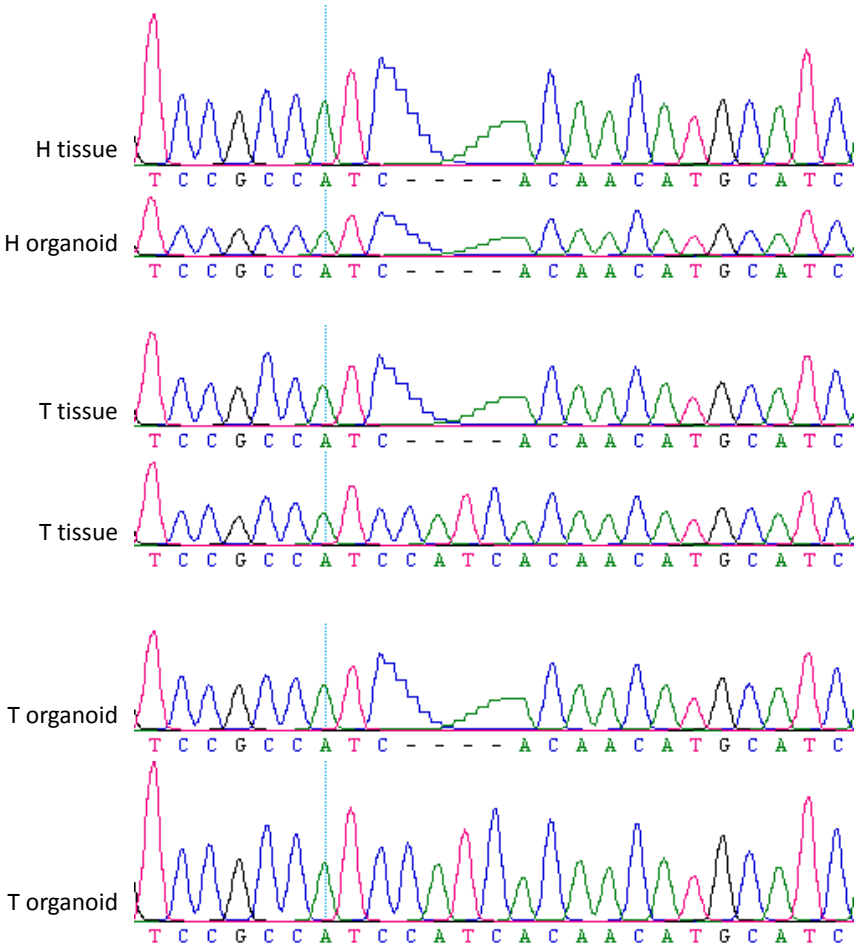

Supplementary Figure 10. Targeted sequencing of *WT1* shows a frameshift mutation in exon 10. Sanger sequencing shows a heterozygous 4 base pair insertion in the tumor tissue (T tissue) and the organoids derived from the tumor tissue (T organoid). This insertion is absent in the healthy kidney tissue (H tissue) and organoids derived from the healthy tissue (H organoid).

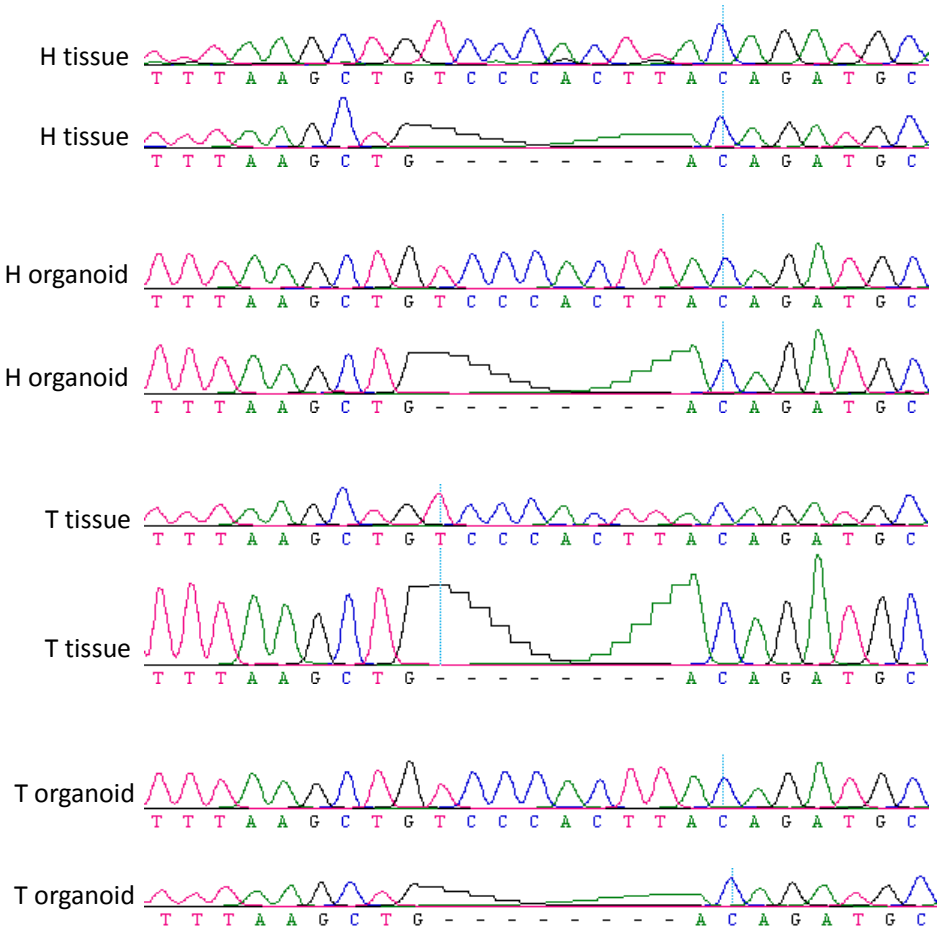

Supplementary Figure 11. Targeted sequencing of *WT1* shows a frameshift mutation in exon 7. Sanger sequencing shows a heterozygous 8 base pair deletion in the healthy kidney tissue (H tissue); organoids derived from the healthy tissue (H organoid); tumor tissue (T tissue) and the organoids derived from the tumor tissue (T organoid).

Supplementary Figure 12. Urine-derived organoids from a subject with CF are kidney organoids. Assessed with a PAX8 staining. Scale bar 100 µm.

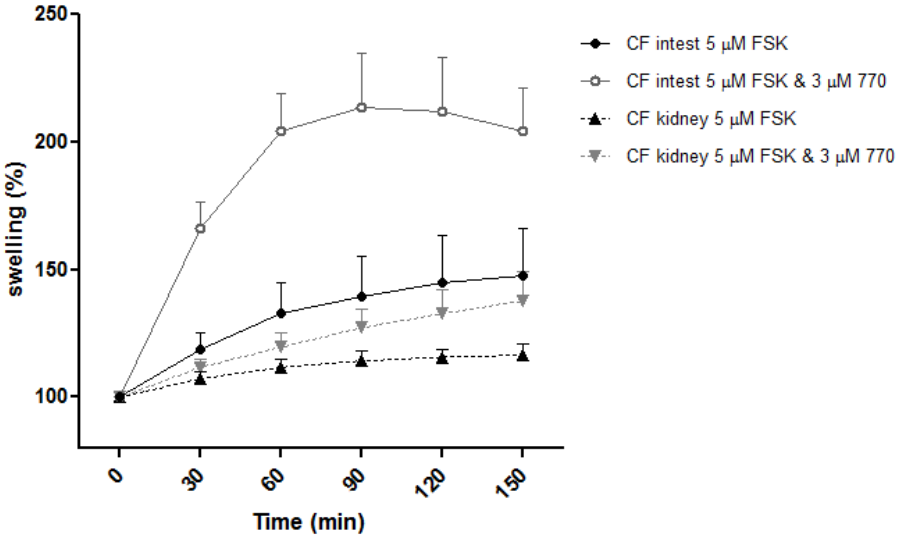

Supplementary Figure 13. The effect of VX-770 on FSK-induced swelling in organoids. In urine-derived organoids and intestinal organoids from the same patient, VX-770 increased FSK induced swelling. Average is plotted of *n* = 2 independent experiments, error bars represent standard deviation.

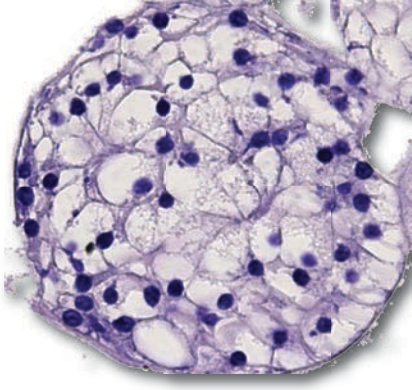

CHAPTER 4

A LIVING ORGANOID BIOBANK OF PEDIATRIC KIDNEY TUMOR PATIENTS

ABSTRACT

Kidney tumors are among the most common solid childhood tumors. These tumors include a wide range of subtypes that differ in terms of frequency of appearance and prognosis. Although prognosis of particular subtypes improved significantly over the last decades, several subtypes have a dismal outcome and harsh chemotherapy causes severe side effects later in life.

Patient-derived organoid cultures have great potential for drug development and personalized medicine. Here, we report the establishment of tumor organoid cultures and matching healthy kidney organoid cultures from 37 children with different subtypes of kidney cancer. These tumor organoids recapitulated properties of the original tumor *in vitro* as assessed by histology and immunohistochemistry.

Our living biobank of pediatric kidney tumor organoid cultures opens up experimental avenues for basic tumor biology research, high-throughput drug screening and personalized medicine.

Frans Schutgens[1,2], Carola Ammerlaan[1,2], Maarten B. Rookmaaker[2], Marry van den Heuvel – Eibrink[3], Ronald de Krijger, Marianne C. Verhaar[2], Hans Clevers[1,3], Jarno Drost[3]

[1] Hubrecht Institute–Royal Netherlands Academy of Arts and Sciences, Utrecht, the Netherlands
[2] Department of Nephrology and Hypertension, University Medical Centre Utrecht, the Netherlands
[3] Princess Máxima Center for Pediatric Oncology, Utrecht, the Netherlands

INTRODUCTION

Three-dimensional (3D) organoid culture models open new opportunities for both fundamental and translational cancer research (*Drost and Clevers, under revision*). Originally established for mouse small intestine,[1] organoids can currently be efficiently established from primary patient material of a wide variety of healthy and diseased tissues.[2] Previously, it was demonstrated that organoids derived from healthy tissue are genomically stable over long periods of time, whereas tumor-derived organoids recapitulate the genetic heterogeneity of the native tissue.

Kidney cancer is the one of the most frequently diagnosed solid cancers in children.[3] The majority (~90%) of the pediatric kidney tumors are Wilms tumors (nephroblastoma), while the most common non-Wilms tumors include malignant rhabdoid tumor of the kidney (MRTK) and renal cell carcinoma (RCC).

Wilms tumors likely result from differentiation defects during kidney development, resulting in nephrogenic rests that may develop into malignant tumors.[4] For Wilms tumors, overall survival rates are high (~90% 5 year survival).[5] However, it leads to loss of the affected kidney and long-term side effects due to the harsh chemotherapy treatment. Additionally, high-risk Wilms tumors (25% of all patients) have adverse outcome with 60% 5 year survival.[5] The classical Wilms tumor is histologically characterized by a tri-phasic pattern, with blastemal, epithelial and stromal components.[6] However, predominance of one of the components may also occur: i.e. stromal, epithelial, and blastemal subtypes, or anaplastic, when diffuse anaplasia is present. A phenomenon that can be observed in the stromal component of Wilms tumor is the differentiation towards muscle, termed rhabdomyomatous differentiation.[19] Rhabdomyomatous differentiation appears as patchy pink structures on H&E that stain for the muscle marker Desmin. The classification in subtypes affects prognosis: anaplastic and pre-treated Wilms tumors of blastemal-type have a poor disease outcome. Therefore, these are categorized as high-risk and treated with more aggressive chemotherapy. Genetically, Wilms tumors are heterogeneous tumors with mutations in *WT1* (often combined with *CTNNB1* mutations) or *WTX* in 30% of the cases.[7, 8] Additionally, mutations in S*IX1* and *SIX2*, and microRNA processing genes, such as *DROSHA* and *DGCR8*, were recently identified in blastemal-type Wilms tumors, whereas the majority of anaplastic Wilms tumors harbor mutations in *TP53*.[9, 10] In addition, in 75% of the Wilms tumors, copy number variations occur, which are typically gain of 1q, chromosome 8, chromosome 12 and loss of 16q.[4, 11-13]

The other kidney tumor types are genetically and histologically distinct from Wilms tumors. At least 95% of MRTKs harbor inactivating mutations in the SWI/SNF protein complex member *SMARCB1* (*INI1*).[14] On histology, MRTKs have a rhabdomyosarcomatoid pattern,[16] but to more conclusively diagnose a MRTK, SMARCB1 immunostainings are routinely used, as SMARCB1 expression is present in all normal cells, but lost in 95% of the MRTKs.[20] RCCs typically have translocations of Xp11.2 or t(6;11).[15, 16] Histologically, RCCs may have a clear or granular cytoplasm with pleomorphic nuclei.[17] Both MRTKs and RCCs have a poor prognosis, with 5 year survival rates of 26%[18] and 60%,[17] respectively. Thus, there is an urgent need to develop more effective and less toxic treatment strategies, for which pre-clinical culture models are highly valuable.

Currently, pre-clinical culture models sustaining efficient and long term *in vitro* propagation of patient-derived kidney tumor tissue are lacking. The most prevalent human-derived *in vitro* model systems are cell lines, which are usually derived from late stage tumors and do not reflect

the heterogeneity of native tumor tissue. Moreover, their establishment is inefficient and matching normal lines are lacking, making them a poor model for drug development and individualized therapy.

Based on our protocol for culturing organoids from healthy and diseased human kidney tissue (**Chapter 3**), we now describe the establishment and histologic characterization of paired organoids derived from different tumor types and healthy epithelium from children with kidney cancer. This biobank may facilitate drug development and individualized therapy in the future.

RESULTS

Establishment of a living organoid pediatric kidney tumor biobank

Tumor and matching normal kidney tissue were obtained after nephrectomy (Figure 1A). We established 37 organoid lines from pediatric kidney tumors and matching normal tissue using our previously described culture protocol (**Chapter 3**). Typically, the first organoids appeared 7 days after seeding and could be passaged 14 days after seeding. Pediatric kidney tumor organoids could be cryopreserved and efficiently recovered (*data not shown*).

Efficiency of establishment (defined as growth of organoids from a patient for at least 3 passages) was 100% for normal tissue and 90% (26 out of 29), 100% (5 out of 5), and 100% (4 out of 4) for Wilms tumor, MRTK, and RCC tissue, respectively. Organoids could not always be established from pre-treated Wilms tumor tissue, likely due to vast amounts of necrotic tissue. From one MRTK, organoids were established from a lymph node metastasis as well as from the primary tumor. In addition, organoids could be established from a metanephric adenoma (1 out of 1; Supplementary Figure 1A) and a metanephric fibroadenoma (1 out of 1; Supplementary Figure 1B), which are tumor types that very rarely occur. An epithelial angiomyolipoma did not expand in our culture conditions (0 out of 1; *data not shown*). Finally, from one clear cell sarcoma of the kidney (CCSK) cells initially grew out, but ceased proliferation after 2 passages (Supplementary Figure 1C), suggesting that culture medium optimizations might be required to sustain growth of this tumor type.

Expansion capacity varied within and among different tumor types. 20 out of 26 Wilms tumor organoids could be for expanded for at least 10 passages with average split ratios of 1:2-1:3 every 10 days. Within this group, 8 tumor organoid lines could be expanded for over 20 passages, including 3 lines that are currently in passage 32, 37 or 43. Of note, the most recent established Wilms tumor cultures did not have the time to reach high a passage number, thereby underestimating the expansion capacity here. MRTKs were roughly passaged weekly with 1:3 split ratios, for > 20 passages. Lastly, 3 pre-treated RCCs (3 out of 3) could be expanded for 6 passages with 1:3 splits every 14 days and one untreated RCC (1 out of 1) could be expanded for at least 10 passages, suggesting that organoids derived from pre-treated RCCs might be more difficult to expand long term.

To assess whether tumor cells were cultured, we performed a histologic analysis of 25 of the organoid lines (Figure 1B, Supplementary Table 1) that were selected on the basis of tumor type and expansion capacity. The selection comprised the major types of pediatric kidney tumors: Wilms tumor (n = 19), MRTK (n = 4) and RCC (n = 1). In addition, we included syndromal tumors (Beckwith Wiedemann; n = 4), a nephrogenic rest (n = 1), and ensured a mix between tumors with (n = 21) or without (n = 4) pre-nephrectomy chemotherapy (Supplementary Table 1).

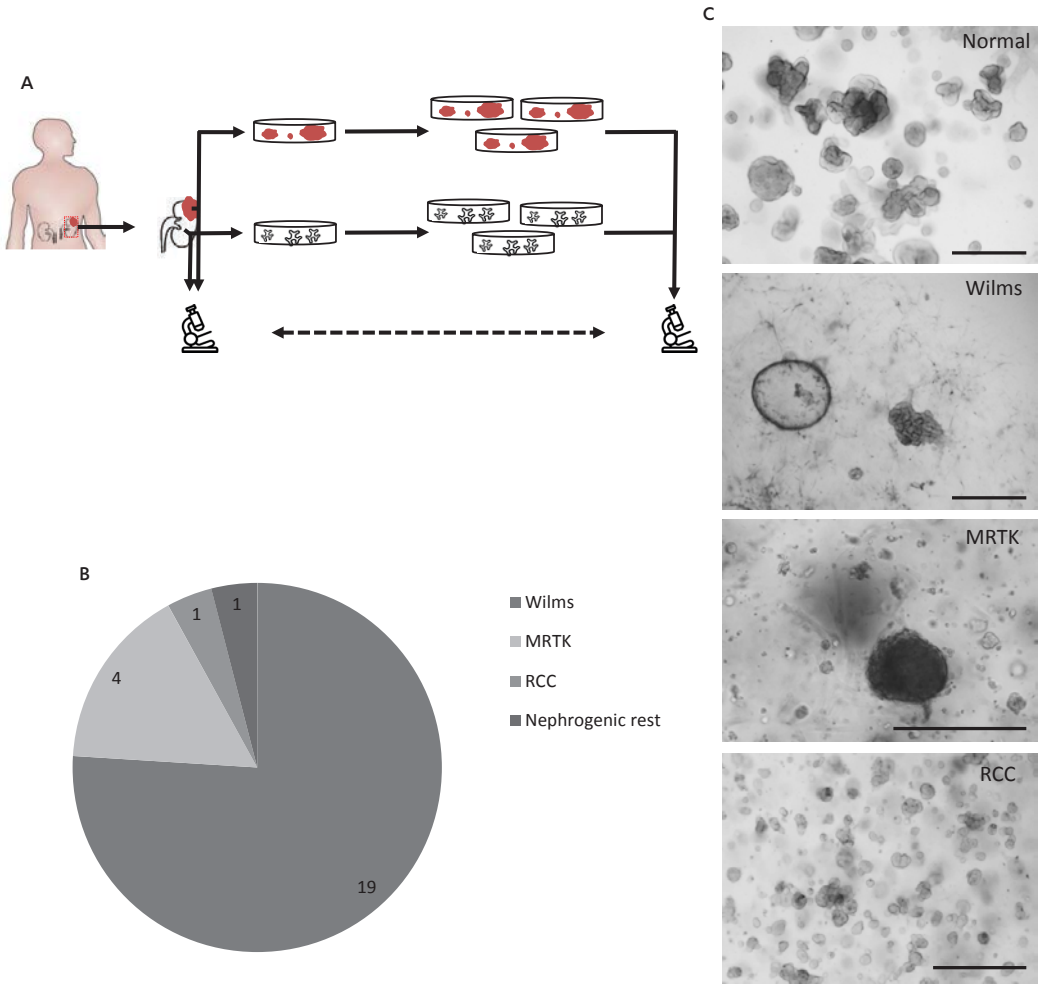

Figure 1. Establishment of a living pediatric kidney tumor organoid biobank. Overview of the study set-up. Organoid lines were established from tumor and matching normal tissue and histology of the organoids was compared with the primary tumor (A). Composition of the 25 organoid samples that were analyzed in detail (B, more characteristics can be found in *supplementary table 1*). Representative brightfield microscopy images of the organoid lines from the different tumor types and one normal sample (which is the matched normal sample of the depicted Wilms tumor) (C). Scale bars: 500 µm.

Morphologically, most organoid lines established from tumor tissue were different from the matched normal organoids (Figure 1C and Supplementary Figure 2), suggesting that the organoids indeed were tumor-derived. As previously described (**Chapter 3**), organoids derived from healthy kidney tissue are usually folded in the first passages (Figure 1C). In contrast, Wilms tumor-derived organoid cultures contained a mix of different components in which some structures were cystic from the start (Figure 1C). MRTK-derived organoids appeared in grape-like clumps of cells and RCC organoids remained small, rounded structures (Figure 1C).

Histologic characterization of pediatric kidney tumor organoids

In several cases, histologic analysis revealed that the organoid lines closely resembled the original tumor tissue. A Wilms tumor where blastema, epithelium and stroma were present, yielded a triphasic culture of organoids that was maintained for at least 10 passages (**Chapter 3**, Figure 3), whereas a Wilms tumor with a significant epithelial component, yielded a predominantly epithelial organoid line (Figure 2A).

In addition, we observed rhabdomyomatous differentiation in the organoids: when Desmin-positive pink structures were found in a Wilms tumor, Desmin-positive pink structures could be detected in the organoid line derived thereof (Figure 2B).

The cellular composition of MRTK organoids displayed the typical rhabdomyosarcomatoid pattern, thereby resembling the primary tumor (Figure 3A). In one organoid line, loss of SMARCB1 was observed in the primary tumor tissue and the lymph node metastasis, as expected. The loss of SMARCB1 was also observed in all organoids established from both tissues (Figure 3B). Not surprisingly, the immune infiltrate in the tumor, as well as the normal tissue and organoids derived thereof, were positive for SMARCB1 (Figure 3B). In a different MRTK-derived line, a mix of normal and tumor cells was observed (Supplementary Figure 3).

The RCC showed typical clear cells in the primary tumor and these were also represented in the organoids (Figure 4).

An overview of the H&E stainings of all organoid lines and tissues is provided in Supplementary Figure 4.

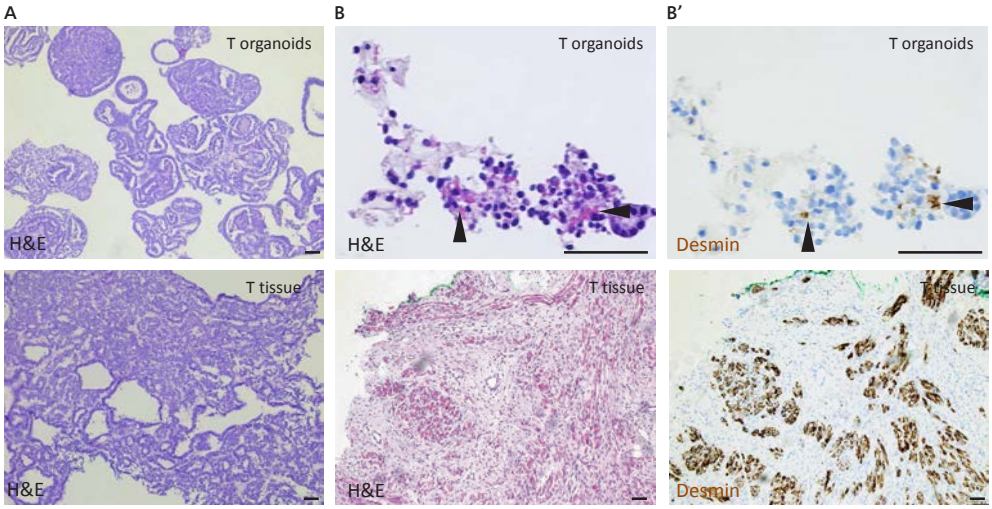

Figure 2. Histology of Wilms tumor organoid lines. Typical example of an epithelial Wilms tumor (*T tissue*) on H&E staining, where the tumor-derived organoid line (*T organoids*) is similarly epithelial in nature (A) Rhabdomyomatous differentiation of stromal cells in the primary tumor tissue (*T tissue*) appears pinkish on H&E staining and in stromal cells present in the tumor organoid (*T organoid*) culture, similar pinkish structures are present (B) The pink-colored structures stained positive for Desmin in the primary tumor tissue (*T tissue*) as well as the organoid line (*T organoids*) (B'). Scale bars: 50 µm.

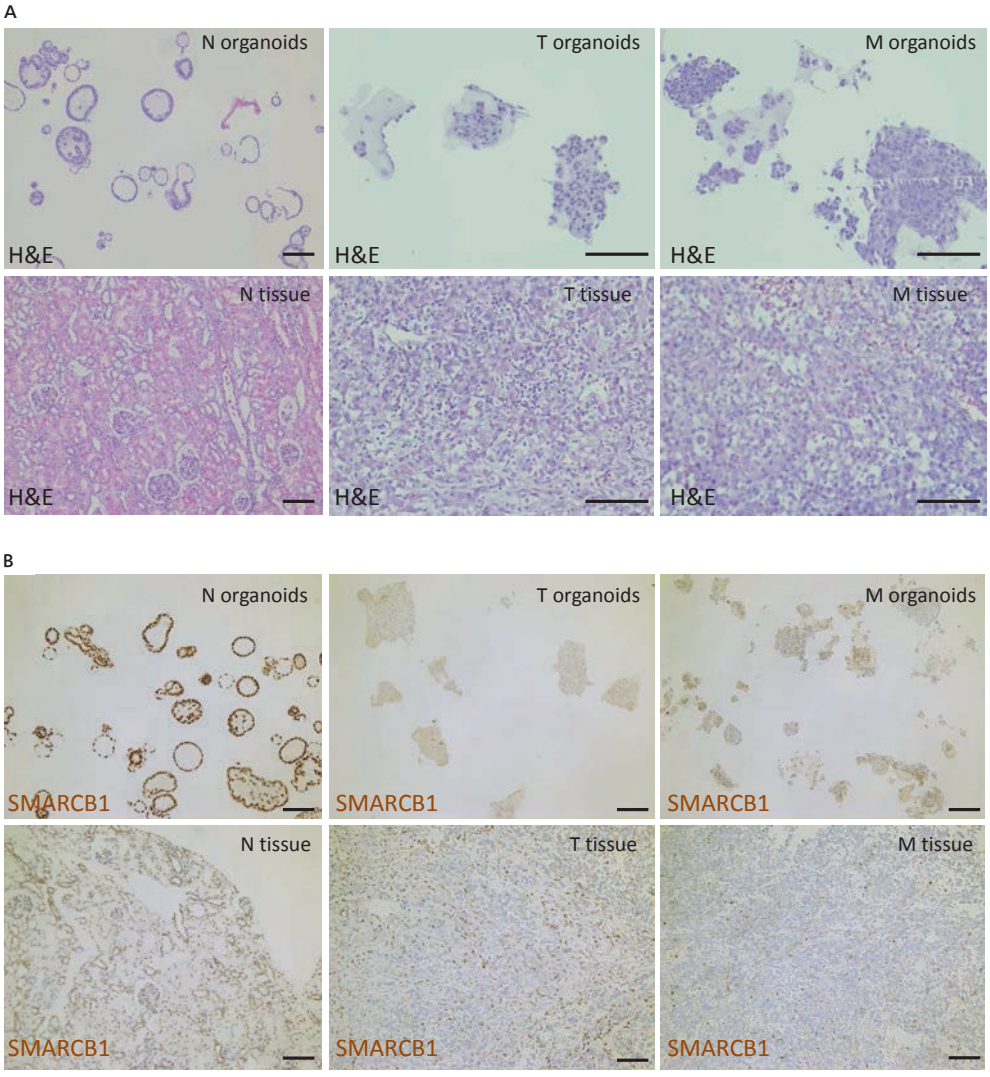

Figure 3. Histology of a MRTK-derived organoid line. Normal tissue-derived organoids (*N organoids*) have the typical cystic structure on H&E staining, whereas MRTK-derived organoids (*T organoids*) and MRTK metastasis-derived organoids (*M organoids*) form clusters of cells that resemble the cells in the primary tumor (*T tissue*) and metastasis (*M tissue*) (A). The tumor tissues (*T tissue; M tissue*) and tumor-derived organoids (*T organoids; M organoids*) do not stain for SMARCB1, except for tumor infiltrating immune cells, whereas normal kidney tissue (*N tissue*) and normal organoids (*N organoids*) do stain for SMARCB1 (B). Scale bars: 100 µm.

DISCUSSION

Here, we describe the establishment and characterization of a living pediatric kidney tumor organoid biobank that includes organoids derived from Wilms tumors, MRTKs and RCCs. Organoids can be established with high efficiency from primary tumor tissue and matching normal tissue. We

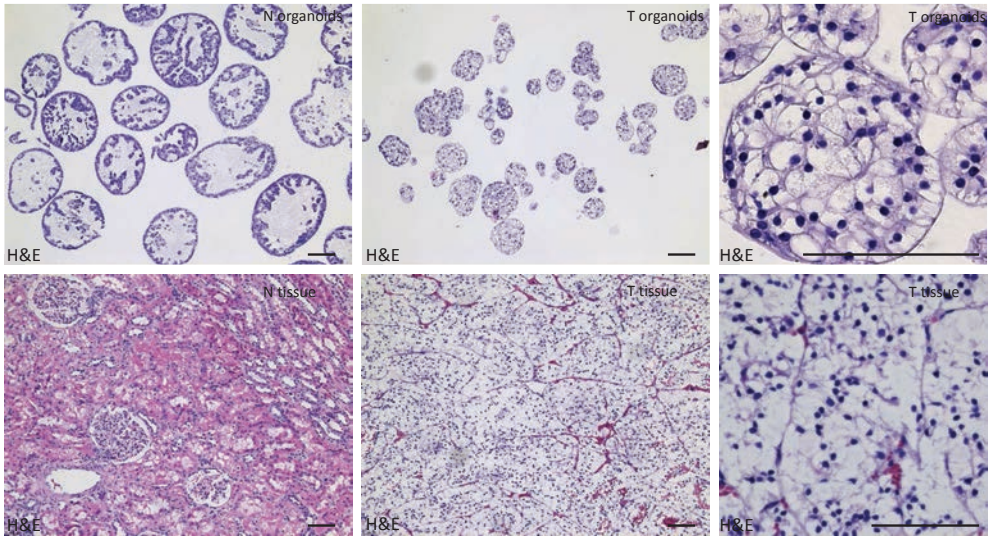

Figure 4. Histology of a RCC-derived organoid line. Normal tissue-derived organoids (*N organoids*) have the typical cystic structure on H&E staining, whereas RCC-derived organoids (*T organoids*) consist of cells with a typical clear cell morphology, that are also present in the primary tumor (*T tissue*). Scale bars: 100 µm.

demonstrate that in many cases tumor organoid lines resemble the native tumor tissue on histology. Our organoid biobank faithfully recapitulates native tumor tissue and may in the future be used for pediatric kidney cancer research and drug discovery.

Methods to study patient-derived pediatric kidney tumors thus far, have been cell lines or patient-derived xenografts. A small subset of cell lines has been established for Wilms tumors harboring *WT1* mutations.[22] In addition, a few MRTK cell lines have been established[23, 24] (one of which was at first falsely identified as Wilms tumor cell line[25]) and a translocation-type RCC[26] cell line is available. Cell lines have been the golden standard for *in vitro* oncological research and although they have contributed immensely to our understanding of tumor biology, cell lines have significant drawbacks. Cell lines are clonal expansions from the original tumor and therefore tumor heterogeneity is lost. Generally, establishing cell lines is not efficient (e.g. 12% reported for adult renal cell carcinoma[27]), but the efficiency of establishing the specific tumor cell lines mentioned above was not reported. In addition, cell lines were only established from sub-sets of tumors, indicating selection effects. Finally, histological characteristics of the tumor are not retained and matching normal cell lines were not established.

Patient-derived xenografts (PDXs), a model in which tumor tissue samples from a patient are transplanted into mice, are available for Wilms tumors.[28] PDXs most likely better retain tumor heterogeneity, but are expensive to establish and high-throughput analyses are complicated by the number of mice required.

Hitherto, a culture protocol sustaining growth of a variety of pediatric kidney tumor subtypes and matching healthy control tissue has been lacking. The high efficiency of establishing tumor

organoid lines reduces potential selection effects, thereby increasing the chance that the whole spectrum of tumors is covered. In addition, as the organoid lines established are non-clonal and multiple cell types are present, *in vivo* tumor heterogeneity is better reflected than in cell lines: to our knowledge it is the first time that non-epithelial cells are expanded in an ASC-organoid culture.

To further validate our biobank additional analyses are to be done. A whole genome sequencing analysis will indicate whether the tumor organoids have the same genetic aberrations as the primary tumor and whether these are absent in the matched normal line. Xenotransplantation into mice will show whether tumor organoids are tumorigenic upon transplantation and whether the tumor grown *in vivo*, reflects the primary tumor. Proof-of-principle drug screening will indicate whether the patient's drug response, reflects the response observed in the organoids.

In addition, by adaptation of culture conditions, it may become feasible to establish long-term cultures for CCSKs, for which no cell lines are available (Gooskens et al., *manuscript submitted*).

Because of the high efficiency, culture of matched normal tissue and heterogeneity of the organoids, we expect that pediatric kidney tumor organoid culture will enhance the study of fundamental tumor biology as well as metastatic potential and drug resistance in the future. In tumor biology, single cell-derived cultures, combined with (single cell) RNA sequencing will be of use to study how blastemal, epithelial, and stromal components develop from one another. Metastatic potential can be studied by transplantation of organoid lines into mice. Organoids will enable drug-screening for the development of new therapies as well as personalized medicine, as demonstrated previously for tumor organoids ([21] and Sachs et al., *under review*).

MATERIAL AND METHODS

Human tissue

All experiments with human tissue were approved by the medical ethical committee of the University Medical Centre Utrecht and written informed consent from patients was obtained.

Organoid culture

Tumor tissue or healthy cortical kidney was minced and collagenase digested (1 mg/ml, C9407, Sigma) for 45 minutes at 37°C. Fragments were seeded in growth factor-reduced BME (R&D Systems) and cultured in medium (ADMEM / F12 supplemented with 1% penicillin / streptomycin, HEPES, Glutamax), with 1.5% B27 supplement (Gibco), 10% Rspo1-conditioned medium,[29] EGF (50 ng/ml, Peprotech), FGF-10 (100 ng/ml, Preprotech); N-acetylcysteine (1.25 mM, Sigma), Rho-kinase inhibitor Y-27632 (10 µM, Abmole) A8301 (5 µM, Tocris Bioscience), primocine (0.1 mg/ml, Invivogen).

Histology and immunohistochemistry

Tissues were fixed in 4% paraformaldehyde, dehydrated and embedded in paraffin. Sections were subjected to H&E and / or immunohistochemical staining. IHC was performed according to standard protocols on 3–4 µm sections. The primary antibodies were Desmine (1:10, NCL-L-DES-DER11, Novocastra) and SMARCB1/INI1 (1:20, 612111, Transduction labs). Sections were counter-stained with haematoxylin.

REFERENCES

1. Sato, T. et al. Single Lgr5 stem cells build crypt-villus structures in vitro without a mesenchymal niche. *Nature* **459**, 262-5 (2009).
2. Clevers, H. Modeling Development and Disease with Organoids. *Cell* **165**, 1586-1597 (2016).
3. Stiller, C.A. Epidemiology and genetics of childhood cancer. *Oncogene* **23**, 6429-6444 (2004).
4. Hohenstein, P., Pritchard-Jones, K. & Charlton, J. The yin and yang of kidney development and Wilms' tumors. *Genes & Development* **29**, 467-482 (2015).
5. Pritchard-Jones, K. et al. Treatment and outcome of Wilms' tumour patients: an analysis of all cases registered in the UKW3 trial. *Annals of oncology*, mds025 (2012).
6. Rivera, M.N. & Haber, D.A. Wilms' tumour: connecting tumorigenesis and organ development in the kidney. *Nature Reviews Cancer* **5**, 699-712 (2005).
7. Maiti, S., Alam, R., Amos, C.I. & Huff, V. Frequent association of β-catenin and WT1 mutations in Wilms tumors. *Cancer research* **60**, 6288-6292 (2000).
8. Ruteshouser, E.C., Robinson, S.M. & Huff, V. Wilms tumor genetics: Mutations in WT1, WTX, and CTNNB1 account for only about one–third of tumors. *Genes, Chromosomes and Cancer* **47**, 461-470 (2008).
9. Bardeesy, N. et al. Anaplastic Wilms' tumour, a subtype displaying poor prognosis, harbours p53 gene mutations. *Nature genetics* **7**, 91-97 (1994).
10. Gordon, D.J., Resio, B. & Pellman, D. Causes and consequences of aneuploidy in cancer. *Nature Reviews Genetics* **13**, 189-203 (2012).
11. Hawthorn, L. & Cowell, J.K. Analysis of wilms tumors using SNP mapping array-based comparative genomic hybridization. *PloS one* **6**, e18941 (2011).
12. Mengelbier, L.H. et al. Deletions of 16q in Wilms tumors localize to blastemal-anaplastic cells and are associated with reduced expression of the IRXB renal tubulogenesis gene cluster. *The American journal of pathology* **177**, 2609-2621 (2010).
13. Hing, S. et al. Gain of 1q is associated with adverse outcome in favorable histology Wilms' tumors. *The American journal of pathology* **158**, 393-398 (2001).
14. Jackson, E.M. et al. Genomic analysis using high-density single nucleotide polymorphism-based oligonucleotide arrays and multiplex ligation-dependent probe amplification provides a comprehensive analysis of INI1/SMARCB1 in malignant rhabdoid tumors. *Clinical cancer research* **15**, 1923-1930 (2009).
15. Song, H.C. et al. Biological characteristics of pediatric renal cell carcinoma associated with Xp11. 2 translocations/TFE3 gene fusions. *Journal of pediatric surgery* **49**, 539-542 (2014).
16. Royer-Pokora, B. Genetics of pediatric renal tumors. *Pediatric Nephrology* **28**, 13-23 (2013).
17. Young, E.E., Brown, C.T., Merguerian, P.A. & Akhavan, A. 42-49 (Elsevier).
18. van den Heuvel-Eibrink, M.M. et al. Malignant rhabdoid tumours of the kidney (MRTKs), registered on recent SIOP protocols from 1993 to 2005: a report of the SIOP renal tumour study group. *Pediatric blood & cancer* **56**, 733-737 (2011).
19. Anderson, J., Slater, O., McHugh, K., Duffy, P. & Pritchard, J. Response without shrinkage in bilateral Wilms tumor: significance of rhabdomyomatous histology. *Journal of pediatric hematology/ oncology* **24**, 31-34 (2002).
20. Sigauke, E. et al. Absence of expression of SMARCB1/INI1 in malignant rhabdoid tumors of the central nervous system, kidneys and soft tissue: an immunohistochemical study with implications for diagnosis. *Modern pathology* **19**, 717-725 (2006).
21. van de Wetering, M. et al. Prospective Derivation of a Living Organoid Biobank of Colorectal Cancer Patients. *Cell* **161**, 933-945 (2015).
22. Royer-Pokora, B. et al. Wilms tumor cells with WT1 mutations have characteristic features of mesenchymal stem cells and express molecular markers of paraxial mesoderm. *Human molecular genetics* **19**, 1651-1668 (2010).
23. Ota, S., Crabbe, D.C.G., Tran, T.N., Triche, T.J. & Shimada, H. Malignant rhabdoid tumor. A study with two established cell lines. *Cancer* **71**, 2862-2872 (1993).
24. Karnes, P.S. et al. Establishment of a rhabdoid tumor cell line with a specific chromosomal abnormality, 46,XY,t(11;22)(p15.5;q11.23). *Cancer Genetics and Cytogenetics* **56**, 31-38 (1991).
25. Garvin, A.J., Re, G.G., Tarnowski, B.I., Hazen-Martin, D.J. & Sens, D.A. The G401 cell line, utilized for studies of chromosomal changes in Wilms' tumor, is derived from a rhabdoid tumor of the kidney. *The American Journal of Pathology* **142**, 375-380 (1993).

26. Mathur, M., Das, S. & Samuels, H.H. PSF-TFE3 oncoprotein in papillary renal cell carcinoma inactivates TFE3 and p53 through cytoplasmic sequestration. *Oncogene* **22**, 5031-5044 (0000).

27. Ebert, T., Bander, N.H., Finstad, C.L., Ramsawak, R.D. & Old, L.J. Establishment and characterization of human renal cancer and normal kidney cell lines. *Cancer Research* **50**, 5531-5536 (1990).

28. Pode-Shakked, N. et al. Developmental tumourigenesis: NCAM as a putative marker for the malignant renal stem/progenitor cell population. *Journal of cellular and molecular medicine* **13**, 1792-1808 (2009).

29. Kim, K.-A. et al. Mitogenic Influence of Human R-Spondin1 on the Intestinal Epithelium. *Science* **309**, 1256-1259 (2005).

SUPPLEMENTARY INFORMATION

Supplementary Table 1. Characteristics of the study participants. A = actinomycin D; V = vincristin; D = doxorubicin.

Line	Gender	Year of birth	Diagnosis	Low/intermediate/ high risk	Pre-op treatment	Predominant Subtypes
1	F	2013	Wilms	intermediate	6 weeks VAD	Regressive type
2	F	2014	Wilms	intermediate	6 weeks AV	Bilateral, material from 1 kidney. 3 tumors, tumor 1 and 2 regressive, tumor 3 nephroblastomasis
3	F	2013	Wilms	intermediate	4 weeks AV	Mixed type (blastema/stroma)
4	F	2010	Wilms	intermediate	4 weeks AV	Mixed type (blastema/stroma/ epithelium)
5	F	2009	Wilms (Beckwith Wiedemann)	intermediate	4 weeks AV	Mixed type (blastema/ epithelium)
6	M	2016	MRTK	n/a	4 weeks AV	n/a
7	F	2015	MRTK	n/a	5 weeks AV	n/a
8	F	2015	Wilms	high	4 weeks AV	Blastemal type
9	M	2011	Wilms	treated as high risk	4 weeks AV	2 tumors: 1 triphasic; and 1 blastemal type AND diffuse anaplasia
10	M	2016	MRTK	n/a	2 weeks AV	n/a
11	F	2013	Wilms	intermediate	4 weeks AV	Mixed type (minimal blastema/ stroma/ epithelium)
12	F	2015	Wilms	intermediate	4 weeks AV + 1 cycle carbo/ etoposide	Stromal type
13	F	2013	Wilms	intermediate	4 weeks AV	Mixed type (blastema/ epithelium)
14	M	2016	Wilms	intermediate	untreated	Epithelial type
15	M	2015	Wilms	intermediate	4 weeks AV	Stromal type
16	F	2016	Wilms	intermediate	4 weeks AV	Mixed type (65% blastema)
17	M	2014	Wilms (Beckwith Wiedemann)	unknown which tumor is which	4 weeks AV	3 tumors: 1) blastemal predominant, 2 and 3) regressive, no anaplasia
18	M	2014	Wilms	unknown which tumor is which	4 weeks AV	4 tumors: 1-3 blastemal predominant, 4) regressive
19	F	2013	Wilms	intermediate	4 weeks AV	Regressive type
20	F	2012	Wilms (Beckwith Wiedemann)	high	8 weeks AV	Bilateral, 3 tumors from right kidney: 1) diffuse anaplasia, 2) regressive, 3) nephrogenic rest
21	F	2014	Wilms	intermediate	6 weeks VAD	Stromal subtype
22	F	2016	Nephrogenic rest (Beckwith Wiedemann)	n/a	4 weeks AV	Nephrogenic rest
23	F	2017	MRTK	n/a	untreated	n/a
24	F	2002	RCC	n/a	untreated	pX11.2 translocation
25	F	2016	Wilms	intermediate	untreated	Mixed type (blastema/epithelium/ small stromal component)

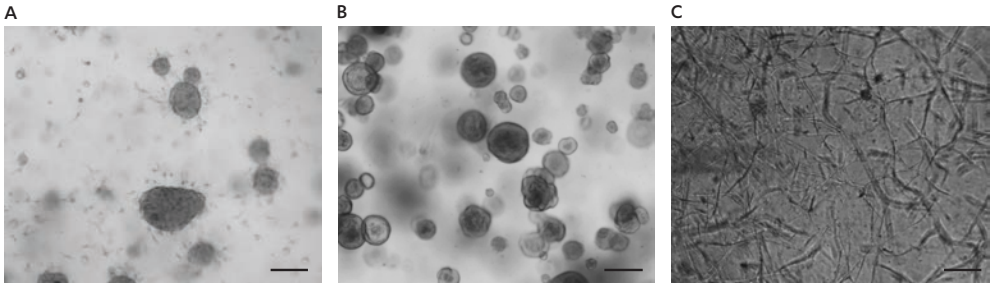

Supplementary Figure 1. Brightfield images of organoids from very rare kidney tumors. Organoids established from a metanephric adenoma (A), metanephric fibroadenoma (B) and a CCSK (C). Scale bars: 200 µm.

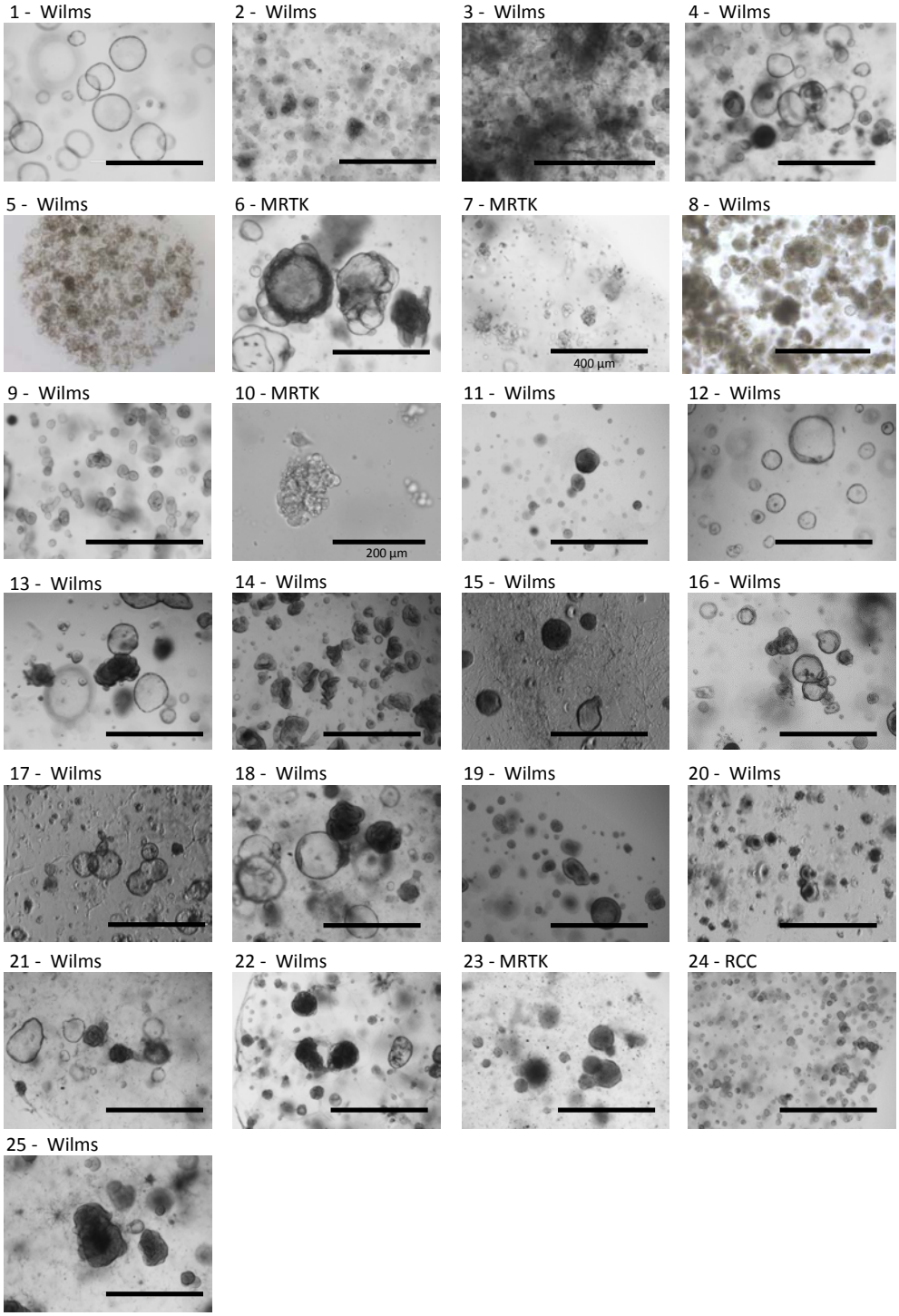

Supplementary Figure 2. An overview of the 25 tumor organoid lines in brightfield. The normal lines are not provided, as these all have a similar morphology. Scale bars: 1000 µm, unless otherwise indicated.

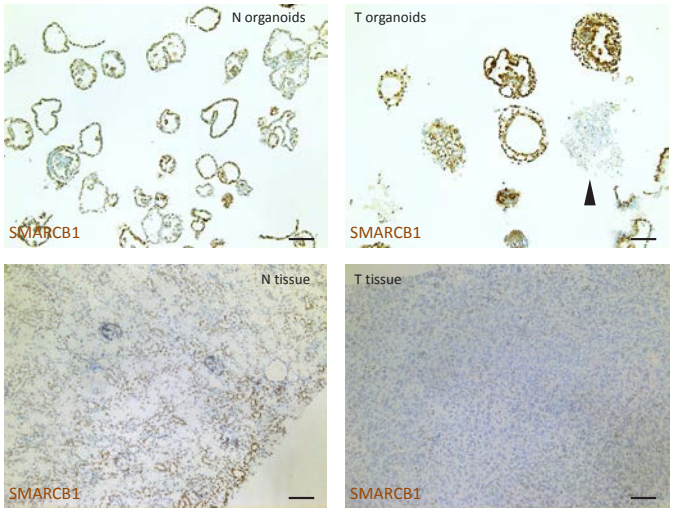

Supplementary Figure 3. A MRTK-derived organoid line is a mix between normal and tumor cells. Normal tissue (*N tissue*) and organoids derived thereof (*N organoids*) stain for SMARCB1. The primary tumor tissue (*T tissue*) is negative for SMARCB1 and the organoid line (*T organoids*) is a mix between SMARCB1 positive and negative (*arrow head*) cells, indicating a mix between tumor and normal cells. Scale bars: 100 µm.

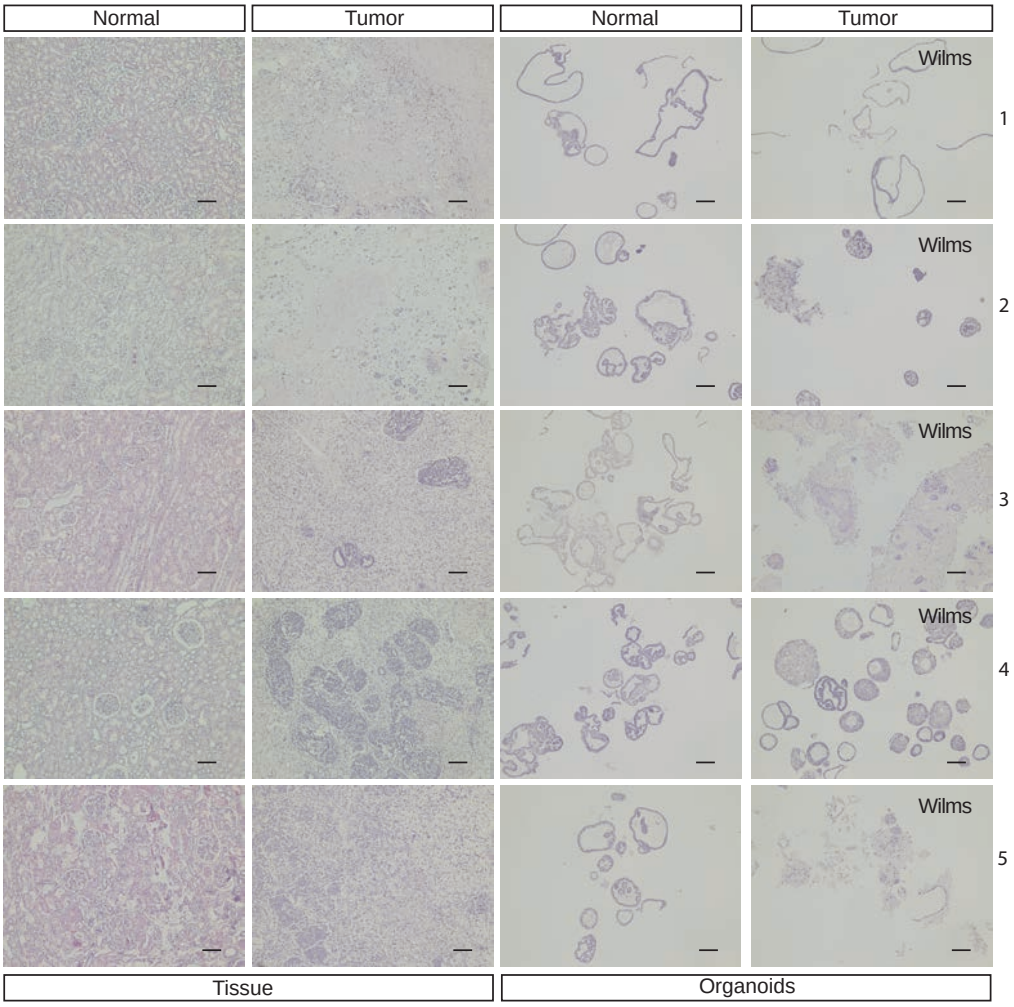

Supplementary Figure 4. An overview of H&E stainings of 25 tumor tissues and organoid lines derived thereof, with matching normal tissues and organoid lines derived thereof. For sample 12, no normal tissue was received and for sample 17, histology is in progress. Scale bars: 100 µm.

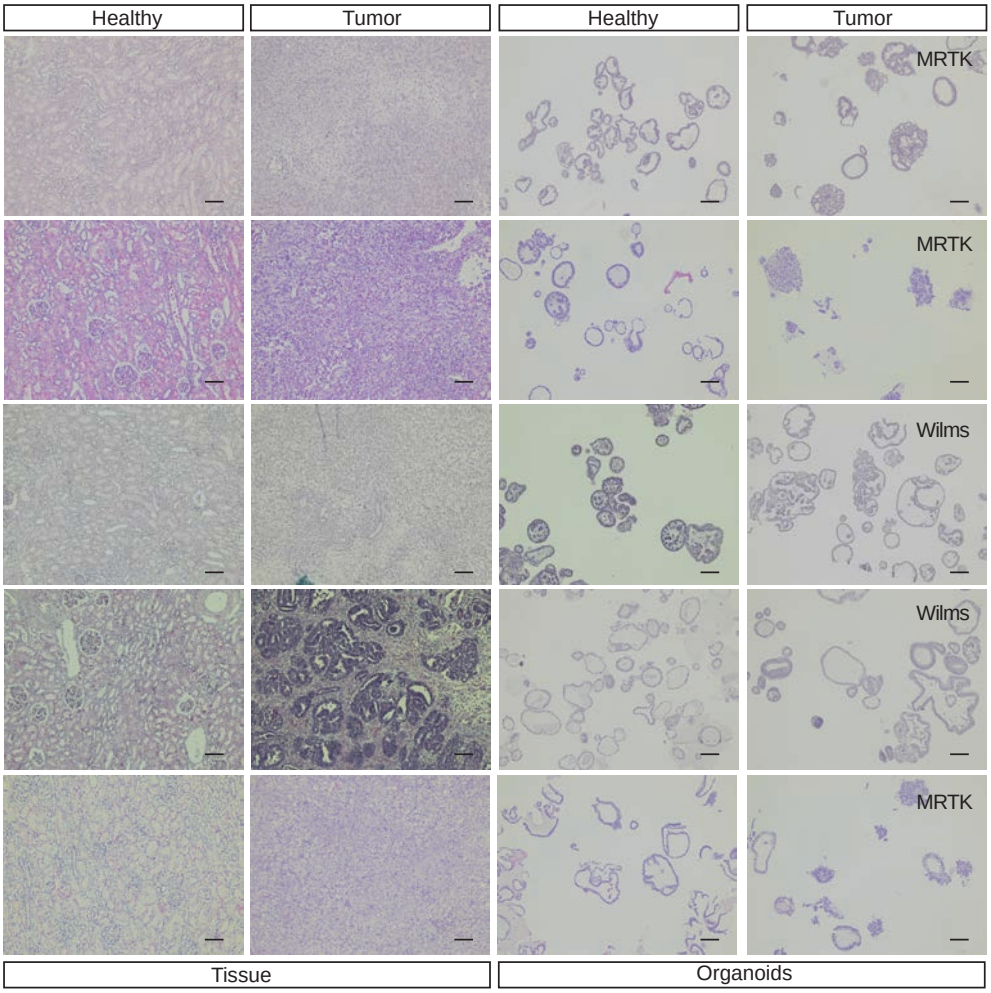

Supplementary Figure 4. (continued)

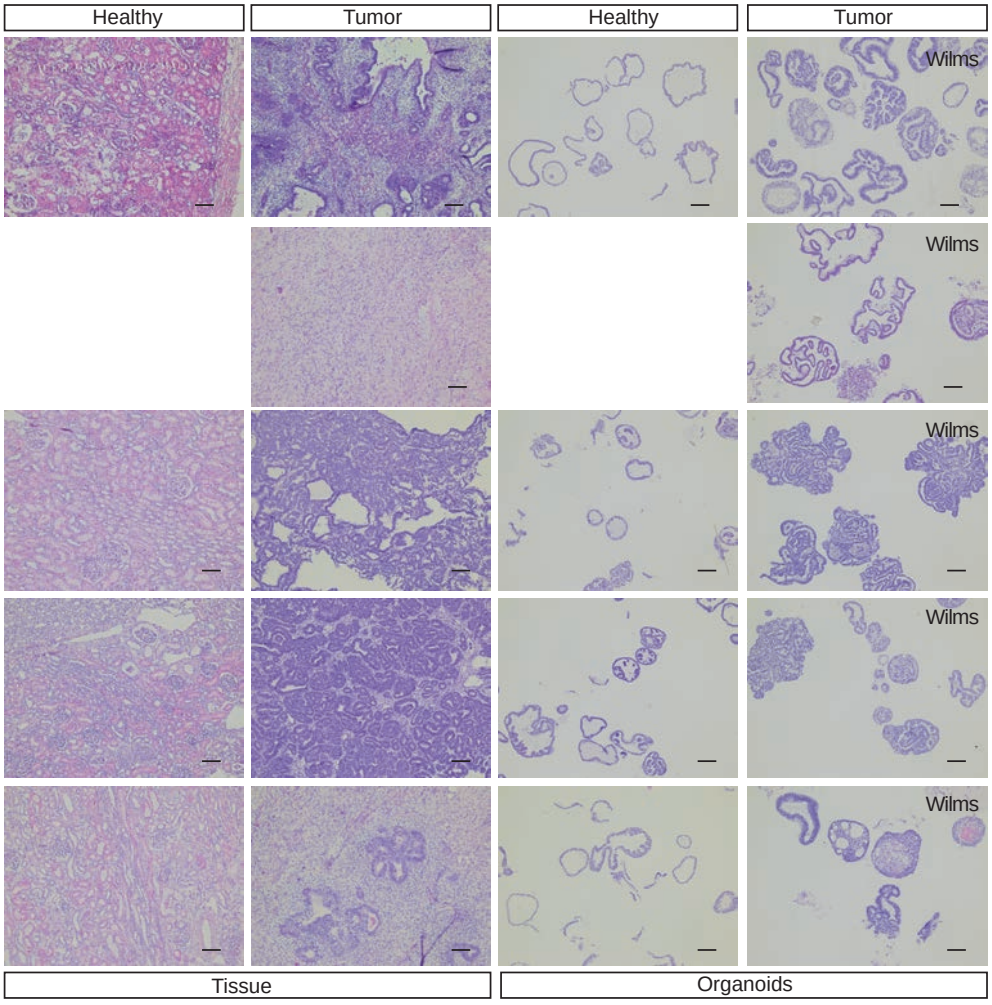

Supplementary Figure 4. (continued)

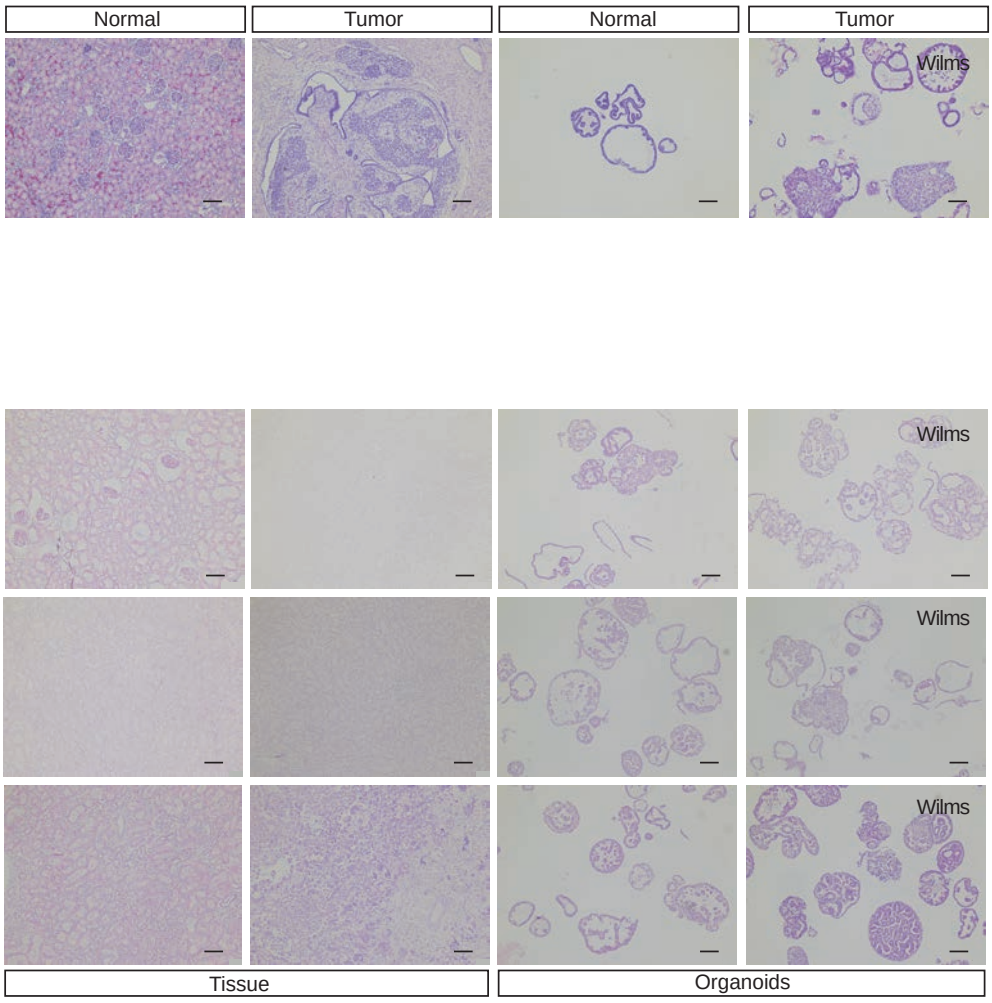

Supplementary Figure 4. (continued)

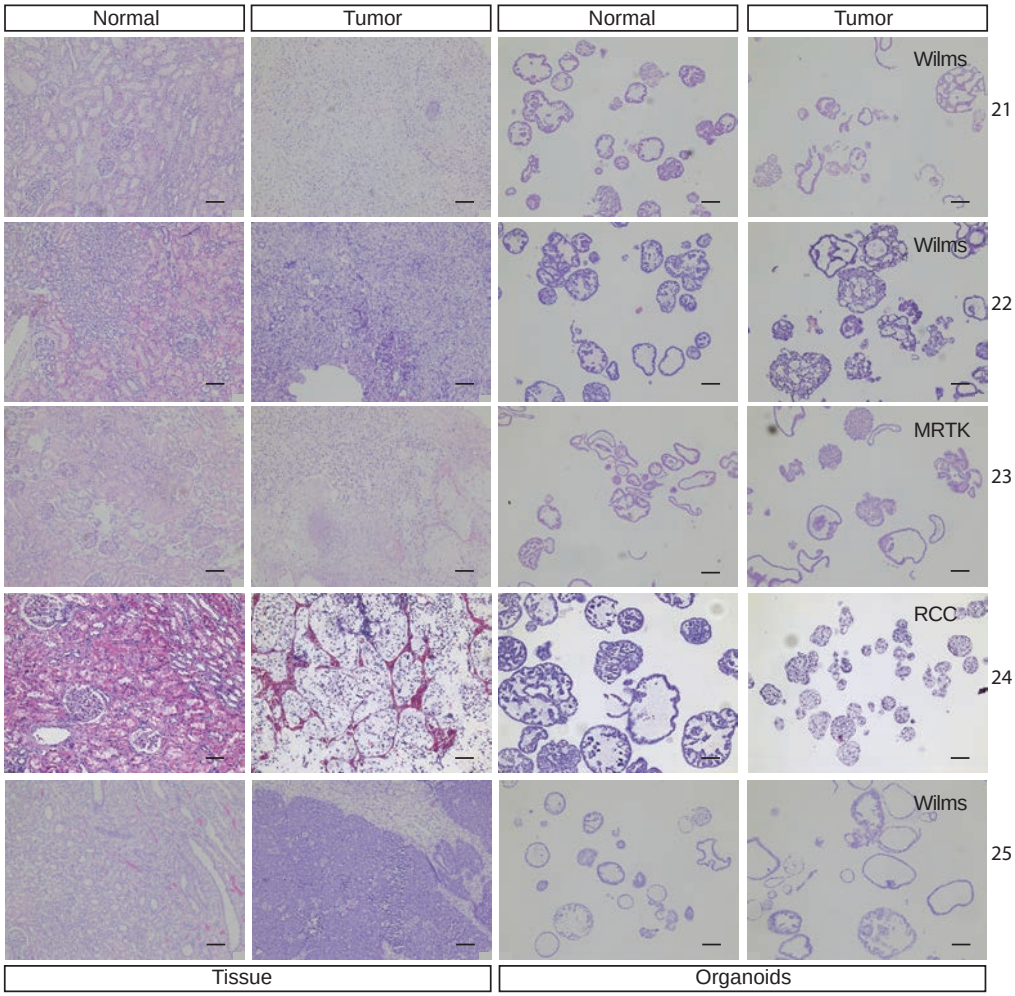

Supplementary Figure 4. (continued)

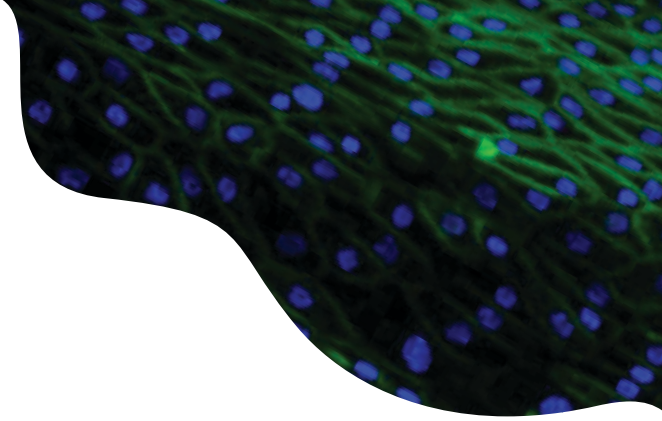

CHAPTER 5

KIDNEY ORGANOID-DERIVED CELLS ON A CHIP AND ON A HOLLOW FIBER

ABSTRACT

Adult Stem Cell (ASC)-derived kidney organoids, 3D epithelial structures that contain self-renewing and organ-specific stem cells, are cultured as cysts in Matrigel or BME. Integration with other culture platforms may broaden the scope of applications of kidney organoids.

Here, organoid-derived cells are cultured on **i.** organ-on-a-chip OrganoPlates – to obtain structures with a uniform tubular morphology that allow high-throughput transporter and toxicity studies and **ii.** hollow fibers that are used as hemodialysis membranes – to create autologous 'living membranes' for renal assist devices to improve the clearance of waste solutes (i.e. uremic toxins).

Organoid cells on OrganoPlates yield polarized, leak-tight epithelial tubules that display (trans-) epithelial transport function and that are damaged after exposure to nephrotoxins. Organoids expand on collagen-coated hollow microPES (PolyEtherSulfone) fibers and display apical and basolateral proximal tubule transporter function.

Thus, organoid cells prove to be robust and amenable to culture substrates other than BME / Matrigel. This designates autologous kidney organoids as cell source for high-throughput transporter analyses and drug screening in personalized medicine and drug development, as well as for 'living membranes' for bioartificial or bioengineered kidneys.

Frans Schutgens[1,2], Linda Gijzen[3], Jitske Jansen[4], Carola Ammerlaan[1,2], Marianne Vormann[3], Henriette Lanz[3], Maarten B. Rookmaaker[2], Rosalinde Masereeuw[4], Marianne C. Verhaar[2], Hans Clevers[1]

[1] Hubrecht Institute–Royal Netherlands Academy of Arts and Sciences, the Netherlands
[2] Department of Nephrology and Hypertension, University Medical Centre Utrecht, the Netherlands
[3] Mimetas, the Organ on a Chip Company, Leiden, the Netherlands
[4] Division of Pharmacology, Utrecht Institute for Pharmaceutical Sciences, Utrecht University, the Netherlands

INTRODUCTION

ASC-derived organoids, 3D epithelial structures that contain self-renewing and organ-specific stem cells, have proved valuable for the expansion and study of healthy as well as diseased tissue.[1-7] An ASC-derived kidney organoid culture system is described in **Chapter 3**. These organoids can be derived from biopsies as well as from cells shed in urine, have a vast expansion capacity, are genetically stable and retain secretory function mediated by transport proteins.

However, ASC-kidney organoids grow as heterogeneous cysts in BME or Matrigel. Integration of the culture system with other technologies to homogenize organoid culture or to culture on substrates more readily transferable to the clinic than in BME or Matrigel, will facilitate the applicability of kidney organoids.

Integrating organoid culture with an organ-on-a-chip platform will guide organoids into a homogeneous, tubule-like conformation, allowing high-throughput and reproducible epithelial transport and toxicity studies. In general, organ-on-a-chip is defined[8] as a microfluidic cell culture device that contains continuously perfused chambers with living cells arranged to simulate tissue-level physiology. The 3-lane OrganoPlate is a specific type of organ-on-a-chip platform with 40 parallel chips with stratified compartments for extracellular matrix and medium perfusion.[9] Cells are cultured in a medium perfusion compartment along the matrix gel, molding the cells in a tube-formation and allowing apical as well as basolateral access (Figure 1A). This set-up enables standardized, high-throughput transporter and toxicity studies, that are both relevant given the abundant presence of proximal tubule cells in regular kidney organoid culture in BME or Matrigel.

Culture of organoid cells on permeable membranes that permit cell growth as well as solute transport, on a platform that allows a vast increase in surface area, will facilitate the development of autologous 'living membranes' for Renal Assist Devices (RADs). RADs are dialysis modalities, combined with an extra cartridge with living kidney proximal tubule cells.[10] The cartridge of living cells is of benefit as it adds excretion of protein-bound uremic toxins, additional reabsorption of useful compounds, and hormone production to a conventional dialysis machine.

Hollow MicroPolyEtherSulfone (MicroPES) fibers are compatible with hemodialysis and have previously been successfully used to create 'living membranes' using an immortalized renal cell line.[11] Also primary allogeneic proximal tubule cells have been used as cell source for RADs. Due to their limited availability and stability, as well as batch-to-batch variability, both immortalized and primary cell lines are not ideal for upscaling the technology.[12] Organoid-derived cells may provide an autologous cell source with a stable and high expansion capacity.

Here, we aim to embed kidney organoid culture in **i.** a technology that enables high-throughput evaluation of transporters and toxicity and **ii.** hollow fiber culture to create autologous 'living membranes' for bioartificial kidneys.

RESULTS

Kidney organoid-derived cells form polarized tubes in OrganoPlates with a proximal tubule phenotype

After seeding organoid cells on OrganoPlates, epithelial tubes formed within 7 days (Figure 1B). The majority of cells expressed proximal tubule microvillus marker Ezrin (Figure 1C). In addition,

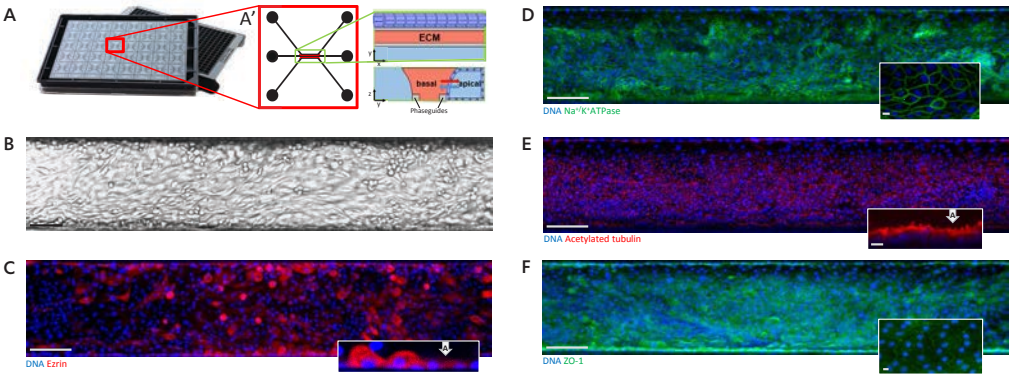

Figure 1. Organoid cells form tubes on OrganoPlates. The OrganoPlate platform with 40 microfluidic cell culture chips embedded in a standard 384-well microtiter plate (A). Schematic lay-out of one chip on the organ-on-a-chip plate, with separate compartments for gel and medium perfusion with cells seeded in one medium channel (A'). 7 days after seeding, a confluent tubular layer is formed as assessed by brightfield microscopy (B). Immunofluorescence shows cells that are positive for Ezrin, a marker for the microvillus on proximal tubule cells (C). Immunofluorescence shows that cells are positive for Na^+/K^+-ATPase on the basolateral side (D) and acetylated tubulin on apical the apical side (E). Cells are positive for ZO1, marker for tight junctions (F). Scale bars are 100 µm with the exception of the zoom in immunofluorescent figures, where they are 10 µm. Immunofluorescent images of the whole tube are max projections (C-F). Zoom in figures of a z-slice of the tube (C, F) are positioned at 50 µm from the bottom glass, where figures (D, E) are positioned on the bottom glass. White arrows (C,F) indicate the apical site of the tube.

the cells building the tubes were polarized, as assessed by immunofluorescence for Na^+/K^+ ATPase (basolateral) and acetylated tubulin (apical) (Figure 1D, E). ZO1 visualized tight junctions (Figure 1F) and suggested leak-tightness of the tubes.

Organoid-derived tubes are leak-tight and exhibit (trans-)epithelial transporter function

Leak-tightness of tubes is essential for the study of transporter function. To show that the tubes were leak tight, we added 20 dextran-FITC to the cell compartment and observed whether it leaked into the ECM or perfusion compartment. After 20 minutes, dextran-FITC remained in the cell compartment in 94 of 108 (86%) tested tubes, whereas in the negative control (no cells plated), dextran-FITC was diffusely present throughout all compartments (Figure 2A, B). The leaking tubes were likely due to seeding too few cells (only a small (2 µl) volume of cells is plated in each chip) or ECM detachment.

Next, we evaluated the function of P-glycoprotein (P-gp, also known as *ABCB1, MDR1*), a transporter that is involved in the excretion of foreign substances. We performed a P-gp transporter assay in the presence and absence of a specific inhibitor (PSC-833), similar to what was described in **Chapter 3** (for a schematic overview: Chapter 3, Supplementary Figure 6). We observed accumulation of intracellular calcein in the presence of PSC-833, demonstrating P-gp activity (Figure 2C, $P = 0.001$).

Subsequently, we tested whether the tubes displayed trans-epithelial transport function. The fluorescent rhodamine 123 is transported into cells by Organic Cation Transporter 1 and 2

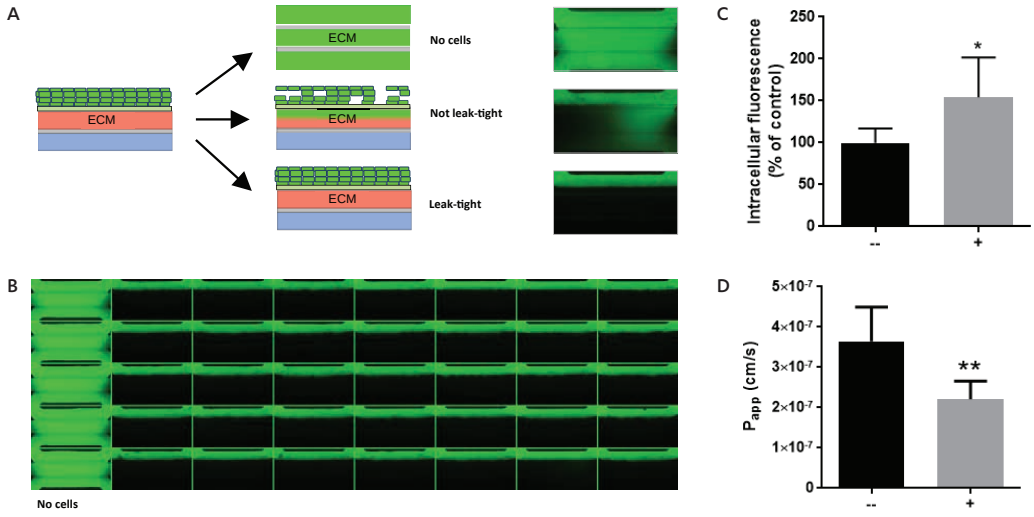

Figure 2. Organoid cells form functional leak-tight tubes on OrganoPlates. Schematic lay-out of a barrier integrity assay, where Dextran-FITC is added to the lumen of the cell compartment (A). In chips with tube formation, no leakage is observed, whereas in the negative control (no cells present), dextran-FITC spreads over the whole chip. A typical organ-on-a-chip plate overview after 20 min of 20 kDa Dextran-FITC exposure, where Dextran-FITC spreads over the whole chip in the negative controls (*no cells*, first column), but not in the chips where cells were plated (B, typical example of $n = 3$ independent experiments). The tubes significantly increase in intracellular calcein, after inhibition of P-gp with PSC-833, demonstrating P-gp activity (C, average is plotted of $n = 3$ independent experiments). Fluorescent Rhodamine123, that was added at the basal side of the tubes, is detected in the lumen at the apical side and the signal can be reduced by the addition of PSC-833, demonstrating that the process is P-gp-dependent (D, average is plotted of $n = 2$ independent experiments). Error bars represent standard deviation. * $P = 0.001$; ** $P < 0.0001$.

(OCT1 and OCT2)[13], which are influx pumps located on the basolateral side of proximal tubule cells. It is secreted from cells at the apical membrane by P-gp.[14] Rhodamine 123 was added at the basal side of the tube in the presence or absence of the P-gp inhibitor PSC-833. After 3 and 5 hours of incubation, fluorescent intensity of rhodamine 123 at the apical side was measured and the difference between the two time points was quantified. A scheme of the experimental set-up is provided in Supplementary Figure 1.

Fluorescence was detected at the apical side, indicating transepithelial transport. The difference between 3 and 5 hours was reduced in the presence of PSC-833 ($P < 0.0001$), showing that efflux of rhodamine 123 was dependent on P-gp function.

Thus, organoid-derived cells formed leak-tight tubes that maintained trans-epithelial transport activity in an organ-on-a-chip format.

Organoid-derived tubes are damaged by clinically used nephrotoxins

We exposed leak-tight tubes to the anti-neoplastic cisplatin and reverse transcriptase-inhibitor tenofovir, which are compounds commonly used in the clinic and known to induce proximal tubule injury.[15,16] Cisplatin is transported into proximal tubule cells by OCT2, a transporter that is functional

in organoid-derived cells in OrganoPlates (Figure 2D), whereas tenofovir depends on Organic Anion Transporters (OATs). After 24 hours and 48 hours of exposure to cisplatin (5 and 90 µM - concentrations in the range of plasma concentrations reached during treatment[17]) and tenofovir (15.6 µM - a concentration in the range of plasma concentrations reached during treatment[18], and 1 mM), morphology of the treated tubes did not change when compared to vehicle controls (*data not shown*). However, LDH activity was significantly increased after exposure to 90 µM cisplatin ($P < 0.0001$) indicating an increase in cell death (Figure 3B). In addition, an increase in γH2AX was observed 24 (Supplementary Figure 2C) and 48 hours (Figure 3C) after cisplatin exposure, showing an increase in DNA double strand breaks. A more subtle increase in γH2AX staining was observed for tenofovir (Figure 3C and supplementary figure 2C).

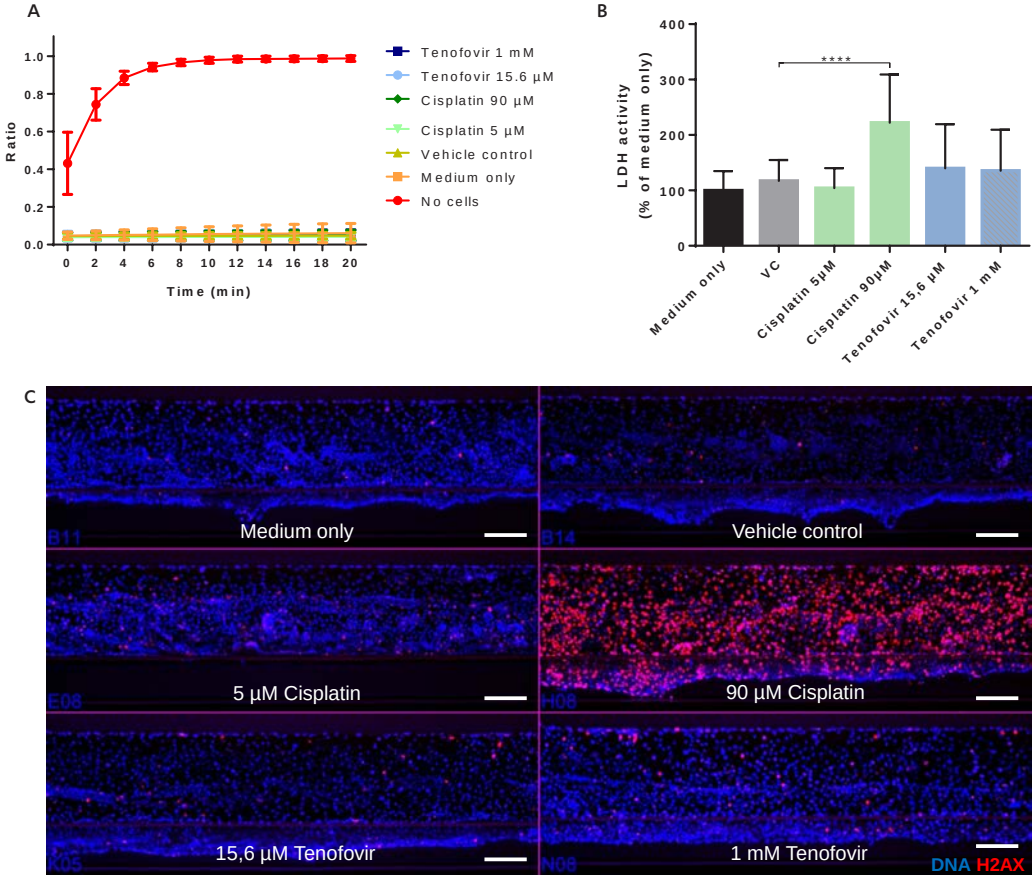

Figure 3. Organoid-derived tubes after 48 hours exposure to cisplatin and tenofovir. Tubes remain leak-tight after cisplatin or tenofovir exposure, as evidenced by apical and basal fluorescent ratio (A, average is plotted of $n = 3$ independent experiments). Cisplatin 90 µM causes a significant increase in LDH activity, compared to vehicle control (VC) (B, average is plotted of $n = 3$ independent experiments). γH2AX staining is increased Cisplatin 90 µM and slightly increased in 1mM tenofovir, compared to vehicle control (C). Immunofluorescent images of the whole tube are max projections. Scale bars: 100 µm. Error bars represent standard deviation. **** $P < 0.0001$.

All tubes were leak-tight before toxin exposure (Supplementary Figure 2A) and surprisingly, all tubes remained leak-tight after 24 and 48 hours (Supplementary Figure 2B and Figure 3A), despite the DNA damage observed with γH2AX staining and the increase in LDH activity.

Thus, we found an increase in cell death and DNA damage in response to cisplatin and a milder increase in DNA damage in response to tenofovir, but all tubes remained leak-tight.

Organoid-derived cells form functional epithelial layers on hollow fibers

We plated organoid cells on L-DOPA and collagen IV-coated MicroPES hollow fiber membranes (~1.5 cm).[11] A cartoon of the set-up is provided in Figure 4A. We observed that the cells attached to the fibers, survived and expanded in such way that large parts of the fibers were covered with cells (Figure 4B, C).

In these cell layers, ZO1 visualized tight junctions (Figure 4C), suggesting leak-tightness. However, functional testing leak-tightness with a barrier integrity assay as performed for the OrganoPlates (Figure 2A, B) was not done, as it was difficult to cover the complete fiber (~1.5 cm) with cells.

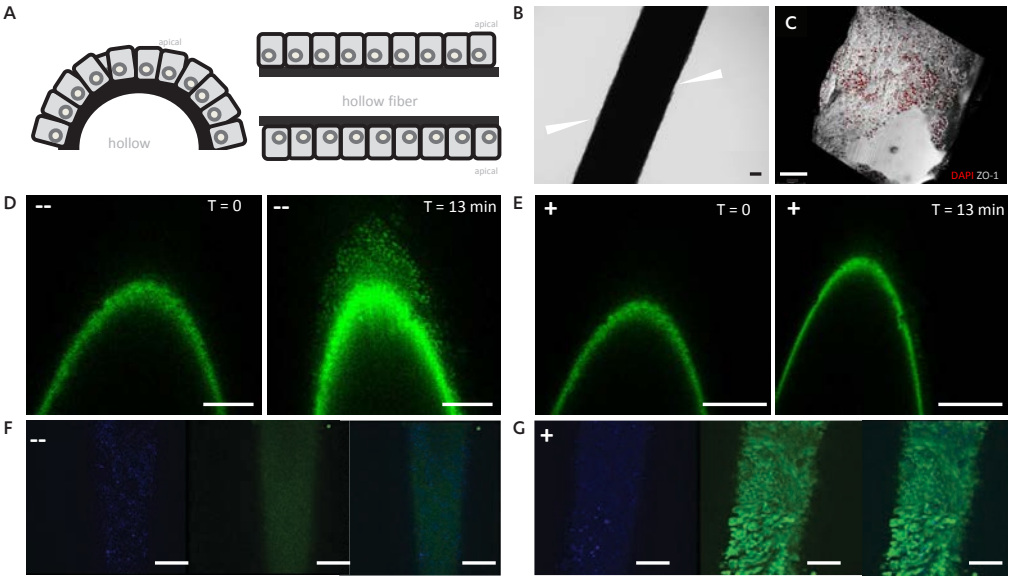

Figure 4. Organoids grow and are functional on hollow fiber membranes. A schematic horizontal (*left*) and vertical (*right*) cross section of a hollow fiber, coated with cells (A) A layer of cells (*arrow heads*) is present 7 days after seeding, as viewed from the side of a fiber (B). A 3D reconstruction of organoid cells on a fiber, showing ZO1 expression and the fiber membrane in the region where no cells are present (C). Exposure on the inside of the hollow fiber of fluorescent OCT substrate ASP, leads to an increase in fluorescent signal on the outside of the fiber within 13 minutes (D, n = 1 experiment). This increase in fluorescence is not observed after 13 minutes in the presence of OCT2 inhibitor cimetidine - solely the autofluorescent edge of the fiber is detected (n = 1 experiment) (E). Fluorescent substrate Calcein AM of efflux pump P-gp is not detected inside cells when P-gp is not inhibited (typical example of n = 2 independent experiments) (F), whereas accumulation of Calcein AM is detected after blocking P-gp activity with 5 μM of PSC-833 (typical example of n = 2 independent experiments) (G). Scale bars: 100 μm.

To test whether the cells were functional, we performed functional assays for OCT2 and P-gp. To determine OCT2 function, we used a previously described live-imaging set-up[11] of which a scheme is provided in Supplementary Figure 3. The fluorescent substrate of OCT2, 4-(4-(dimethylamino) styryl)-N-methylpyridinium iodide (ASP), was infused through the hollow fiber with or without OCT2-inhibitor cimetidine. In this way, the substrate with or without cimetidine was presented to the basolateral side of the cells. Transport was visualized with live confocal microscopy, imaging the cells at the apical side (i.e. the other side of the hollow fiber) for 13 minutes. In the absence of cimetidine, we observed an increase in the fluorescent signal over time, showing transport activity of OCT2 (Figure 4D). In presence of cimetidine, the signal did not increase over time and only the autofluorescent signal at the edge of the fiber was detected (Figure 4E).

P-gp function was determined as described above and before (**Chapter 3**, Supplementary Figure 6). We observed an accumulation of calcein in the presence of PSC-833 (Figure 4G), compared to the condition without P-gp inhibitor PSC-833 (Figure 4F), showing P-gp activity of organoid cells on fibers.

Thus, organoid cells on hollow fibers showed activity of transporters at the basolateral as well as the apical side of cells and were potentially leak-tight.

DISCUSSION

Here, by combining organ-on-a-chip and organoid technology, we cultured kidney organoid-derived leak-tight, functional tubes in OrganoPlates, allowing high-throughput transporter and toxicity studies. In addition, organoid cells on hollow fibers form tight junctions and show basolateral and apical transport, which are essential characteristics for potential application as autologous cell source to create 'living membranes.'

Traditionally, organ-on-a-chip and organoid technologies have been regarded as mutually exclusive tools and thus far, predominantly cell lines have been used as cell source for organ-on-a-chip models: for example, kidney-on-a-chip devices have been seeded with a rat Inner Medullary Collecting Duct (IMCD) cells[19] or Madin Darby Canine Kidney (MDCK)[20] cells. This proof-of-principle of compatibility of these technologies offers opportunities for human, autologous and genetically stable organ-on-a-chip models. In addition, it may set a precedent for autologous organ-on-a-chip models of other tube-like organs with established organoid cultures, such as the intestine.

The study of trans-epithelial transport and drug toxicity in tubes established from an autologous and potentially non-invasively acquired cell source (**Chapter 3**, Figure 4), has hitherto not been described.

It needs to be determined, in a direct comparison, whether organoid cells perform better in resembling the *in vivo* situation than cell lines in toxicity and transporter assays. In addition, the differentiation of the organoid tubes can be improved. Limited differentiation may explain the relatively small effect of tenofovir: tenofovir is transported into cells by OATs, which are only lowly expressed in organoids (*data not shown*), whereas cisplatin is transported into cells by OCT2, a transporter that we showed is functional in organoid-derived cells. Adaptation of the culture medium or matrix prior to assays may increase differentiation. Furthermore, the tubes are currently purely epithelial and predominantly proximal tubule in nature. The addition of interactions with

vasculature, immune cells and fibroblasts, which is feasible in a controlled fashion in separate compartments in OrganoPlates, may increase similarity to *in vivo* kidneys. To enable the modeling of compound handling throughout the nephron (i.e. from proximal tubule towards collecting duct), differentiation could be directed towards segments that are currently under-represented, or segment-specific organoid cultures could be established.

In the future, 'organoids-on-a-chip' may function as a platform for standardized, high-throughput drug screening and personalized medicine. Establishing organoid biobanks from urine from healthy volunteers and patients with genetic transporter diseases (such as Gitelman and Bartter), combined with seeding in OrganoPlates, would be a valuable tool for disease modeling and drug efficacy / toxicity studies.

Organoid-derived cells grow and function on hollow fibers, designating organoids as candidate for autologous and non-immunogenic cell source for bioartificial kidneys. Conventional dialysis does not recapitulate active and selective transport function of the proximal tubule, which are features considered to contribute significantly to the high morbidity and mortality of dialysis patients. Organoid cells show aspects of these functions on hollow fibers. Importantly, the hollow fibers are suitable for surface enlargement and are permeable, the latter allowing active and selective transport, whereas cells themselves have tight junctions.

It needs to be determined whether the organoid cells on hollow fibers are truly leak-tight in a barrier integrity assay. Additionally, also on the hollow fibers, differentiation needs to be improved. Currently, expression of organic anion transporters (OATs) is low in organoids. OATs are important transporters that excrete protein-bound uremic toxins, which are compounds that cannot be properly excreted by conventional hemodialysis.

In the future, expression of OATs might be induced by adaptation of the organoid culture medium: optimization of growth factor composition, concentration and timing may increase differentiation and guide organoid cells to more mature proximal tubule cells. Alternatively, OAT expression may be upregulated by the presence of the substrates of the transporters, uremic toxins. Similar mechanisms have been observed before: for example, expression and activity of alcohol dehydrogenase increases after ethanol consumption.[21]

In conclusion, organoid cells prove to be robust and amenable to culture methods other than in BME / Matrigel. This allows the embedding of organoid culture in other technologies, which in turn broadens the scope of applications for organoid culture: standardized, high-throughput transporter analyses and drug screening become feasible and the development of bioartificial kidneys comes one step closer.

MATERIAL AND METHODS

Human organoid culture

From cortical kidney tissue, tubular fragments were isolated by collagenase digestion (C9407, Sigma) for 45 minutes at 1 mg/ml. Fragments were seeded growth factor-reduced Matrigel (Corning) or Basement membrane extract (BME; R&D Systems) and cultured in medium (ADMEM / F12 supplemented with 1% penicillin / streptomycin, HEPES, Glutamax), with 1.5% B27 supplement (Gibco), 10% Rspo1-conditioned medium,[22] EGF (50 ng/ml, Peprotech), FGF-10 (100 ng/ml,

Preprotech); N-acetylcysteine (1.25 mM, Sigma), Rho-kinase inhibitor Y-27632 (10 µM, Abmole) A8301 (5 µM, Tocris Bioscience), primocine (0.1 mg/ml, Invivogen).

Coating and cell seeding

Dialysis fibers

MicroPES (polyethersulfone) hollow fiber membranes were coated and seeded as described before.[11] Briefly, after sterilizing fiber membranes with 70% (v/v) ethanol, the fiber membranes were coated with L-3,4-dihydroxyphenylalanine,(L-DOPA; Sigma-Aldrich; 2 mg/ml) for 5 hours at 37 °C. Subsequently, the fibers were coated with human collagen IV (Sigma, 25 µg/ml) for 1 hour at 37 °C, after which the collagen IV solution was washed away with Hank's Balanced Salt Solution (HBSS) buffer. The next day, organoids were trypsinized into a single cell suspension and 50,000 cells were added per fiber (~ 1.5 cm in length). Next, fibers in cell suspension (in 0.5 ml eppendorf tubes) were placed horizontally in an incubator (37 °C, 5% (v/v) CO2) and the tubes were turned 90° every hour. After 4 hours, fibers were placed in wells of a 12 well plate with organoid culture medium with medium changes 3x / week. When cells formed a confluent layer on the fiber (after 5-7 days of culture) fibers were either fixed in 2% (w/v) PFA for 15 min at room temperature and prepared for immunofluorescence, or used for transporter assays.

OrganoPlates culture

In each of the 40 chips in the 3-lane 400 µm OrganoPlate microfluidic system (Mimetas, 4003400B), 2 µl of extracellular matrix (ECM) gel composed of 4 mg/ml Collagen I (AMSbio Cultrex 3D Collagen I Rat Tail, 5 mg/mL), 100 mM HEPES (Life Technologies) and 3.7 mg/mL NaHCO3 (Sigma) was dispensed in the gel inlet, incubated for 30 min at 37°C and covered with 30 µl HBSS (Sigma). The next day, organoids were trypsinized, made into a single cell suspension and applied to the OrganoPlate by seeding 2 µl of 10 x 10^6 of cells/ml in the inlet of the top medium channel. Next, 50 µl of human organoid culture medium was added to the same inlet and the plate was placed on the side in an incubator for 5 hours to allow the cells to attach to the ECM. Afterwards, an additional 50 µl of culture media was added to each of the remaining in- and outlets of the top and bottom medium channels. Subsequently, the OrganoPlate was placed horizontally in the incubator (37°C, 5% CO2) on an interval rocker (every 8 minutes switching between +7° and -7° inclination) allowing bi-directional flow. Medium (50 µl each on in- and outlets) was refreshed every 2 to 3 days. After 7 days, cells were either formaldehyde-fixed for immunofluorescent staining or used for barrier integrity or transport assays.

Immunofluorescence

Kidney organoid tubes cultured in the OrganoPlate were fixed with 50 µl 3.7% formaldehyde (Sigma) in HBSS for 15 min, washed twice with HBSS and permeabilized with 0.3% Triton X-100 (Sigma) in HBSS for 10 min. Next, cells were washed with 4% FCS (Sigma) in HBSS and incubated with blocking solution (2% FCS, 2% bovine serum albumin (BSA) (Sigma), 0.1% Tween20 (Sigma) in HBSS) for 30 min. Afterwards, cells were incubated with primary antibodies for 1 hour at RT, washed twice, incubated with secondary antibodies for 30 min at RT and washed twice with 4% FCS in HBSS. The following antibodies were used: Mouse anti-Ezrin (1:125, #610602, BD Transduction), Rabbit anti-ZO-1 (1:125,

#339100 or #402200, Life tech), Mouse anti-Acetylated tubulin (1:2000, #T6793, Sigma), Rabbit anti-Na^+/K^+ ATPase (1:400, #ab76020, Abcam), mouse isotype (Life tech), rabbit isotype (Life tech), goat anti-mouse Alexa Fluor 647 (Life tech, 1:250) and goat anti-rabbit Alexa Fluor 488 (Life tech, 1:250). Finally, the nuclei were stained with Hoechst 33342 (Life tech) and cells were stored in HBSS. The kidney organoid tubules were images with ImageXpress Micro XLS-C High Content Imaging Systems (Molecular Devices).

OrganoPlates barrier integrity assay

Medium in the apical perfusion channel was replaced by medium containing 0.5 mg/ml FITC-dextran (20 kDa, Sigma) and 0.5 mg/ml TRITC-dextran (155 kDa, Sigma). Leakage of the fluorescent dye from the lumen of the renal tubular structure into the ECM compartment was imaged every 2 minutes for 20 min on an ImageXpress XLS Micro (Molecular Devices). The ratio between the fluorescent signal in the basal and apical part of the tube was analyzed using FiJi.[1]

Transporter assays

Hollow Fibers

P-gp activity was determined as described before.[23] Briefly, fibers were washed twice with HBSS and pre-incubated with or without P-gp-inhibitor PSC-833 (5μM) in HBSS. Next, fluid was replaced with Calceine-AM in HBSS (either with or without P-gp-inhibitor PSC833 at 5 μM) and the fibers were incubated (protected from light) for 1 hour at 37° C, 5% (v/v) CO2. Subsequently, the buffer was removed and washed once with cold Krebs Henseleit HEPES (KHH) buffer. Then, cells were fixed cells in 2% (w/v) PFA for 5 min, washed and mounted in mounting medium with DAPI (Vectashield, Vectorlabs).

OCT2 activity was determined real-time with a live imaging set-up in a microfluidic system as described previously.[11] Briefly, fibers were perfused on the basolateral side (i.e. the inside of the hollow fiber, 6 ml/h) with the fluorescent OCT2 substrate 4-(4-(dimethylamino)styryl)-N-methylpyridinium iodide (ASP, 10 μM) in KHH buffer in the presence or absence of OCT2-inhibitor cimetidine (100 μM). Confocal imaging (SP8, Leica) was performed for 13 min at 37 °C, 5% (v/v) CO2.

OrganoPlates P-gp assay

Cells were incubated with calcein-AM (Life tech, 1μM) at the apical side of the tube in the presence or absence of PSC-833 (Sigma) at 5μM in OptiHBSS (33% Opti-MEM (Gibco), 66% HBSS (Sigma) for 1 hour in the incubator (37°C, 5% CO2) on an interval rocker (8 min, 7°). After incubation, cells were washed once with OptiHBSS, nuclei were stained with Hoechst 33342 and the tubes were imaged with ImageXpress Micro XLS-C High Content Imaging Systems (Molecular Devices). The intracellular fluorescent values were corrected for total cell numbers of each microfluidic chip, for background values, and were normalized to the calcein-AM only condition.

OrganoPlates trans-epithelial transport

Medium in the apical channel was replaced with medium containing 5 μM PSC833 or 0.2% DMSO. Medium in the basal channel was replaced with medium containing 10 μM rhodamine 123 (Sigma) and 5 μM PSC833 or 0.2% DMSO respectively. To determine the concentration of rhodamine 123,

a concentration curve was added to extra chips. Tubules were incubated for 5 hours on the rocker (8 min, 7°) in the incubator (37°C, 5% CO2). After 3 and 5 hours, the rhodamine 123 concentration was measured by imaging the top inlets with the FITC filter on the ImageXpress Micro XLS-C High Content Imaging Systems (Molecular Devices). The apparent permeability (P_{app}) was calculated by using the following formula:

$$P_{app} = \frac{\Delta C_{receiver} \times V_{receiver}}{\Delta t \times A \times C_{donor}} \text{ (cm/s).}$$

In this formula, $C_{receiver}$ is the measured intensity difference in the top wells over time, $V_{receiver}$ is the receiving volume in the reservoirs of the top inlets, t is the time difference, A is the surface of the ECM interface with the medium channel, and C_{donor} is the donor concentration of 10 µM rhodamine 123.

Toxicity assays

Tubes were exposed from both apical and basolateral side to cisplatin (Sigma, 5 and 90µM) or tenofovir (Santa Cruz, 15.6 and 1000µM) for 24 or 48 hours in the incubator (37°C, 5% CO2) on an interval rocker (8 min, 7°). Cisplatin was dissolved in 0.9% NaCl (Sigma) and tenofovir in DMEM F12 phenol red-free (Gibco). After incubation, cells were imaged with ImageXpress Micro XLS-C High Content Imaging Systems for morphology assessment. Subsequently, a barrier integrity assay was performed as described above and the plates were fixed with 50 µl 3.7% formaldehyde in HBSS (Sigma) for 15 min. The kidney tubular structures were immunofluorescently labelled for DNA damage according to the protocol described above. The following antibodies were used: Rabbit a-Phospho-Histone H2A.X (Cell signaling technology, 1:200), Rabbit isotype (Life tech) and Goat a-Rabbit Alexa Fluor 555 (Life tech, 1:250).

LDH activity assay

After incubation, medium samples were collected by combining the in- and outlet of each channel in a 96-well plate. The lactate dehydrogenase (LDH) activity of each sample was measured with the Lactate Dehydrogenase Activity Assay Kit (Sigma) according to manufacturer protocol. The absorbance was measured with the Multiskan™ FC Microplate Photometer (Thermo scientific).

Statistics and data analysis

Image analysis was carried out by using FiJi.[1] Data analysis was performed using Microsoft Office Excel 2016 and GraphPad Prism version 6.07 (GraphPad Software Inc., La Jolla, CA). All data are expressed as mean ± standard deviation (SD). Statistical analysis was performed using a student T test or one-way ANOVA with Dunnett's Multiple Comparison test. Statistical significance was considered at $P < 0.05$.

REFERENCES

1. Huch, M. *et al.* Long-Term Culture of Genome-Stable Bipotent Stem Cells from Adult Human Liver. *Cell* **160**, 299-312, doi:10.1016/j.cell.2014.11.050 (2015).
2. Boj, S. F. *et al.* Organoid models of human and mouse ductal pancreatic cancer. *Cell* **160**, 324-338, doi:10.1016/j.cell.2014.12.021 (2015).
3. Drost, J. *et al.* Sequential cancer mutations in cultured human intestinal stem cells. *Nature* **521**, 43-47, doi:10.1038/nature14415 http://www.nature.com/nature/journal/v521/n7550/abs/nature14415.html#supplementary-information (2015).
4. Gao, D. *et al.* Organoid cultures derived from patients with advanced prostate cancer. *Cell* **159**, 176-187, doi:10.1016/j.cell.2014.08.016 (2014).
5. Bartfeld, S. *et al.* In vitro expansion of human gastric epithelial stem cells and their responses to bacterial infection. *Gastroenterology* **148**, 126-136 e126, doi:10.1053/j.gastro.2014.09.042 (2015).
6. van de Wetering, M. *et al.* Prospective Derivation of a Living Organoid Biobank of Colorectal Cancer Patients. *Cell* **161**, 933-945, doi:10.1016/j.cell.2015.03.053 (2015).
7. Sato, T. *et al.* Single Lgr5 stem cells build crypt-villus structures in vitro without a mesenchymal niche. *Nature* **459**, 262-265, doi:10.1038/nature07935 (2009).
8. Bhatia, S. N. & Ingber, D. E. Microfluidic organs-on-chips. *Nat Biotech* **32**, 760-772, doi:10.1038/nbt.2989 (2014).
9. Trietsch, S. J., Israëls, G. D., Joore, J., Hankemeier, T. & Vulto, P. Microfluidic titer plate for stratified 3D cell culture. *Lab on a Chip* **13**, 3548-3554 (2013).
10. Humes, H. D., Buffington, D., Westover, A. J., Roy, S. & Fissell, W. H. The bioartificial kidney: current status and future promise. *Pediatric nephrology* **29**, 343-351, doi:10.1007/s00467-013-2467-y (2014).
11. Jansen, J. *et al.* Human proximal tubule epithelial cells cultured on hollow fibers: living membranes that actively transport organic cations. *Scientific Reports* **5**, 16702, doi:10.1038/srep16702 http://www.nature.com/articles/srep16702#supplementary-information (2015).
12. Westover, A. J. *et al.* A bio-artificial renal epithelial cell system conveys survival advantage in a porcine model of septic shock. *Journal of Tissue Engineering and Regenerative Medicine*, n/a-n/a, doi:10.1002/term.1961 (2014).
13. Jouan, E., Vee, M., Denizot, C., Da Violante, G. & Fardel, O. The mitochondrial fluorescent dye rhodamine 123 is a high–affinity substrate for organic cation transporters (OCTs) 1 and 2. *Fundamental & clinical pharmacology* **28**, 65-77 (2014).
14. Yumoto, R. *et al.* Transport of rhodamine 123, a P-glycoprotein substrate, across rat intestine and Caco-2 cell monolayers in the presence of cytochrome P-450 3A-related compounds. *Journal of Pharmacology and Experimental Therapeutics* **289**, 149-155 (1999).
15. Herrera-Pérez, Z., Gretz, N. & Dweep, H. A Comprehensive Review on the Genetic Regulation of Cisplatin-induced Nephrotoxicity. *Current Genomics* **17**, 279-293, doi:10.2174/1389202917666160202220555 (2016).
16. Fernandez-Fernandez, B. *et al.* Tenofovir Nephrotoxicity: 2011 Update. *AIDS Research and Treatment* **2011**, 354908, doi:10.1155/2011/354908 (2011).
17. Laurell, G. & Jungnelius, U. High-Dose cisplatin treatment: Hearing loss and plasma concentrations. *The Laryngoscope* **100**, 724-734, doi:10.1288/00005537-199007000-00008 (1990).
18. Rodríguez-Nóvoa, S. *et al.* Impairment in kidney tubular function in patients receiving tenofovir is associated with higher tenofovir plasma concentrations. *AIDS* **24** (2010).
19. Jang, K.-J. & Suh, K.-Y. A multi-layer microfluidic device for efficient culture and analysis of renal tubular cells. *Lab on a Chip* **10**, 36-42, doi:10.1039/B907515A (2010).
20. Baudoin, R., Griscom, L., Monge, M., Legallais, C. & Leclerc, E. Development of a Renal Microchip for In Vitro Distal Tubule Models. *Biotechnology progress* **23**, 1245-1253, doi:10.1021/bp0603513 (2007).
21. He, L., Ronis, M. J. J. & Badger, T. M. Ethanol induction of class I alcohol dehydrogenase expression in the rat occurs through alterations in CCAAT/enhancer binding proteins β and γ. *Journal of Biological Chemistry* **277**, 43572-43577 (2002).
22. Kim, K.-A. *et al.* Mitogenic Influence of Human R-Spondin1 on the Intestinal Epithelium. *Science* **309**, 1256-1259 (2005).
23. Jansen, J. *et al.* A morphological and functional comparison of proximal tubule cell lines established from human urine and kidney tissue. *Experimental cell research* **323**, 87-99, doi:http://dx.doi.org/10.1016/j.yexcr.2014.02.011 (2014).

SUPPLEMENTARY INFORMATION

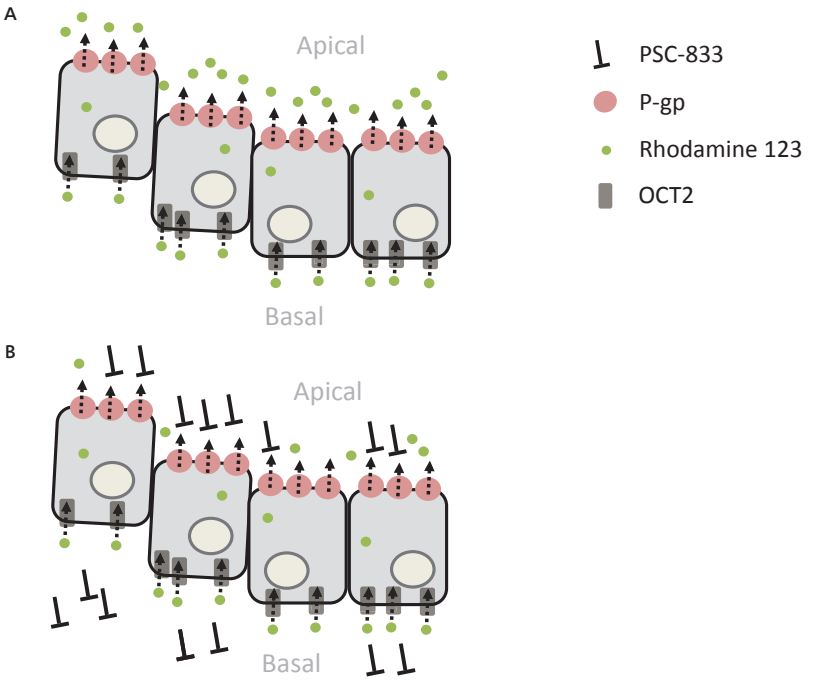

Supplementary Figure 1. Overview of the trans-epithelial transporter assay. Rhodamine 123 is transported into cells at the basal side by OCT-transporters and removed at the apical side by by efflux pump P-gp (A) In the presence of P-gp inhibitor, rhodamine 123 fluorescence in the lumen at the apical side, should be reduced (B).

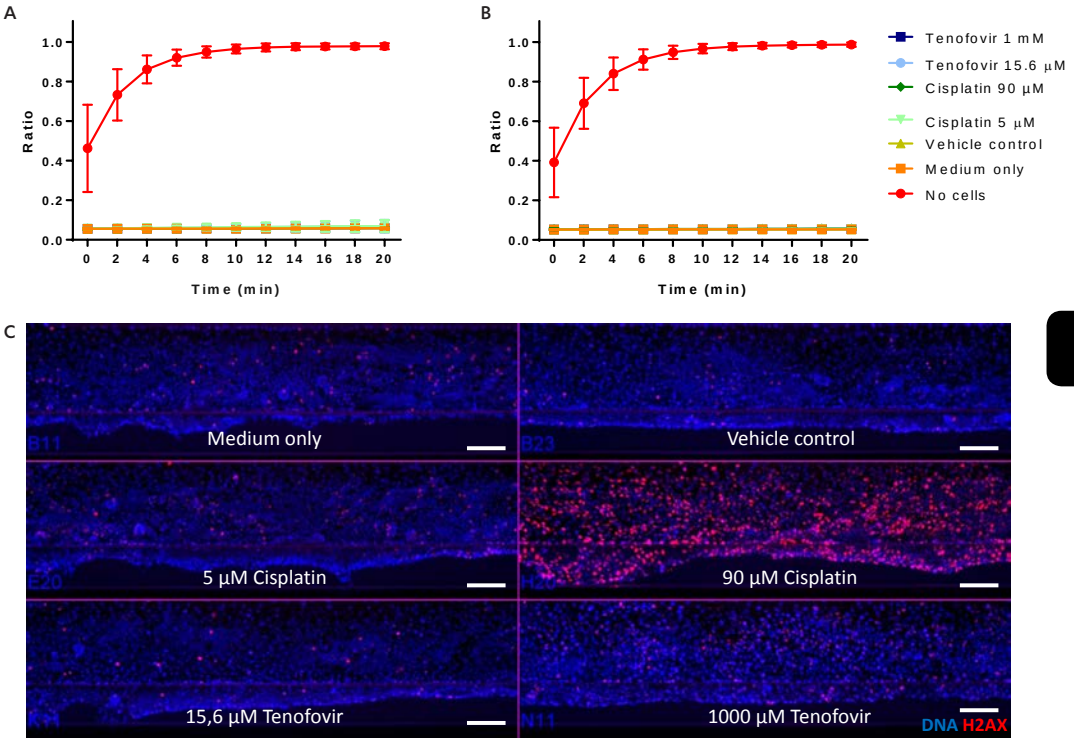

Supplementary Figure 2. Organoid-derived tubes before and after cisplatin and tenofovir exposure. Before exposure to cisplatin and tenofovir, tubes are leak-tight (A, data plotted of *n* = 3 independent experiments). 24 hours after exposure to cisplatin and tenofovir, tubes remain leak-tight (B, data plotted of *n* = 3 independent experiments). γH2AX staining after 24 hours of exposure to cisplatin and tenofovir (C).

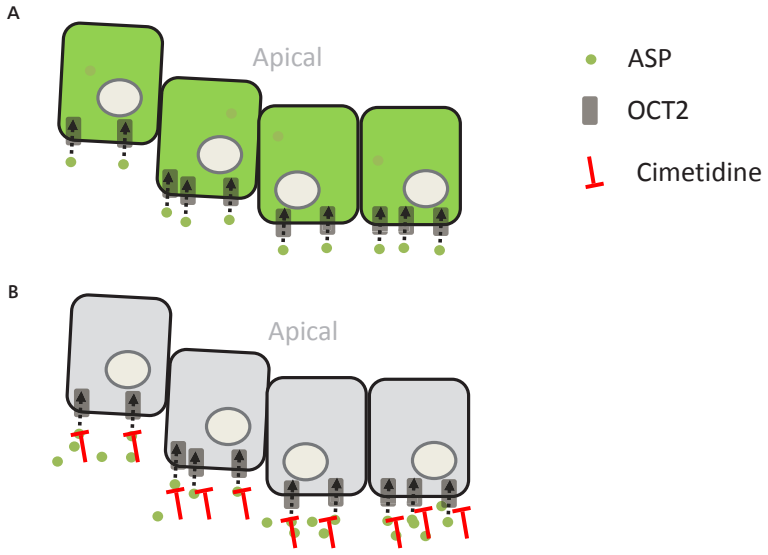

Supplementary Figure 3. Overview of the OCT2 assay. Fluorescent ASP is transported into cells at the basal side by OCT2 (A). This can be inhibited by OCT2-inhibitor cimetidine, thereby reducing the intracellular fluorescent signal (B).

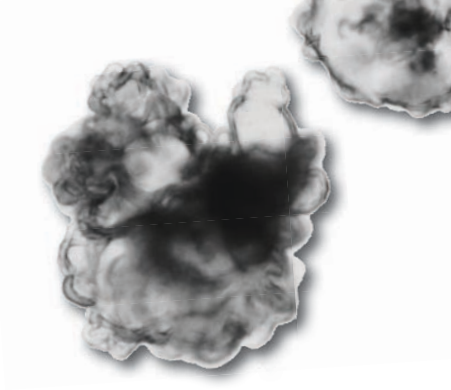

CHAPTER 6

TRACING ORGANOID-FORMING CELLS *IN VIVO*

Troy/TNFRSF19 marks epithelial cells with progenitor characteristics during kidney development that continue to contribute to turnover of the collecting duct in adult kidney

ABSTRACT

During kidney development, progressively committed progenitor cells give rise to the distinct segments of the nephron, the functional unit of the kidney. Similar segment-committed progenitor cells are thought to be involved in the homeostasis and regeneration of adult kidney. However, markers for most segment-committed progenitor cells remain to be identified. Here, we evaluate *Troy/TNFRSF19* as a segment-committed nephron progenitor cell marker.

Troy is expressed in the ureteric bud during embryonic development. During post-natal nephrogenesis, Troy+ cells are present in the cortex and papilla and display an immature tubular phenotype. Tracing of Troy+ cells during nephrogenesis demonstrates that Troy+ cells give clonally rise to tubular structures that persist for up to 2 years after induction. Troy+ cells have a 40-fold higher capacity than Troy- cells to form organoids, which is considered a stem cell property *in vitro*. In the adult kidney, Troy+ cells are present in the papilla and these cells continue to contribute to collecting duct formation during homeostasis and repair.

Our data show that Troy marks a renal stem/progenitor cell population in the developing kidney that in adult kidney contributes to collecting duct homeostasis and regeneration.

Frans Schutgens[1,2], Maarten B. Rookmaaker[1], Francis Blokzijl[3], Ruben van Boxtel[3], Robert Vries[4], Edwin Cuppen[3], Marianne C. Verhaar[1], Hans Clevers[2]

[1] Department of Nephrology and Hypertension, University Medical Center Utrecht
[2] Hubrecht Institute–Royal Netherlands Academy of Arts and Sciences
[3] Center for Molecular Medicine, Cancer Genomics Netherlands, Department of Genetics, University Medical Center Utrecht
[4] Hubrecht Organoid Technology (HUB), Utrecht, the Netherlands

Under Review

INTRODUCTION

The kidney plays a crucial role in blood pressure regulation, interior milieu homeostasis and hormone production. The human kidney consists of one million nephrons, which are the functional units of the kidney. In mammals, nephrons arise exclusively during embryonic development, and in some species, including mouse, this process is continued during early post-natal development. After nephrogenesis has ceased, a low level of tubular cell turnover persists. However, no new nephrons are formed. The formation of insufficient nephrons during development, commonly referred to as 'low nephron endowment', poses a risk for kidney disease in later life.[1] Moreover, damage exceeding the capacity of renal tubules to replace injured cells, leads to loss of nephrons without replacement. The progressive loss of nephrons is the final common pathway of renal disease. Identification of the mechanisms and progenitor cells involved in renal development as well as adult organ homeostasis provides insights into kidney (patho)physiology and will facilitate the development of new diagnostic and therapeutic strategies.

Historically, research has focused on progenitor cells involved in nephrogenesis during embryonic development. Developmental studies have shown that the kidney is formed by the interaction of two distinct mesodermal cell populations, the ureteric bud (UB), where the self-renewing stem cell population particularly resides in the tips,[2,3] and the metanephric mesenchyme (MM). Upon the interaction between the UB and MM, nephrons are formed in a process that is dependent on Wnt-signaling.[4] Quickly after the induction of nephron formation, differentiation towards the distinct segments of the nephron, which are all derived from the MM except for the collecting duct (CD),[5] occurs. Indeed, it has been demonstrated using lineage tracing that clonal expansions occur during development that do not cross segment barriers,[6] showing that segment-committed progenitor cells exist. In line with this, we demonstrated that one single Lgr5+ segment-committed stem cell is responsible for the expansion of the thick ascending limb of Henle's loop (TAL) in each nephron.[7] However, until now, no other segment-committed progenitor cells have been identified in the developing kidney.

More recently, also in adult kidneys the presence of stem cell populations has been suggested. With elegant lineage tracing experiments, the gold standard for identification of stem cell populations, it has been demonstrated that during adult homeostasis and repair, clonal expansions occur that do not cross segment barriers. This suggests that adult segment-committed progenitor cells exist that clonally expand.[6] However, no markers for these segment-committed stem cells have been identified.

In this study, we evaluate the Wnt target gene *Troy* (*TNFRSF19*) as a stem cell marker in the developing and adult kidney. Wnt target genes and proteins are of specific interest for the identification of renal progenitor cells, as Wnt signaling is both essential for kidney development, and involved in adult tubular cell turnover.[4,7,8] In addition, *Troy* has been shown to mark stem/progenitor cells in the stomach and brain.[9-11] Here, we document the presence, localization and identity of Troy+ cells and its progeny in the developing kidney, as well as during normal cell turnover and regeneration in the adult kidney.

RESULTS

Troy-EGFP+ cells are present in the UB during embryonic development and mark undifferentiated cells in the post-natal kidney

To document *Troy* expression during embryonic development, we isolated embryonic kidneys from *Troy-Enhanced Green Fluorescent Protein (EGFP)-ires-CreERT2* mice (n=8). Embryonic kidneys were isolated at 12 days post coitum (12 dpc), when the UB starts to invade the MM, and were cultured *ex vivo* for 1, 2, or 6 days (Figure 1A, B, C). Troy-EGFP-expression was observed in the ureteric bud from the moment of isolation and remained present during the culture period. When kidneys were isolated at post-natal day 1 and 2 (P1 and P2, n=6), Troy-EGFP was detected in the outer cortex as well as in the papilla (Figure 1D).

Next, we phenotypically characterized the Troy-EGFP+ cells at P1 and P2 by immunofluorescent staining for nephron-segment specific markers. It showed that the majority of the Troy-EGFP+ cells did not co-stain with segment-specific differentiated tubular cell markers: megalin (proximal tubule; Figure 1E), Tamm Horsfall Protein (thick ascending limb of Henle's loop; Figure 1F), calbindin (distal tubule; Figure 1G), AQP2 (principal cells of the collecting duct; Figure 1H), AE1 (α-intercalated cells, collecting duct; Figure 1I) and Pendrin (non-α-intercalated cells, collecting duct; Figure 1J). It is of note that we detected only a limited number of Pendrin+ intercalated cells at post-natal day 3 (that do not co-stain with Troy), which is in accordance with findings from others.[12] Although most of the Troy-EGFP+ cells did not co-stain for these differentiation markers, occasionally some double-staining for Troy-EGFP+ cells with AQP2 or megalin is observed (supplementary information, Figure 1).

Thus, most Troy-EGFP+ cells are relatively undifferentiated cells directly post-natally.

Troy-EGFP+ cells in the developing kidney express UB/collecting duct specific genes

To further characterize the Troy-EGFP+ positive cells during renal development, we performed RNA sequencing of Troy-EGFP+ cells isolated from kidneys from early postnatal (p2) *Troy-EGFP-ires-CreERT2* mice (n=3) to determine the signature transcriptome. Single cells were FAC-sorted into three fractions: strongly Troy-EGFP positive (Troy-EGFP++) weakly Troy-EGFP positive (Troy-EGFP+) and Troy-EGFP negative (Troy-EGFP-) populations (Figure 2A). 5-10% of the living cells at post-natal day 2 were Troy-EGFP++ (with these gating settings, 0.5% of the kidney cells from a wildtype mouse were part of the EGFP+ population). We found that *Troy* expression was highest in the Troy-EGFP++ population as compared to Troy-EGFP+ and Troy-EGFP-, confirming their identity as the endogenous *Troy+* kidney population (Figure 2B).

From a previously published dataset,[13] we extracted lists of genes that are enriched in the UB and a list of genes that are specifically expressed in the MM. We compared these lists, with the genes that are differentially expressed in the Troy++ population, compared with the Troy- population. We found that genes that were enriched in Troy++ population, were much more likely to be typical UB genes than MM genes. These findings indicate a predominant UB-identity of Troy-EGFP++ cells, and MM-identity for Troy-EGFP- cells (Figure 2C).

Next, we performed a similar analysis to assess in greater detail the stages of UB development, by comparing our expression data to an additional data set[14] that we accessed through the Gudmap database. This micro-array based data set includes two time points, E11.5 and E15.5 and examines multiple laser-captured compartments. It is of note that this reference data set did not find

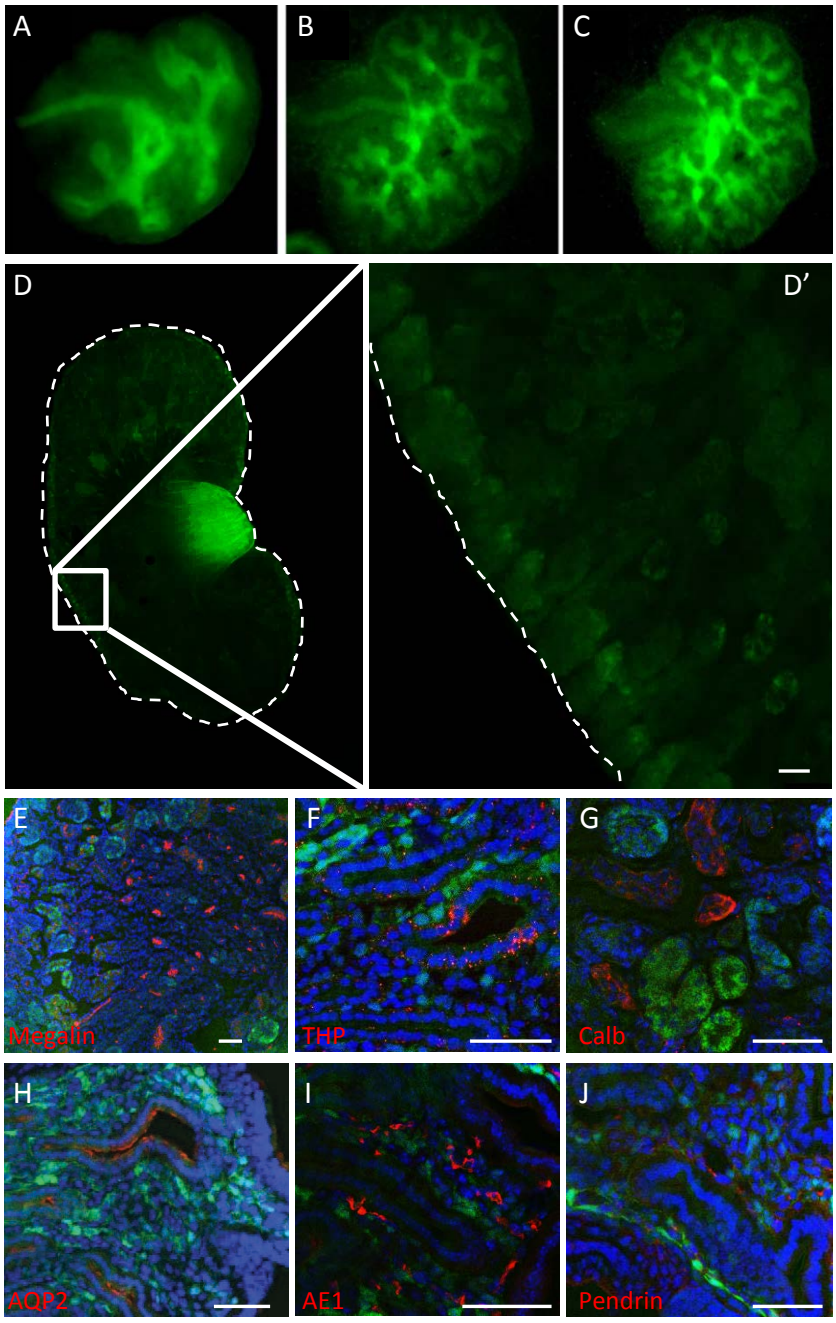

Figure 1. Troy expression during kidney development. Troy was expressed during embryonic development in the UB at E12.5 (A), E13.5 (B) and E18.5 (C) dpc in *ex vivo* kidney culture. At post-natal day 1 and 2, Troy was expressed in the papilla (D) and outer cortex (D,D'). Troy-EGFP+ cells did not overlap with tubular differentiation markers megalin (E), THP (F), Calbindin (G), AQP2 (H) AE1 (I), or Pendrin (J). Of note, we detected only a limited number of Pendrin+ intercalated cells at post-natal day 2, which is what is expected at P3.[12] E-J visualized with immunofluorescence. Scale bars: 50 µm.

large differences in gene expression across compartments[14] and therefore it appeared that many compartments were enriched in the Troy-EGFP++ population (Figure 2D). However, within the UB-related compartments, Troy-EGFP++ cells had highest upregulation in E15.5 ureteric tip-specific genes, showing a ureteric tip identity of Troy-EGFP++ cells (Figure 2D). Surprisingly, genes specific to the S-shaped body, a non-UB related compartment, were also highly upregulated in the Troy-

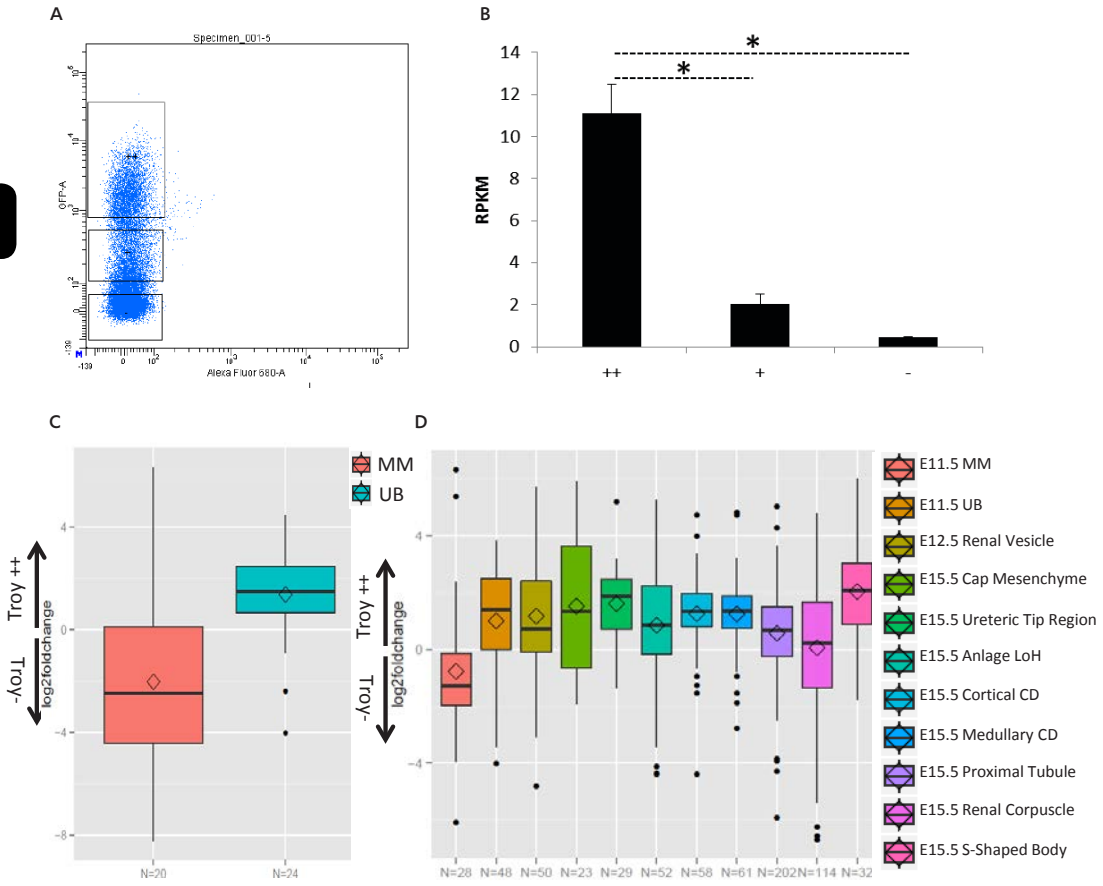

Figure 2. Transcriptome analysis of P2 Troy-EGFP++ versus Troy-EGFP- cells. Profile of FAC-sorted Troy-EGFP++, Troy-EGFP+ and Troy-EGFP- cells, from *Troy-EGFP-CreERT2* mice at P2 (A) EGFP++ cells had high Troy expression, compared to EGFP+ and EGFP- cells, confirming its identity as the endogenous Troy population. Values depicted as Reads per Kilobase per million Mapped Reads (RPKM). Error bars are SD from two replicates and significance is calculated with a one way anova, followed by Tukey post-hoc test * $P < 0.01$ (B). EGFP++ cells had high *Troy* expression, compared to EGFP+ and EGFP- cells, confirming its identity as the endogenous *Troy* population. * Indicates $P \leq 0.0001$ (B). UB-associated genes were upregulated in Troy-EGFP++ cells, when compared to Troy-EGFP- population, and MM-specific genes downregulated. The total number of genes in the compartment-specific gene sets are indicated below the graph. Gene sets are from Schwab and colleagues[13] (C). Within the UB compartments, upregulation of E15.5 ureteric tip region-specific genes in Troy++ compared with Troy- cells was largest. Within adult compartments, Troy-EGFP++ cells are particularly upregulated in medullary and cortical collecting duct genes. Compartment-specific gene lists were derived from Brunskill and colleagues.[14] The number of the genes per compartment is indicated below the graph (D). Diamonds in the box plots (C, D) depict the mean.

EGFP++ fraction. However, during the S-shaped body stage of kidney development, fusion to the ureteric bud has already taken place, potentially explaining why – at least part of – Troy-EGFP++ cells are also enriched for S-shaped body genes.

Interestingly, of the compartments in the data set that remain present in adult kidney (proximal tubule, Loop of Henle, cortical collecting duct and medullary collecting duct), Troy-EGFP++ cells have on average the highest upregulation in collecting duct-specific genes.

Troy-EGFP+ cells in the developing kidney exhibit organoid-forming capacity *in vitro*

Formation of spheres or organoids *in vitro* is considered a stem cell capacity.[15-17] To assess organoid-forming capacity of Troy-EGFP++ cells, we FAC-sorted cells derived from P2 kidneys (n=3 mice) into Troy-EGFP++, Troy-EGFP+ and Troy-EGFP- populations (Figure 3A) and we seeded 15,000 cells of each fraction in Matrigel as described previously.[18] Cells were cultured in culture media supplemented with Wnt3A-, Rspo1- and Noggin- conditioned medium and addition of B27, N-acetylcysteine, EGF, FGF10 and A8301.

Sorted Troy-EGFP++ cells clonally proliferated, leading to typical cystic organoids, as previously observed for multiple other organs (Figure 3C, D).[17] After 5 days, by scoring cystic structures as depicted in 3C and E, a 40-fold higher colony-forming efficiency of Troy-EGFP++ (2.0%) cells was observed, compared to the Troy-EGFP- cells (0.05%), whereas the Troy-EGFP+ population had an intermediate efficiency of 0.87% (Figure 3B). In the organoids derived from single Troy-EGFP++ cells, both EGFP+ positive as well as negative cells were present, suggesting loss of the expression of stem / progenitor cell marker Troy (Figure 3E).

To provide definitive proof that the organoids arose in a clonal fashion, we FAC-sorted single Troy-EGFP+ cells from the culture of cystic structures (as depicted in Figure 3C and E), directly into Matrigel (i.e. one single cell per well). We found that the same epithelium that formed cystic structures, formed complex branching structures that could subsequently be expanded into multiple structures (Figure 3F).

Troy-EGFP+ cells clonally expand into tubular structures during renal development

We used *in vivo* lineage tracing to determine whether the Troy+ populations residing within the developing kidney were functioning as renal stem cells *in vivo*. *Troy-EGFP-ires-CreERT2; Rosa-LacZ* mice were tamoxifen-induced at post-natal day 1 and traced for 1 (= day 2), 9 and 29 days as well as 2 years. At day 2 (n=2), LacZ+ cells were confined to the cortex, whereas at day 10 (n=3), LacZ+ structures started to extend into the medulla (Figure 4A-C). At day 30 (n=3), LacZ+ clones extended into the papilla (Figure 4D-F). In accordance with the histology, quantification of tracing clones revealed that these clones significantly increased in size over this period of time ($p < 0.01$; 4H). In addition, we observed that these clones not only continuously expand, but that they also persist for at least 2 years after induction (Figure 4G). To identify to which nephron segment Troy-expressing cells gave rise, immunohistochemistry (IHC) for differentiated tubular markers was performed (Figure 4I-L). IHC revealed that clones predominantly co-stained for AQP2, a collecting duct marker rather than for markers for the proximal tubule (Figure 4J), loop of Henle (Figure 4K), or distal tubule (Figure 4L). However, particularly in the long-term tracings, also co-staining was observed for megalin, THP and calbindin (supplementary information, Figure 2).

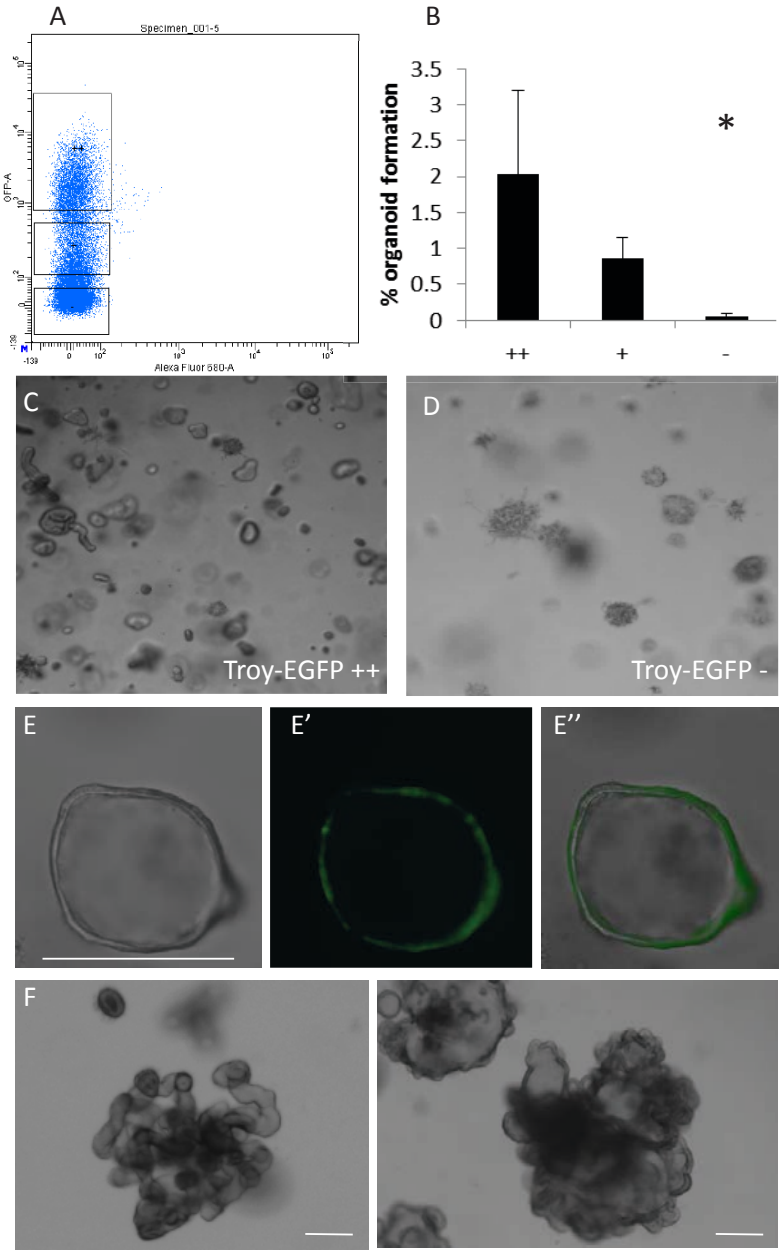

Figure 3. Troy+ cells have organoid-forming capacity. Profile of FAC-sorted EGFP populations from P2 kidneys (n=3) isolated from *Troy-EGFP-ires-CreERT2* mice: Troy++ and Troy+ were discriminated from the Troy- populations according to their EGFP expression level (A). Organoid-forming capacity was significantly ($P<0.05$) increased in the Troy-EGFP++ population compared to the Troy-EGFP- after 5 days. Error bars signify SD. (B) In the Troy-EGFP++ cultures, cystic organoids were observed after 5 days (C), whereas EGFP- cultures gave rise to mesenchymal-like colonies (D). The organoids formed in the Troy-EGFP++ culture contained both Troy-EGFP+ as well as Troy-EGFP- cells (E). To prove that the structures were clonal, we FAC-sorted one single cultured Troy-EGFP+ cell per well and complex branching structures formed. Images are from passage 2 (F). Scale bars: 250 µm.

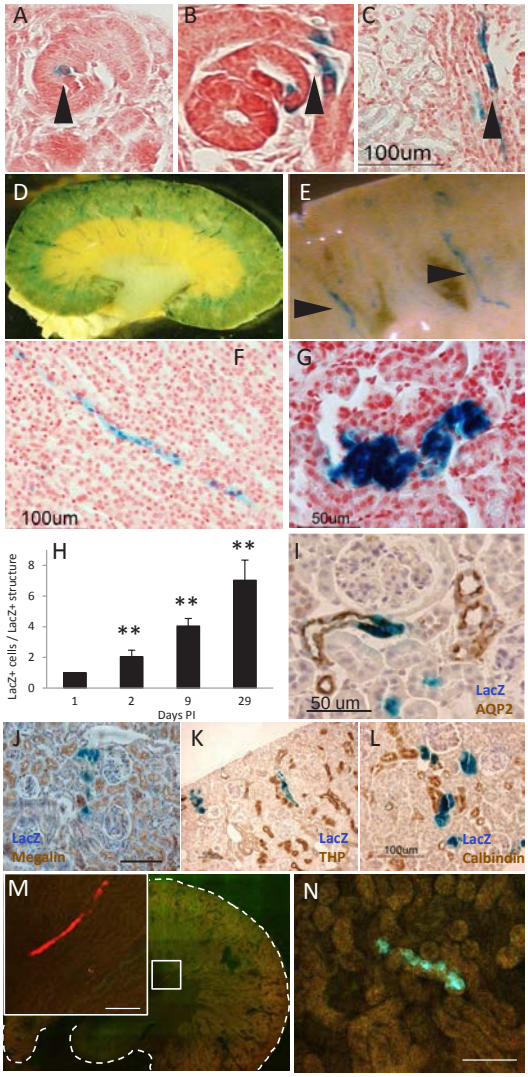

Figure 4. Troy+ cells formed tubular structures during post-natal kidney development. Kidney sections of P1 induced *Troy-EGFP-ires-CreERT2; Rosa- LacZ* mice, traced for 1 (A), 2 (B) or 9 (C) days, indicating the expansion of Troy+ clones (arrow heads). Whole mount images of *Troy-EGFP-ires-CreERT2; Rosa- LacZ* kidneys traced for 29 days and stained for LacZ, indicated that tubular structures (arrow heads) were formed (D, E). The formation of tubular structures was confirmed with histology on 29 day traced *Troy-EGFP-ires-CreERT2; Rosa- LacZ* kidney (F). Tubular structures persisted up to two years, which was the last time point included in the experiment (G). Quantification of the number of LacZ+ cells per LacZ+ structure shows the significant expansion of LacZ+ clones, as assessed by a One Way Anova, followed by a post-hoc Tukey test. P-values of the differences between 1 day post-induction on the one hand, and different tracing time points on the other hand are indicated in the graph ** P <0.01. (H). LacZ+ clones co-stained predominantly with AQP2 (I), and not with megalin (J), THP (K) or calbindin (L). Confetti lineage tracing from neonate Troy+ populations revealed the activity of individual Troy+ stem/progenitor cells. Confocal images of the kidneys of P1 induced *Troy-EGFP-ires-CreERT2; R26R-confetti* mice, where a RFP clone that was traced for traced for 1 year (M) and a CFP clone that was traced for 90 days (N). The single color shows the stem/progenitor outcome of one Troy+ cell. Scale bars: 100 µm, except in G and I: 50 µm.

To assess whether these LacZ+ expansions were clonal (and not the result of clustering of multiple independent Troy+ cells that together gave rise to a tubular structure), we employed *Troy-GFP-ires-CreERT2; R26R-confetti* mice that after tamoxifen-induction randomly express one of four fluorescent proteins.[19] Again, mice were induced at post-natal day 1 and traced for 30 (n=3), 60 (n=3), 90 (n=3), 180 (n=3), 365 (n=3) and 540 days (n=2). Single-colored clones were detected at distinct time points (Figure 4M, N), indicating that one clone arose from one single Troy+ cell (otherwise, clones of mixed colors would have been detected). In addition, clones persisted for at least 1.5 years. Fewer clones were observed per induced kidney than in the LacZ tracings,[7] in agreement with the lower sensitivity of the *R26R-confetti* allele.[19]

Troy-EGFP+ cells are present in the papilla in the adult kidney

Next, we assessed the presence of Troy+ cells in the kidney after completion of nephrogenesis. In 5-week-old *Troy-EGFP* mice, the presence of Troy-EGFP+ cells was limited to the papilla (Figure 5A) and Troy expression was more limited in the adult kidney compared to P1 kidney. No co-staining was observed with megalin, THP, calbindin and pendrin (supplementary information, Figure 3). Co-staining occurred with AE1 (α-intercalated cells of the collecting duct, Figure 5B) and AQP2 (principal cells of the collecting duct, Figure 5C).

Troy-EGFP+ cells clonally expand into tubular structures during adult renal cell turnover

We induced *Troy-GFP-ires-CreERT2; Rosa-LacZ* mice with tamoxifen at post-natal day 35 and followed tracing for up to 1 year (1, 7, 21, 63, 181, 365 days). As expected, the LacZ+ cells were present in the papilla only, and the number of LacZ+ cells was limited, compared to P1-induced kidney, but the labelled LacZ+ structures increased significantly over time (Figure 5D-F, J, K). IHC revealed predominant co-staining with AQP2, a marker of principal cells of the collecting duct (Figure 5H) and AE1 (marker of intercalated cells of the collecting duct, Figure 5I).

As the number and size of the LacZ tracing clones was limited, we employed *Troy-GFP-ires-CreERT2; Rosa-tdTomato* mice, with a higher reporter efficiency, to confirm our LacZ-tracings. We induced at day 56 and found that 14 days after induction, Troy-derived tubular structures were present, predominantly in the papilla (supplementary information, Figure 4). These structures increased in size over time and remained present on the long term, as assessed after 1 year of tracing (Figure 5L and L').

Troy-cells contribute to regeneration after reversible injury

To further substantiate the findings of Troy+ cells as stem/progenitor cell, we assessed whether Troy+ cells contributed to regeneration. Injection of folic acid is known to induce injury in both proximal tubule and collecting duct.[20] To confirm that folic acid induced tubular damage, histology was assessed. After 7 days, histology revealed signs of tubular kidney injury, including tubular dilation, cast formation and cell shedding (Figure 6A (vehicle) and A' (folic acid)). Ki-67 staining showed an increase in proliferating cells in the folic acid-injected mice, compared to vehicle-injected mice (Figure 6B (vehicle) and B' (folic acid)). To confirm injury, blood urea levels were measured and these were increased compared to control (Figure 6C).

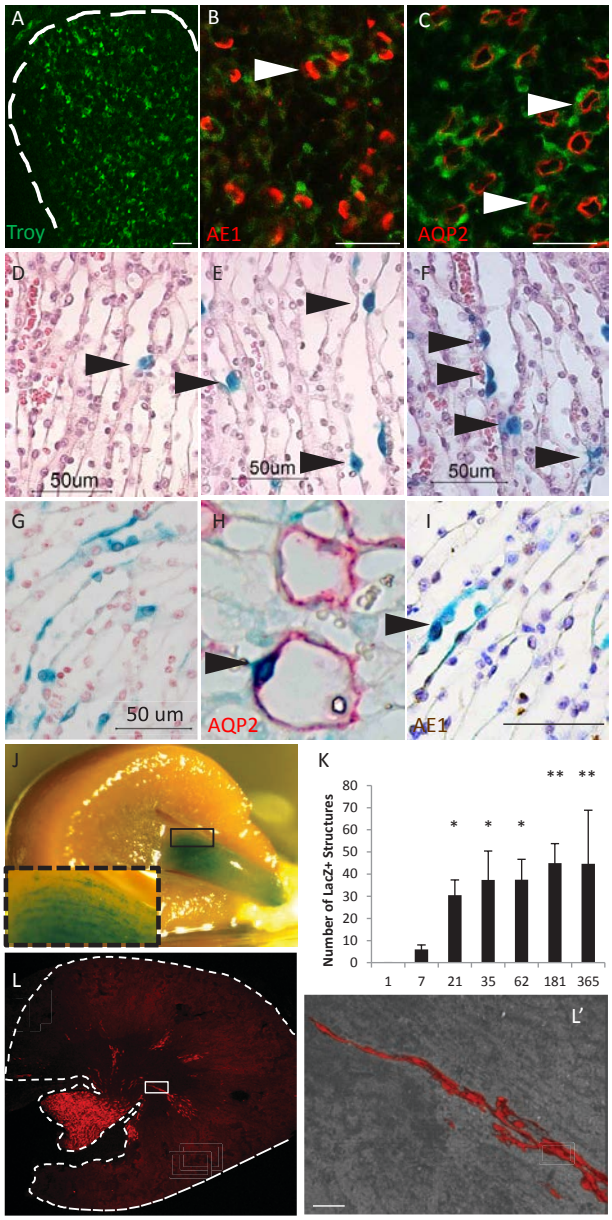

Figure 5. Troy is expressed in adult kidney and Troy+ cells accumulate over time. Troy expression in adult kidney was limited to the papilla, as visualized with confocal imaging. Dashed white line indicates the circumference of the papilla (A). Co-staining (arrow heads) of Troy+ cells with collecting duct markers AE1 (B) and AQP2 (C), as assessed with immunofluorescence. Sections of *Troy-EGFP-ires-CreERT2* mice show LacZ+ cells (arrow heads) induced at day 35, and traced for 14 (D), 30 (E) or 90 days (F), up to 1 year (G). Part of the LacZ+ cells co-stained with AQP2 (arrow head) (H) and AE1 (arrow head) (I). Whole-mount image of an adult kidney traced for 63 days (J), with detail of the papilla in the dashed box. The number of LacZ+ structures per kidney section increases significantly over time. P-values of the differences between 1 day post-induction on the one hand, and different tracing time points on the other hand are indicated in the graph* P <0.05 ** P <0.01 (K). Adult-induced (day 56) tracings in *Troy-GFP-ires-CreERT2; Rosa-tdTomato mice,* confocal image of a cross-section, 1 year after induction (L and L'). L' is a 3D-reconstruction from the clone in the white box in L. Scale bars: 50 µm.

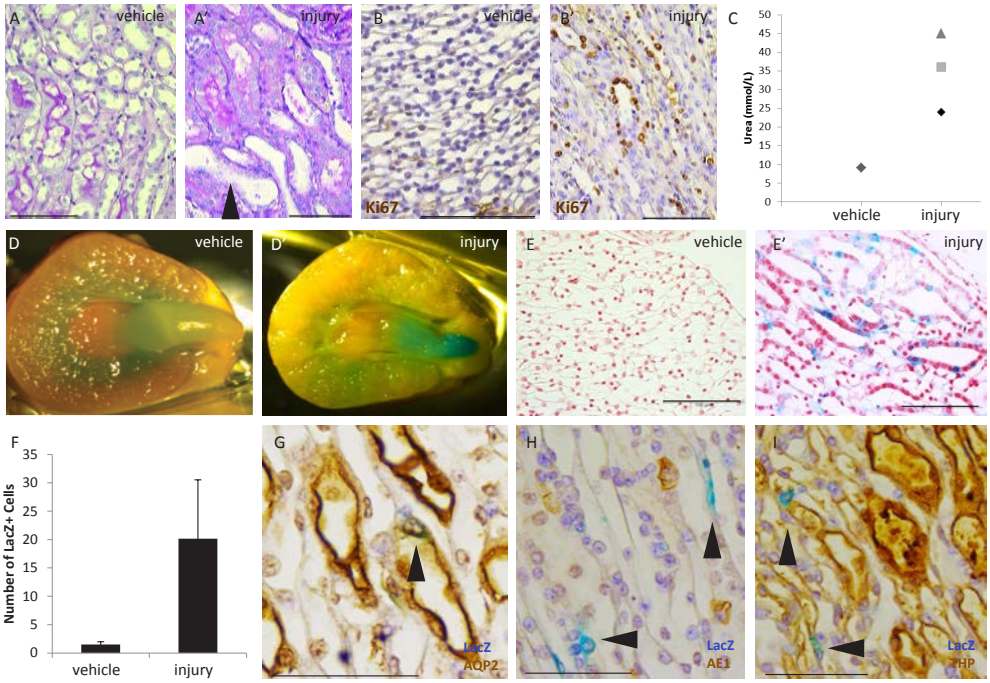

Figure 6. Troy-derived cells increase after injury-induction. Histology of a kidney, 7 days after folic acid injection, revealed signs of tubular injury, including tubular dilation, cast formation and cell shedding (arrow head), which was not present in the vehicle-treated animals (A (vehicle) and A' (injury)). Ki-67 staining showed an increase in proliferating cells in the folic acid-injected group compared to vehicle-injected mice (B (vehicle) and B' (injury)). Folic acid injection led to a significant increase in blood urea levels one day after folic acid injection, compared to vehicle injection, indicating kidney injury (C). Whole-mount kidney image from injured and tamoxifen-induced Troy-EGFP-ires-CreERT2 mice, revealed increased tracings in the papilla after 7 days, compared to a vehicle-injected animal (D (vehicle) and D' (injury)). Sections from injured and tamoxifen-induced Troy-EGFP-ires-CreERT2 mice, revealed increased tracings after 7 days in the injured animals compared to vehicle-injected animal (E (vehicle) and E' (injury), with the number of LacZ+ cells quantified per kidney section. N = 2 vehicle animals; N = 6 injury; error bars signify SEM (F). These cells (arrow heads) co-stain with AQP2 (G) and not with AE1 (H) or THP (I). Scale bars: 100 µm, except G,H,I: 50 µm.

After injection of folic acid and tamoxifen-induction of *Troy-EGFP-ires-CreERT2; Rosa-LacZ* mice, an increase in LacZ+ cells was observed in 3 out of 6 mice, compared to non-injured and solely tamoxifen-induced (n = 2) mice after 7 days (Figure 6D, D'; 6E, E' and F). The Troy-derived cells were present in the papilla and co-stained with AQP2 (Figure 6G) and not with AE1 (Figure 6H) or THP (Figure 6I).

DISCUSSION

Our data show that *Troy* marks a progenitor cell population during renal development that also contributes to collecting cell turnover in the adult kidney. A progenitor cell phenotype was supported by the absence of staining for differentiated tubule segment markers and

the organoid-forming capacity *in vitro*. Morphologically, *Troy* appears to be expressed in the UB during embryonic development. At postnatal day 1, the gene expression profile of the Troy+ cells matched the UB rather than MM, and within the UB, resembled the expression of the ureteric tip region. Moreover, lineage tracing showed that Troy+ cells clonally contributed to distinct nephron segments, including the collecting duct, during postnatal development, as well as collecting duct turnover and regeneration in the adult kidney. Whether this stem/progenitor phenotype of Troy+ cells is hard-wired, or rather a state that cells can enter and leave (a "stem cell state"), remains to be identified.

Our findings are in line with other research on renal stem/progenitor cells. Classic recombination experiments have demonstrated that the UB gives rise to the collecting duct, and later others[21] extended this finding and showed that progenitor cell capacity of the early (12 dpc) UB is not restricted to a limited number of UB cells. Accordingly, we note the diffuse Troy expression of the UB in kidneys harvested 12 dpc. More recent experiments demonstrated that self-renewing progenitor cells are predominantly located in the tips of the UB[2,3,22] and indeed, we find that Troy++ cells have a UB-tip gene signature. Moreover, previous *in vivo* tracing studies have suggested clonal expansion of single segment-committed stem cells during renal development, homeostasis and regeneration.[6] Our study confirms and extends these findings by providing a marker for a subset of these clonally expanding cells. In addition, our study is complementary to our previous study[7] where we identified Lgr5 as a marker for the loop of Henle, and we elaborate the findings into the adult maintenance and regeneration phase. Although both *Troy* and *Lgr5* are Wnt-target genes, their expression pattern as well as the location and identity of their daughter cells is clearly different. However, there appears to be some overlap in Lgr5 and Troy expression in the kidney: for example, P1-induced *Troy* tracings yields some clones that co-stain with TAL-marker THP (TAL is the predominant phenotype of *Lgr5*-traced cells). A similar situation with different fates for *Troy* and *Lgr5* stem cells exists in the stomach epithelium.[11,23]

We find that the location and relative number of Troy+ cells change during renal development (Figure 7). During early nephrogenesis (12dpc), Troy appears to be expressed in almost all UB cells, whereas Troy is expressed in the papilla and outer cortex immediately after birth, when nephrogenesis still takes place. Expression is limited to the papilla when nephrogenesis has ceased 5 weeks later. The fact that, although predominantly located at the UB tips, all UB cells have stem cell capacity during early nephrogenesis is in line with previous findings[21] as described above. The cortical localization of perinatal Troy+ stem cells appears to be in line with the notion that nephrogenesis still takes place at the renal cortex at this time point, suggesting the presence of UB stem cells in the cortex. However, at P1 Troy appears to be expressed in progenitor cells of other nephron segments, which is supported by the increased presence of non-collecting duct phenotypes of Troy progeny in the P1-induced tracing experiment, and the co-staining of Troy cells with non-collecting duct markers like megalin. Localization of progenitor cells in the papilla at P1 and at 5 weeks of age extends the findings of the papilla as stem cell niche. The papilla as adult stem cell niche was previously suggested on the basis of DNA label-retaining experiments. [24-29]

The relative reduction in number of Troy+ cells in adult kidney as compared to the developing kidney can be explained by the increased number of cells per nephron in adult kidney, causing a relative decrease in stem cells. The reduced Troy expression in adult kidneys compared to

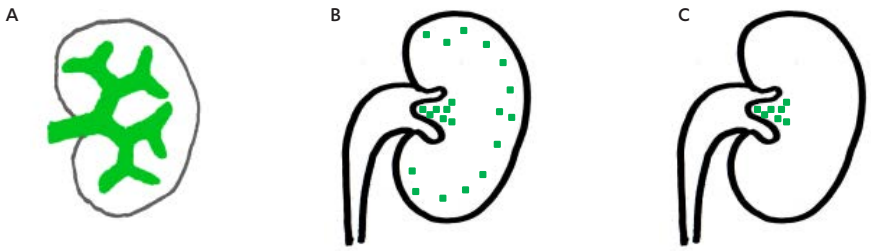

Figure 7. Localization of Troy expression at different time points. Troy is expressed in the ureteric bud during embryonic development (A). Troy is expressed in the nephrogenic zone and in the papilla in the post-natal kidney (B). Troy is expressed in the papilla in the adult kidney during homeostasis and repair (C).

the developing kidney could also be explained by the low-turnover of the kidney during homeostasis (i.e. proliferation of less Troy-EGFP+ cells), which eliminates a requirement for active Troy+ stem cell populations, such as present in the gut.[30] Alternatively, stem cells may lose Troy expression and expression might be induced upon injury. Indeed, we observed an increase in Troy-derived cells after folic acid-induced injury. We did not resolve the mechanism behind this response. It could either be that after injury, Troy expression was induced in a dedicated stem cell, as is observed in the liver[31] and pancreas,[32] or it could be that any differentiated cell could enter a (Troy+) stem cell state, which is a mechanism that is also observed in the intestine, where differentiated cells can, when Lgr5+ stem cells are removed, fill the stem cell niche.[33] In the proximal tubule of the kidney, it seems that all differentiated epithelial cells have the capacity to dedifferentiate and proliferate.[34] Similarly, in the physiological UB stem cell capacity is localized to the UB tips,[3] but after dissociation (i.e. damage), all UB cells have stem cell capacity.[21]

In contrast to the *in vivo* tracing studies mentioned above, a variety of *ex vivo* studies have demonstrated differentiation of (mouse and human) adult renal progenitor cells into more than one nephron segment. Rat proximal tubule are *in vitro* capable of differentiation into structures containing all segments of the nephron, even including the collecting duct.[35] A mouse MSC-like collecting duct progenitor cell population has the *in vitro* capacity to differentiate into adipocytes and chrondrocytes,[36] although upon transplantation *in vivo* these cells are solely able to contribute to the collecting duct. Multi-potent human adult stem cells, marked by CD133 and isolated from cortical kidney tissue, have the *in vitro* capacity to differentiate into podocytes, endothelial and epithelial cells[37] or epithelial, osteogenic cells and adipocytes.[38] For obvious reasons, lineage tracings have not been carried out.

Thus, to our knowledge, whenever a lineage tracing or *in vivo* study is performed, mainly segment-restricted progenitors are found, whereas after *in vitro* culture, multi-potent progenitors are also found, possibly due to non-physiological trans-differentiation.

In our study, Troy cells give almost exclusively rise to collecting duct cells in the 12dpc and 5 week-old mouse kidneys. However, LacZ+ structures from the tracing experiments in P1 induced kidneys also have co-staining with megalin, calbindin and THP, particularly at long-term tracings. One explanation is that these markers display some expression in collecting ducts: calbindin expression has been observed in collecting duct,[39,40] whereas Kumar and colleagues[41] observed

THP in collecting duct cells. Alternatively, immediately after birth Troy might also be expressed in progenitor cells for other nephron segments.

To definitively determine the lineage capacity of Troy+ cells, a Troy knock-out allele and recently developed explant cultures based on primary embryonic renal cells,[42,43] will be of use. The progressive identification of nephron segment-committed stem cells provides fundamental insight in normal physiology and facilitates the evaluation of abnormal development as a first step towards clinical application. Although the relative number of these segment-committed stem cells appears to be low, especially in the adult kidney, previous studies by others[6] and by our group[7] suggest that a single segment-committed progenitor is responsible for the formation and homeostasis of that particular nephron segment and, together, the integrity of a whole nephron.[5] The ability to determine the number and quality of (committed) progenitor cells (i.e. regenerative capacity) in a renal biopsy may improve its prognostic value. Interestingly, Troy has already been used as a prognostic marker in oncology.[44-46] Moreover, the importance of assessing the quality of progenitor cells is highlighted by studies that show that proliferating cells with a prolonged G2/M cell cycle phase, have pro-fibrotic effects leading to chronic kidney disease.[47] The fundamental insight in the development and maintenance of nephrons provided by the progressive identification of segment-committed nephron progenitor cells, will fuel the development of new diagnostic and therapeutic strategies for renal disease.

MATERIAL AND METHODS

Mice

Troy-EGFP-ires-CreERT2; *Rosa-lacZ, Troy-GFP-ires-CreERT2; Rosa-tdTomato* and *Troy-EGFP-ires-CreERT2; R26R-confetti* mice were generated as described previously.[30] *Rosa26RlacZ* mice were obtained from Jackson Labs. All animal experiments were approved by the Animal Experimentation Committee of the Royal Dutch Academy of Science and UMC Utrecht.

Tamoxifen induction

Cre-recombinase was activated in *Troy-EGFP-ires-CreERT2*; *Rosa-LacZ* by intraperitoneal injection of 4-hydroxytamoxifen (Sigma). For post-natal day 1 inductions, a single dose of 10 µl tamoxifen in corn oil at 10 mg/ml was used; for post-natal day 35 inductions a single dose of 200 µl was applied.

Embryonic *ex vivo* culture

Embryos from timed pregnant mice were isolated 12 days after fertilization using a dissecting microscope.[48] Subsequently, they were placed in a petri dish with cold PBS. Head and tail were removed, the abdominal wall was opened and intra-abdominal organs were removed, by which the retroperitoneum was exposed. The retroperitoneum was carefully removed and kidneys were isolated from it. The embryonic kidneys were placed on a 4 mm pore size transwell membrane and cultured at the medium-air interface. Medium (Advanced Dulbecco's Modified Eagle's medium (ADMEM) / F12 supplemented with 1% penicillin / streptomycin, HEPES, Glutamax and 10% fetal calf serum) was refreshed every second day. The culture was maintained for one week in a fully humidified 37°C incubator with 5% CO2.

β-Galactosidase staining

To visualize the localization of Troy after tamoxifen-induction, kidneys were isolated, halved, and incubated for 2 hours in a 20-fold volume of ice-cold fixative (1% formaldehyde, 0.2% glutaraldehyde, 0.02% nonyl phenoxypolyethoxylethanol (NP40) in PBS) at 4°C on a rolling platform. Staining for the presence of β-galactosidase (LacZ) activity was performed as described.[23]

Histology and immunohistochemistry

H&E, PAS and IHC was performed according to standard protocols on 3–4 µm paraffin-embedded sections. The primary antibodies were goat anti-AQP2 (1:200, C-17, Santa Cruz), goat anti-THP (1:500, G-20, Santa Cruz); goat anti-calbindin D28K (1:200, N-18, Santa Cruz), goat anti-megalin (1:200; P-20, Santa Cruz), rabbit anti-AE1 (1:500, Alpha Diagnostics International), rat-anti-KI67 (1:1000, eBioscience). All primary antibodies were dissolved in 0.05% Bovine Serum Albumin (BSA) in PBS. If required, the secondary antibody rabbit- α-goat-HRP (1:500, Dako) in PBS in 0.05% BSA was used. Goat-α-Rabbit Powervision-Alkaline Phosphatase or Goat-α-Rabbit Powervision-Horse Radish Peroxidase (both Leica Biosystems) were used as secondary or tertiary antibodies, depending on the mode of detection. Staining with Permanent Red (Dako) or Nova Red (Vector laboratories) and counter-stained with haematoxylin or light green (Vector Laboratories).

Cryo- and vibratome- sectioning and confocal imaging

Isolated kidneys were sliced open and fixed for 30 minutes (postnatal) or 1 hr (adult kidney) in 4% PFA solution at 4 degrees. For cryosectioning, kidneys were dehydrated in a 30% sucrose solution in PBS overnight, followed by embedding in tissue freezing medium (Leica) and cyrosectioning. For vibratome sectioning, fixed organs were embedded in 4% UltraPure LMP Agarose (Invitrogen) and vibratome sectioned (Leica VT 1000S) at 150 µm as described previously.[49] Subsequenly, immunofluorescent stainings were carried out with goat anti-AQP2 (1:100, C-17, Santa Cruz), goat anti-THP (1:100, G-20, Santa Cruz); goat anti-calbindin D28K (1:100, N-18, Santa Cruz), goat anti-megalin (1:100; P-20, Santa Cruz); rabbit anti-pendrin (1:100; H-195 Santa Cruz); rabbit anti-AE1 (1:100, Alpha Diagnostics International). Alexa Fluor 568 donkey anti-goat and donkey anti-rabbit immunoglobulin G (IgG) were used as secondary antibodies (1:500; Invitrogen).

Then, 150 µm sections were mounted in Hydromount (National Diagnostics) and analyzed for fluorescent protein expression or immunofluorescence by confocal microscopy (Leica SP5).

RNA sequencing

Kidneys were isolated from neonatal mice (P2). *Troy-EGFP-ires-CreERT2* expressing kidneys were identified by confocal microscopy and this was later confirmed by a genotyping PCR. Kidneys were mechanically disrupted and enzymatically digested with collagenase (C9407, Sigma) and dispase (Invitrogen) and subsequently with TrypLE (Sigma-Aldrich) and DNase. Troy-EGFP++, Troy-EGFP+ and Troy-EGFP- cells (n=100,000) were sorted by flow cytometry (Moflo; Dako). Cells were collected centrifuged and lysed in TriZol reagent (Ambion Life Technologies). Samples from n=3 mice from two different sorts were pooled and a technical replicate was included.

RNA was extracted using TRIzol (Life Technologies) according to manufacturer's instructions. RNA quality was determined using a Bioanalyser 2100 (Agilent) with an RNA 6000 Nano Kit. Libraries

were generated from 100 ng total RNA using a TruSeq Stranded Total RNA kit with Ribo-zero human/mouse/rat (Illumina # RS-122-2201) according to manufacturer's instructions. For final application, 15 cycles of PCR were used. Quality of the libraries was determined and libraries were quantified using a bioanalyser 2100 (Agilent) with a DNA 1000 Kit. Equimolar amounts of libraries were pooled and subjected to single end, 75 base-pair sequencing using an Illumina Nextseq.

RNA sequencing analysis

RNA-seq reads were aligned to the mouse reference genome NCBIM37 using STAR.[50] The BAM files were sorted with Sambamba v0.5.1[51] and transcript abundances were quantified with HTSeq-count.[52] Subsequently, DESeq 1.16.0[53] was used to normalize gene counts and to test for differential expression between Troy++, Troy+ and Troy- samples. *P* values were adjusted for multiple testing using Benjamini-Hochberg FDR correction. Adjusted *P* values of < 0.05 were considered significantly up- or downregulated.

To determine which embryonic compartment resembles Troy++ cells the most in gene expression, we assessed the differential expression between Troy++ and Troy- cells of available compartment-specific gene sets of embryonic mouse kidney.[13,14] Gene symbols were converted to Ensembl Gene ID using org.Mm.eg.db[54] and genes that occurred in multiple segments or genes that we could not link to an Ensembl Gene ID were excluded from the analysis. From Brunskill and colleagues,[14] genes that were most specific to a compartment (> 20 fold upregulated compared to median expression over all compartments) were included in the analysis.

Organoid assay

Organoid formation assay is based on the original protocol by Sato and colleagues.[18] Kidneys were isolated and digested into a single cell suspension and sorted into Troy-EGFP++, Troy-EGFP+ and Troy-EGFP- populations as described under "RNA sequencing." 15,000 cells were resuspended for each condition in growth factor-reduced Matrigel (Corning) and cultured for a week in culture medium (ADMEM / F12 supplemented with 1% penicillin / streptomycin, HEPES, Glutamax), with 1.5% B27 supplement (Gibco), 40% Wnt3a conditioned medium (produced using stably transfected L cells) 10% Noggin conditioned medium, 10% Rspo1-conditioned medium,[55] EGF (50 ng/ml, Peprotech), FGF-10 (100 ng/ml, Preprotech); N-acetylcysteine (1.25 mM, Sigma) A8301 (5 µM, Tocris Bioscience). Colony-forming capacity was calculated after 5 days of culture.

For the cultures established from a single Troy-EGFP cell, a single cell suspension from cultured neonatal kidney cells from *Troy-EGFP-ires-CreERT2 mice* was made. Troy-EGFP++ cells were sorted (Facsjazz, BD) directly into Matrigel, one Troy-EGFP++ cell per well of a 96 well plate. After polymerization of the Matrigel, organoid culture medium was added and organoid cultures (n =3) were established.

Folic acid injury model

Adult *Troy-EGFP-ires-CreERT2*; *Rosa-lacZ,* were subjected to IP Folic acid injections at 125 mg /ml. 1 day after injury, Troy expression was induced with tamoxifen as described above. After 7 days, mice were sacrificed for analysis and blood samples were collected for determination of plasma urea (DiaSys Urea CT FS, DiaSysDiagnostic Systems).

Statistical analysis (except RNA sequencing analysis)

Error bars signify mean ± Standard Deviation (SD), unless otherwise indicated. In case of multiple groups, a one way ANOVA was performed, combined with Tukey post-hoc tests. A P-value <0.05 is considered statistically significant.

Accession numbers

The RNA sequencing data have been deposited at the European Nucleotide Archive (http://www.ebi.ac.uk/ena/) under accession number ERP019784.

ACKNOWLEDGMENTS

We thank Harry Begthel and Jeroen Korving for preparation of histological and immunohistochemical specimens. We thank Johan van Es and Maaike van den Born for support with the mouse work. We thank the Hubrecht Imaging Center for assistance with (confocal) microscopy. We thank the Hubrecht FACS facility for help the sort of Troy-EGFP cells. This work was supported by a grant from the Dutch Kidney Foundation (DKF14OP04).

REFERENCES

1. Hoy, W. E., Hughson, M. D., Bertram, J. F., Douglas-Denton, R. & Amann, K. Nephron Number, Hypertension, Renal Disease, and Renal Failure. *Journal of the American Society of Nephrology* **16**, 2557-2564 (2005).
2. Michael, L. & Davies, J. A. Pattern and regulation of cell proliferation during murine ureteric bud development. *Journal of anatomy* **204**, 241-255 (2004).
3. Shakya, R., Watanabe, T. & Costantini, F. The role of GDNF/Ret signaling in ureteric bud cell fate and branching morphogenesis. *Developmental cell* **8**, 65-74, doi:10.1016/j.devcel.2004.11.008 (2005).
4. Carroll, T. J., Park, J.-S., Hayashi, S., Majumdar, A. & McMahon, A. P. Wnt9b Plays a Central Role in the Regulation of Mesenchymal to Epithelial Transitions Underlying Organogenesis of the Mammalian Urogenital System. *Developmental cell* **9**, 283-292, doi:http://dx.doi.org/10.1016/j.devcel.2005.05.016 (2005).
5. Hendry, C., Rumballe, B., Moritz, K. & Little, M. H. Defining and redefining the nephron progenitor population. *Pediatric nephrology (Berlin, Germany)* **26**, 1395-1406, doi:10.1007/s00467-010-1750-4 (2011).
6. Rinkevich, Y. *et al.* In vivo clonal analysis reveals lineage-restricted progenitor characteristics in mammalian kidney development, maintenance, and regeneration. *Cell reports* **7**, 1270-1283, doi:10.1016/j.celrep.2014.04.018 (2014).
7. Barker, N. *et al.* Lgr5(+ve) stem/progenitor cells contribute to nephron formation during kidney development. *Cell reports* **2**, 540-552, doi:10.1016/j.celrep.2012.08.018 (2012).
8. Kawakami, T., Ren, S. & Duffield, J. S. Wnt signalling in kidney diseases: dual roles in renal injury and repair. *The Journal of pathology* **229**, 221-231, doi:10.1002/path.4121 (2013).
9. Hisaoka, T., Morikawa, Y., Kitamura, T. & Senba, E. Expression of a member of tumor necrosis factor receptor superfamily, TROY, in the developing olfactory system. *Glia* **45**, 313-324, doi:10.1002/glia.10323 (2004).
10. Shao, Z. *et al.* TAJ/TROY, an Orphan TNF Receptor Family Member, Binds Nogo-66 Receptor 1 and Regulates Axonal Regeneration. *Neuron* **45**, 353-359, doi:10.1016/j.neuron.2004.12.050 (2005).
11. Stange, D. E. *et al.* Differentiated Troy+ chief cells act as reserve stem cells to generate all lineages of the stomach epithelium. *Cell* **155**, 357-368, doi:10.1016/j.cell.2013.09.008 (2013).
12. Song, H.-K. *et al.* Origin and Fate of Pendrin-Positive Intercalated Cells in Developing Mouse Kidney. *Journal of the American Society of Nephrology* **18**, 2672-2682 (2007).
13. Schwab, K. *et al.* A catalogue of gene expression in the developing kidney. *Kidney international* **64**, 1588-1604 (2003).
14. Brunskill, E. W. *et al.* Atlas of Gene Expression in the Developing Kidney at Microanatomic Resolution. *Developmental cell* **15**, 781-791, doi:10.1016/j.devcel.2008.09.007 (2008).
15. Reynolds, B. A. & Weiss, S. Clonal and population analyses demonstrate that an EGF-responsive mammalian embryonic CNS precursor is a stem cell. *Developmental biology* **175**, 1-13, doi:10.1006/dbio.1996.0090 (1996).
16. Seaberg, R. M. *et al.* Clonal identification of multipotent precursors from adult mouse pancreas that generate neural and pancreatic lineages. *Nature biotechnology* **22**, 1115-1124, doi:10.1038/nbt1004 (2004).
17. Clevers, H. Modeling Development and Disease with Organoids. *Cell* **165**, 1586-1597, doi:10.1016/j.cell.2016.05.082 (2016).
18. Sato, T. *et al.* Single Lgr5 stem cells build crypt-villus structures in vitro without a mesenchymal niche. *Nature* **459**, 262-265, doi:10.1038/nature07935 (2009).
19. Snippert, H. J. *et al.* Intestinal crypt homeostasis results from neutral competition between symmetrically dividing Lgr5 stem cells. *Cell* **143**, 134-144, doi:10.1016/j.cell.2010.09.016 (2010).
20. Fang, T.-C. *et al.* Proliferation of Bone Marrow-Derived Cells Contributes to Regeneration after Folic Acid-Induced Acute Tubular Injury. *Journal of the American Society of Nephrology* **16**, 1723-1732 (2005).
21. Unbekandt, M. & Davies, J. A. Dissociation of embryonic kidneys followed by reaggregation allows the formation of renal tissues. *Kidney international* **77**, 407-416, doi:10.1038/ki.2009.482 (2010).

22. Riccio, P., Cebrian, C., Zong, H., Hippenmeyer, S. & Costantini, F. <italic>Ret</italic> and <italic>Etv4</italic> Promote Directed Movements of Progenitor Cells during Renal Branching Morphogenesis. *PLoS biology* **14**, e1002382, doi:10.1371/journal.pbio.1002382 (2016).

23. Barker, N. *et al.* Lgr5(+ve) stem cells drive self-renewal in the stomach and build long-lived gastric units in vitro. *Cell stem cell* **6**, 25-36, doi:10.1016/j.stem.2009.11.013 (2010).

24. Lin, S.-L. *et al.* Macrophage Wnt7b is critical for kidney repair and regeneration. *Proceedings of the National Academy of Sciences of the United States of America* **107**, 4194-4199, doi:10.1073/pnas.0912228107 (2010).

25. Whitehouse, T., Stotz, M., Taylor, V., Stidwill, R. & Singer, M. Tissue oxygen and hemodynamics in renal medulla, cortex, and corticomedullary junction during hemorrhage-reperfusion. *American journal of physiology. Renal physiology* **291**, F647-653, doi:10.1152/ajprenal.00475.2005 (2006).

26. Mohyeldin, A., Garzon-Muvdi, T. & Quinones-Hinojosa, A. Oxygen in stem cell biology: a critical component of the stem cell niche. *Cell stem cell* **7**, 150-161, doi:10.1016/j.stem.2010.07.007 (2010).

27. Oliver, J. A., Maarouf, O., Cheema, F. H., Martens, T. P. & Al-Awqati, Q. The renal papilla is a niche for adult kidney stem cells. *The Journal of clinical investigation* **114**, 795-804, doi:10.1172/JCI20921 (2004).

28. Oliver, J. A. *et al.* Proliferation and Migration of Label-Retaining Cells of the Kidney Papilla. *Journal of the American Society of Nephrology : JASN* **20**, 2315-2327, doi:10.1681/ASN.2008111203 (2009).

29. Al-Awqati, Q. & Oliver, J. The kidney papilla is a stem cells niche. *Stem Cell Rev* **2**, 181-184, doi:10.1007/s12015-006-0046-3 (2006).

30. Barker, N. *et al.* Identification of stem cells in small intestine and colon by marker gene Lgr5. *Nature* **449**, 1003-1007, doi:10.1038/nature06196 (2007).

31. Huch, M. *et al.* In vitro expansion of single Lgr5+ liver stem cells induced by Wnt-driven regeneration. *Nature* **494**, 247-250, doi:10.1038/nature11826 (2013).

32. Huch, M. *et al.* Unlimited in vitro expansion of adult bi-potent pancreas progenitors through the Lgr5/R-spondin axis. *The EMBO journal* **32**, 2708-2721, doi:10.1038/emboj.2013.204 (2013).

33. Tetteh, Paul W. *et al.* Replacement of Lost Lgr5-Positive Stem Cells through Plasticity of Their Enterocyte-Lineage Daughters. *Cell stem cell* **18**, 203-213, doi:10.1016/j.stem.2016.01.001 (2016).

34. Kusaba, T., Lalli, M., Kramann, R., Kobayashi, A. & Humphreys, B. D. Differentiated kidney epithelial cells repair injured proximal tubule. *Proceedings of the National Academy of Sciences of the United States of America* **111**, 1527-1532, doi:10.1073/pnas.1310653110 (2014).

35. Kitamura, S., Sakurai, H. & Makino, H. Single Adult Kidney Stem/Progenitor Cells Reconstitute 3-Dimensional Nephron Structures in Vitro. *Stem cells*, n/a-n/a, doi:10.1002/stem.1891 (2014).

36. Li, J. *et al.* Collecting Duct-Derived Cells Display Mesenchymal Stem Cell Properties and Retain Selective In Vitro and In Vivo Epithelial Capacity. *Journal of the American Society of Nephrology* **26**, 81-94 (2015).

37. Bombelli, S. *et al.* PKH(high) cells within clonal human nephrospheres provide a purified adult renal stem cell population. *Stem cell research* **11**, 1163-1177, doi:10.1016/j.scr.2013.08.004 (2013).

38. Sagrinati, C. *et al.* Isolation and characterization of multipotent progenitor cells from the Bowman's capsule of adult human kidneys. *Journal of the American Society of Nephrology : JASN* **17**, 2443-2456, doi:10.1681/ASN.2006010089 (2006).

39. Kumar, R., Schaefer, J., Grande, J. P. & Roche, P. C. Immunolocalization of calcitriol receptor, 24-hydroxylase cytochrome P-450, and calbindin D28k in human kidney. *American Journal of Physiology - Renal Physiology* **266**, F477-F485 (1994).

40. Davies, J. Control of calbindin-D28K expression in developing mouse kidney. *Developmental Dynamics* **199**, 45-51, doi:10.1002/aja.1001990105 (1994).

41. Kumar, S., Jasani, B., Hunt, J., Moffat, D. & Asscher, A. W. A system for accurate immunolocalization of Tamm-Horsfall protein in renal biopsies. *The Histochemical journal* **17**, 1251-1258, doi:10.1007/BF01002506 (1985).

42. Junttila, S. *et al.* Functional Genetic Targeting of Embryonic Kidney Progenitor Cells Ex Vivo. *Journal of the American Society of Nephrology* **26**, 1126-1137 (2015).

43. Halt, K. J. *et al*. CD146+ cells are essential for kidney vasculature development. *Kidney international* **90**, 311-324, doi:http://dx.doi.org/10.1016/j.kint.2016.02.021 (2016).

44. Spanjaard, R. A., Whren, K. M., Graves, C. & Bhawan, J. Tumor necrosis factor receptor superfamily member TROY is a novel melanoma biomarker and potential therapeutic target. *International Journal of Cancer* **120**, 1304-1310, doi:10.1002/ijc.22367 (2007).

45. Paulino, V. M. *et al*. TROY (TNFRSF19) Is Overexpressed in Advanced Glial Tumors and Promotes Glioblastoma Cell Invasion via Pyk2-Rac1 Signaling. *Molecular Cancer Research* **8**, 1558-1567 (2010).

46. Loftus, J. C. *et al*. TROY (TNFRSF19) Promotes Glioblastoma Survival Signaling and Therapeutic Resistance. *Molecular Cancer Research* **11**, 865-874 (2013).

47. Canaud, G. & Bonventre, J. V. Cell cycle arrest and the evolution of chronic kidney disease from acute kidney injury. *Nephrology Dialysis Transplantation* **30**, 575-583 (2015).

48. Giuliani, S. *et al*. Ex Vivo Whole Embryonic Kidney Culture: A Novel Method for Research in Development, Regeneration and Transplantation. *The Journal of urology* **179**, 365-370, doi:10.1016/j.juro.2007.08.092 (2008).

49. Snippert, H. J., Schepers, A. G., Delconte, G., Siersema, P. D. & Clevers, H. Slide preparation for single-cell-resolution imaging of fluorescent proteins in their three-dimensional near-native environment. *Nat. Protocols* **6**, 1221-1228, doi:http://www.nature.com/nprot/journal/v6/n8/abs/nprot.2011.365.html#supplementary-information (2011).

50. Dobin, A. *et al*. STAR: ultrafast universal RNA-seq aligner. *Bioinformatics* **29**, 15-21 (2013).

51. Tarasov, A., Vilella, A. J., Cuppen, E., Nijman, I. J. & Prins, P. Sambamba: fast processing of NGS alignment formats. *Bioinformatics* **31**, 2032-2034 (2015).

52. Anders, S., Pyl, P. T. & Huber, W. HTSeq—a Python framework to work with high-throughput sequencing data. *Bioinformatics* (2014).

53. Anders, S. & Huber, W. Differential expression analysis for sequence count data. *Genome Biology* **11**, 1-12, doi:10.1186/gb-2010-11-10-r106 (2010).

54. Carlson, M. org.Mm.eg.db: Genome wide annotation for Mouse. *R package* (2016).

55. Kim, K.-A. *et al*. Mitogenic Influence of Human R-Spondin1 on the Intestinal Epithelium. *Science* **309**, 1256-1259 (2005).

SUPPLEMENTARY INFORMATION

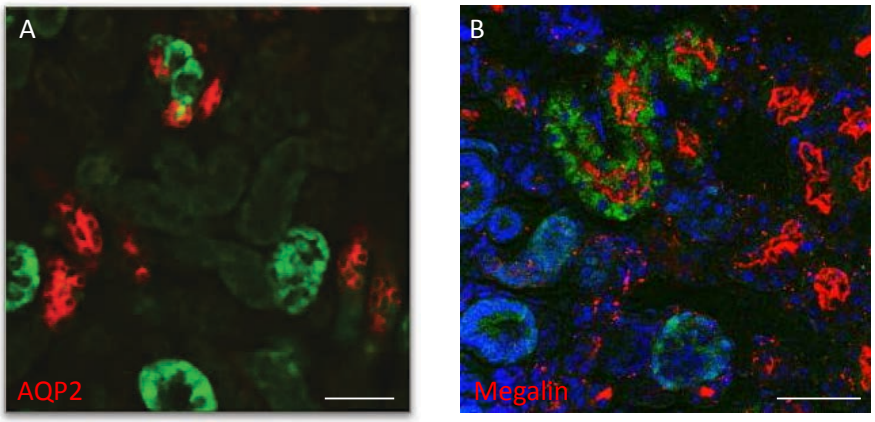

Supplementary Figure 1. Characterization of Troy-EGFP+ cells in neonatal kidney. Co-staining of Troy-EGFP+ P1 with differentiation markers AQP2 (A) and megalin (B) is observed occasionally. Scale bars: 50 µm.

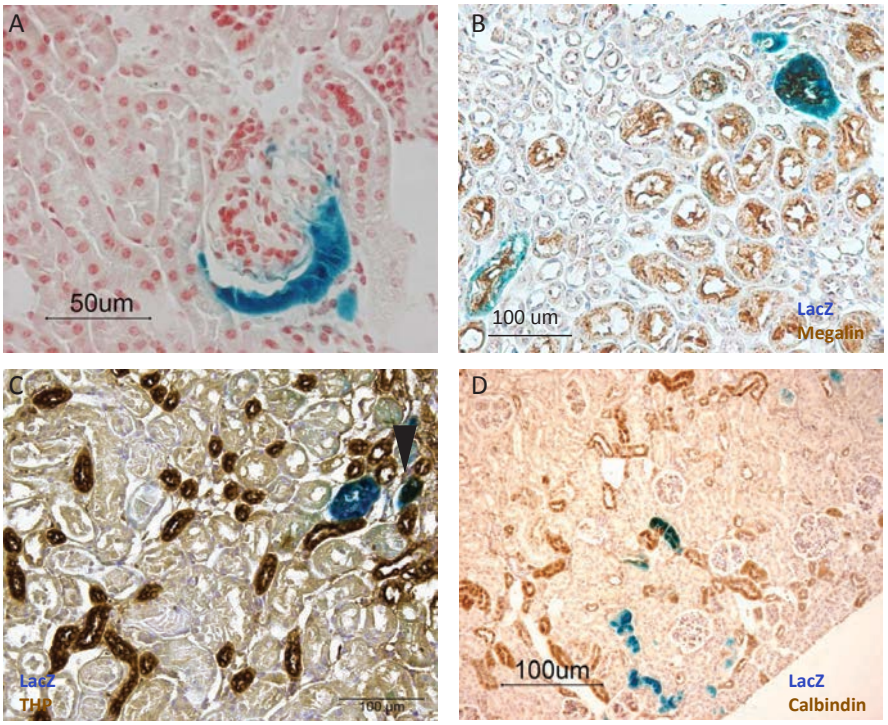

Supplementary Figure 2. Non-collecting duct tubular structures derived from Troy+ cells. Some tracings occur in close proximity to glomeruli (A) and co-staining occurs with Megalin (B) THP (*arrow head*) (C) and Calbindin (D).

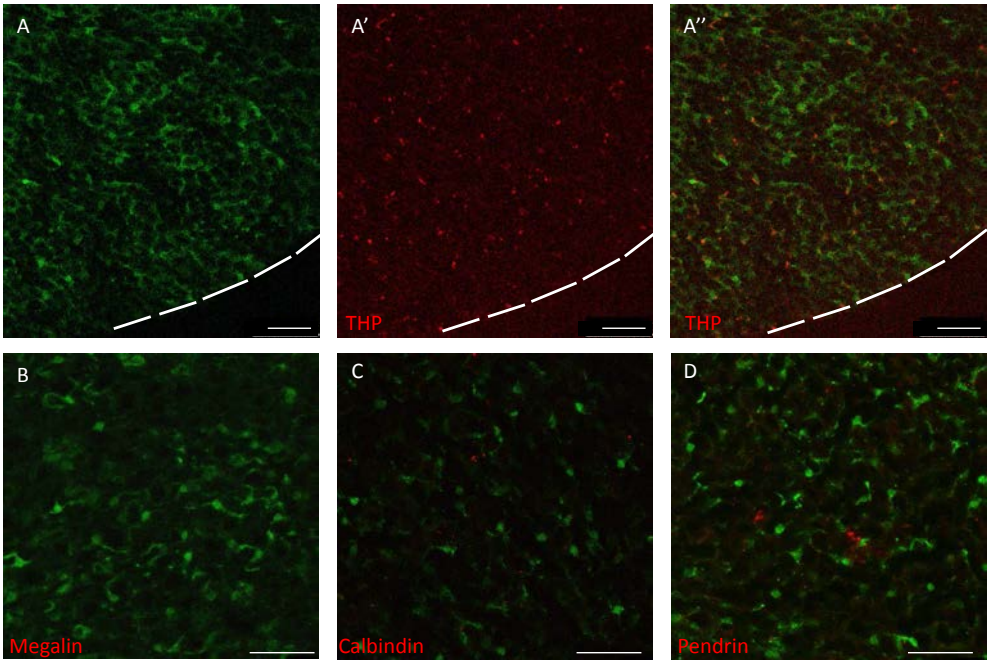

Supplementary Figure 3. Characterization of Troy-EGFP+ cells in adult kidney. Adult Troy-EGFP cells in the kidney do not co-stain with THP, as there is some THP staining present, separated channels are provided for clarity (A: GFP signal; A' THP-signal; A'': overlay), Megalin (B) Calbindin (C) and Pendrin (D), as assessed with immunofluorescence. Scale bars: 50 µm.

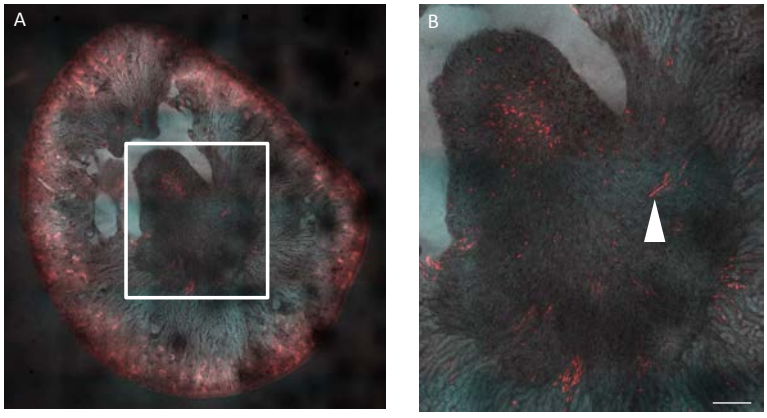

Supplementary Figure 4. Adult-induced (day 56) tracings in *Troy-GFP-ires-CreERT2; Rosa-tdTomato mice*. Confocal image of a cross-section 14 days after induction (A and insert: A') with clones present (white arrow head). Scale bar: 250 µm.

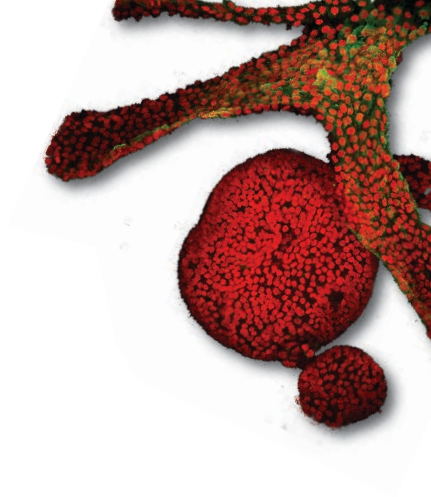

CHAPTER 7

SUMMARIZING DISCUSSION

Kidney disease is a worldwide public health problem. The population prevalence exceeds 16% in many countries and this number is expected to increase in the next decades, due to the rise in the prevalence of risk factors for kidney disease, such as diabetes, hypertension and cardiovascular disease.[1, 2] The causes of kidney disease can be classified in different dimensions: genetic (e.g. autosomal dominant polycystic kidney disease) versus acquired (e.g. infectious disease - BK virus-induced nephropathy); acute (e.g. after myocardial infarction) versus chronic (e.g. diabetic nephropathy); oncological (e.g. Wilms tumor) versus non-oncological.

The kidney has a high regenerative capacity in response to acute injury, such as infectious, ischemic or drug-induced toxic insults.[3] However, when damage exceeds a threshold, nephrons are lost without replacement. Then, regardless of the type of disease, kidney disease may progress to the final common pathway of end-stage renal disease. Treatment options for end-stage renal disease are either dialysis or kidney transplantation, and both have limitations and co-morbidities. Dialysis does not recapitulate all kidney functions and patients on regular hemodialysis have a mortality rate of up to 20% per year.[4] There is a shortage of organs for transplantation and the use of immunosuppressive drugs after transplantation increases the risk of infections and malignancies.[5, 6]

A better understanding of kidney function, regeneration and disease, preferably on a personalized level, is essential to identify new therapeutic targets, reliably test efficacy and toxicity of drugs and ultimately enhance the prognosis of patients with kidney disease. To achieve these goals, adequate human *in vitro* models are indispensable, since mouse models may not fully capture human disease.

Human *in vitro* models for kidney research before this thesis

For *in vitro* kidney research, two types of models have been predominantly used. First, our understanding of kidney (patho)physiology would not be where it is today, without the use of kidney cell lines. Proximal tubule cell lines display transporter function, rendering them useful for fundamental transporter studies and *in vitro* toxicity studies (as proximal tubule cells excrete toxic compounds).[7, 8] Genetic alterations in adult renal cell carcinoma have been identified in tumor cell lines.[9] However, cell lines have significant drawbacks. Cell lines from adult healthy kidney require an immortalization step, for example by introducing telomerase reverse transcriptase (TERT)[10] or HPV 16 E6/E7,[7] thereby making cell lines unsuitable for cell therapy. Establishing cell lines from tumors is difficult and has a low efficiency (e.g. 12% for renal cell carcinoma)[11], thereby complicating the establishment of patient-specific cell lines with matched normal lines: assuming that the efficiency for establishing a healthy cell line is also 12%, the success rate of establishing a tumor cell line with matched normal would be approximately 1.5%. Furthermore, cell lines are clonal expansions from one cell, which leads to loss of heterogeneity and selection bias, particularly in the field of tumor biology.

Second, pluripotent stem cell (PSC)-derived organoids have been developed over the last 3 years as highly relevant and exciting new tools for *in vitro* research (protocols reviewed in **Chapter 2**). This organoid culture system adds complexity to existing *in vitro* models: PSC-kidney organoids contain multiple cell types with a nephron-segmented orientation and grow as 3D structures.[12] As PSCs are used as start material, it is an excellent model for the study of normal or (genetically) impaired

human kidney development. Given that the architecture is similar to *in vivo* kidneys, the prediction of nephrotoxicity of compounds and the study of the cross-talk and feedback loops between different cell types in the proximal and distal nephron, will most likely be improved when compared to cell lines. However, PSC-derived organoids do not enable the culture of primary diseased tissue, such as kidney tumors, and the reprogramming process required to obtain the organoids may affect cell stability and behavior. [13]

This thesis: adult stem cell-derived kidney organoid culture

A third type of *in vitro* model system that has been developed, is adult stem cell (ASC)-derived organoid culture. The field has developed at a tremendous pace over the last years and yielded exciting results for other organs (reviewed in **Chapter 1**), including personalized medicine for cystic fibrosis (CF)[14] and modeling the development of colon cancer *in vitro*.[15]

In this thesis, an ASC-derived kidney organoid culture system was developed and investigated. This is of great relevance for kidney research. First, it allows the expansion of healthy kidney cells without immortalization or reprogramming, providing a platform for the study of kidney function that potentially better resembles the *in vivo* situation. Second, it allows the culture of primary diseased cells directly from patients, enabling the heterogeneous culture of tumor cells, disease modeling and personalized medicine. These two features have proved difficult or even impossible with cell lines and PSC-derived organoids, making ASC-derived organoids a useful and complementary tool for *in vitro* kidney research.

Establishment

After adaptation of existing (non-kidney) ASC-organoid protocols (**Chapter 1**) and by using knowledge of the PSC-kidney organoid protocols (**Chapter 2**), it is possible to grow organoid structures from nephrectomy material (**Chapter 3**). Tubular fragments are resuspended in BME or Matrigel, in order to mimic the components of the kidney extracellular matrix, particularly laminin and collagen.[16] Rspo-conditioned medium is added to enhance canonical Wnt signaling, known to be essential for embryonic kidney development,[17, 18] whereas FGF10 is supplemented to promote survival of kidney progenitor cells.[19] To prevent growth arrest and TGF-β-induced epithelial to mesenchymal transition,[20] ALK4/5/7 receptors are inhibited with A8301. Lastly, to stimulate cell division EGF is added and Rho-kinase inhibitor is supplemented to prevent anoikis of dissociated cells.[21]

Characterization

However, merely "growing something" is not particularly valuable on itself and before organoids can be applied as a model, an in-depth characterization on multiple levels is required. These (RNA, protein and functional) analyses have mainly been presented in **Chapter 3**. A crucial aspect is determination of what these organoid structures represent (i.e. what cell types are propagated), because this determines the diseases that can be modeled in the culture system. Mouse organoid lines established from adult bulk kidney have a predominant distal nephron phenotype, whereas human organoids are more heterogeneous mix, tending towards a proximal tubule predominant phenotype. This difference can be explained by differences in start material: for setting up a mouse organoid line, a whole mouse kidney is digested, whereas for human cultures, cortical kidney tissue

(~80% proximal tubule cells) is used. Furthermore, the high expansion capacity of both mouse and human cultures makes it likely that stem /progenitor cells are propagated.

It is also relevant to perform functional characterization and determine whether the structures display features of normal kidney physiology, such as transporter function. In **Chapter 3**, we showed that mouse organoids increase *aqp2* expression in response to anti-diuretic hormone exposure, resembling *in vivo* collecting duct function. Human organoids display P-gp function (**Chapter 3**), which is a typical proximal tubule efflux transporter. Thus, organoids show characteristics of *in vivo* kidney function.

For personalized medicine and drug screening, it is important to know whether structures can be established efficiently, ensuring that organoids can be easily established from every individual, and whether they are genetically stable on the long-term, ensuring reliable drug screening results. Efficiency of establishment is 100% under optimized conditions and karyotyping indicates that the cells retain a normal number of chromosomes.

In **Chapter 6**, a stem / progenitor cell type with a particularly high organoid-forming capacity was identified using reporter mice. Neonatal Wnt-responsive Troy+ cells, that have multi-lineage capacity with a tendency towards distal nephron, have a high organoid formation compared to Troy- population. This suggests that Wnt-responsive progenitor cells are the start cells of (mouse) organoid lines. In **Chapter 6**, organoid-forming capacity is used as an argument, besides the lineage-tracing experiments presented, as proof for the stemness of Troy+ cells. However, with the risk of making a circular argument, these data can also be interpreted otherwise: the fact that organoid cultures from other organs are ASC-derived and that Troy+ cells have a higher organoid formation, **Chapter 6** can also be interpreted as an analysis of the behavior of an organoid-forming cell *in vivo*. Then, it shows that neonatal organoid-forming cells contribute to all tubular lineages (with a predominant distal nephron phenotype) in a segment-specific way (which is in line with the literature, where segment-specific stem cells have been identified[22, 23]). In adult kidney, Troy-derived cells have a more specific collecting duct phenotype and the number of cells that originated from organoid-forming cells may increase after damage. It is of note that the organoid-formation analysis was done with neonatal Troy+ cells and not adult cells, complicating extrapolation of the data to the adult and/or human situation. However, in accordance with the lineage tracing data in **Chapter 6**, mouse organoid lines established from adult bulk kidney have a predominant distal nephron phenotype (**Chapter 3**).

Thus, organoids contain tubular cells of multiple nephron segments and are stem / progenitor cell-derived.

Non-invasive start material

The need for biopsy or nephrectomy material as a source of cells for establishing kidney organoids poses a major limitation for establishing cultures from kidney diseases for which biopsy and nephrectomy are not the standard of care. Therefore, a non-invasive cell source was pursued. After adaptation of protocols that others[24] established to isolate cells from urine, it is possible to isolate single cells (either kidney or urothelial in nature) from urine that develop into organoids in ~10-20% of the cases (**Chapter 3**). The low efficiency can partly be explained by bacterial and fungal contaminations of the urine. This may be solved by optimization of antibiotic use. A question that remains is whether ultimately organoid cultures can be established from every individual's

urine (by repeated isolations), or that some individuals shed too few cells, making isolation futile. The latter may be solved by interventions to induce cell shedding, such as fluid consumption or medication.

Applications

We developed kidney organoid-based disease models, to show proof-of-principle for personalized medicine and to embed organoids as cell source in other technologies. Here, the focus was on human organoids, rather than mouse, as it is the most relevant for the majority of applications. We used two different approaches, first, starting with healthy organoids and applying the disease, and second, starting with primary diseased tissue.

Disease modeling

To provide proof-of-principle for the modeling of acquired kidney disease, organoids were infected with BK virus infection. Typical characteristics of the *in vivo* infection (patchy pattern of infection; increase in size of the nucleus of infected cells) are recapitulated in organoids (**Chapter 3**). The focal infection pattern in organoids resembles the *in vivo* infection more than in cell lines, where a more diffuse pattern is observed (20% of the cultured cells are infected within 6 days).[25] It is possible to maintain organoid cultures with BK virus for at least 30 days, modeling the chronic nature of the infection. Importantly, infection of organoids could be established with urine from patients with BK virus-induced nephropathy. This reduces selection or adaptation effects of virus strains that may occur during the expansion of the virus in human embryonic lung fibroblasts (MRC-5 cells), which is the current laboratory standard. Furthermore, we demonstrated that virus replication can be inhibited dose-dependently by the clinically used drugs, which indicates that future therapies can be tested for efficacy and toxicity in organoids.

Pediatric solid tumors are commonly found in the kidney. Treatment encompasses nephrectomy, leading to loss of the affected kidney and chemotherapy, causing long-term side effects that damage the contra-lateral kidney. Organoid lines from the major types of pediatric kidney tumors (Wilms, RCC and MRTK) with matched normal organoid lines were established in order to create a "living biobank" (**Chapter 4**). This biobank may eventually lead to the development of more efficient and less toxic treatment strategies. Tumor organoid lines can be established with 95% overall efficiency, implicating that there are hardly selection effects. A large number of tumor cells expands after seeding, suggesting that tumor heterogeneity is maintained. We show that the organoid lines histologically reflect the tumor tissue that they are derived from: an epithelial type Wilms tumor, yields an organoid culture with predominant epithelial structures, whereas an organoid line from a classic tri-phasic tumor, is composed of all three (epithelial, blastemal, stromal) components. Similarly, clear cells are present in an organoid line derived from a renal cell carcinoma containing exclusively clear cells, and SMARCB1 is absent in an organoid line derived from a MRTK where SMARCB1 is lacking. In addition, preliminary genetic analyses of two Wilms tumor lines show that tumor organoids have the same genetic aberrations as the tumor that the organoids were derived from and that these are absent in the matched normal tissue and organoids (**Chapter 3**).

The high efficiency of establishing organoid lines from pediatric kidney tumors is in stark contrast with the efficiency of adult kidney tumors. Repeated attempts, in different culture conditions, of

culturing adult renal cell carcinomas were not successful. We can only speculate as to why this difference exists. Adult renal cell carcinomas typically have inactivating mutations in *VHL* that are mostly absent in pediatric kidney tumors. Inactivation of *VHL* may lead to metabolic changes that in turn require other culture conditions (in terms of growth factor or matrix composition). More comprehensively testing different types of matrices and growth factor combinations may improve the efficiency of adult kidney tumor organoid culture in the future.

Personalized medicine

Because of the easy access to start material (urine) for cultures, applications of kidney organoids in other fields than nephrology are conceivable. Indeed, the first proof-of-principle for personalized medicine of kidney organoids derived from non-invasive biological material was demonstrated for a disease that is not kidney-related (**Chapter 3**). In CF research, the forskolin-induced swelling assay can be used to determine the efficacy of CFTR-restoring compounds with rectal organoids.[14] Urine-derived organoids from a CF-patient react similarly to forskolin exposure and CFTR-restoring compounds as the intestinal organoids established from the same patient. It remains to be determined whether the results obtained for the one patient (ΔF508/S1251N mutation) presented in this thesis, can be replicated for patients with different CFTR mutations. In addition, the question remains whether urine is a viable alternative for rectal biopsies as material for forskolin-induced swelling assays: i.e. is it cost-effective, taking into account the reduced invasiveness as well as the lower efficiency of establishing cultures?

Studies on organoid cultures from patients with kidney transporter diseases are on the brink of starting.

Integrating organoid cells in emerging technologies

Organoid cells can be integrated into other technologies. A bioartificial kidney adds a cellularized cartridge to conventional hemodialysis, in order to better recapitulate kidney function (e.g. increased excretion of uremic toxins and hormone production) than hemodialysis does. The development of bioartificial kidneys is hampered by the lack of an appropriate cell source.[26] In **Chapter 5**, it is demonstrated that organoid cells display basolateral and apical transport functions – characteristics that are required for application in a bioartificial kidney. This indicates that organoid cells may function as autologous cell source for bioartificial kidneys.

Additionally, organ-on-a-chip platforms and organoid models are often viewed as two competing "next generation" cell culture models. However, in **Chapter 5** is shown that organoid cultures and "organ-on-a-chip" models are not necessarily mutually exclusive and that these may be combined synergistically.

A summary of the key findings of this thesis is provided in **Box 1**.

Future developments

Four expected developments for applications of kidney organoids are listed below.

Fundamental studies

Organoids will be of use to study epithelial physiology, such as transporter function. Fluorescent substrates for specific transporters may conveniently accumulate in the organoid lumen (for

Box 1. Summary of the key findings of this thesis

1. Mouse and human ASC-derived, long-term, kidney organoid cultures can be established.
2. Kidney organoid cultures contain epithelial cell types of multiple nephron segments.
3. Kidney organoids can be used to model infectious kidney diseases (BK-virus nephropathy).
4. Kidney organoids can be established from urine.
5. Urine-derived organoids can be used test treatment efficacy for cystic fibrosis (personalized medicine).
6. Organoids can be established from the most common types of pediatric kidney tumors and recapitulate the tumor that the organoids are derived from.
7. Organoid-derived cells cultured on an "organ-on-a-chip" platform form leak-tight tubes that enable high-throughput transporter and toxicity studies.
8. Organoid-derived cells can be cultured on dialysis membranes, designating organoids as potential cell source for autologous bioartificial kidneys.
9. *Troy* marks a progenitor cell type in the developing and adult kidney that has a high organoid formation capacity.

apically located efflux transporters), or can be injected into the lumen (for apically located influx transporters), allowing straightforward quantification of transport. Alternatively, organoid cells may be forced into a tube-like structure on "organ-on-a-chip" plates with access to both basolateral and apical sides. This will also reduce the heterogeneity of regular organoid culture, facilitating the standardized and high-throughput evaluation of kidney transporters. Of note, as organoids enrich for stem / progenitor cells, further differentiation of organoid cultures may be required for transporter studies, which necessitates the optimization of differentiation culture media.

In addition, biobanks of specific diseases will facilitate the study of pathophysiology. Analogous to the pediatric kidney tumor biobank (**Chapter 5**), we will establish biobanks for genetic kidney diseases (e.g. channelopathies, such as Gitelman or Bartter syndromes). Additionally, in order to include isogenic controls, healthy organoid lines will be genetically modified with CRISPR/CAS9 to create genetic disease models.

Drug development

Urine as start material for organoid cultures offers opportunities for establishing living biobanks of human healthy and diseased kidney organoids that can be used for drug development. Kidney organoid biobanks of a broad, healthy population will help pre-clinical high-throughput efficacy and toxicity studies: this will facilitate the testing of widely prescribed diuretics or chemotherapeutic agents that are often nephrotoxic. With biobanks established from patients with genetic diseases, easy read-outs for efficacy will fuel drug development: e.g. for channelopathies, similar assays to the forskolin-induced swelling assay in CF, may be developed.

Personalized medicine

Organoids open up the high-throughput screening of candidate drugs for an individual patient. This has been demonstrated for tumor organoids from colon[27] and breast (*manuscript under review*), as well as rectal organoids from CF patients.[14] Analogous efficacy and toxicity screenings are expected for kidney organoids. For pediatric kidney tumors, organoids may be established from tumor biopsies and subsequent drug screens will determine what the most effective pre- or post-nephrectomy chemotherapy is. This is particularly relevant for tumors with a poor prognosis, such as MRTKs (20% 5 year survival)[28, 29] from which we have established four organoid lines. Eventually, it is expected that personalized medicine treatment regimens will be developed, so that treatment is based on what is effective for an individual rather than what works best on average for a whole population. Similar personalized medicine can be developed for channelopathies.

Towards building a bioartificial kidney

It would be straightforward to repeat the study from Humes and colleagues,[30] where dogs were subjected to kidney injury and subsequently treated with a bioartificial kidney. The sole difference in set-up will be that an additional group is included in the study: autologous (dog-derived) organoid cultures, established prior to injury, will be used to seed the living cell cartridge. This will indicate whether organoid-derived cells perform better than cell lines.

Instead of embedding organoid cells in existing bioartificial set-ups, completely new types of bioartificial kidneys may ultimately be developed. Dialysis membranes (that are used as filters), can potentially be replaced by micron-scale printed filters to recapitulate the glomerulus function of the kidney. Autologous leak-tight tubes, cultured on "organ-on-a-chip" platforms, may recapitulate the tubule function of the kidney by selective reabsorption and excretion. Attaching the filters to the tubes may yield a device that can be connected to the circulation and is small enough to allow implantation.

REFERENCES

1. Eckardt, K.-U. et al. Evolving importance of kidney disease: from subspecialty to global health burden. *The Lancet* **382**, 158-169 (2013).
2. Couser, W.G., Remuzzi, G., Mendis, S. & Tonelli, M. The contribution of chronic kidney disease to the global burden of major noncommunicable diseases. *Kidney international* **80**, 1258-1270 (2011).
3. Benigni, A., Morigi, M. & Remuzzi, G. Kidney regeneration. *The Lancet* **375**, 1310-1317 (2010).
4. Pastan, S. & Bailey, J. Dialysis Therapy. *New England Journal of Medicine* **338**, 1428-1437 (1998).
5. Fishman, J.A. Infection in solid-organ transplant recipients. *New England Journal of Medicine* **357**, 2601-2614 (2007).
6. Engels, E.A. et al. Spectrum of cancer risk among US solid organ transplant recipients. *Jama* **306**, 1891-1901 (2011).
7. Ryan, M.J. et al. HK- an immortalized proximal tubule epithelial cell line from normal adult human kidney. *Kidney Int* **45** (1994).
8. Jansen, J. et al. A morphological and functional comparison of proximal tubule cell lines established from human urine and kidney tissue. *Experimental Cell Research* **323**, 87-99 (2014).
9. Brodaczewska, K.K., Szczylik, C., Fiedorowicz, M., Porta, C. & Czarnecka, A.M. Choosing the right cell line for renal cell cancer research. *Molecular Cancer* **15**, 83 (2016).
10. Kogan, I. et al. hTERT-immortalized prostate epithelial and stromal-derived cells: an authentic in vitro model for differentiation and carcinogenesis. *Cancer research* **66**, 3531-3540 (2006).
11. Ebert, T., Bander, N.H., Finstad, C.L., Ramsawak, R.D. & Old, L.J. Establishment and characterization of human renal cancer and normal kidney cell lines. *Cancer Research* **50**, 5531-5536 (1990).
12. Takasato, M. et al. Kidney organoids from human iPS cells contain multiple lineages and model human nephrogenesis. *Nature* **526**, 564-568 (2015).
13. Kim, K. et al. Epigenetic memory in induced pluripotent stem cells. *Nature* **467**, 285-290 (2010).
14. Dekkers, J.F. et al. A functional CFTR assay using primary cystic fibrosis intestinal organoids. *Nat Med* **19**, 939-45 (2013).
15. Drost, J. et al. Sequential cancer mutations in cultured human intestinal stem cells. *Nature* **521**, 43-47 (2015).
16. Genovese, F., Manresa, A.A., Leeming, D.J., Karsdal, M.A. & Boor, P. The extracellular matrix in the kidney: a source of novel non-invasive biomarkers of kidney fibrosis? *Fibrogenesis & tissue repair* **7**, 4 (2014).
17. Stark, K., Vainio, S., Vassileva, G. & McMahon, A.P. Epithelial transformation of metanephric mesenchyme in the developing kidney regulated by Wnt-4. *Nature* **372**, 679-683 (1994).
18. Carroll, T.J., Park, J.-S., Hayashi, S., Majumdar, A. & McMahon, A.P. Wnt9b Plays a Central Role in the Regulation of Mesenchymal to Epithelial Transitions Underlying Organogenesis of the Mammalian Urogenital System. *Developmental Cell* **9**, 283-292 (2005).
19. Poladia, D.P. et al. Role of fibroblast growth factor receptors 1 and 2 in the metanephric mesenchyme. *Developmental Biology* **291**, 325-339 (2006).
20. Xu, J., Lamouille, S. & Derynck, R. TGF-β-induced epithelial to mesenchymal transition. *Cell research* **19**, 156-172 (2009).
21. Watanabe, K. et al. A ROCK inhibitor permits survival of dissociated human embryonic stem cells. *Nat Biotech* **25**, 681-686 (2007).
22. Rinkevich, Y. et al. In vivo clonal analysis reveals lineage-restricted progenitor characteristics in mammalian kidney development, maintenance, and regeneration. *Cell Rep* **7**, 1270-83 (2014).
23. Barker, N. et al. Lgr5(+ve) stem/progenitor cells contribute to nephron formation during kidney development. *Cell Rep* **2**, 540-52 (2012).
24. Zhou, T. et al. Generation of human induced pluripotent stem cells from urine samples. *Nat. Protocols* **7**, 2080-2089 (2012).
25. de Kort, H. et al. Primary human renal-derived tubular epithelial cells fail to recognize and suppress BK virus infection. *Transplantation* (2017).
26. Westover, A.J. et al. A bio-artificial renal epithelial cell system conveys survival advantage in a porcine model of septic shock. *Journal of Tissue Engineering and Regenerative Medicine*, n/a-n/a (2014).
27. van de Wetering, M. et al. Prospective Derivation of a Living Organoid Biobank of Colorectal Cancer Patients. *Cell* **161**, 933-945 (2015).
28. Weeks, D.A., Beckwith, J.B., Mierau, G.W. & Luckey, D.W. Rhabdoid Tumor of Kidney: A Report of

111 Cases from the National Wilms' Tumor Study Pathology Center. *The American journal of surgical pathology* **13**, 439-458 (1989).

29. Vujanić, G.M., Sandstedt, B., Harms, D., Boccon–Gibod, L. & Delemarre, J.F.M. Rhabdoid tumour of the kidney: a clinicopathological study of 22 patients from the International Society of Paediatric Oncology (SIOP) nephroblastoma file. *Histopathology* **28**, 333-340 (1996).
30. Humes, H.D., Buffington, D.A., MacKay, S.M., Funke, A.J. & Weitzel, W.F. Replacement of renal function in uremic animals with a tissue-engineered kidney. *Nature biotechnology* **17**, 451-455 (1999).

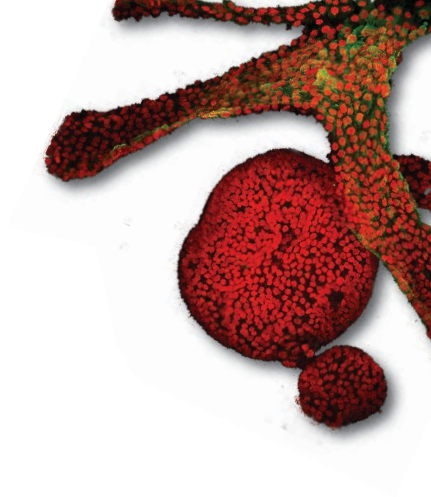

ADDENDUM

NEDERLANDSE SAMENVATTING
CURRICULUM VITAE AND LIST OF PUBLICATIONS
DANKWOORD

&

NEDERLANDSE SAMENVATTING

– ook voor niet-ingewijden

Het aantal mensen met nierschade en nierfalen in de wereld neemt toe. Dit is voornamelijk te wijten aan de toename van risicofactoren voor nierschade, zoals overgewicht en diabetes. We begrijpen nog niet alles van nierziekten en de behandeling bestaat in eerste instantie dan ook uit het remmen van de progressie van nierschade, in plaats van het genezen ervan. Als de nierfunctie dusdanig is aangedaan en eindstadium nierfalen is bereikt, dan is niervervangende therapie de enige optie. Hiervan bestaan twee varianten: niertransplantatie en dialyse. Beide hebben belangrijke nadelen: wat transplantatie betreft, is er een tekort aan donororganen en bij dialyse worden niet alle functies die de nier in het lichaam heeft, overgenomen.

Kortom, nierziekten vormen een groot probleem, waarvoor geen optimale behandelingen bestaan. Beter begrijpen hoe de nier zichzelf onderhoudt in gezondheid en wat er mis gaat tijdens ziekte, kan leiden tot verbetering van de bestaande behandelingen. Om deze doelen te bereiken, zijn er humane laboratoriummodellen (*in vitro*) nodig, die een goede nabootsing zijn van de nier in het lichaam (*in vivo*).

Bij aanvang van dit promotieonderzoek waren er twee types *in vitro* modellen beschikbaar voor nieronderzoek: cellijnen en nierorganoïden ('mini-nieren') uit embryonale stamcellen.

Cellijnen zijn gekweekte cellen, die zijn gegroeid vanuit één enkele cel en die vaak met kunstgrepen in het laboratorium onsterfelijk zijn gemaakt. De afgelopen decennia hebben cellijnen de kennis over de nier enorm doen toenemen, maar zij hebben ook nadelen. Doordat ze gegroeid zijn uit één enkele cel is er sprake van verlies aan diversiteit in cellen die *in vivo* in de nier aanwezig is. Daarnaast zijn de cellen genetisch niet 'normaal': ze hebben bijvoorbeeld extra chromosomen.

In de afgelopen jaren is er een techniek ontwikkeld om nierorganoïden uit embryonale stamcellen te maken. Grofweg zijn er twee types stamcellen: embryonale stamcellen en volwassen stamcellen. Embryonale stamcellen zijn cellen die kort na de bevruchting ontstaan en waaruit het embryo zich ontwikkelt. Na de embryonale ontwikkeling zijn deze cellen niet meer aanwezig. Dit in tegenstelling tot volwassen stamcellen, die bij volwassen individuen volop aanwezig zijn. Volwassen stamcellen zijn orgaan-specifiek en zorgen voor reparatie en onderhoud van het betreffende orgaan.

Nierorganoïden gegroeid uit embryonale stamcellen, zijn daadwerkelijk 'mini-nieren' omdat ze qua structuur erg op de *in vivo* nier lijken, waardoor ze heel nuttig kunnen zijn voor onderzoek. Twee zaken die ontbreken in dit kweeksysteem zijn de mogelijkheid om de cellen te expanderen (uit een klein aantal cellen, heel veel cellen maken) en om direct cellen te isoleren uit zieke nieren en die vervolgens te expanderen. In **hoofdstuk 2** worden de protocollen beschreven die zijn ontwikkeld om vanuit embryonale stamcellen nierorganoïden te maken.

In onze onderzoeksgroep is een kweeksysteem ontwikkeld, waarbij volwassen stamcellen worden gebruikt om organoïden van te groeien. Een stamcel uit een volwassen darm, kan in een kweekbakje in het laboratorium uitgroeien tot een 'mini-darm.' Na de ontwikkeling van de darmorganoïden, zijn er ook kweken opgezet voor andere organen. Dit heeft onder andere geleid tot maag-, lever-, alveesklier- en prostaatorganoïden. Deze kweken blijken zeer nuttig voor

zowel fundamenteel biomedisch onderzoek als klinische toepassingen (bijvoorbeeld het patiënt-specifiek testen van medicatie).

In **hoofdstuk 1** worden de ontwikkeling van deze techniek, de essentiële componenten en toepassingen ervan beschreven.[1]

Ook wordt in **hoofdstuk 1** aandacht besteed aan de vraag waarom een nierorganoïdkweek uit volwassen stamcellen, een systeem dat nog niet ontwikkeld is, nuttig zou kunnen zijn. De duidelijkste toegevoegde waarde is dat het met dit systeem waarschijnlijk mogelijk is om met een hoge efficiëntie zieke cellen, die direct uit ziek nierweefsel zijn gehaald, te laten groeien. Deze eigenschap ontbreekt bij andere kweeksystemen. Dit maakt het mogelijk om nieuwe medicijnen op effectiviteit en toxiciteit te testen en eveneens om op een patiënt-specifieke manier te testen: zo zou je uit een niertumor van een patiënt tumor-organoïden kunnen laten groeien en daar 100 verschillende chemotherapeutica op testen, om te kijken welke middelen het beste werken voor deze specifieke tumor.

Het doel van dit proefschrift is dan ook om een nierorganoïdenkweek uit volwassen stamcellen op te zetten en toepassingen hiervoor te ontwikkelen.

In **hoofdstuk 3** wordt de ontwikkeling van zo'n kweeksysteem beschreven. Met aanpassingen in de groeifactorcocktail die voor darmorganoïden wordt gebruikt, is het mogelijk om nierorganoïden (zowel van muis als mens) ongeveer een half jaar te laten groeien en van een klein beetje weefsel, heel veel weefsel te maken. Nierorganoïden zijn een bepaald deel van het nefron (de functionele eenheid van de nier), namelijk de tubulus en dan vooral het proximale deel. Om aan te tonen dat het systeem nuttig is om ziekten te modelleren, wordt beschreven dat BK virus (een virus dat de nieren bij transplantatiepatiënten infecteert en de nieren daarmee kapot maakt) de nierorganoïden infecteert en aspecten van de *in vivo* infectie nabootst. Een andere belangrijke bevinding is dat het mogelijk is om uit urine cellen te isoleren die te gebruiken zijn voor het opzetten van een organoïdkweek. Dit kan nuttig zijn om op een niet-invasieve manier medicijnen te testen. Het principe hiervoor wordt aangetoond met het testen van medicatie voor een patiënt met taaislijmziekte (cystische fibrose). Het is bekend dat mini-darmen van patiënten met taaislijmziekte gebruikt kunnen worden om de werkzaamheid van een medicijn te voorspellen. In **hoofdstuk 3** wordt beschreven dat vergelijkbare tests kunnen worden gedaan op mini-nieren die vanuit urine zijn gegroeid. Dit heeft mogelijk het voordeel dat er in de toekomst geen rectumbiopt (dat weer nodig is voor het kweken van mini-darmen) nodig is voor het uitvoeren van deze test.

In **hoofdstuk 4** wordt het kweekprotocol uit **hoofdstuk 3** gebruikt om organoïden te maken uit niertumoren die bij kinderen voorkomen. Pediatrische tumoren komen frequent in de nier voor en de behandeling bestaat uit het verwijderen van de nier en chemotherapie (die schadelijke effecten heeft op de lange termijn). In **hoofdstuk 4** worden organoïden uit verschillende typen niertumoren (Wilms tumor, rabdoid tumor en heldercellig niercarcinoom) beschreven en wordt aangetoond dat deze organoïden qua histologie lijken op de tumor waaruit ze gegroeid zijn. Van een paar tumoren (zie hiervoor **hoofdstuk 3**) wordt aangetoond dat de organoïden ook dezelfde genetische fouten bevatten als het tumorweefsel. Kortom, tumor-organoïden lijken op de primaire

[1] Het nut van organoïden in het algemeen leg ik ook uit in een college voor de Universiteit van Nederland dat op hun website (www.universiteitvannederland.nl) bekeken kan worden.

tumor, zowel histologisch als genetisch. Dit kan in de toekomst nuttig zijn voor onderzoek van deze tumoren, maar ook voor het testen van medicijnen. Dit zou uiteindelijk kunnen leiden tot de ontwikkeling van efficiëntere en minder toxische behandelingen.

In **hoofdstuk 5** wordt geprobeerd om de nierorganoïdkweek compatibel te maken met twee andere technologieën die in opkomst zijn, namelijk de bioartificiële nier en een organ-on-a-chip platform. De bioartificiële nier combineert conventionele dialyse met een cartridge met levende cellen, met als doel om ook nierfuncties die door standaard dialyse niet uitgevoerd worden, te vervangen. Een probleem waardoor de ontwikkeling van de bioartificiële nier spaak loopt, is dat er geen adequate bron van niercellen beschikbaar is. In **hoofdstuk 5** worden de eerste aanwijzingen beschreven dat organoïden een mogelijke geschikte bron van cellen zijn voor de bioartificiële nier. Daarnaast worden organoïd-cellen in een buisvorm 'gedwongen' op een organ-on-a-chip platform. Organ-on-a-chip technologie probeert, net als organoïd technologie, *in vitro* modellen te maken die meer op de *in vivo* situatie lijken. In het geval van de nier, bestaat er een organ-on-a-chip platform dat cellen dwingt in de vorm van een buis te groeien, dezelfde vorm die de tubulus van het nefron heeft in het lichaam. Er wordt aangetoond dat organoïd-cellen buisjes vormen die lekdicht zijn en dat ze ook enkele transportfuncties van de nier uitvoeren. Uit deze studies blijkt voor het eerst dat organoïd technologie en organ-on-a-chip technologie goed met elkaar samen gaan en dat voor sommige toepassingen de combinatie van de twee technologieën synergistisch kan werken.

Organoïden ontstaan uit stamcellen. In **hoofdstuk 6** wordt een celtype dat met een relatief hoge efficiëntie nierorganoïden vormt, beschreven. Door die hoge organoïd-vormende efficiëntie, is er het vermoeden dat dit celtype een stamcel is. Op vier manieren wordt aangetoond dat dit daadwerkelijk zo is. Ten eerste door te laten zien dat eiwitten die specifiek zijn voor gedifferentieerde cellen en dus alleen voorkomen bij niet-stamcellen, afwezig zijn in deze cellen (*kenmerk van een stamcel*). Ten tweede, door te laten zien dat in het lichaam van een muis één enkele cel, hele stukken nierbuis vormt (*kenmerk van een stamcel*). Ten derde, door te laten zien dat er genen tot expressie komen die belangrijk zijn voor nierontwikkeling (*kenmerk van een stamcel*). Ten vierde, door te laten zien dat bij sommige muizen, deze cellen toenemen na schade (*kenmerk van een stamcel*).

Tenslotte wordt in **hoofdstuk 7** het proefschrift samengevat en in een context geplaatst. Ook worden er suggesties gedaan voor vervolgonderzoek.

CURRICULUM VITAE

Frans Willem Godfried Schutgens was born in Beek on June 10th, 1987. He graduated from Trevianum Gymnasium in Sittard (*cum laude*), where he majored in nature and health track and nature and technology track. In 2005 he enrolled in University College Utrecht, the honors college from Utrecht University, where he opted for the pre-medical school track. During his bachelor's degree, he spent one semester at the University of California, Berkeley, as part of an exchange program. He obtained his Bachelor of Science at University College Utrecht in 2008 (*summa cum laude*). He continued his studies, supported by a Huygens Talentenbeurs from the Dutch government, at the Imperial College of Science, Technology and Medicine, in London, to pursue a Master of Science degree in molecular medicine. He graduated in 2009 (*with distinction*). In September 2009, he started the Selective Utrecht Medical Masters (SUMMA) program at Utrecht University to obtain an MD degree. During his research internship in last year of SUMMA, he was working on a combined project in Hans Clevers' lab (Hubrecht Institute) and Marianne Verhaar's lab (UMC Utrecht), under supervision of Maarten Rookmaaker. He worked on kidney stem cells and organoids. He continued this research after his graduation in a combined PhD project and the results of this research are printed in this thesis.

LIST OF PUBLICATIONS RELATED TO THIS THESIS

M.B. Rookmaaker*, F. Schutgens*, M.C. Verhaar, H. Clevers. Development and application of human adult stem or progenitor cell organoids. Nature Reviews Nephrology. 2015. 11(9):546-554.
(* *Contributed equally to the work*)

F. Schutgens, M.C. Verhaar, M.B. Rookmaaker. Pluripotent stem cell-derived kidney organoids: an *in vivo*-like in vitro technology. European Journal of Pharmacology. 2016. 790: 12-20.

F. Schutgens, M.B. Rookmaaker, F. Blokzijl, R. van Boxtel, R. Vries, E. Cuppen, M.C. Verhaar, H. Clevers. Troy/TNFRSF19 marks epithelial cells with progenitor characteristics during kidney development that continue to contribute to turnover of the collecting duct in adult kidney. *Under review*

F. Schutgens, M.B. Rookmaaker, C. Ammerlaan, J. Jansen, M. Viveen, L. Gijzen, A. Vonk, K.M. de Winter - de Groot, A.P.A. Hendrickx, M.M. van den Heuvel – Eibrink, E. Heitzer, H. Lanz, J. Beekman, J. Murk, R. Masereeuw, J. Drost, M.C. Verhaar, H. Clevers. Human adult kidney-derived organoids as personalized disease models in a dish and on a chip. *Under review*

DANKWOORD

Een proefschrift schrijf je niet alleen. Ik ben velen dankbaar die aan dit proefschrift hebben bijgedragen. Een aantal wil ik hier in het bijzonder bedanken.

Mijn promotoren **Hans** en **Marianne**.

Hans, bedankt voor al je input over de jaren heen en voor het overbrengen van jouw visie op wetenschap. Ik heb veel van je geleerd tijdens de dinsdagochtend werkbesprekingen, waar je altijd blijft doorvragen en daardoor stimuleert om het meeste uit experimenten te halen. Naast formele werkbesprekingen, blijf je op de hoogte en geef je duidelijke adviezen door langs te lopen tussen jouw afspraken door. Dit gaat vaak gepaard met de klassieke vraag: 'En, heb je nog wat ontdekt?' Aan deze korte interacties heb ik veel gehad. Ik blijf het indrukwekkend vinden hoe je, ondanks je overvolle agenda, steeds binnen een dag of, vaker nog, binnen een uur antwoordt op e-mails.

Marianne, dank voor de kans om bij jou te promoveren en voor het opstarten van het project. Door je begeleiding en het vertrouwen dat je in me hebt, heb ik het maximale uit vier jaar promotieonderzoek gehaald. Tijdens meetings heb je focus in mijn project weten aan te brengen. Bovendien heb je me constant aangespoord om na te denken over de toekomst en carrière na het promotietraject. Daarmee heb je me altijd goed geholpen – zelfs toen bleek dat die toekomst mogelijk buiten de nefrologie ligt.

Mijn copromotoren **Maarten** en **Rob**.

Maarten, toen ik als masterstudent stage kwam lopen, was je vanaf de eerste dag betrokken als begeleider. Na deze stage is door jou dit PhD project überhaupt van de grond gekomen. Tijdens het PhD-traject ben je altijd zeer betrokken gebleven. Dank voor je kritische vragen, oplossingsgerichtheid, onverstoorbaar enthousiasme (zelfs met slaapgebrek na een drukke dienst), bijdehante opmerkingen en droge humor. Nadat je me vier jaar lang hebt bestempeld als 'future Apple user,' heb je ook hierin gelijk gekregen... Wat ik in het bijzonder heb gewaardeerd is de gelegenheid die je me hebt geboden om klinische ervaring op te doen tijdens de maandelijkse nefrogenetica poli: jouw begeleiding hierbij heb ik als heel prettig ervaren.

Rob, ik heb veel aan je gehad bij het opstarten in het lab en bij discussies over mijn projecten toen je nog als project manager werkzaam was.

Mijn paranimfen **Else** en **Laurens**.

Else, BN'er en rockster uit Dronten (en dus ABN-sprekend, dat blijkt uit 'feestie' en 'schoenties'), CRISPR-koningin, koffiecompagnon van het eerste uur, Lowlandsganger, fietsmaat, steun en toeverlaat in het lab: supercool dat jij mijn paranimf wil zijn! Altijd een luisterend oor voor werk of niet-werk gerelateerde zaken. Je hebt de afgelopen jaren altijd figuurlijk achter me gestaan en ook nog redelijk wat uren in de week letterlijk, in lab of kantoor. Dat je dit tijdens de verdediging ook zal doen, geeft veel vertrouwen.

Laurens, wat vind ik het mooi dat jij mijn paranimf bent. Ik kan me enkele middagen herinneren waar we samen op zaterdagmiddag in de Maxwell met een speciaalbiertje op onze laptops aan onze proefschriften aan het typen waren. Bovendien ben je het symbool voor en immer-aanwezig deel van een hechte groep vrienden. Je geeft altijd goed advies, bent nooit in paniek en hebt vertrouwen dat dingen goedkomen. Dit alles zal goed van pas komen bij de verdediging.

Ik wil iedereen van de Clevers groep en de HUB bedanken. Ik vind het erg waardevol en motiverend om met zo'n gedreven groep mensen te werken die zoveel enthousiasme toont voor de wetenschap. Ik heb ervan genoten. Meer nog dan van het uitvoeren van mijn eigen onderzoeksproject, heb ik van jullie inzichten, intelligente vragen en suggesties geleerd.

Van diegenen die rondliepen toen ik begon en inmiddels weer verdere stappen hebben gezet, ben ik met name dank verschuldigd aan **Nobu** (for all the hours of culturing in the hood next to you, talking about the oddities of Dutch culture) en **Norman** (jouw fascinatie voor microscopie en filmpjes heb je zeker op me kunnen overdragen – en als ik ook maar een fractie van jouw skills heb overgenomen, vind ik het gezegend!). In het bijzonder **Jarno**: je gedrevenheid en efficiëntie zijn bewonderenswaardig en heb ik veel van kunnen leren. Ondanks je voorkeur voor een bepaald voetbalteam, is het een feest om met je samen te werken. Ik hoop dat we in de toekomst nog veel projecten samen kunnen doen. Veel succes met de Drost groep!

Wat de huidige Clevers groep betreft: **Carola**, dank voor al je inzet en harde werk in de laatste 1,5 jaar van het onderzoek - ik vind het fijn om met je samen te werken. **Harry** & **Jeroen** dank voor de ontelbare paraffine blokjes die jullie hebben verwerkt. **Maaike** & **Johan** voor de essentiële hulp bij het muiswerk. Ik vind het indrukwekkend hoe strak jullie de muizen georganiseerd hebben. **Jasper** (waar is die running title nou?!), voor het enthousiaste Limburgse gegroet op de vroege morgen, om mij me wat beter thuis te laten voelen. Zeker ook voor je verwoede pogingen om, naar eigen zeggen, wat meer een voetbalkantinesfeer te creëren in het lab. **Oded**, for all the trust you have in my choice of music and for our GoT discussions. **Benedetta**, for a daily dose of wonderful Italian irony. Thanks to all other post-docs for ideas and feedback to improve my project: **Kai**, **Helmuth, Talya**, **Inha**, **Yotam**, **Marrit**, **Angelos**, **Huili**, **Lena**, **DJ**, **Onur**, **Tomo**, **Yoshi**, **Florijn**, **Georg**, and **Jochem** (als ik nog een keer een intens complex immunologie paper moet reviewen, weet ik je weer te vinden).

De andere PhD studenten in de groep: **Kim**, **Kadi**, **Dymph**, **Marie**, **Else**, **Joep**, **Jens** & **Yorick**. Dank voor de gezelligheid binnen en buiten het lab (PhD avonden, borrels, Lissabon) en succes met jullie toffe projecten. **Joep** (BMP gradient!), bedankt dat je er altijd was om sportwedstrijden te analyseren en Tour te kijken. Alte Schnupert **Jens** (good stuff!) voor alle slechte grappen die je hebt uitgehaald en ik vond het beremooi om met zo'n tafeltenniskoning te tafeltennissen. Slangenbezweerder **Yorick** voor alle kopjes koffie, Haagse humor en potjes voetbal (voetballen in de gang mag, na 18.00).

Dan mijn kantoorgenoten **Karien** & **Stieneke**, die, samen met **Laura**, absoluut drijvende krachten zijn in het lab. **Karien**, dank voor je al je hulp! **Stieneke**, het was gezellig om naast je te zitten de afgelopen jaren en ik heb genoten van je scherpe commentaar op de gang van zaken in het lab. **Wim** (Willibrordus!), de nestor van het lab die van zijn hobby zijn werk heeft gemaakt, alles weet en alles heeft meegemaakt: 'Zal ik je daarbij helpen? Dat heb ik al 1000x gedaan en werkt altijd.' **Janny**, voor al je hulp over de jaren heen. Zeker bij het regelen van de promotie, maar ik zal ook je boerenkool, hummus en andere culinaire hoogstandjes niet vergeten.

De HUB: **Rob**, **Sylvia**, **Farzin**, **René**, **Tulay**, **Marvin**, dank voor jullie hulp bij mijn onderzoek!

Daarnaast wil ik de afdeling nefrologie en het hele UMCU nefrologie lab bedanken: **Gisela**, **Nynke**, **Olivier**, **Bas** (succes met de organoids!), **Hendrik** (sowieso moeten er meer studies worden uitgevoerd, puur omdat je er een goed acronym van kunt maken), **Tim**, **Rachel**, **Chris**, **Laura**, **Caroline**, **Jaap**, **Joost**, **Petra** & **Petra**, **Glenn** (alles stabiel?), **Merle**, **Femke**, **Paul** en **Arda**.

Alle mensen met wie ik heb mogen samenwerken buiten de eigen onderzoeksgroep. Het transporter-team van **Roos**, met name **Jitske**, voor de transporter assays die ik van je geleerd heb. De nefropathologie **Roel** en **Tri** voor alle consulten, waardoor ik ook een interesse voor pathologie heb ontwikkeld. **Francis** en **Ruben** voor waardevolle hulp bij het opzetten en analyseren van RNA seq experimenten. **Jean-Luc** en **Marco** voor de succesvolle BK-virus experimenten. **Antoni** voor hulp met de scanning EM. Ik bedank ook het team van de pediatrische niertumoren, met o.a. **Marry**, **Ronald** (ook voor het meelopen en je carrière-advies) en **Janna** (moeten we nou het formulier voor of na de OK inleveren? Dat blijft een van de grotere mysteries van mijn PhD ☺). **Marc**, voor het opzetten van de PMC tumor meetings en voor al je ideeën voor onderzoek. Mimetas (**Linda** en **Henriëtte**) voor alle lekdichte buisjes die we samen gemaakt hebben. Het CF-team van **Jeffrey**, vooral **Annelot** voor de toffe experimenten in het laatste deel van mijn onderzoek.

Labs United en **Labs United 2.0.** Thanks **Pieterjan**, **Axel, Ollie**, **Javi**, **Joppe**, **Max**, **Mauro**, **Enric**, **Samu**, **Lucas**, **Geert** and **Alex** for awesome Thursday nights with games of football, beers, one cup final and one championship. United we stand, divided we fall!

Voor essentieel geklaag ("DPhil, DPhil, doe mij maar een refill") en ontspanning na een lange dag mislukte experimenten: mijn vrienden. **Berend**, **Jannis**, **Laurens**, **Krijn**, **Eelke**, **Gijs**, **Sander**, **Pieter**, **Casimir**, **Eduard**, **Ruben**, **Neles**, **Bram**, **Eva**, **Iona**, **Sanne**, **Leonie**, **Johanneke**, **Roos**, **Jeanette**. Dank voor jullie onmisbare rol in mijn leven. Ik hoop dat we nog menig (kerst)diner, festival, GoT aflevering, kroeg- en/of spelletjesavond, weekend weg, groot of klein avontuur in Nederland of het buitenland samen mogen beleven.

Papa en **mama** (ook voor proofreaden ☺), voor onvoorwaardelijke steun bij wat ik ook uitspook en voor jullie aansporing van jongs af aan om nieuwe dingen te blijven leren en een studie/vak te kiezen waar je veel voldoening uit haalt. **Laura**, **Christine**, **Ivo** en **Michel** (een proefschrift schrijven is een beetje als een escape room): ik hoop dat jullie door dit boekje een beter inzicht hebben gekregen waar ik de afgelopen vier jaar mee bezig ben geweest.